THE UNIVERSITY of EDINBURGH

This thesis has been submitted in fulfilment of the requirements for a postgraduate degree (e.g. PhD, MPhil, DClinPsychol) at the University of Edinburgh. Please note the following terms and conditions of use:

Techno-Economic Study of the Calcium Looping Process for CO₂ Capture from Cement and Biomass Power Plants

Dursun Can Ozcan

Thesis submitted for the degree of Doctor of Philosophy to
The University of Edinburgh

The School of Engineering, The University of Edinburgh

2014

Declaration

I certify that the work presented in this dissertation was composed by me and that the work contained herein is my own except where explicitly stated otherwise in the text. Furthermore, I declare that this work has not been submitted for any other degree or professional qualification except as specified.

The work presented in this dissertation has contributed to 5 scientific papers, including the journals of Greenhouse Gas Control and Industrial & Engineering Chemistry Research, has been presented in 8 international conferences, including the AIChE Annual Meeting and the IEAGHG HTSLCN Meeting, and has received 2 awards from Honeywell and Association of British and Turkish Academics. Further details are available in Appendix E.

Dursun Can Ozcan

Lay Summary

The greenhouse effect is a natural process where greenhouse gases trap heat from the Sun in the atmosphere, warming the surface of the Earth. The greenhouse gases include water vapour, carbon dioxide (CO_2), methane and nitrous oxide and naturally exist in the atmosphere. This process maintains the Earth's temperature at a safe level to support life. Nevertheless, some human activities particularly burning fossil fuels and clearing of forests intensify the greenhouse effect because more greenhouse gases are released into the atmosphere. For this reason, the amount of heat absorbed by the greenhouse gases increases, which results in a rise in global surface temperatures and sea levels due to the melting of land ice. CO_2 is the most important greenhouse gas acting in climate change. It is expected that the anthropogenic CO_2 emissions will continue to increase if fossil fuels remain as the major source of energy production.

Carbon capture and storage (CCS) is a promising and an emerging way of reducing CO_2 emissions from large point sources, especially fossil-fuelled power stations and industrial processes such as cement plants. In addition, the use of sustainably-grown biomass as a renewable energy source in combustion systems is linked to zero net CO_2 emissions. We have developed comprehensive process flowsheets where fully integrated CCS systems are fitted to cement and biomass-fired power plants. Calcium looping (Ca-looping) process where CO_2 reacts with calcium oxide (CaO) and is thereby separated from flue gas has been selected as the main option for this purpose. The Ca-looping process uses relatively cheap and abundant CaO-based sorbents and is currently being piloted at the ~2 MW_{th} scale. We have evaluated the techno-economic performance of the Ca-looping process as well as several alternative CCS technologies. The findings of this dissertation contribute to the development of efficient and cost effective CCS systems applicable to cement and biomass-fired power plants.

Abstract

The first detailed systematic investigation of a cement plant with various carbon capture technologies has been performed. The calcium looping (Ca-looping) process has emerged as a leading option for this purpose, since this process applied to a cement plant provides an opportunity to use the CaO purge for clinker production. The Ca-looping process is comprised of two interconnected reactors where the carbonator captures CO_2 from flue gases and the calciner regenerates the $CaCO_3$ into CaO by oxy-combustion. Fully integrated process flowsheets have been developed and simulated in UniSim Design Suite from Honeywell. The detailed carbonator model has been implemented using Matlab and incorporated into UniSim to provide a full flowsheet simulation for an exemplary dry-feed cement plant as a user-defined operation. The base cement plant simulation was also modified to integrate three different carbon capture processes: membrane; indirect calcination; and amine-scrubbing. Furthermore, an advanced configuration of Ca-looping process has been investigated where the energy intensive air separation unit was replaced with a chemical looping combustion (CLC) cycle. Each case has been optimised to minimise its energy consumption and compared in terms of levelised cost of cement and its resulting cost of CO_2 avoided at the same CO_2 avoidance rate.

The proposed integration of the Ca-looping process is capable of achieving over 90% CO_2 avoidance with additional fuel consumption of 2.5 to 3.0 GJ_{th}/ton CO_2 avoided. By using an advanced configuration of the Ca-looping process with a CLC cycle, the additional fuel consumption can be reduced to 1.7 GJ_{th}/ton CO_2 avoided, but the cost of the oxygen carrier is the major concern for this system. Among the other CO_2 capture options, the membrane process is a promising alternative for the Ca-looping process since it has a potential of achieving the target CO_2 avoidance rate and purity requiring lower energy consumption. The indirect calcination process provides moderate levels of CO_2 avoidance (up to 56%) without a need of an external capture process whereas the integration of the amine process in a cement plant is challenging as a result of the requirement of steam for solvent regeneration.

Furthermore, considering zero net CO_2 emissions associated with biomass combustion systems, a novel concept has been analysed to capture of CO_2 in-situ with the Ca-looping process while operating the combustor of a dedicated biomass power plant at sufficiently low temperature. This process is capable of achieving 84% overall CO_2 capture rate with an energy penalty of 5.2% when a proper heat exchanger network is designed with the support of a pinch analysis. The techno-economic performance of the biomass power plant with in-situ Ca-looping CO_2 capture process was compared with that of the alternative biomass-air-fired and biomass-oxy-fired power plants.

Acknowledgements

Table of Contents

List of Figures

3

List of Tables

Nomenclature

a   Decay constant of solid concentration in the lean region (m^{-1})

A_t Cross sectional area of the reactor (m^2)

b   Decay constant of contacting efficiency in the lean region (m^{-1})

C_{CO_2} Actual CO_2 concentration in the CFB riser (mol/m^3)

C_{CO_2*} Equivalent CO_2 concentration in the CFB riser (mol/m^3)

$C_{CO_2,d}$ CO_2 concentration in the dense region exit (mol/m^3)

$C_{CO_2,eq}$ CO_2 concentration allowed by chemical equilibrium (mol/m^3)

$C_{CO_2,in}$ CO_2 concentration in the reactor inlet (mol/m^3)

$C_{CO_2,out}$ CO_2 concentration in the reactor exit (mol/m^3)

d_p Particle diameter (m)

E_{ac} Activation energy of calcination (kJ/mol)

E_{CO_2} Fraction of CO_2 captured to total CO_2 entering the carbonator

f_{carb} Extend of carbonation of the particles ($X_{ave}/X_{max,ave}$)

f_t Fraction of sorbent particles with a residence time t

F   Molar flow rate (kmol/s)

F_{ash} Molar flow rate of ash entering the Ca-looping system (kmol/s)

F_0 Make-up ($CaCO_3$) flow rate (kmol/s)

F_{CO_2} Molar flow rate of CO_2 in a flue gas stream entering the carbonator (kmol/s)

F_R Circulated sorbent (CaO) flow rate (kmol/s)

F_S Molar flow rate of sulfur entering the Ca-looping system (kmol/s)

g   Acceleration of gravity (m/s^2)

H_d Height of the dense region (m)

H_l Height of the lean region (m)

H_t Total height of the carbonator (m)

k_c Kinetic constant for the calcination reaction ($m^2 kmol^{-1} s^{-1}$)

k_{c0} Pre-exponential factor ($m^3 kmol^{-1} s^{-1}$)

k_r Kinetic constant of the carbonation reaction ($m^3/mol/s$)

k_{ri} Kinetic constant of the carbonation reaction (s^{-1}): $k_r \rho_{s,a}/M_{s,a}$

$k_{ri,ave}$ Average kinetic constant of the population of potentially active Ca-based solids (s^{-1})

k_s Rate constant for the carbonation reaction at the surface of CaO ($m^4/mol/s$)

K_{cw} Core-wall mass transfer coefficient (s^{-1})

M_s Molar mass of total solids (kg/kmol)

$M_{s,a}$ Molar mass of potentially active Ca-based solids (kg/kmol)

$n_{s,a}$ Moles of potentially active Ca-based solids (kmol)

N Number of carbonation/calcination cycles

p Pressure (Pa)

$P_{CO_2,eq}$ Equilibrium CO_2 partial pressure (Pa)

r_N Mass fraction of particles after N cycles of carbonation-calcination

s Flow rate per unit of width (membrane) (kmol/ms)

S_N Specific surface area available after N cycles of carbonation-calcination (m^2/m^3)

t Time (s)

t_c^* Time required to achieve full calcination (s)

t_{lim} Time required for a particle to reach its maximum carbonation (s)

T Temperature (K)

T_C Condenser temperature (C)

T_H Superheated steam temperature (C)

u_0 Superficial velocity of a gas (m/s)

v   Flow rate per unit of length (membrane) (kmol/ms)

V_g Volume of gas phase (m^3)

V_s Volume of solid phase (m^3)

$V_{g,in}$ Volumetric flow rate of inlet gas stream (m^3/s)

$V_{g,out}$ Volumetric flow rate of outlet gas stream (m^3/s)

W_s Solid inventory in the carbonator (kg)

x   Molar fraction

x_{ash} Molar fraction of ash

x_{CaSO_4} Molar fraction of $CaSO_4$

X   Carbonation degree of a lime particle

X_{ave} Average carbonation level

$X_{max,ave}$ Maximum average carbonation degree of the sorbent after N cycles of carbonation-calcination

$X_{max,N}$ Maximum carbonation conversion rate after N cycles of carbonation-calcination

Greek letters

ε_s^* Asymptotic solid volumetric fraction

$\varepsilon_{s,c}$ Volume fraction of solids in the lower dense region leaner core zone

$\varepsilon_{s,d}$ Volume fraction of solids in the lower dense region

$\varepsilon_{s,e}$ Volume fraction of solids at the carbonator exit

$\varepsilon_{s,l}$ Volume fraction of solids in the lean region

$\varepsilon_{s,w}$ Volume fraction of solids in the lower dense region denser wall zone

ρ_g Density of gases (kg/m^3)

ρ_s Density of total solids (kg/m^3)

$\rho_{s,a}$ Density of potentially active Ca-based solids (kg/m^3)

ΔX_{CaSO_4} Average fraction of sorbent sulfated at each cycle

μ Viscosity (kg/m/s)

η Net electrical efficiency (kW$_e$/kW$_{th}$)

η_l The contact efficiency of the lean region

η_{sd} The contact efficiency of the dense region

η_T Steam turbine efficiency

δ The core volumetric fraction of the dense region

ξ Volume ratio between the potentially active solids and the total solids

τ Average residence time of solids particles (s)

π Permeance (GPU)

Acronyms

ASU	Air separation unit
BECCS	Bio-energy with CO_2 capture and storage
BFB	Bubbling fluidized bed
Ca-looping	Calcium looping process
CCS	Carbon capture and storage
CF	Capacity factor
CFB	Circulating fluidized bed
CHP	Combined heat and power
CLC	Chemical looping combustion
COC	Cost of cement
COE	Cost of electricity
COM	Component object model
COP	Coefficient of performance
ESP	Electrostatic precipitator
ETS	Emission trading system
FC	Fuel cost
FCF	Fixed charge factor
FGD	Flue gas desulphurization
FWH	Feedwater heater
GC	Green certificate
GCC	Grand composite curve
GPU	Gas permeation unit
IGCC	Integrated gasification combined cycle
LCOC	Levelised cost of cement
LCOE	Levelised cost of electricity

LHV	Lower heating value
M&S	Marshall&Swift cost index
MEA	Monoethanolamine
MER	Minimum energy requirement
MOFS	Metal-organic frameworks
O&M	Operating & maintenance
OTM	Oxygen transport membrane
PC	Pulverised coal
PSA	Pressure swing adsorption
ROC	Renewable obligation certificates
SCR	Selective catalytic reduction
TCR	Total capital requirements
TGA	Thermal gravimetric analysis
TSA	Temperature swing adsorption
VOM	Variable operating and maintenance

Chapter 1 Introduction

1.1 Background

Global CO_2 emissions hit a new record of 34.5 Gt in 2012 (Olivier et al., 2013) and are predicted to increase further, reaching 40.2 Gt by 2030 (IEA, 2009a). The National Oceanic and Atmospheric Administration (NOAA)/Earth System Research Laboratory reported that the global CO_2 concentration reached 400 ppm in 2013, representing an increase of 24% from 1958 (Dlugokencky and Tans, 2014). According to the latest Intergovernmental Panel on Climate Change report (IPCC, 2014), it is more certain than ever that CO_2 emission from fossil fuel burning is the major contributor to changing the earth's climate. Unless alternative energy systems are developed and rapidly deployed, it is expected that fossil fuels will remain as the major contributor for energy production (IEA, 2012) while world energy demand is envisioned to increase by 40% from 2007 to 2030 (IEA, 2009b).

The increasing demand in electricity will trigger CO_2 emissions dramatically if applicable technologies to reduce such emissions are not developed. For the sake of restraining the severe effects of climate change and limiting the increase in the atmospheric temperature to 2°C (EG Science, 2008), substantial reductions of global CO_2 emissions by at least 50% are required by 2050 (IPCC, 2007). The UK aims for at least 80% reduction in its CO_2 emissions relative to 1990 levels by 2050 as stated in the Climate Change Act (UKP, 2008). Moreover, the Kyoto Protocol ratified in 1997 (Kyoto, 1997) and the Bali Declaration issued at the United Nations Climate Change Conference in 2007 (UNFCC, 2007) also emphasize the requirement for reductions in greenhouse gases, especially for CO_2 which accounts for 77% of the total anthropogenic emissions (IEA, 2009c) originating from the combustion of fossil fuels and from transport/households.

Being one of the primary environmental targets, the reduction of net CO_2 emissions to the atmosphere can be achieved by (IPCC, 2005): (i) improving the efficiency of energy conversion and/or utilization to reduce energy consumption, (ii) inducing the use of renewable and less carbon intensive fuels, (iii) enhancing the biological absorption capacity in forests and soils and (iv) capturing and storing CO_2.

1.2 Carbon Capture and Storage

Carbon capture and storage (CCS) is a promising and an emerging way of reducing CO_2 emissions from the main contributors: fossil-fuelled power stations and industrial processes such as cement, iron and steel production plants (DOE, 1999). The IEA (2010) estimates that up to 19% reductions in CO_2 emissions by 2050 can be achieved when CCS is applied to these main emission sources. In the framework of CCS, CO_2 emissions from a process are captured and the high concentration CO_2 product is separated. Thus, part of the CO_2 (depending on the efficiency of a carbon capture process) is not emitted to the atmosphere.

The captured CO_2 can be injected into geological formations (Torp and Gale, 2004) but is also used for enhanced oil recovery (Jaramillo et al., 2009). The technology needed to deploy CCS already exists in the natural gas, oil and chemical industries, where CO_2 and other gases such as H_2 and O_2 have been separated from different gas mixtures (Rodriguez et al., 2010). It has been proven by an economic analysis given in Rao and Rubin (2002) that CO_2 capture accounts for 75-85% of the overall cost associated with CCS. Therefore, it is important to develop efficient and cost-effective carbon capture technologies, which are usually split into three general routes: pre-combustion, oxy-combustion and post-combustion as presented in Figure 1-1. In addition, chemical looping combustion (CLC) is a new generation combustion technology with inherent CO_2 capture. These technologies are briefly detailed in the sections that follow.

1.2.1 Pre-combustion

The main objective of this technology is to convert a fuel to carbon-free H_2 prior to combustion. It involves three steps. First, a hydrocarbon containing fuel such as coal or biomass reacts with steam or air and/or oxygen to produce syngas or fuel gas. Second, CO generated in the first step catalytically reacts with steam to generate CO_2 and more H_2 through the water gas shift reaction. Finally the product gas containing mainly CO_2/H_2 proceeds to a carbon capture process where CO_2 is separated from H_2.
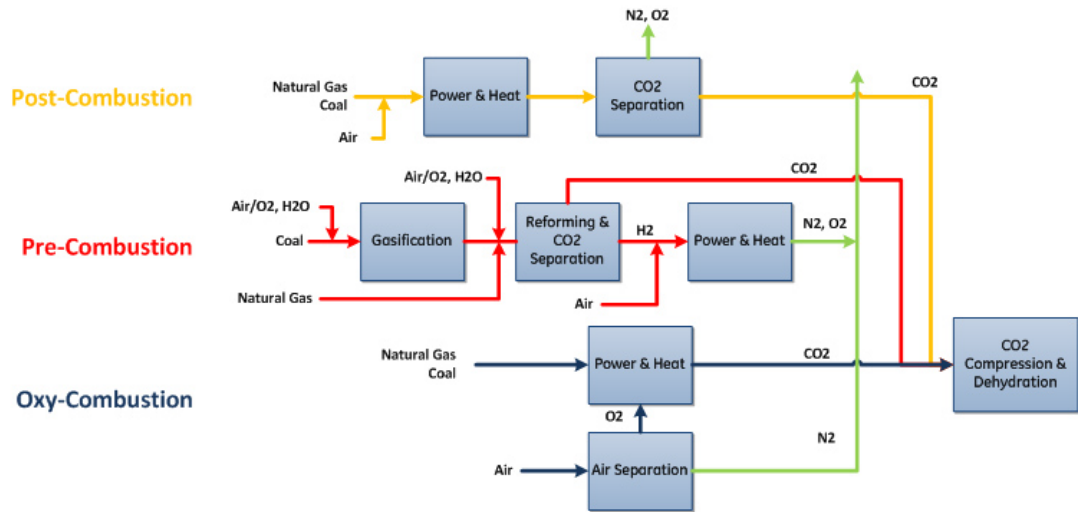
Figure 1-1 The primary routes for CO_2 capture (IPCC, 2005).

The potential carbon capture technologies for this purpose include adsorption, absorption and membrane separation. The resulting H_2-rich product can be fired in boilers, furnaces, heaters or as a fuel in vehicles (Harrison, 2008; Pennline et al., 2008). This technology is close to commercial reality in the form of the Integrated Gasification Combined Cycle (IGCC) (CCSGI, 2010) where the use of physical sorbents, such as Selexol (Kapetaki et al., 2013) is preferable because of the high temperature and pressure gas streams. Nevertheless, since only CO_2 emissions from fuel combustion can be avoided by pre-combustion technologies, only moderate carbon capture efficiencies can be achieved when this technology is applied into the cement industry, where CO_2 is generated by two different sources: fuel combustion and calcination of limestone. In general pre-combustion is only applicable for new plants rather than existing ones, which is the opposite of post-combustion for which retrofit integration is often possible.

1.2.2 Oxy-combustion

In this technology, almost pure oxygen ($\geq$95 mol%) is supplied to a combustor instead of air, so that it is in principle possible to increase the CO_2 concentration in the flue gases to more than 90 mol% after condensation of water vapour compared with 10-15 mol% for air-based combustion systems (Jared et al., 2010). To maintain the same boiler flame temperature as in air-combustion, part of the exit gas stream is

generally recycled to lower the concentration of the inlet oxygen. The type of fuel, the excess quantity of oxygen and the potential air-leakages are the main elements determining the final CO_2 purity. Consequently, a CO_2 purification stage could be needed to increase the purity further to meet storage specifications ($\geq$95 mol%). The currently available oxy-combustion technologies are based on cryogenic air separation unit (ASU) for oxygen production, which is an expensive and energy-intensive process. Promising progress on the development of membrane-based systems for oxygen production to reduce power consumption by 70% to 80% compared to a cryogenic system has been reported (Stadler et al., 2011). The Babcock & Wilcox Company has already demonstrated oxy-combustion of coal on a 30 MW_{th} boiler (McCauley et al., 2009).

1.2.3 Chemical Looping Combustion

CLC is a new generation energy technology allowing inherent production of pure CO_2 after condensation of steam (Lyon and Cole, 2000; Ishida and Jin, 2004). In contrast to the conventional combustion process, oxygen for combustion is provided by the reduction of metal oxides in a fuel reactor as presented in the following reaction. Some well-known oxygen carriers are the oxides of Ni, Cu, Fe and Mn supported by inert materials such as Al_2O_3, MgO and TiO_2 (Hossain and de Lasa, 2008). The exit gas stream from the fuel reactor contains CO_2 and H_2O.

$$(2n + m)Me_xO_y + C_nH_{2m} \rightarrow (2n + m)Me_xO_{y-1} + mH_2O + nCO_2 \qquad \text{(Rn. 1.1)}$$

H_2O can then be condensed to obtain pure CO_2. The reduced metal oxide from the fuel reactor is then re-oxidized with air in an air reactor.

$$Me_xO_{y-1} + {}^1\!/_2\, O_2 \rightarrow Me_xO_y \qquad \text{(Rn. 1.2)}$$

The total amount of heat generated by reduction and oxidation in the two reactors is equal to that of combustion of a fuel. The main advantages of the CLC process compared to the oxy-combustion technology are the absences of an ASU and the excess oxygen for combustion that reduces the CO_2 purity. A considerable number of studies have been conducted to improve the stability and performance of the metal

oxides in use (Leion et al., 2009; Adanez et al., 2012). Mature circulating fluidized bed (CFB) technology is well-suited for the application of the CLC process.

1.2.4 Post-combustion

Post-combustion refers to the separation of CO_2 from any flue gas streams containing CO_2 mixed with other gases. It can be adapted to any industrial process emitting large quantities of CO_2 as an end-of-pipe solution without needing excessive modifications to the actual process scheme. There is a vast potential for retrofitting post-combustion technologies to large anthropogenic CO_2 emission sources in the UK where nearly a third of electricity is generated from coal (Mellows-Facer, 2010). In addition, the IPCC (2005) indicated that approximately 8000 large stationary CO_2 sources around the world releasing 14 Gt CO_2 per year could potentially be retrofitted with CCS.

The most common types of post-combustion technologies are summarized in the next section. However, it should be first highlighted that the leading post-combustion carbon capture technology should provide high capture efficiencies with less expense, meaning lower energy and cost requirements. Therefore, one of the milestones in the development of these technologies is the evaluation of their techno-economic performance. For this purpose, the transfer of knowledge from experimental studies would enable the development of reactor models, which can then be employed in fully integrated process flowsheets.

1.3 Types of Carbon Capture Technology

The most common methods for the separation of CO_2 from gas streams include:

1) Absorption

2) Membrane Separation

3) Cryogenic Separation

4) Adsorption
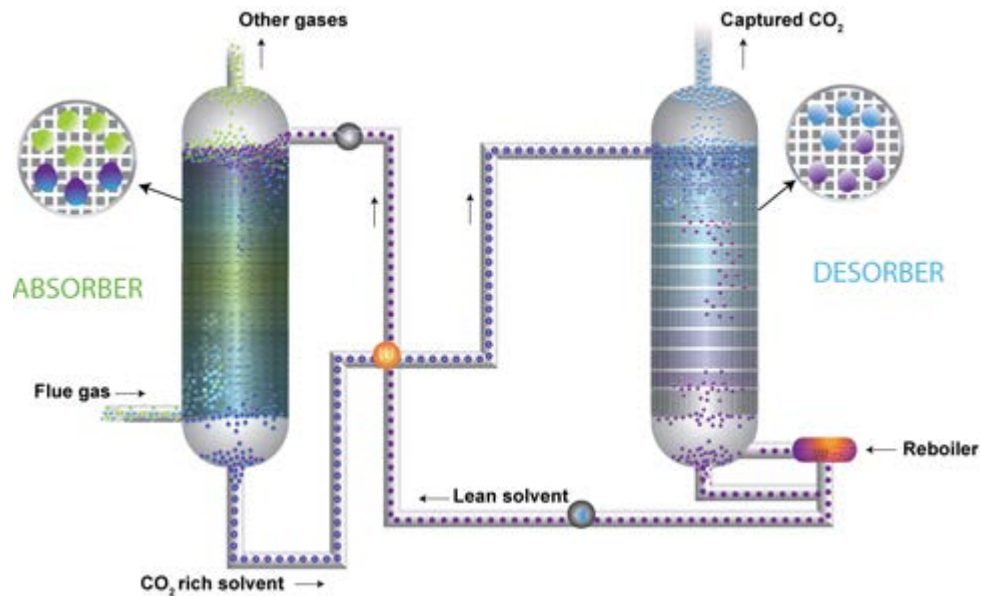
Figure 1-2 Process schematic of the amine process (CO2CRC, 2014).

1.3.1 Absorption

This technology relies on the principle that CO_2 in the feed gas is transferred into the liquid phase by selective absorption in a solvent. The solvent rich in CO_2 can then be regenerated by the application of heat while pure CO_2 is released. The absorption process typically works at low temperatures, between 40°C (absorption) and 120°C (desorption). The CO_2 separation can be achieved either physically or chemically. Physical absorption relies on the selective solubility of different gases while the solubility of the absorbent increases at high partial pressures. In chemical absorption (or reactive absorption), however, CO_2 reacts with the absorbent and better absorption performance can be achieved at low partial pressures.

Amine process, based on removal of acidic gases from gas streams by chemical absorption with aqueous amine solutions, is the most mature technology for post-combustion CO_2 capture applications from low pressure and low CO_2 concentration flue gases. It has been used for over 80 years (Bandyopadhyay, 2011) and several techno-economic studies are available for this system (Finkenrath, 2011; EPRI, 2009). The well-known and most widely used amine is monoethanolamine (MEA). The base schematic diagram for the amine process is shown in Figure 1-2 where the CO_2 in flue gases reacts chemically with the solvent in an absorber, and the solvent is

regenerated in a desorber (stripper). The clean flue gases from the absorber, a vertical and packed column, generally go through a water wash tower to remove any MEA slip. The CO_2 rich solvent from the absorber is fed into the top of the stripper column after being heated up in a heat exchanger. The chemically bound CO_2 is separated from the solvent in the stripper while heat is provided in a reboiler.

The level of NO_x and SO_x concentrations in the feed gas stream is crucial for the amine process. These components react with amine to produce amine salts which cannot be dissociated in the stripper. The spent solvent needs to be replaced with fresh solvent which increases the variable cost. Therefore, flue gas desulphurization (FGD) and selective catalytic reduction (SCR) units need to be included in the process to limit SO_x and NO_x emissions. Applying this technology within a power plant, the heat requirement in the stripper is usually provided by the steam dilution from steam cycle of the power plant. In Ahn et al. (2013), ten different advanced amine process configurations were systematically evaluated for the purpose of CO_2 capture from a power plant, and the heat duty in the stripper was reduced to as low as 2.22 MJ_{th}/kg CO_2 from 3.52 MJ_{th}/kg CO_2 for the conventional system by enhancing heat recovery and increasing solvent working capacity.

1.3.2 Membrane Separation

Gas separation using membranes relies on selective and specific permeation of different gases. The driving force for the separation can be expressed as the difference in partial pressure between the two sides (retentate and permeate), and feed compression and/or vacuum at the permeate side are often adopted. The schematic representation of the membrane separation principle is presented in Figure 1-3. The permeability represents the ability of the molecules to permeate through the membrane film and can be written as the product of diffusivity and solubility according to the solution diffusion theory (Baker, 2002; Baker, 2004). For effective removal of CO_2 from a gas stream, membrane materials should possess a number of properties including high CO_2 permeability and selectivity as well as thermal and chemical stability.
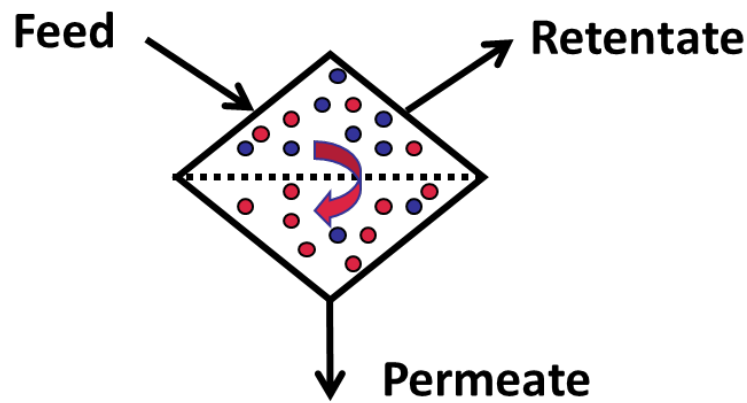
Figure 1-3 Schematic representation of the separation through a membrane (Bocciardo, 2014).

Currently this technology is only applied to the removal of CO_2 from natural gas but numerous membranes have been developed and commercialised for gas separations since the 1970s (Robeson, 2008). Dense polymeric membranes are the main candidates for post-combustion carbon capture (Merkel et al., 2010). Unfortunately it was reported that the selectivity of membranes can possibly be affected by impurities, i.e. SO_x, NO_x and H_2O in flue gases (Scholes et al., 2011). Furthermore multiple stages and considerable membrane areas would be required to achieve high capture efficiencies and CO_2 purities (e.g. ~90% capture and over 95 mol% purity). This technology is still not available commercially for CO_2 capture applications in spite of promising results from pilot-scale investigations (NETL, 2012).

1.3.3 Cryogenic Separation

For the separation of CO_2 from other gases, the cryogenic separation process uses low temperatures and high pressures to reach a condition where CO_2 is in liquid phase. The operating conditions in this system are maintained by the use of compressors and heat exchangers in series. This technology is commercially used for the purification of gas streams at high CO_2 concentrations (>90 mol%). However, the major disadvantage of cryogenic separation of CO_2 is the excessive energy requirement for the refrigeration step, particularly at very low CO_2 concentrations. It has an advantage in that the separated CO_2 by this system is already in liquid phase which is beneficial for certain transport options.

1.3.4 Adsorption

Adsorption is a cyclic process where CO_2 in a gas stream is initially adsorbed on the surface of a solid either physically or chemically and thereby removed from the gas stream. In physical adsorption, the bonding between the CO_2 and the surface is due to weak van der Waals forces, and low temperatures are favourable whereas strong chemical bonding in chemical adsorption is favourable at higher temperatures (>200°C). The main types of adsorption processes involve pressure swing adsorption (PSA) and temperature swing adsorption (TSA). In PSA, the regeneration is provided by the difference in pressure whereas it is the temperature which allows regeneration of the sorbent in TSA. The currently available most effective sorbents are activated carbons, zeolites and aluminas. Researchers have been working on a large scale application of this technology in the industrial process, which requires highly selective and efficient adsorbents (Harlich and Tezel, 2004; Boot-Handford et al., 2014; Hu et al., 2014). The need for sorbents with elevated performance characteristics leads to the development of novel sorbents.

1.4 Overview of Carbon Capture Technologies

Figure 1-4 illustrates the potential of CO_2 capture technologies for commercialization and cost reduction benefit. Currently amine-based post combustion technology is closest to the market. However, the integration of an amine process into an existing power plant is energetically intensive and economically prohibitive. The reason for the latter is also related to the necessity to prevent solvent degradation as a result of reaction with SO_x and NO_x in flue gases in addition to the high cost of solvents. Reports suggest that the SO_2 concentration in the flue gas needs to be maintained below 10 ppm before an amine process, revealing the requirement of over 98% SO_2 removal even for the lowest sulphur coals (Rao and Rubin, 2002). Another potential technology that is close to the market is the oxy-combustion process. Nevertheless, this process requires an energy intensive ASU to produce significant amounts of oxygen for combustion. In addition to that, very stringent safety management along with the control of air-leakages is needed.
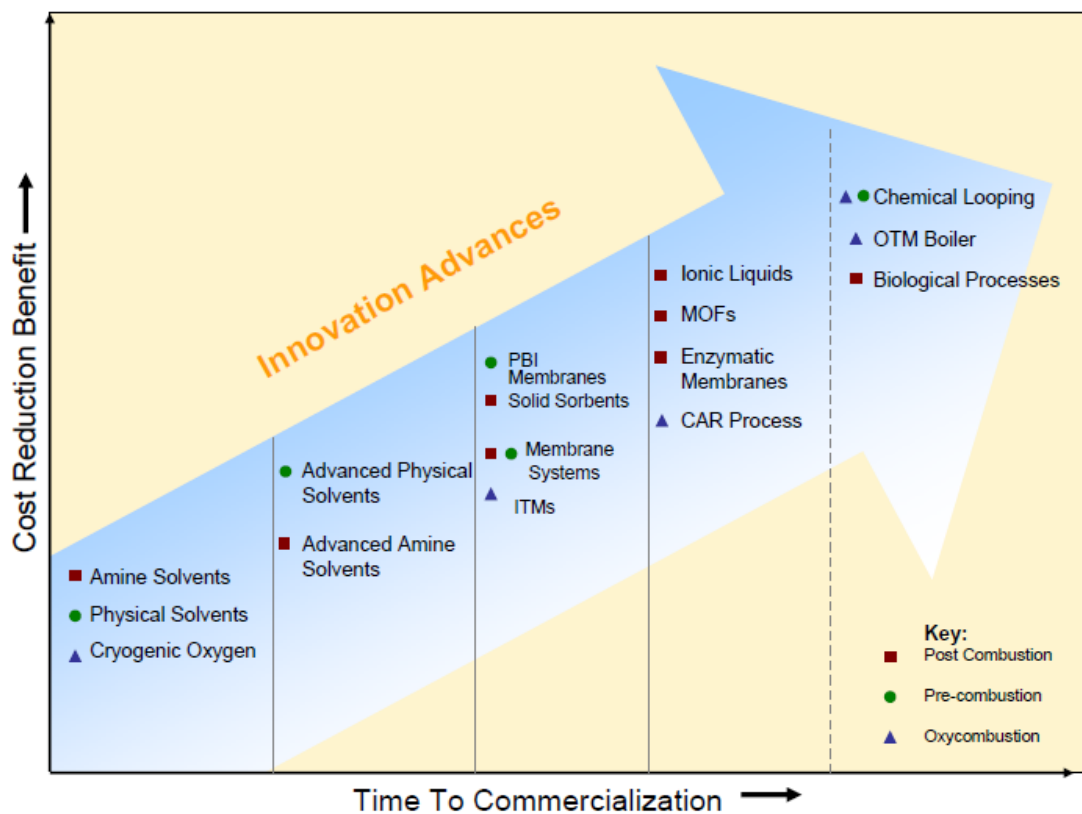
Figure 1-4 Cost reduction benefit vs. time to commercialization for innovative CO_2 capture technologies (Figueroa et al., 2008).

For some of the next generation technologies, for example, ionic liquids, metal-organic frameworks (MOFs) and oxygen transport membrane (OTM) boilers, a considerable number of investigations at pilot scale have been continuing but significant R&D efforts are still needed before these technologies reach large-scale applications. Because of such deficiencies associated with most conventional CO_2 capture technologies, there is an urgent need to develop more advanced and less expensive methods by which the above issues can be minimized.

One of such promising technologies for carbon capture from industrial sources is an absorption process based on the reversible reaction of CO_2 on specific metal oxides at high temperatures. The CaO-based sorbents have attracted the most attention owing to their high absorption capacity, wide availability and low cost. The concept of utilizing CaO for CO_2 capture was first introduced by DuMotay and Marechal for enhancing coal gasification in 1869 (Squires, 1967) and named the calcium looping (Ca-looping) process. The Ca-looping process is applicable to pre-

combustion (Albrecht, 2008a; Weimer et al., 2008; Blamey et al. 2010) and post-combustion (Shimizu et al., 1999; Abanades and Alvarez, 2003; Abanades et al., 2005; Berstad et al., 2012) CO_2 capture applications. It has attracted great interest owing to the use of a cheap sorbent, a relatively small energy penalty (6-8%) compared to 8-10% for post combustion amine scrubbing (Florin and Fennell, 2010), the potential use of large scale CFB systems as a mature technology, the reduction of ASU power consumption (approximately 1/3 of that for the oxy-combustion) (Abanades et al., 2005), and the possible use of the purge stream in cement manufacturing plants which has a potential to improve the economics of the system and to de-carbonize both industries.

1.5 Calcium Looping Process

1.5.1 Basics of the Cycle

The post-combustion Ca-looping process that was first proposed by Shimizu et al. (1999) uses state-of-the-art CFB systems due to the huge flue gas flow coming into contact with a solid stream as presented in Figure 1-5. In this process, CO_2 containing flue gases are fed to a reactor, called carbonator, and CO_2 is captured at 600-750°C according to the following reaction:

$$CaO + CO_2 \leftrightarrow CaCO_3 \ (\Delta H_{923\ K} = -171 \ kJ/mol) \tag{Rn. 1.3}$$
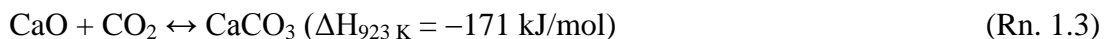
The solids from the carbonator are separated in a cyclone and sent to a calciner where the product of carbonation, $CaCO_3$ is regenerated and high purity CO_2 at 870-950°C is obtained. The heat requirement in the calciner, which is a relevant fraction (35-50%) of the total energy entering the entire system (i.e. the power plant and Ca-looping process together) (Abanades et al., 2007; Rodriguez et al., 2008a), is often provided by oxy-combustion of a fuel (Romeo et al., 2008; Romeo et al., 2009). Otherwise, if air is used for combustion, the N_2 from the air dilutes the gas stream from the calciner. The use of transfer mediums, such as hot CaO particles from a high temperature combustor has also been suggested as a means of providing heat for the calciner (Abanades et al., 2005).
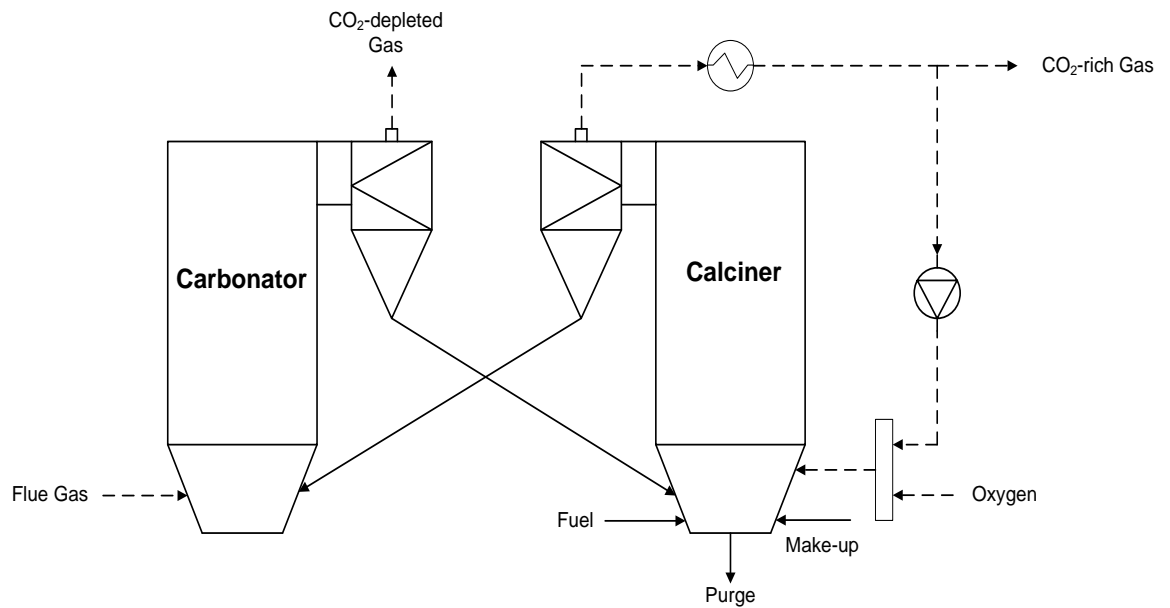
Figure 1-5 The simplified schematic diagram of the Ca-looping process.

The thermal energy requirement in the calciner depends mainly on the flow rate of make-up sorbent and solid circulation rates between the reactors, which are directly linked to overall capture efficiency. Despite the fact that additional heat is required in the calciner, one of the advantages of this system is the possibility of recovering surplus energy from hot gas and solid streams leaving the reactors as well as the exothermic carbonation reaction. The recovered heat can then be used to drive a steam cycle to generate electricity, reducing the energy penalty of the system.

A plot of temperature vs. equilibrium CO_2 vapour pressure (Garcia-Labiano et al., 2002) is given in Figure 1-6. This shows that above the equilibrium line carbonation is favourable while below the line $CaCO_3$ decomposes into CaO and CO_2. The graph also provides a convenient means for the estimation of the minimum calcination temperature which depends on CO_2 partial pressure inside the calciner. In order to produce a suitable gas from the calciner for storage, the calciner should operate at high CO_2 partial pressures. According to CaO-$CaCO_3$ equilibrium, high CO_2 partial pressure in the calciner imposes a temperature of more than 900°C if the calciner operates at atmospheric pressure. For a calciner operating at atmospheric pressure, calcination starts at around 600°C under pure nitrogen but the starting temperature delays to 880°C under pure CO_2 (Ozcan, 2010).
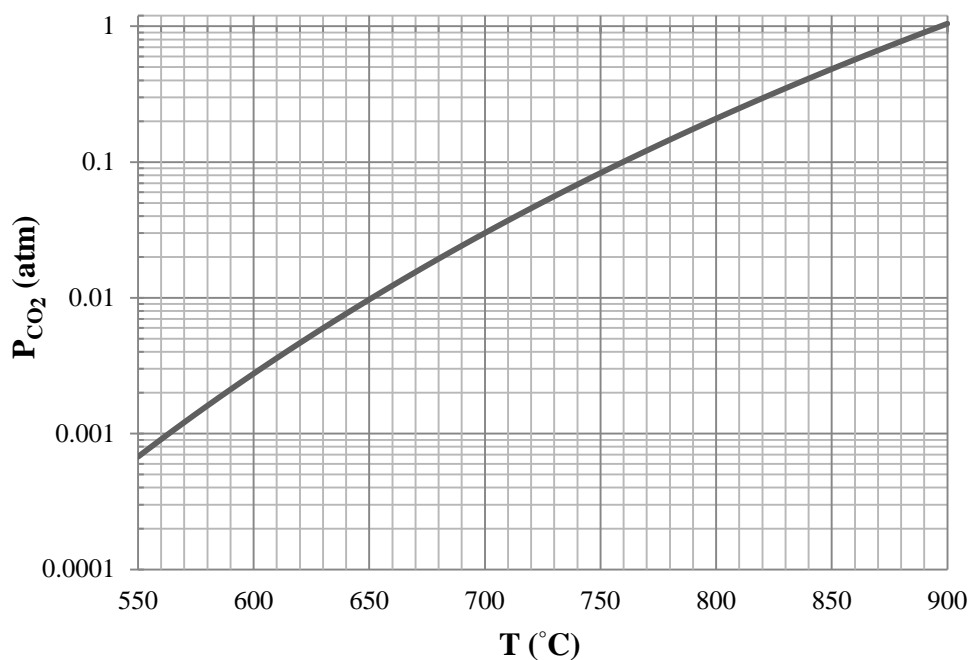
Figure 1-6 The equilibrium vapor pressure of CO_2 over CaO (Garcia-Labiano et al., 2002).

Even though there are various experimental studies where the CO_2 uptake performance of a CaO-based sorbent was evaluated under mild calcination conditions (Salvador et al., 2003; Ryu et al., 2006), the need for $CaCO_3$ calcination in a CO_2 rich atmosphere (>90%) for production of a high purity CO_2 stream significantly affects the carbonation behaviour of the sorbent. Thus, the calciner temperature is often determined by a compromise between the production of high CO_2 partial pressure and the expense of sorbent degradation. At high temperatures, calcination kinetics is very fast which allows complete calcination to occur rapidly, but also high calcination temperatures trigger loss in the sorbent capacity because of sintering. Sintering is a term referring to changes in the sorbent structure, pore shape, pore shrinkage and grain growth. Similarly, the carbonator reaction is governed by the equilibrium between temperature and CO_2 partial pressure. The effect of sintering is more prominent at high temperatures and in severe calcination conditions (high steam and CO_2 partial pressures) (Abanades and Alvarez, 2003; Chrissafis et al., 2005). Thus, sintering of CaO is more effective in the calciner than the carbonator because of the operating conditions.

A method of reducing CO_2 partial pressure in the calciner is the dilution of the calcination environment with steam. It allows the reduction of the required calcination temperature for complete calcination and prevents calcination at high temperatures (Garcia-Labiano et al., 2002). The steam in the CO_2-rich gases can then be condensed and separated from the CO_2. Khinast et al. (1996) indicated that the calcination rate increases exponentially with decreasing CO_2 partial pressure at a constant temperature. Wang et al. (2008) illustrated that the calcination conversion of 72% at 100% CO_2 atmosphere increases to 98% with 60% steam dilution at a bed temperature of 920°C and average residence time of 40 mins. It should be noted that the selection of a steam source to dilute calcination atmosphere can be challenging. If it is need to be taken from the steam cycle of a power plant, the steam dilution results in a decrease in the output of the power plant and is thus a potential energy penalty for the capture process. Another solution to minimize the calcination temperature is the application of a vacuum to reduce pressure in the calciner (Abanades et al., 2005). It has been shown that the calcination of a sorbent under vacuum conditions at a lower temperature improves the kinetics of the sorbent by reducing the effect of sintering (Skadjian et al., 2007). However, the application of a vacuum is expensive especially at larger scales.

As presented in Figure 1-7 for a cycle of carbonation-calcination reaction (Ozcan, 2010), the carbonation reaction contains two steps. After an initial rapid, kinetically controlled first stage, the second stage is very slow and diffusion controlled (Bhatia and Perlmutter, 1983). The calcination stage generally proceeds to completion. The materials used in the Ca-looping process can be any widely available and low cost natural sorbents such as limestone and dolomite (Silaban et al., 1996; Grasa et al., 2008b). A CaO-based sorbent can also be manufactured from synthetic precursors such as $Ca(OH)_2$, $Ca(C_2H_3O_2)_2$ etc. Grasa et al. (2007) demonstrated that the sorbents derived from synthetic CaO precursors present similar behaviour to the limestone under realistic calcination conditions (high temperature and CO_2 partial pressure) even though these sorbents show much better stability and performance under mild calcination conditions.
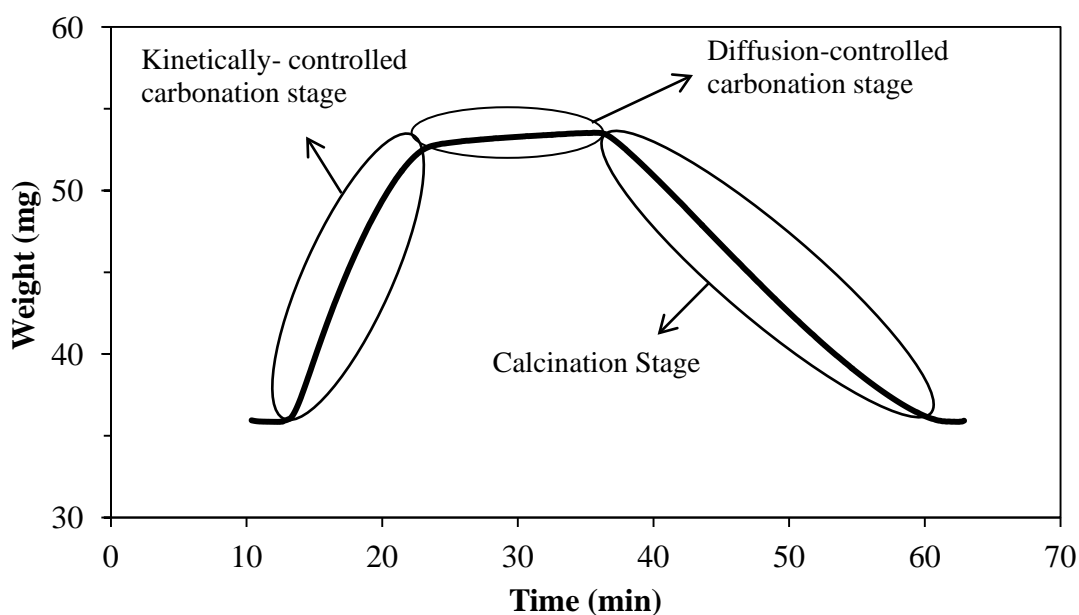
Figure 1-7 A cycle of carbonation and calcination observed by a TGA (Ozcan, 2010). The test of absorption capacity was conducted isothermally at 750°C under atmospheric pressure.

One of the greatest challenges in the Ca-looping process is the deterioration of the CO_2 capture capacity when these materials are used over a number of cycles of carbonation and calcination reactions (Curran et al., 1967; Silaban and Harrison, 1995; Grasa and Abanades, 2006). For continuous processes, it would be preferable to use a sorbent for countless numbers of cycles. However, the evolution of the capture capacity of natural sorbents reveals that the capture capacity significantly decreases during the first 20 cycles but then stabilizes at around 8% even after 500 cycles (Grasa and Abanades, 2006). For the carbonation reaction, a sufficiently large pore volume needs to be ensured but the available pore volume in the sorbent derived from limestone decreases through the cycling progress. Figure 1-8 shows the CO_2 uptake capacities of CaO samples prepared from different precursors: pure CaO, Microna 10 limestone, dolomite and calcium acetate (Ozcan et al., 2011). The samples demonstrate a decrease in their absorption capacities through the cycles while that of dolomite seems more stable compared to others owing to MgO acting as a stabilizer. The major reason for lowering residual activity was sintering of experimentally tested sorbents at high temperatures while the potential challenges could be extended to include sulphation and attrition in large scale applications of the Ca-looping process.

27
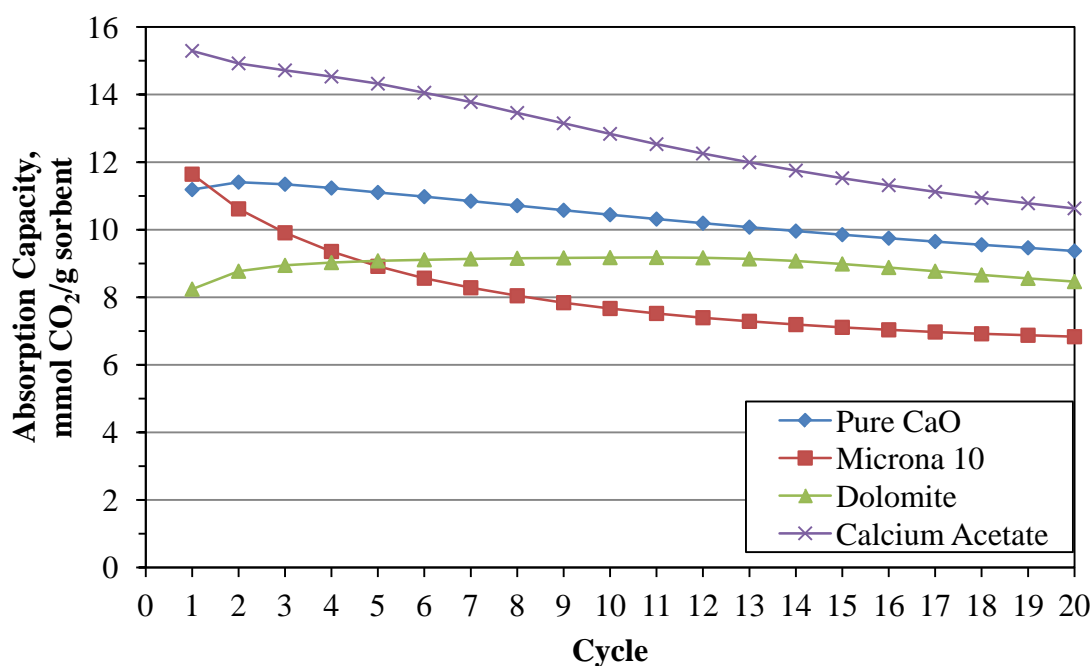
Figure 1-8 CO_2 uptake capacities of CaO samples manufactured from the given precursors at 1000°C in N_2 for 1 hr (Ozcan et al., 2011).

CaO-based sorbents have a very strong affinity to absorb SO_2 existing in the flue gases and generated by coal combustion in the calciner in the form of $CaSO_4$, as shown in (Rn. 1.4), because of very high Ca/S ratio in the reactors.

$$CaO + SO_2 + \frac{1}{2} O_2 \rightarrow CaSO_4 \quad (\Delta H = -506 \text{ kJ/mol}) \tag{Rn. 1.4}$$
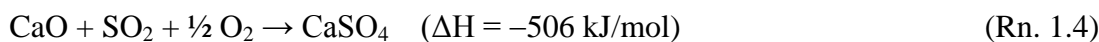
$CaSO_4$ is stable under the conditions of carbonation and calcination, thus, in order to regenerate $CaSO_4$ back to CaO, either high temperatures (>1250°C) or a reducing atmosphere is needed. The reaction between CaO and SO_2 can be considered as loss in reactive sites for carbonation in the Ca-looping process. Sun et al. (2007) indicated that sulphate formation results in pore blockage as it has a much larger volume and prevents CO_2 flow to the centre of a particle. On the other hand, CaO derived from calcination of natural limestone has been commercialized in CFB power plants for sulphur control (Srivastava et al., 2001). In such systems, there is no need for an external FGD unit, which is necessary for pulverised-coal (PC) combustion power plants, unless the emission regulations are extremely strict. The absence of FGD can be, therefore, counted as profit for its capital cost. Furthermore, the attrition of the

limestone can be problematic in large scale CFB systems where the CaO particles can break apart by collision with other particles, and resulting fine particles escape the system with the gas stream (Coppola et al., 2012). In a recent study, pelletisation of artificial sorbents using calcium aluminate cements as binders has presented both high reactivity and resistance against the attrition (Manovic and Anthony, 2009a).

Substantial research efforts are currently being undertaken to reduce the decay in reactivity of CaO or to improve the reactivity of the used sorbent (Lu et al., 2006; Manovic and Anthony, 2009b). These methods include thermal pre-treatment (Manovic and Anthony, 2008; Arias et al., 2011), reactivation of spent sorbent by hydration (Fennell et al., 2007; Sun et al., 2008; Manovic and Anthony, 2011a; Wang et al., 2012) and doping of natural sorbents with inert materials (Manovic and Anthony. 2009c; Sun et al., 2012).

Lysikov et al. (2007) investigated the effects of thermal activation on sorbent performance. It was observed that prolonged exposure of the sorbent derived from limestone to severe calcination/carbonation conditions is beneficial for the cyclic CaO conversion. The severely sintered sorbent initially possesses a low CO_2 uptake capacity in the first cycles because of reduced pore volume but the conversion actually increases later, which is referred to self-reactivation. Recently, it was indicated that the improvement in the CO_2 uptake capacity of the thermally pre-treated sorbents is not significant after 100 cycles (Ozcan et al., 2011). It was proven that the reactivity of hydrated limestone is even better than fresh limestone (Manovic and Anthony, 2007); however, the side effect of hydration was reported to be the deterioration of the mechanical strength of reactivated sorbents resulting in high rates of attrition (Manovic et al., 2008).

Another approach for improving the cyclic stability of the sorbent involves the incorporation of the limestone with a variety of dopants such as Al (Pacciani et al., 2008), Mg (Albrecht et al., 2008b) or Si (Huang et al., 2010) because of their high Tammann temperatures in the sorbent. The Tammann temperature is approximately half of the melting point and is often considered as the point where sintering becomes rapid. The incorporated inert material is expected to suppress the sintering.

The inert supports often do not react with CaO, forming mixed oxides but the reverse is also possible (Manovic and Anthony, 2010).

Unless highly stable and efficient CaO-based sorbents are derived, some spent sorbents need to be removed as a purge from the system while fresh sorbent is introduced. From the viewpoint of process economics, there is a trade-off between the sorbent cost and performance. In general, the production of synthetic sorbents is more costly compared to natural sorbents. Thus, the expectation would be manufacturing synthetic sorbents that possess high and stable CO_2 uptake capacities to minimize the requirement of the sorbent replacement. However, if this is not achievable, the use of natural sorbents with affordable purge flow rates would be preferable.

1.5.2 Use of Spent Sorbent for Cement Production

The purge stream from the coal-fired calciner fed with limestone is mainly composed of CaO with small amounts of $CaSO_4$ and ash. According to Hurst et al. (2012), a coal-fired power plant integrated with a Ca-looping process could be a carbon negative if the purge sorbent is used in the cement industry or disposed in the ocean forming bicarbonate. If the spent sorbent from the Ca-looping process can be used as a raw material for cement manufacture, the CO_2 released by the calcination of limestone in the cement process can be eliminated. Moreover, the heat requirement for calcination and the costs of limestone and fuel in the cement plant can be reduced.

Even though it was conceivable in earlier studies that the purge CaO could be sent to a kiln to make a clinker, there has been an issue that the deactivated CaO may deteriorate the clinker quality and the factors which can potentially limit or affect the re-use of purge CaO have been discussed (Dean et al., 2011a). The study raised issues that sulphur conveyed by a purge stream can lead to expansion and cracking of the cement paste upon hydration and also affects the formation of cement phases. Moreover, the trace elements released from fuel combustion in the calciner as well as attrition and agglomeration have been identified as other potential issues in using purge materials. In the latter work of this group, it has been shown experimentally

that cement can be successfully produced from the purge by utilizing CaO which has experienced many cycles of calcination and carbonation (Dean et al., 2011b). In a more recent work (Telesca et al., 2014), the spent sorbent from a pilot scale Ca-looping plant, purged after 60 cycles of carbonation and calcination, was employed in place of limestone in a lab-scale cement manufacturing process. It was concluded that the burnability of this mixture is better than one including fresh limestone while the mineralogical composition and hydration behaviour of both samples were found to be identical.

1.5.3 Pilot Calcium Looping Projects

In addition to outstanding efforts in lab-scale investigations (Alonso et al., 2010; Rodriguez et al., 2011a), several different projects around the world have been initiated to scale up the Ca-looping technology, including a 1.7 MW_{th} pilot plant which has been in operation to test the concept in La Pereda, Spain funded under "CaOling" project since January 2012 (Arias et al., 2013). The pilot plant treats 1/150 of the flue gases emitted from La Pereda CFB power plant and includes two interconnected CFB reactors: a carbonator and an oxy-fired calciner, which are 15 m in height. It has been operated more than 380 hours in steady state mode and demonstrated to achieve CO_2 capture efficiencies over 90% with the supply of sufficient CaO. Furthermore, promising results have also been reported from a 1 MW_{th} pilot plant in Darmstadt (Plötz et al., 2012). In this plant, the capture efficiencies over 80% have been achieved in the carbonator (overall >90%) for several hours of operation, and the limitations of reactions kinetics and chemical equilibrium on CO_2 capture efficiency have been demonstrated by changing process parameters. The heat requirement in the calciner is provided by combustion of either propane or pulverised hard coal. The height of the CFB carbonator was set to 8.7 m while that for the calciner is 11.3 m, where a maximum flow of 150 kg/h can be introduced.

Initial experience on 10 kW_{th} facility led IFK Stuttgart to scale up their Ca-looping plant to 200 kW_{th} (Dieter et al., 2004). The main purpose of the large scale Ca-looping plot is to investigate different fluidization regimes and concepts for solid

circulations. Three interconnected fluidized bed reactors were built, which provides flexibility to operate the carbonator in two modes: either a fast fluidized bed or a turbulent fluidized bed. While the calciner is 10 m in height, the carbonator is either 10 m (the fast fluidized) or 6 m (the turbulent fluidized). Even though it was concluded that the turbulent reactor offers greater flexibility for the variations in flue gas load compared to the fast fluidized bed, the latter was reported to allow more flue gas load and has been preferred at equal active space times because of better performance. Moreover, a great attention has been given to sorbent attrition which was defined as one major hurdle during the operation. A minimum 3 wt%/h solid inventory lost was observed regarding to the attrition.

Canmet Energy, Canada operates 75 kW_{th} dual fluidized bed system (Lu et al., 2008). The carbonator was constructed as a BFB, and the calciner is an oxy-fired CFB. The calciner can be operated under three different modes: oxy-combustion of biomass or coal and electrical heating. With continuous operations more than 50 h, promising CO_2 capture efficiencies have been achieved. Attrition of sorbent was also defined as the major problem in this plant while the attrition rate was found to be ~50% for Havelock limestone particles, in the range 0.4-0.8 mm, which eventually became less than 0.1 mm.

A 1.9 MW_{th} Ca-looping pilot designed by ITRI, Taiwan is currently being erected (Chang et al., 2013). The design of this pilot was based on experimental results obtained by a 3 kW_{th} bench-scale system. The carbonator was built as a BFB with a diameter of 3.3 m and height of 4.2 m, and operates at 650°C with gas residence time of 8 – 10 s. The 36 water-cooled double steel jackets were installed to remove excess heat from the carbonator because of the exothermic carbonation reaction and the high temperature solid stream from the calciner. The calciner was designed as a rotary kiln, as existing in the cement manufacturing process, and 5 m in length. It was facilitated with an oxy-combustion system including flue gas recirculation. Even though the system is able to run smoothly at this stage, the evaluation of process parameters is still under investigation.

1.5.4 Economics of the Calcium Looping Process

Abanades et al. (2007) reported the cost structure for a post-combustion Ca-looping process comprising of three key components: a power plant, an oxy-fired CFB power plant as a calciner and a fluidized bed carbonator. The capital cost of the calciner was estimated based on that for a CFB oxy-fired power plant as both systems works under the same principle and contain similar units: a CFB oxy-fired combustor, a steam cycle, an ASU and a CO_2 compression unit. Detailed capital cost estimation for the carbonator was not included and that of this unit was roughly estimated to be 10% of the total capital requirement of the oxy-fired system. According to the reported values, the cost of CO_2 avoided for the Ca-looping process was around 15 \$/ton CO_2 in comparison to 24 \$/ton CO_2 for a CFB oxy-fired power plant. It is needed to be highlighted that the given cost estimates reflect the capital and variable cost data available around the publication year of the reference and should be adjusted using the cost indices to assess current values. MacKenzie et al. (2007) estimated a cost for CO_2 avoided of 20 \$/ton CO_2 for the Ca-looping process while the value of the conventional amine process was around 55 \$/ton CO_2 (Tuinier et al., 2011). It was emphasized that the sorbent cost is a crucial parameter in cost calculations. Thus, when two processes using different sorbents are compared, it is really important to do this comparison in terms of both energy consumption and cost of CO_2 avoided as it does not mean that the one with less energy consumption will provide lower cost of CO_2 avoided. Romeo et al. (2009) concluded also that the sorbent costs should be maintained at reasonably low levels to achieve a low cost of CO_2 avoided. A modified sorbent would be preferable only if it provides significantly better CO_2 uptake capacity compared to natural limestone, which may allow a reduction in purge flow rates.

1.6 Objectives of the Dissertation

Cement is a key construction material. Owing to the increasing demand in rapidly developing countries such as India, China and Brazil, the demand of cement has increased by around 6% in 2012 when compared to 2011, reaching 3.78 billion tons (CW Group, 2012). The cement industry is the second largest stationary CO_2

emission source in the world and accounts for over 2 billion tonnes of CO_2 emitted per year (IEA, 2009b; CW Group, 2012). Thus, it can be specified as a potential candidate for the implementation of CCS technology. On the other hand, there is a growing trend of using sustainably-grown biomass as a renewable energy source in combustion systems as this is associated with zero net CO_2 emissions (Faaij et al., 1998). The application of CCS to biomass fired systems was reported to produce negative emissions of CO_2 (Ishitani and Johansson, 1996). Therefore, the principal objective of this dissertation is to evaluate the techno-economic performance of the Ca-looping process to mitigate CO_2 emissions from cement plants and biomass-fired power plants. This study also contributes to the assessment of various alternative carbon capture processes including oxy-combustion, amine, indirect calcination and membrane. In addition, an advanced configuration of the Ca-looping process where the energy intensive ASU is replaced with a CLC cycle has also been considered as an option to reduce the energy penalty associated with this system. The primary aims of research can be given as:

(i) **Development of full process simulations:** To investigate the process performance of the carbon capture technologies, the first task was to develop and simulate full process flowsheets considering all major units having an influence on mass and energy balances, and chemical reactions in UniSim Design Suite from Honeywell. The detailed analysis of the base plants was used for the selection of optimal process configurations and the determination of a variation in energy consumption when a CO_2 capture facility is present. Technical challenges involved in process arrangements have been addressed, and innovative solutions have been provided. To be able to predict accurately CO_2 recovery in the carbonator of the Ca-looping process, a rigorous carbonator model that is not available in the commercial process simulator has been incorporated into UniSim as a user defined operation.

(ii) **Application of an economic analysis:** The comparison of different carbon capture systems should take economic criteria into account. A detailed economic study based on the assessments of total capital requirement, operating and maintenance, and variable costs has been carried out to reveal economics of the proposed carbon capture processes. Since the available

methods to estimate the cost of carbon capture has been built on the similarity of carbon capture systems with commercially available technologies, i.e. the calciner in the Ca-looping process vs. an oxy-fired power plant, and limited variable cost data, a sensitivity analysis had to be included to illustrate variation in current estimates for different scenarios.

1.7 Organization of the Dissertation

This dissertation has been organized into six chapters. A brief overview of the content of each chapter is as follows:

Chapter 2 describes the technical details of an exemplary dry-feed cement plant and presents a conceptual design of integrating the Ca-looping process in the cement plant. It also considers the purge rate of part of the circulating CaO, given the tendency of the material to sinter and reduce its capture capacity. The purge stream from the calciner substitutes limestone in raw meal for clinker production. The effect of molar flowrate ratio of lime make-up to feed CO_2 (F_0/F_{CO2}) between two operational limits has been investigated.

In Chapter 3, alternative carbon capture systems have been evaluated for the purpose of CO_2 capture from cement plants. A variety of process configurations to incorporate a CLC cycle into the Ca-looping process have been initially investigated. This system allows a reduction in energy penalty regarding to use of oxygen from an energy intensive ASU. The process integration of an indirect calcination process analysed in this chapter aims to minimize the thermal energy consumption by using excess heat from hot gas streams for raw meal preheating. Since the achievable CO_2 avoidance rate by the standalone indirect calcination process is only at moderate levels, an amine process has been added to increase the avoidance rate further. Besides this, a standalone application of an amine process where a combined heat and power (CHP) plant provides heat for solvent regeneration has been analysed. Lastly, two feed gas locations and different multi-stage membrane configurations have been assessed for the process integration of a membrane separation process.

In Chapter 4, the economic performances of the carbon capture technologies reported in Chapters 2 and 3 have been evaluated. A detailed cost methodology and resulting levelised cost of cement (LCOC) and cost of CO_2 avoided estimations have been presented for each case. In addition, sensitivities on cost parameters have been examined. It is the final chapter regarding to CO_2 capture from cement industry.

In Chapter 5, the main purpose is to present in-situ CO_2 capture by using the Ca-looping process from a large-scale (>100 MW_e) dedicated biomass-fired power plant. The techno-economic performance of the proposed system has been compared against that of the alternative biomass-air-fired and biomass-oxy-fired power plants. A heat exchanger network design has been proposed by conducting a pinch analysis to recover the maximum amount of excess heat from the high temperature gas and solid streams available in the Ca-looping process.

Finally, Chapter 6 provides a number of conclusions and recommendations for future work.

Chapter 2 Process Integration of a Ca-looping Carbon Capture Process in a Cement Plant

2.1 CO$_2$ Emissions from Cement Production

The cement industry accounts for more than 5% of global CO$_2$ emission from stationary sources amounting to 1.88 Gt CO$_2$/year in 2006 (IEA, 2009). It is foreseen that the emissions for the cement sector will continue to grow in a parallel with increasing demand for cement (CW Group, 2012) and reach 4.3 Gt CO$_2$/year by 2050 (WWF, 2008). This is regarded as one of the major industrial carbon emission sources for which it is worth implementing carbon capture and storage solutions. The CO$_2$ emissions from cement plants originate from different sources; over 50% of the emissions result from the calcination of limestone in the raw material while the rest is generated by fuel combustion (40%) and indirect emissions due to use of electricity (IEA, 2011). The fuel consumption is significant due to the highly endothermic calcination reaction and high temperature operation in a kiln (around 1450°C). It has been reported that, in the modern technology, the average energy consumption in a cement plant has been reduced to around 2.9 GJ$_{th}$/ton clinker (WBCSD, 2009) and CO$_2$ emission by calcination can be increased to almost 70% by a more efficient use of the fuel and correspondingly lowering CO$_2$ emissions from fuel combustion (Rodriguez et al., 2009).

CO$_2$ emissions in the cement production process can be partially reduced by modifications: improving the process for more efficient use of fuel, replacing fossil fuels with alternative renewables including waste residues, and mixing clinkers with mineral additives (Hasanbeigi et al., 2012). Even though these measures can reduce CO$_2$ emissions resulting from fuel combustion significantly, they cannot tackle the CO$_2$ emission originating from the calcination reaction. Therefore, it is essential to deploy a carbon capture technology on cement processes in order to reduce CO$_2$ emissions by more than 90%.

2.2 CO$_2$ Capture Technologies for the Cement Industry

Several carbon capture technologies including amine scrubbing (IEA, 2008; Hassan, 2005), ammonia scrubbing (Dong et al., 2012), oxy-combustion (IEA, 2008; ECRA, 2009), anti-sublimation (Pan et al., 2013), Ca-looping (Bosoaga et al., 2009; Vera, 2009; Rodriguez et al., 2012; Stallman, 2013) and indirect calcination (Rodriguez et al., 2011b) have received great interest to capture CO$_2$ from cement industry. Cement plants are characterized by a single source of emission (the cooled flue gas from the preheater), with CO$_2$ concentrations of 15-30 mol%, typically released to the environment from one or two emission points, after providing heat for raw material drying. Since a certain percent of CO$_2$ emissions from cement plants originate from the calcination of carbonated materials, fuel decarbonisation by pre-combustion capture processes is not effective in reducing the emissions from cement plants. Thus on-going research has been focused on post-combustion and oxy-combustion processes as the most conventional capture technologies since they are considered mature technology or at least ready to be implemented shortly.

In the case of oxy-combustion, oxygen is fed to the burners instead of air. There are two locations in a cement plant where combustion takes places; the pre-calciner, where fossil fuel or wastes are burnt to reach the calcination temperature of ~900°C, and the kiln where cement clinker is produced at 1450°C. Oxy-combustion in the pre-calciner is suggested as a viable option to capture CO$_2$ from fuel combustion and raw material calcination, avoiding technical uncertainty of operating the cement kiln under oxy-combustion conditions (IEA, 2008). Dual preheaters with oxy-combustion pre-calciner have been designed while raw mill, kiln and clinker cooler operate conventionally. Part of the CO$_2$-rich flue gases from the pre-calciner is recycled back and mixed with oxygen to prevent excessive flame temperatures. The CO$_2$ avoidance rate by oxy-combustion in the pre-calciner is 61% since only part of the CO$_2$ can be captured. The European Cement Research Academy (ECRA, 2009; ECRA 2012) has been investigating the operation of the cement kiln as well as the precalciner under conditions of oxy-combustion for new installed cement plants. The theoretical and experimental outputs of this new design would allow utilization of oxy-combustion in the kiln, resulting in higher CO$_2$ avoidance rates. The applicability of advanced

oxygen production technologies, such as OTM systems, should be investigated to reduce energy and economic penalties involved in conventional cryogenic air separation which would reduce the energy consumption of oxy-combustion further. However, since the OTM are best coupled with a combustion turbine providing hot and high pressure air (IEA, 2007), it is reasonable that a combined cycle power plant would be needed for the OTM integration. Therefore, allocation of additional CO_2 emissions from fuel combustion to the cement plant should be accepted, or a decarbonized fuel should be used in the turbine, bringing about additional cost and plant complexity.

Post-combustion CO_2 capture represents the alternative option for end-of-pipe CO_2 abatement and provides low technical risk. The high CO_2 concentration in the flue gas would make amine-based post-combustion absorption attractive for the cement industry. However, a significant amount of steam is required for solvent regeneration and this is expected to have high energy penalties since a separate steam boiler is needed to supply steam to the solvent regeneration stripper (in case of capture rates > 80%, only 10 to 50% of the heat required for solvent regeneration can be recovered from the plant waste heat) (Kuramochi et al., 2012). The steam generator could generate some electricity with one back pressure turbine as well as steam (IEA, 2008); however, such a steam cycle design results in very low plant efficiency. If the separate steam cycle could be built in a way of having such a high complexity as one found in coal-fired power plants, similar energy penalty can be expected but no one would build a steam cycle with such a high complexity for the purpose of carbon capture. The amine-scrubbing (MEA) based post-combustion method has been proposed to reduce CO_2 emissions from a cement plant (Hassan, 2005; IEA, 2008). A coal-fired CHP plant has been designed to provide the steam for solvent regeneration (IEA, 2008). The flue gases resulting from fuel combustion in the CHP plant is also fed to the amine process. The need of the FGD and the SCR units are major limits of this configuration, in which up to 85% of the released CO_2 can be captured, corresponding to 74% of CO_2 emission avoided.

2.2.1 Application of the Ca-looping Process in Cement Plants

It has been argued that the Ca-looping process would have lower net energy consumption than the amine process since the heat of reaction can be recovered by generating steam and running a steam cycle due to their relatively higher operating temperature. The Ca-looping process may be even more advantageous when integrated with cement plants than those combined with any other industrial plants. The by-products of the process, i.e. the purge flow from the calciner, which is needed to maintain sorbent activity, can be used as kiln feed while it must be dumped as waste or transferred to other sites where a cement plant is present for reuse when combined with power plants. Since ECRA (2007) listed Ca-looping technologies as one of the promising capture technologies for cement plants, there have been conceptual studies which proposed various integration models, such as utilization of purge flow for the cement clinker and synergy between cement and power plants (Bosoaga et al., 2009; Naranjo et al., 2011).

Rodriguez et al. (2011b) proposed a way of producing CO_2 from the calciner by indirect heating using hot CaO circulating between calciner and external combustor instead of oxy-combustion, which is named the indirect calcination process. The proposed design tackles CO_2 emission resulting from limestone calcination only, which accounts for around 50 - 70% of CO_2 emission, and is not effective for CO_2 emission relating to fuel combustion. To enhance the performance, it was also suggested that the hot streams leaving the capture system could be utilized as a heat source for electricity generation. It should be noted that there is no carbonator in this design as distinct from the regular Ca-looping configuration so the CO_2 that both external combustor and kiln generate cannot be recovered in the process, which means that this process would be worth considering only if a moderate level of CO_2 capture is adequate. The key operating parameters and performances in this process are summarized below in Table 2-1.

Table 2-1 Summary of process configuration models on integration of Ca-looping process with cement plants.

Authors	Rodriguez et al. (2011b)	Rodriguez et al. (2012)	Romeo et al. (2011)
Type of integration	Hot CaO circulates between calciner and CFB combustor. There is no carbonator in the scheme.	Kiln gas is sent to carbonator for carbon capture. All $CaCO_3$ from carbonator and fresh limestone are calcined in one common calciner.	The industrial symbiosis of cement and power plants through Ca-looping process has been proposed. The flue gases from both power and cement plants are fed to the Ca-looping process.
Capacity of reference plant	3000 ton cement/day	3000 ton cement/day	3000 ton cement/day 500 MW_e power plant
Fuel (existing plant and calciner) *Composition*	Petroleum coke used in CFB combustor [wt%]: C: 82.2 H: 3.1 O: 0.5 S: 5.5 N: 1.9 Ash: 0.3 Moisture: 6.5	Petroleum coke used in cement kiln and calciner [wt%]: C: 82.2 H: 3.1 O: 0.5 S: 5.5 N: 1.9 Ash: 0.3 Moisture: 6.5 18% excess oxygen is used.	In the <u>power plant</u>, the coal composition [wt%]: C: 61.6 H: 4.9 O: 15.5 N: 1.2 Ash: 6.7 Moisture: 10.1 No information was given for fuel compositions used in the kiln and calciner.
Carbonator *Operating temperature* *Pressure* F_0/F_{CO2} F_R/F_{CO2} W_s u_0 *Reactor height* *Ca conversion* *Capture efficiency in the carbonator* *Net CO_2 avoidance rate* *Gas pressure drop* *Model used*	No carbonator in this system - - - - - - - - - 33%, it becomes 38% if CO_2 emission by extra electricity is excluded. - -	 650°C 1.0 atm 4.5 - - - - CaO conversion: 30% - 99% - There is no a reactor model implemented.	 650°C 1.0 atm A purge of 3.2% of the total solid inventory is assumed. 4 (fixed) - - - - 90% 95.3% (for cement plant) - There is no a reactor model implemented.

Calciner			
Operating temperature *Calcination efficiency* *O₂ content in oxidant stream*	937°C 100% calcination Air used	950°C 100% calcination 25 vol% O_2 (75 vol% CO_2 and H_2O)	950°C 100% calcination -
Steam cycle	A sub-critical steam cycle was chosen. (120 bar/520°C/520°C) No steam bleeds are performed.	Assumed that the lower temperature limit for energy recovery is 150°C. The net thermal efficiency of 33% is estimated for steam cycle.	180 bar/50 bar 600°C/600°C A pinch analysis has been conducted to recover maximum amount of surplus energy.
Air separation unit			
Electricity consumption *O₂ purity*	- -	160 kWh/ton O_2 -	220 kWh/ton O_2 -
CO₂ compression and purification			
Final CO₂ pressure *Final CO₂ purity* *Compression train (Compressor efficiency)* *Overall specific consumption*	100 bar > 95 vol% CO_2 5 turbo compressors + pump (75% isentropic efficiency) -	- - - - 100 kWh/ton CO_2	- - - -
Results *Total power demand* *Power production by steam cycle* *Energy demand of the base cement plant* *Energy demand of the base cement plant + Ca-looping process*	- 31.6 MW$_e$ 3.0 GJ$_{th}$/ton cement 6.1 GJ$_{th}$/ton cement	37.0 MW$_e$ 41.0 MW$_e$ 2.9 GJ$_{th}$/ton cement 5.5 GJ$_{th}$/ton cement	The total thermal energy consumption of reference case (power + cement plants) increases 6.7% for the integrated system (power + cement + Ca-looping plants) The thermal energy requirement in the cement plant decreases by 39.5% since purge CaO can be fed to kiln without calcination.

Given the postulate that the calciner purge can be used as kiln feed, a symbiosis model of a power plant, a Ca-looping process and a cement plant has been proposed with its mass and energy balances (Romeo et al., 2011) (see Table 2.1). The flue gases from both plants are sent to the Ca-looping process, and the CaO purge of this capture unit is returned to the cement plant, mixed with CaO from fresh raw material, and used as kiln feed. In this way, the CO_2 emission and energy consumption of the cement plant can be drastically decreased due to reduced load for calcination. The surplus energy from the capture unit has been utilized to generate electricity by running a separate steam cycle. A pinch analysis has been conducted in order to recover maximum energy from the carbonator, solid purge, clean flue gases and CO_2 stream before compression. Part of this electricity has been used for CO_2 compression and air separation units. The total thermal energy consumption increases by about 6.7% for the integrated system due to addition of capture unit. CO_2 emission avoided was estimated to be 94% on a basis of total CO_2 emission at both industries by this integration system. It must be highlighted that co-location of the power plant and the cement plant is needed in these cases, since transporting large amounts of solids between the two plants over long distances would bring about additional costs and logistic issues. Furthermore, the heat integration between the two systems could not be implemented.

A similar assessment has been performed by Romano et al. (2013), who considered the effect of the actual composition of the purge on the maximum "substitution rate" of the cement plant raw meal. The large amount of $CaSO_4$ and ashes from coal combustion in the calciner can limit the maximum amount of Ca-looping purge that can be used in the cement plant. Such a maximum "substitution rate" strongly depends on the fuel used in the calciner and on the parameters of the Ca-looping process.

As a direct integration of Ca-looping with a cement plant, Rodriguez et al. (2012) investigated two alternative processes (see Table 2.1). One is a retrofit replacing the existing pre-calciner with an oxy-calciner which can achieve 89% CO_2 avoidance and the other is capturing CO_2 from the kiln gas using a carbonator in addition to capturing CO_2 by oxy-calciner to improve avoidance rate up to 99%. As similar with

other Ca-looping processes, the surplus energies from high temperature streams are recovered by an integrated steam cycle. It was reported that the total energy consumption of cement plant increases from 2.93 GJ_{th}/ton cement to 5.45 GJ_{th}/ton cement by retrofit for carbon capture. Nevertheless, the carbonation efficiency of the solid stream containing CaO with clay minerals was roughly estimated in the reference study. Furthermore, the CO_2-rich gas stream from the calciner was transferred to the preheater for raw meal heating, which may cause a significant reduction in CO_2 purity if any air-leakage into this unit cannot be prevented. The design of Ca-looping process in a cement plant can be further improved if the concerns raised are resolved.

In this chapter, the aim is to present a detailed analysis of a typical cement manufacturing process and study the reasonable selection of location of the capture process with respect to process conditions when a Ca-looping process is integrated in a cement plant. Process simulation includes the implementation of a detailed carbonator model and its incorporation into a full cement process simulation. Effects of key operating parameters on Ca-looping process have also been investigated.

2.3 Process Simulation of a Cement Plant (Base Case)

Figure 2-1 shows the block flow diagram of a dry cement process, hereinafter named the base case configuration. The base case includes all the major units in the cement plant: raw mill; preheaters; pre-calciner; kiln and cooler. The base case simulation takes into account key reactions taking place in the process of cement production. Several auxiliary units, such as crushing and milling of the raw materials, cement mixing and milling with fly ash and gypsum are not included since their contribution to the energy balance is not as important as the major units included. In addition, their operations are not affected by retrofitting the carbon capture units into the cement plant. It should be highlighted that the base configuration has a separate pre-calciner upstream of a kiln instead of having a single reactor for calcination and clinkerization since it is well-known that it can provide a lower energy consumption and shorter kiln length (IEA, 2008).
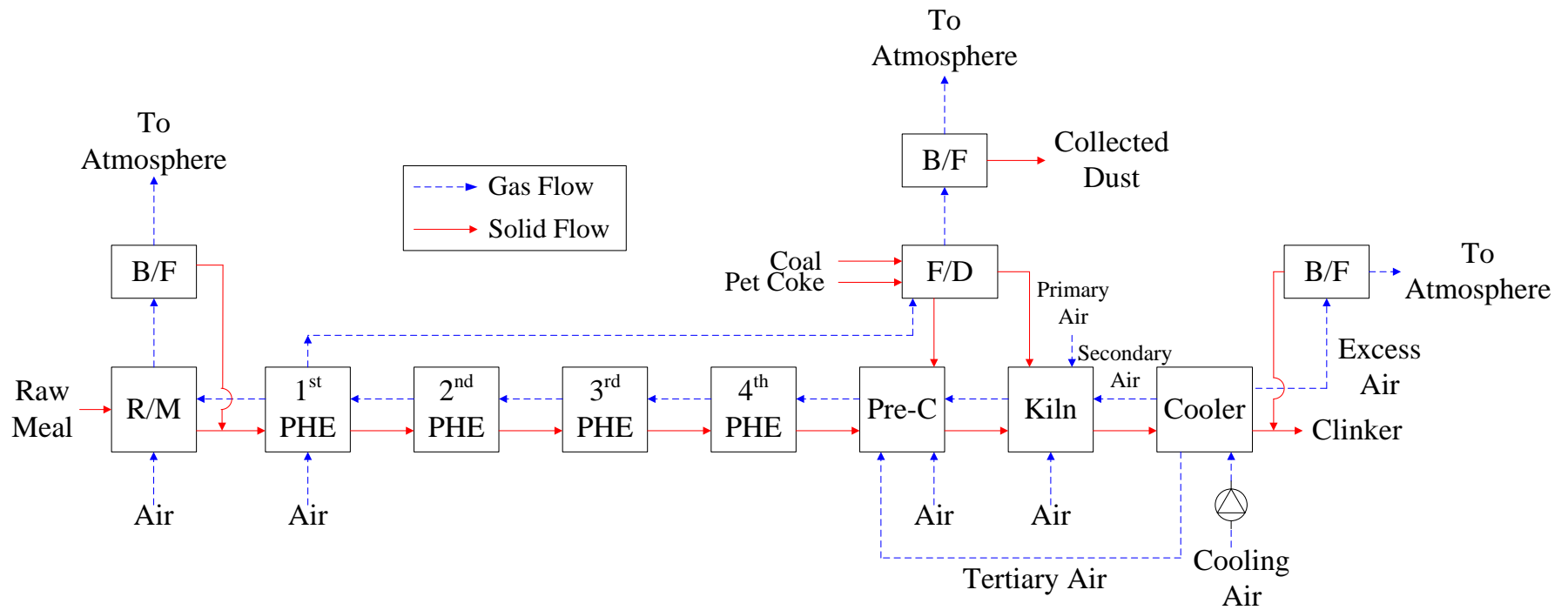
Figure 2-1 Schematic diagram of a cement plant without a CO_2 capture unit (Base Case) (IEA, 2008). Abbreviations: **R/M**, Raw Mill; **B/F**, Bag Filter; **F/D**, Fuel Drying; **PHE**, Preheater; **Pre-C**, Pre-calciner.

Table 2-2 Chemical reactions and their standard enthalpies considered in this cement plant simulation (Taylor, 1990).

Reaction	ΔH (kJ/kg)	Reference
$CaCO_3$ (calcite) → $CaO + CO_2(g)$	+1,782	$CaCO_3$
AS_4H (pyrophyllite) → $\alpha\text{-}Al_2O_3 + 4SiO_2$ (quartz) + $H_2O(g)$	+224	AS_4H
AS_2H_2 (kaolinite) → $\alpha\text{-}Al_2O_3 + 2SiO_2$ (quartz) + $2H_2O(g)$	+538	AS_2H_2
$2FeO\cdot OH$ (goethite) → $\alpha\text{-}Fe_2O_3 + H_2O(g)$	+254	$FeO\cdot OH$
$2CaO + SiO_2$ (quartz) → $ß\text{-}C_2S$	-734	C_2S
$3CaO + SiO_2$ (quartz) → C_3S	-495	C_3S
$3CaO + \alpha\text{-}Al_2O_3$ → C_3A	-27	C_3A
$4CaO + \alpha\text{-}Al_2O_3 + \alpha\text{-}Fe_2O_3$ → C_4AF	-105	C_4AF
$S + O_2$ → SO_2	-17,813	S
$CaO + SO_2 + 0.5O_2$ → $CaO\cdot SO_3$	-7,656	SO_2

Table 2-3 Composition of the raw meal fed to the raw mill (Taylor, 1990).

	wt %
Calcite	72.5
Quartz	6.0
Pyrophyllite	9.0
Kaolinite	2.4
Goethite	1.8
Moisture	8.0
Sulphur	0.3
Total	**100.0**

It is crucial to identify the chemical reactions occurring in each unit and determine their conversion rate in order to have accurate mass and energy balances. Table 2-2 shows the reactions being considered which can be classified into the decomposition of the raw materials and the clinkerization stages (Taylor, 1990). Given the raw meal composition in Table 2-3, the approximate chemical composition of the four main clinker phases (wt%), C_3S, C_2S, C_3A, and C_4AF, can be estimated by the Bogue equation (Bogue, 1929).

$$C_3S = 4.0710CaO - 7.6024SiO_2 - 6.7187Al_2O_3 - 1.4297Fe_2O_3 \qquad \text{(Eq. 2.1)}$$

$$C_2S = -3.0710CaO + 8.6024SiO_2 + 5.06383Al_2O_3 + 1.0785Fe_2O_3 \qquad \text{(Eq. 2.2)}$$

$$C_3A = 2.6504Al_2O_3 - 1.6920Fe_2O_3 \qquad \text{(Eq. 2.3)}$$

$$C_4AF = 3.0432Fe_2O_3 \qquad \text{(Eq. 2.4)}$$

Table 2-4 Comparison of Bogue equation approximation and the simulation results.

Mineral	Bogue calculation [wt %]	Simulation [wt%]
Alite (C_3S)	60.6	60.4
Belite (C_2S)	17.5	17.2
Tricalcium Aluminate (C_3A)	11.0	10.9
Tetracalcium Aluminate (C_4AF)	8.6	8.2
Free CaO	0.0	0.0
CaO·SO3	2.3	2.5
Ash	0.0	0.8
Total	**100.0**	**100.0**

The simulated clinker compositions are in good agreement with those estimated by the Bogue equation as shown in Table 2-4. It is assumed that 30% of sulphur in the raw material reacts with oxygen to become SO_2 in the first preheater and then leaves the plant via the raw mill. The remaining sulphur is converted into SO_2 in the pre-calciner and subsequently all the SO_2 formed reacts with CaO and oxygen to form CaO·SO_3 in the pre-calciner and is included in the clinker product (IEA, 2008). The raw meal having 8% moisture is dried passing the raw mill where it is heated by contacting the flue gas leaving the preheaters directly. The flue gas flowrate to be fed to the raw mill is determined such that both gas and solid streams leave the raw mill at around 110°C. The gas stream, leaving the pre-calciner at 915°C, is cleaned of the entrained fine particles passing the four cyclones in series comprising the preheater where it heats up the raw meal up to 760°C. The solid removal efficiency is assumed to be 94%, 90%, 85% and 80%, respectively from the preheater stage 1 to 4 (Alsop et al., 2007). It should be noted that calcination and clay decomposition start to take place at the 4th preheater with the 10% for calcination and 30% for clay decomposition referring the phase diagram shown in Figure 2-2 (Taylor, 1990). It is assumed that entire formed CaO reacts with SiO_2 in the 4th preheater stage and is converted belite (C_2S).

The preheated raw meal enters the pre-calciner where 90% of the remaining calcites are calcined and all clays are decomposed into their constituents, such as alumina, silica, and ferrite, at the operating temperature of 915°C. The conversion efficiency is set to 70% for the belite formation in this reactor. As the calcination and clay decomposition reactions are all endothermic, the pre-calciner is supplied with the heat generated from coal combustion with the tertiary air heated up to 908°C by

the clinker cooler. The flue gas leaving the kiln at 1025°C flows into the pre-calciner in order to lower the CO_2 partial pressure and supply an additional heat source for the endothermic reaction.

The rotary kiln, where cement clinker is produced by counter-current contact of the gas and solid streams, has been simulated in three separate units so that the temperature change along the length can be simulated. The first unit, corresponding to the solid feed end of the kiln, is simulated as a heat-exchanger to heat the solid stream from 915°C to 1250°C by its direct contact with the kiln gas flowing in the opposite direction. Subsequently, the temperature of the solid stream increases up to 1450°C by fuel combustion with primary and secondary air in the reactor (second unit) in order to calcine the remaining calcite and make all clinkerization reactions completed. Finally, the kiln product formed in the second unit is cooled to 1370°C with the incoming secondary air at the solid product end (third unit) (see Appendix A).
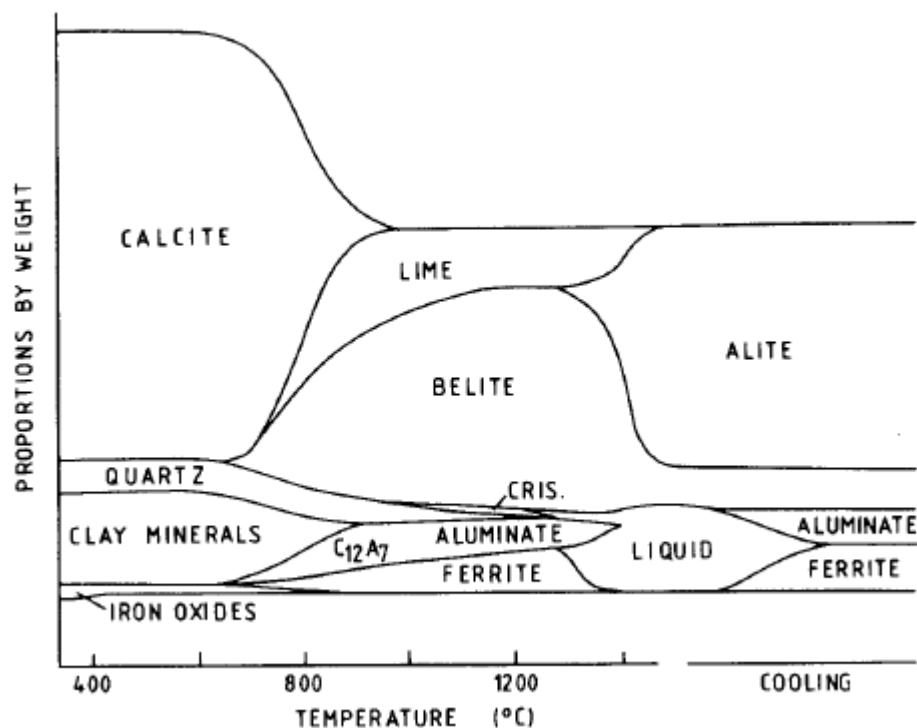
Figure 2-2 Clinker phase diagram (Taylor, 1990).

The kiln product is sent to the clinker cooler in which it is cooled to 60°C by ambient air. Even though there is a potential to burn alternative fuels such as tyres and biomass fuels in the pre-calciner, coal is selected as a heat provider in a parallel with the reference (IEA, 2008). The high temperature requirement in the kiln restricts the fuel flexibility; therefore, pet coke with low ash content is generally combusted in this reactor. Both fuel streams are dried completely by the hot flue gases from preheater. The excess air ratio is set as 10% to guarantee complete combustion in both reactors. The compositions of the fuels used in this study has been constructed from IEA (2008) report and presented in Table 2-5.

Tables 2-6 and 2-7 show the mass and energy balance around the cement plant obtained by the base case simulation. Given the raw meal composition, 1.66 kg/s of raw meal is required to produce 1 kg/s of clinker. The CO_2 generation intensity is around 0.8 ton CO_2/ton clinker that is within the range of 0.65 – 0.92 ton CO_2/ton cement given as the average CO_2 intensity for cement manufacture (IEA, 2007). Based on the energy balance, the required thermal energy for unit clinker production is estimated to be 3.13 MJ_{th}/kg clinker. The ratio of heat supply into the pre-calciner and kiln is maintained at 6 to 4.

Table 2-5 Composition of the fuels fed to the pre-calciner, kiln and calciner (* Data from IEA, 2008).

	Precalciner (Coal*) wt %	Kiln (Pet coke*) wt %	Calciner (Pet coke) wt %
Carbon	64.4	85.6	87.2
Hydrogen	4.5	3.5	3.6
Nitrogen	1.4	1.8	1.8
Sulfur	0.9	5.3	3.6
Ash	12.1	0.2	0.2
Oxygen	7.2	1.8	1.8
Moisture	9.5	1.8	1.8
Total	**100.0**	**100.0**	**100.0**

Table 2-6 Mass balance of the base case simulation [kg/s].

Mass in		Mass out		
Raw meal	52.41	Clinker		31.61
Air	99.55	Flue gas		
Fuel			From fuel drying	4.30
Wet coal to pre-calciner	2.26		From raw mill	75.49
Wet pet-coke to kiln	1.18	Excess Air		44.00
Total in	**155.40**	**Total out**		**155.40**

The overall heat of chemical reactions involved in conversion of raw meal to clinker is estimated about 178.4 GJ_{th}/h (1.57 MJ_{th}/kg clinker) by the difference between enthalpy in and out. The overall heat of reaction is lower in this simulation than in the reference (Taylor, 1990) (1.76 MJ_{th}/kg clinker) since it also takes into account the heat of the two highly exothermic reactions of sulphur conversion to SO_2 and its reaction with CaO.

2.4   Process Simulation of a Ca-looping Process

Different carbonator modelling studies have been published in recent years. These models have been developed with the support of the experimental results from either lab or pilot trials of the Ca-looping process as well as those for the CFB hydrodynamics. Shimizu et al. (1999) proposed a bubbling fluidized bed (BFB) model for the carbonator, which was based on the Kunii and Levenspiel (K-L) model (Kunii and Levenspiel, 1991) considering bubble and emulsion regions. This model was then modified by Abanades et al. (2004) to include the kinetic model proposed by Bhatia and Perlmutter (1983). Abanades (2002) proposed a simplified carbonator model that neglects the effects of reactor hydrodynamics. This model only considers the maximum average carbonation degree of the sorbents based on the maximum carbonation degree after a number of cycles and the mass fraction of these particles in the system. The simplified model has been used in many studies for the estimation of carbonation efficiency (see Appendix B). Later, the model developed by Alonso et al. (2009) combined the sorbent kinetics and residence time distribution functions. Although very simple assumptions about the fluid dynamics: plug flow for the gas phase and the perfect mix of the solids were considered, it has been proven to be accurate for carbonator design and optimization.

Table 2-7 Energy balance of the base case simulation [GJ_{th}/hr].

Enthalpy in			Enthalpy out		
	Sensible Heat	***Heat by combustion**		**Sensible Heat**	**Heat of Reaction**
Raw Meal	1.82		Clinker	5.12	
Air	3.25		Flue gas		
Fuel			From fuel drying	4.29	
Wet coal to pre-calciner	0.12	216.58	From raw Mill	72.95	
Wet pet-coke to kiln	0.05	139.25	Excess Air	45.77	
			Heat lost by radiation and convection	54.54	
			Overall heat of reaction		178.4 (1.57 MJ_{th}/kg)
Total in	**361.07**		**Total out**	**361.07**	

The reference state for enthalpy is at 0°C and 101 kPa.

* The heat by combustion of the fuel is a standard heat of combustion at 25°C and 101 kPa.

Lasheras et al. (2011) implemented a 1D carbonator model into a full-scale power plant. The carbonator was modelled as a CFB, and the model was divided into three main parts: particle distribution in the riser, absorption kinetics and calculation of overall carbonation efficiency. The particle distribution part was developed for fast fluidization as given in Kunii and Levenspiel (1991). Two regions were distinguished inside the carbonator: a lower dense region and an upper lean region. The rate of carbonation takes the boundary layer diffusion and the spherical grain model suggested by Abanades et al. (2004) into account. To estimate the carbonation efficiency, the model for gas conversion in catalytic reactions was used (Kunii and Levenspiel, 1991).

The model employed for predictions of carbonation efficiency in this dissertation was developed by Romano (2012). The vital difference between this model and others is the application of the effects of coal ash and sulphur species to CO_2 capture efficiency. The fast fluidized bed carbonator model is briefly presented here while further details, including the manner in which it performs integration with a full process flowsheet, can be found in the original paper (Romano, 2012) and Appendix B. The model assumes: (i) uniform temperature, (ii) no gas side mass transfer, (iii) perfect mixing, (iv) uniform particle size and (v) uniform superficial velocity. Similar to the model proposed by Lasheras et al. (2011), the carbonator model presented in Romano (2012) was based on the K-L theory for CFB systems. The reaction model describing the reaction rate of cycled particles was defined as the following equation (Grasa et al., 2008a):

$$\frac{dX}{dt} = k_r\big(C_{CO2} - C_{CO2,eq}\big) = k_s S_N (1-X)^{2/3}\big(C_{CO2} - C_{CO2,eq}\big) \qquad \text{(Eq. 2.5)}$$

where X is the carbonation degree, t is time, k_r is the kinetic constant, S_N is the specific surface area after each carbonation-calcination cycle, and k_s is the instinct kinetic constant. C_{CO2} and $C_{CO2,eq}$ refer to actual and equilibrium CO_2 concentrations, respectively. Despite being neglected in most modelling studies, Grasa et al. (2008b) indicated experimentally that a strong effect on the structure can be detected when limestone experiences sulphation after each cycle. To reflect the impact of sulphation on CO_2 capture efficiency in the carbonator, the experimental data from Grasa et al.

(2008b) was adapted to the model. The experimental data from the reference is fitted using the following equation and employed in the carbonator model for the calculation of the maximum carbonation degree of the sorbent.

$$X_{max,N} = \frac{1}{1/(1-X_r)+kN} + X_r \qquad \text{(Eq. 2.6)}$$

where X_r and k are the constants and N is the cycle number.

The reactor was divided into a dense region with a core-annulus radial distribution and a lean upper region. The use of the K-L model allows the estimations of solid distribution, the heights of the bottom dense and upper lean regions as well the mass velocity of solids. The gaseous phase mass balance was developed by rearranging the kinetics given in Eq. 2.5 in the form of:

$$\frac{d(C_{CO2}-C_{CO2,eq})}{dt} = -\frac{\xi\,V_s}{V_g}\frac{\rho_{s,a}}{M_{s,a}} k_r\left(C_{CO2} - C_{CO2,eq}\right) \qquad \text{(Eq. 2.7)}$$

where ξ is the volume ratio between potentially active sorbents and the total solids (including ash and $CaSO_4$). V_s and V_g refer to volumes of solid and gas phase, respectively. $M_{s,a}$ and $\rho_{s,a}$ are the molecular weight and density of potentially active sorbents, respectively. Eq. 2.7 can be solved for the core and wall regions in the bottom dense section. The final form of the equation representing CO_2 concentration at the dense region outlet is given in Appendix B. The following material balance was arranged for the lean region.

$$u_0 \frac{d(C_{CO2}-C_{CO2,eq})}{dz} = -\xi\,\varepsilon_{s,l}\eta_l k_{ri}\left(C_{CO2} - C_{CO2,eq}\right) \qquad \text{(Eq. 2.8)}$$

Here, u_0 is the superficial velocity of gas, $\varepsilon_{s,l}$ is the volumetric solid fraction in the lean region and k_{ri} is the first order kinetic constant of the carbonation reaction. η_l is the contact efficiency in the lean region starting from that in the dense region to take into account the non-ideality of the reactor.

The volume ratio of active solids and the average kinetic constant should be known in order to find a numerical solution for the mass balance equations. Thus, the second part of the model was dedicated to the estimation of solid population in the

bed, where the impact of ash and $CaSO_4$ contents in feed sorbent on solid residence is included. Overall, there are two solution steps for the carbonator model. The first step is related to solid distribution in the reactor and mass balance for the dense and lean regions, while the second step is dedicated to the estimation of solid residence time and the average carbonation degree of the sorbent. The numerical solution is relevant to the calculation of the same CO_2 capture efficiency in these two parts. Despite the fact that the first results for pilot-scale applications have just been released, the model has provided satisfactory results against those from the lab-scale facilities operating at Stuttgart University, Germany and INCAR-CSIC, Spain (Charitos et al., 2011). In all simulations, the operating condition of the carbonator is carefully chosen to capture 90% CO_2 from the feed gas and the $CaCO_3$ fed to the calciner is regenerated to CaO at complete conversion. The calciner temperature is selected to be 930°C, which is higher than the pre-calciner temperature (915°C), to guarantee complete calcination due to the CO_2 partial pressure in the calciner close to 1 atm. The temperature of the carbonator, which should be kept as close to the calciner temperature as possible in order to save the energy consumption for reheating the circulating solid, is fixed at 650°C in this study.

It is assumed that all SO_2 generated by combustion in the calciner is captured by CaO. As a result of the deterioration of the CO_2 absorption capacity through the carbonation/calcination cycles, fresh $CaCO_3$ needs to be added into the calciner while same amount of spent sorbents (CaO) are removed from the calciner on molar basis. The $CaCO_3$ make-up, fuel, and oxygen streams fed to the calciner are neither preheated nor dried but directly fed to the calciner due to the lack of flue gas availability for preheating. All the mathematical models for the carbonator are solved in Matlab and then the carbonator unit was incorporated into the UniSim process simulation for cement plant as a user defined operation. The Visual Basic code in a user defined operation transfers the input values from the UniSim into the Matlab environment where the design calculations are implemented via a component object model (COM) interface. The calculated values are then sent back to UniSim and used for the mass and energy balance calculations in the complete process flowsheet (see Appendix B).

(a)
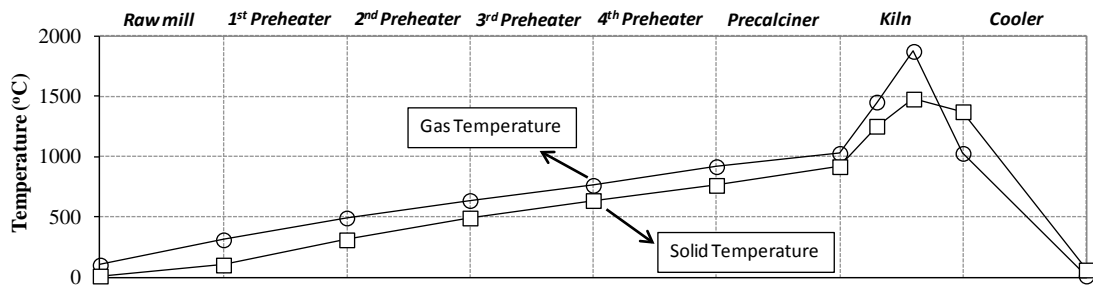
(b)
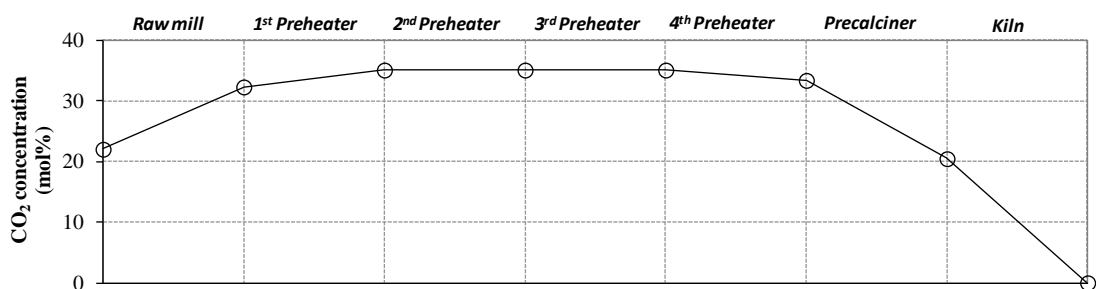
Figure 2-3 Variations of (a) gas and solid temperatures and (b) CO_2 concentration along the cement plant.

2.5 Process Integration of a Ca-looping Unit with a Cement Plant

One of the important issues while integrating a Ca-looping unit with a cement plant is the selection of a feed gas stream for the Ca-looping process. As the flue gas from pre-calciner flows through the process in the opposite direction to the solid flow for heat recovery, its temperature and CO_2 mol fraction varies over the process as shown in Figure 2-3. Therefore, the flue gas stream for the capture process should be selected taking into account the operating condition of a selected capture unit, ease of heat integration, and CO_2 partial pressure.

For the ease of retrofit, it can be envisaged that the flue gas stream after the raw mill and fuel drying would be an optimal feed for the capture unit. However, the flue gas at this location has around 22 vol% CO_2 as shown in Figure 2-3(b), which is the lowest value over the entire process. The volumetric flowrate is at its highest at this point so a larger equipment size of the capture unit would be required. Furthermore,

the flue gas may need to be reheated prior to being fed to the carbonator in order to initiate the carbonation reaction as the temperatures of the flue gases are around 110°C. In addition, the heat of the CO_2-depleted gas from the carbonator needs to be recovered to improve the energy efficiency but an additional facility for heat recovery should be deployed for this purpose.

In conclusion, the applications of Ca-looping processes to the end-of-the-pipe gas streams of the cement plants would require a complexity similar to those of power plants. However, the flue gas at the exit of the 3rd preheater has a temperature of around 650°C, as shown in Figure 2-3(a), which is similar to the operating temperature of the carbonator. It indicates that the flue gas from the 3rd preheater would not require any pre-heating of the feed gas and would be preferable for the start-up of the carbonator. Moreover, there is no need to recover the heat from the CO_2-depleted flue gas stream for power generation and instead it is possible to return it back to the cement plant in order to heat up the raw materials in a similar way to the operation in the conventional cement plant. The flue gas at the 3rd preheater exit has a higher CO_2 concentration (~35 vol%) compared to the end-of-pipe stream (~22 vol%) as shown in Figure 2-3(b) and, in proportion, such a lower gas flow rate would require smaller carbonator size leading to lower capital expenditure. Therefore, a decision was made that the flue gas from the 3rd preheater stage is diverted to a Ca-looping unit for CO_2 capture as shown in Figure 2-4. The CO_2-depleted flue gas from the carbonator is routed to the 2nd preheater stage for preheating the raw material further. It should be noted that it is still possible to capture CO_2 from all sources including calcination and fuel combustion with this configuration, which was initially proposed by ECRA (2007).

The CO_2 depleted flue gas flowing from the carbonator to the 2nd preheater would have a lower flowrate than that in the base case as a result of carbon capture and its heat duty is not large enough to heat the raw material up to a temperature that would be reached in the base case. Thus, part of the excess air from the clinker cooler as well as CO_2-depleted flue gas should be utilised for heating raw material as shown in Figure 2-4. In all cases of this study, the flowrate of excess air being sent to the raw mill was determined to heat up the raw material entering the 1st preheater up to

110°C. It should be noted that the clay components are not fed into the capture unit in this study as distinct from the reference (Rodriguez et al., 2012) since the sorbent performance has not been proven for this mixture yet and there would be a need of additional efforts for the circulation of inerts. As the purge stream of the Ca-looping unit is mixed with pre-calcined raw materials and then the mixture is sent to the kiln for clinker production, the mass and energy balance in the cement plant is significantly affected by changing the $CaCO_3$ make-up flow rate of the Ca-looping process. Firstly, since the CaO for clinkerization can be produced in the calciner as well as the pre-calciner, the ratio of calcite to clay in the raw meal should be decreased with an increasing F_0/F_{CO2} in order to maintain the same clinker composition as that in the base case. Subsequently, the decreasing ratio of calcite to clay in the raw meal results in reduction in heat demand in the pre-calciner and, to a less extent, kiln. In order to save the energy consumption for a Ca-looping process further, it is possible to recover the heat of reaction in the carbonator, the heat from the CO_2-rich stream and excess air. The heat of those hot streams can be recovered by way of generating steam for a steam cycle. The power generated can be utilised for the cement plant operation, the CO_2 compression unit, the ASU, etc.

Since the solid removal efficiency is not 100% on the 3rd preheater stage, a new cyclone with higher efficiency has been included to prevent the solid transfer from cement plant to capture unit for precise prediction of the carbonation efficiency in this unit. It is estimated that the additional pressure increment of the gaseous feed flowing to carbonator would be approximately 0.16 bar that would be sum of the pressure loss in operating the carbonator (pressure drop along the carbonator bed, 0.10 bar + gas injection through the nozzle, 0.03 bar) and the pressure drop relating to the additional cyclone (0.03 bar) (Alsop et al., 2007). 0.20 bar of a total pressure loss including a 25% safety margin is estimated. The boost of the gas stream pressure has been made by increasing the cooling air pressure flowing to the cement kiln. The ASU power consumption is set as 231 kWh per ton O_2 product at 99.5% oxygen purity (DOE, 2003).
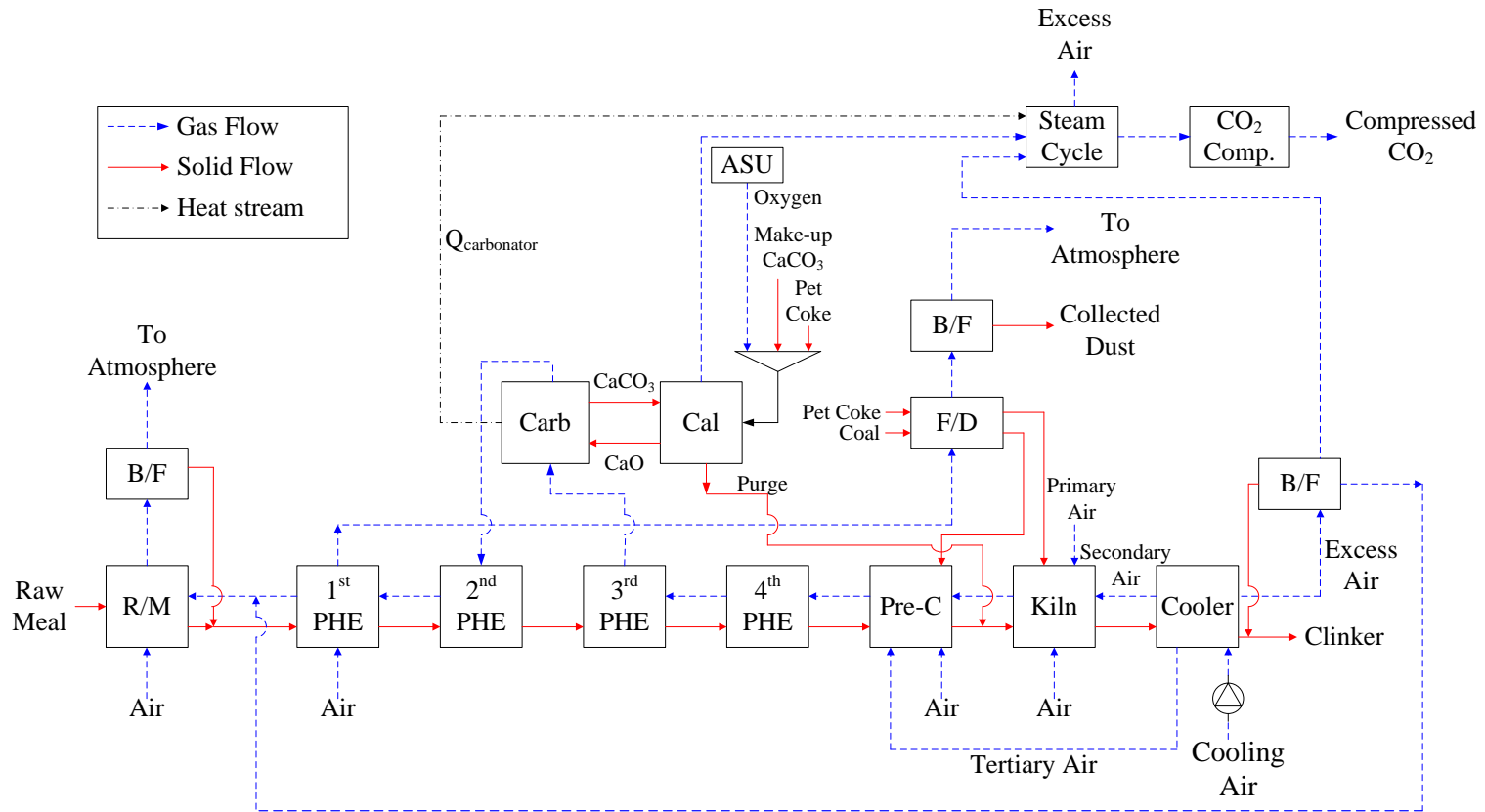
Figure 2-4 Schematic diagram of the proposed process integration of a cement plant with a Ca-looping unit. Abbreviations: **R/M**, Raw Mill; **B/F**, Bag Filter; **F/D**, Fuel Drying; **PHE**, Preheater; **Pre-C**, Pre-calciner; **Carb**, Carbonator; **Calc**, Calciner; **ASU**, Air Separation Unit; **CO₂ Comp**, CO₂ Compression.

The CO_2 compression unit consists of a four-stage turbo compressor with intermediate cooling, followed by a pump once the CO_2 becomes a dense phase. The inlet temperatures of each stage are fixed at 45°C and adiabatic efficiency of each compressor is assumed to be 75%. The power requirement for CO_2 compression up to 150 bar is estimated at 1.08 MJ_{th}/kg CO_2 using a 0.4 conversion factor of power to equivalent thermal energy. An example mass and energy balance calculations for the capture cases can be seen in Appendix A.

2.6 Results and Discussion

Two mathematical models for the carbonator have been compared in this study as shown in Appendix B. While it is assumed that all the active fraction of CaO reacts with CO_2 in the feed gas in the 'simple model', the 'rigorous model' includes the effects of both hydrodynamics and reaction kinetics in the fluidised bed reactor. Moreover, the effects of sulphation on the maximum carbonation degree were taken into account in the rigorous model based on the experimental data of Piaseck for limestone sulphation up to 1% in each carbonation/calcinations cycle (Grasa et al., 2008b). Given a F_0/F_{CO2}, the corresponding F_R/F_{CO2} to achieve 90% CO_2 capture has been evaluated using the simple and rigorous models with results shown in Figure 2-5. The minimum value of the F_0/F_{CO2} being examined is set as 0.20 since the heat demand at the raw mill cannot be met even by employing the entire excess air in addition to the flue gas at a F_0/F_{CO2} less than 0.20. The heat requirement in the raw mill keeps decreasing with increasing F_0/F_{CO2} since the flowrate of raw meal into the raw mill decreases with an increase of the ratio. The upper limit of the F_0/F_{CO2} ratio is determined as 5.10 since there is no calcite in the raw meal at this condition, that is to say, all the calcites in the feed are fed to the calciner. Therefore, the carbonator captures CO_2 generated only from the fuel combustion at this ratio.
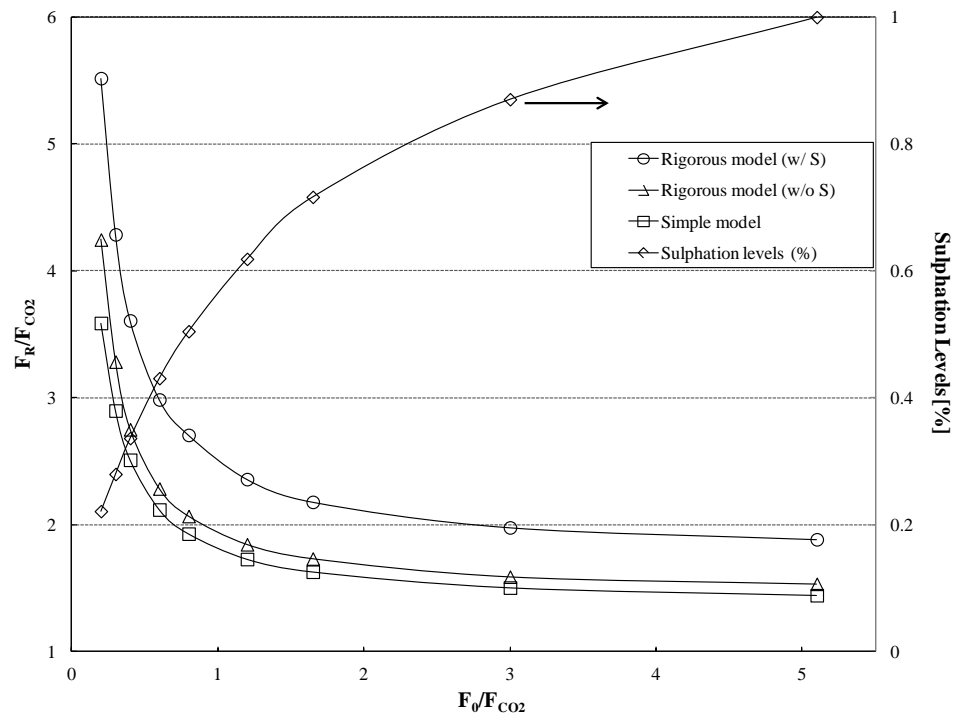
Figure 2-5 Corresponding F_R/F_{CO_2} in range of F_0/F_{CO_2} ratio to reach 90% capture efficiency in the carbonator of proposed configuration (For the rigorous model, the carbonator temperature and pressure drop along the column were set as 650°C and 0.1 bar, respectively while superficial velocity, u_0, was estimated to be 6 m/s. The sulfidation level is shown at each F_0/F_{CO_2}).

As shown in Figure 2-5, it is clear that as the F_R/F_{CO_2} ratios estimated by the rigorous model using sulphur-free fuel are definitely higher than those by the simple model in range of the F_0/F_{CO_2} investigated. The extent of difference between the two models is affected by the residence time of sorbents in the carbonator which is determined by the amount of sorbent inventory in the reactor. However, when utilising the fuel having sulphur in the calciner, the required F_R/F_{CO_2} ratios need to be increased way above those with sulphur-free fuel since the CaO is significantly deactivated by sulphation. In this study the sulphur content in the fuel used in the calciner was adjusted so that the maximum sulphation, obtained at the 5.10 F_0/F_{CO_2} case can be 1%. It implies that the use of sulphur-free fuel would alleviate the severity of its operation condition due to the lower amount of solid circulation required given a F_0/F_{CO_2} ratio.

60

Figure 2-6(a) shows the variation of the thermal energy requirement per unit clinker in terms of fuel combustion (pre-calciner, kiln, and calciner) and power consumption (ASU and blower) with the F_0/F_{CO2}. The thermal requirement for the pre-calciner decreases with increasing F_0/F_{CO2} as the heat requirement for the pre-calciner decreases in proportion to the reduction in calcite fed to the raw mill. The thermal requirement for the kiln has decreasing trends with the F_0/F_{CO2} too since it is assumed that the calcite is completely calcined in the calciner while its conversion is only 90% in the pre-calciner. However, the reduction of energy demand in the kiln is not as significant as that in the pre-calciner because the solid flowrate to the kiln are almost constant regardless of the F_0/F_{CO2} due to nearly constant clinker production rate in all cases.

The heat requirement for the calciner shows a minimum over the F_0/F_{CO2} range investigated. Before the minimum, it is decreasing due to decreasing circulating amount of solid, that is to say, the F_R/F_{CO2} as shown in Figure 2-5. However, after the minimum, the effect of the increase in the heat duty at the calciner caused by the F_0/F_{CO2} increase dominates. The total fuel requirement shows a steady overall decrease with the increase of the F_0/F_{CO2} ratio. The energy requirement for the ASU is proportional to the fuel consumption in the calciner and that for the cold air blower is constant with the F_0/F_{CO2} ratio. The electric power consumptions in the ASU and blower are converted to their corresponding thermal energy consumption using a power plant efficiency of 0.4. This allows an overall comparison of different options in terms of the equivalent total thermal energy required. At least, in terms of total thermal energy consumption for the fuel, the ASU and the blower it is preferable to operate a Ca-looping process at as high F_0/F_{CO2} ratio as possible.

(a)
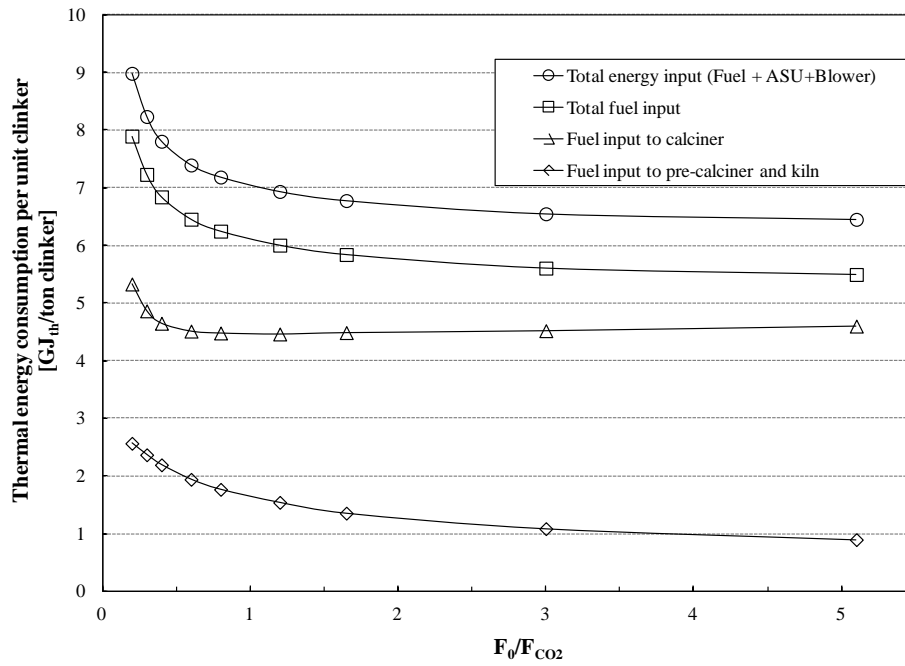
(b)
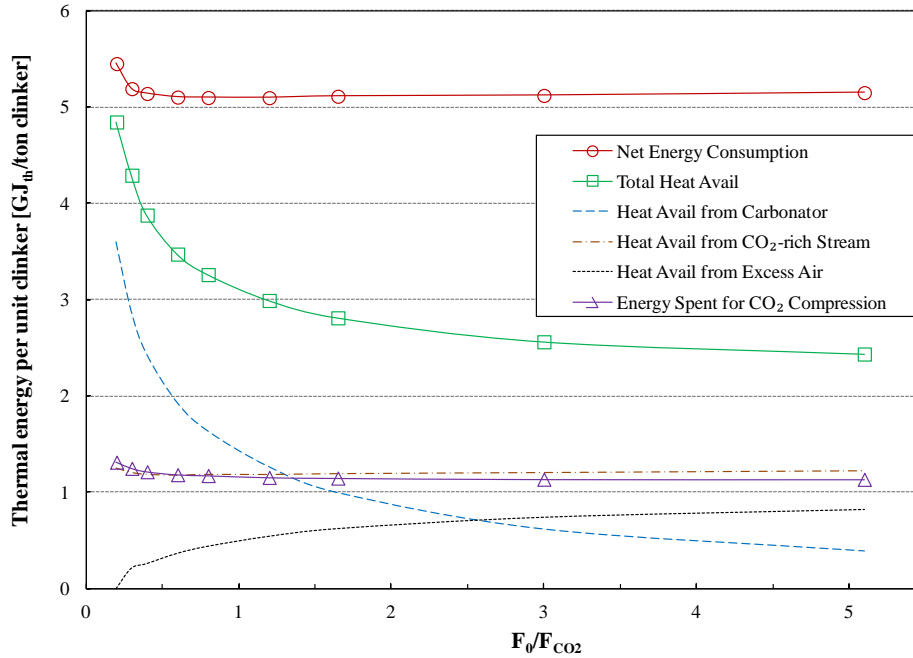
Figure 2-6 (a) Energy consumption per unit clinker with respect to fuel and power and (b) net energy consumption per unit clinker considering heat recovery for power generation.

On the other hand, it is intuitively conceivable that a Ca-looping process can be made more efficient in terms of energy consumption if it is combined with a steam cycle for heat recovery. There are three different sources from which the heat can be recovered by generating steam and subsequently running a steam turbine. It is possible to generate steam by evaporating the water inside the carbonator in order to keep the reactor temperature constant at 650°C and also recovering the heat from a CO_2-rich stream and the excess air as shown in Figure 2-4. In case of heat recovery from the two gaseous streams, it is assumed that the hot gas can supply the steam cycle with thermal energy which is estimated as an enthalpy to be generated when cooled down to 150°C.

At 0.2 F_0/F_{CO2}, as shown in Figure 2-6(b), the heat that can be recovered in the carbonator is a maximum over the range due to the greatest heat of reaction generated in the carbonator and the largest amount of hot solids conveyed from calciner to carbonator (see Figure 2-5). There is no heat to be recovered from the excess air since all the excess air should be diverted to the raw mill in order to compensate the deficiency of heat duty of the flue gas. Considering energy consumption inclusive of CO_2 compression, the net energy consumption per unit clinker production is in the range of 5.2 to 5.5 GJ_{th}/ton clinker. This is equivalent to around 66% increase in energy consumption of a cement plant in producing same amount of clinker.

A work on preliminary steam cycle design to evaluate the power generation from the recovered heat has been conducted. The turbine adiabatic efficiencies have been fixed at 86%, 86% and 95% for HP, IP and LP turbines, respectively (Ahn et al., 2013). With the support of proposed configuration (see Appendix A), a lumped conversion factor of 0.44 has been applied throughout this study for rough estimation of power generation out of the total heat to be recovered from the cement plant integrated with the Ca-looping process. The estimated power generation is shown in Figure 2-7. It is predicted that the power generated in steam cycle can exceed the power demand in the cement plant integrated with a Ca-looping process up to ~1.5 F_0/F_{CO2}. The power use for the cement plant operation is assumed as 120 kWh/ton clinker (IEA, 2008; Taylor, 1990) regardless of the F_0/F_{CO2}.
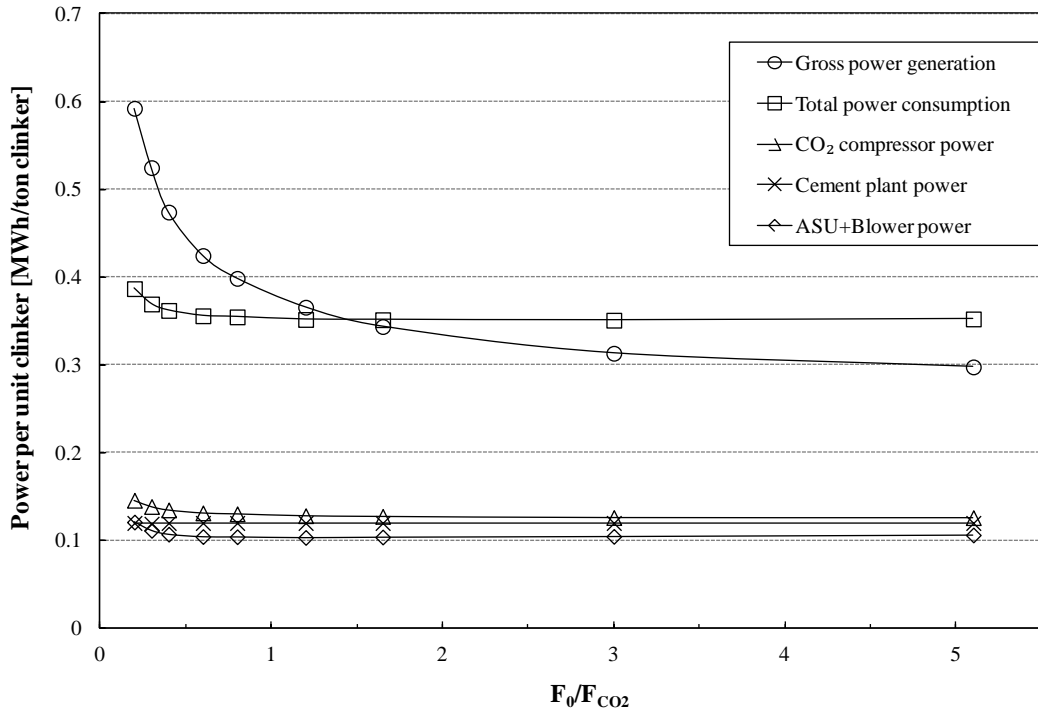
Figure 2-7 Variation of power generation by heat recovery and power consumption with F_0/F_{CO_2} ratio.

The following equations can be used to calculate CO_2 intensity, CO_2 avoidance rate and incremental energy consumption when a carbon capture technology is integrated with a cement plant.

$$CO_2\ intensity = \frac{Amount\ of\ CO_2\ emitted}{Clinker\ production\ capacity} \tag{Eq. 2.9}$$

$$CO_2\ avoidance\ rate\ = \frac{CO_2\ intensity_{base\ cement\ plant} - CO_2\ intensity_{capture\ case}}{CO_2\ intensity_{base\ cement\ plant}} \tag{Eq. 2.10}$$

$$Incremental\ energy\ consumption =$$

$$\frac{Net\ energy\ consumption_{capture\ case} - Net\ energy\ consumption_{base\ cement\ plant}}{CO_2\ intensity_{base\ cement\ plant} - CO_2\ intensity_{capture\ case}} \tag{Eq. 2.11}$$

The CO_2 emissions in each case can be taken from process simulations while the clinker production capacity remains almost constant with a value calculated for the base cement plant. The net energy consumption estimates for the Ca-looping process inclusive of heat recovery have already been given in Figure 2-6(b).

It should be noted that what is initially fixed in this study is not the CO_2 avoidance rate in overall cement process but a CO_2 recovery in the carbonator. As shown in Figure 2-8, therefore, the percentage of CO_2 avoidance is as low as 92% at 0.2 F_0/F_{CO2} since most CO_2 is captured in the carbonator with 90% capture rate but it increases up to 99% at 5.10 F_0/F_{CO2} because most CO_2 is captured with 100% CO_2 recovery in the calciner. It is important to highlight at this point that CO_2 avoidance rate differs from overall CO_2 capture rate for the Ca-looping process integrated with a cement plant because it does not take the capture of additional CO_2 releasing by oxy-combustion in the calciner into account. Although the comparison among various carbon capture technologies has been based on a fixed CO_2 avoided rate in this dissertation, it is worth to mention that the incremental energy consumption estimates given in Figure 2-8 can be reduced when it is based on total amount of CO_2 captured. Furthermore, additional power generation from surplus heat in the Ca-looping process does not have any influence on CO_2 intensity calculations in Eq. 2.9 as it does when the Ca-looping process is integrated with a power plant.

Another limiting case named 'oxy-calciner only' has been simulated such that all calcites are calcined in the calciner separate from the pre-calciner in a similar way to the 5.10 F_0/F_{CO2} case but there is no carbonator for carbon capture from the kiln gas. In this case, the percentage of CO_2 avoidance is 90% since this process can capture CO_2 relating to calcinations and fuel combustion in the calciner and cannot capture CO_2 generated by fuel combustion in the kiln. The incremental energy consumption per CO_2 avoided without heat recovery also shows decreasing trends with F_0/F_{CO2} similarly to the total energy input per unit clinker in Figure 2-6(a). It implies that it would be better to generate CaO by oxy-combustion rather than by the pre-calciner in the existing plant if no heat recovery system is added. The incremental energy consumption per CO_2 avoided at the 'oxy-calciner only' and 5.10 F_0/F_{CO2} cases are 5.1 and 5.5 GJ_{th}/ton CO_2 avoided respectively without heat recovery. It is thought that the difference between the two cases (0.4 GJ_{th}/ton CO_2) can be explained by additional energy consumption resulting from circulating solids between the carbonator and the calciner. With heat recovery put in place, the resulting energy consumption further decreases to 2.5 GJ_{th}/ton CO_2 avoided for the 5.10 F_0/F_{CO2} case and 2.3 GJ_{th}/ton CO_2 avoided for the 'oxy-calciner' case.
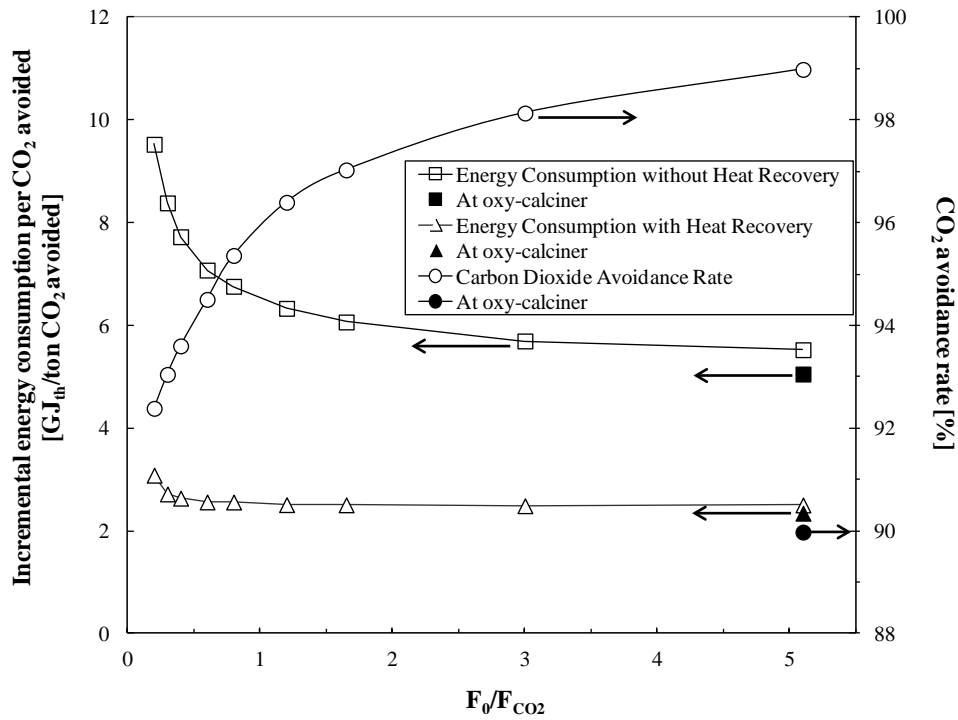
Figure 2-8 Variation of CO_2 recovery based on CO_2 emission at base case and incremental energy consumption per CO_2 avoided with F_0/F_{CO2} ratio.

Table 2-8 shows the quantitative difference of fuel and power consumptions between the cement plant without capture and those integrated with Ca-looping units and heat recovery steam cycle at various F_0/F_{CO2} conditions. Table 2-8 also includes the change of mass flow rates of limestones entering the plant through raw mill and calciner with the F_0/F_{CO2}. Since the proposed cement plants integrated with Ca-looping units are designed such that they can recover heat contained in the hot excess air by a steam cycle that would be lost in the conventional cement plant, the net thermal energy consumption in the cement plants with Ca-looping units are always lower than that in the conventional cement plant as shown in Table 2-8.

For further analysis, the simulations have been repeated to fix CO_2 avoidance rate at 90%, rather than keeping the CO_2 recovery in the carbonator at 90% as presented in Figure 2-8. The F_0/F_{CO2} ratio is limited to 3.0 in this instance because the CO_2 avoidance rate is always greater than 90% at 5.10 F_0/F_{CO2}. It is because the 'oxy-calciner only' case that provides the target avoidance rate without a carbonator. Figure 2-9 presents the incremental energy consumption and CO_2 recovery in the carbonator estimates for the current case.

Table 2-8 Detailed constituents of the incremental energy consumption per CO_2 avoided considering heat recovery [# **Unit: GJ_{th}/ton CO_2 avoided**].

| F_0/F_{CO2} | Mass Flow Rates (kg/s) | | | $\Delta H^{\#}$ | $ASU^{\#}$ | CO_2 compression# | Cold air blower# | Total# |
| | Clay | Limestone | | | | | | |
		Raw Mill	Calciner					
0.2*		28.85	9.09	-0.24	1.30	1.75	0.15	2.96
0.3		25.57	12.37	-0.23	1.18	1.65	0.15	2.75
0.4		22.82	15.12	-0.22	1.12	1.59	0.15	2.64
0.6		18.70	19.24	-0.20	1.07	1.54	0.15	2.56
0.8	10.28	15.67	22.27	-0.16	1.06	1.51	0.15	2.56
1.2		11.81	26.13	-0.15	1.04	1.47	0.15	2.51
1.65		8.62	29.32	-0.13	1.04	1.45	0.14	2.50
3.0		4.02	33.92	-0.11	1.04	1.42	0.14	2.49
5.1**		0	37.94	-0.09	1.04	1.41	0.14	2.50
Oxy		0	37.94	-0.08	1.05	1.37	-	2.34

* The lower limit was defined as the heat requirement in the raw mill can not be met below this point

** The upper limit was defined as no calcite is fed to the raw mill at this F_0/F_{CO2} and more calcite would be fed to the cement plant through the oxy-calciner than required above this point.
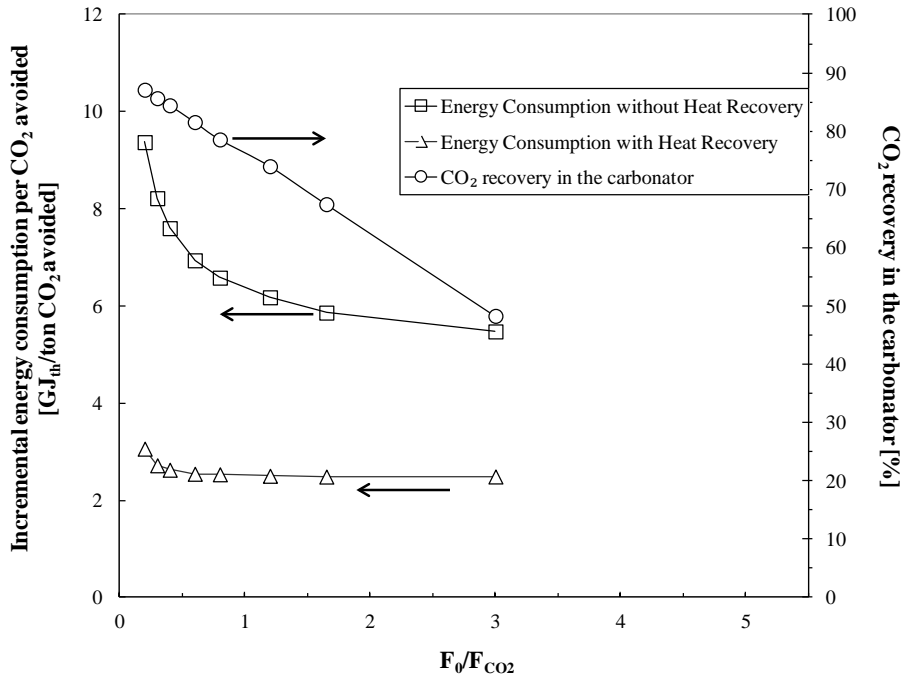
Figure 2-9 Variation of carbonation efficiency and incremental energy consumption per CO_2 avoided with F_0/F_{CO2} ratio at 90% CO_2 avoidance.

At very low F_0/F_{CO2} ratios in the 90% CO_2 avoidance case, the CO_2 recovery in the carbonator needs to be high since only small amount of CaO is provided from the oxy-calciner. In contrast, it reduces to around 48%, when majority of CaO is transferred from the capture system. The results for incremental energy consumption with heat recovery are very similar to those presented in Figure 2-8. Although the energy requirement in the calciner reduces as a result of a reduction in the amount of circulated sorbent, the CO_2 intensity of the plant increases in parallel so there is not any significant change in the incremental energy consumption estimates.

In both cases, it is clear that it would be extremely inefficient to operate a Ca-looping unit at low F_0/F_{CO2} ratio without heat recovery but CO_2 can be recovered with almost constant energy consumption regardless of the F_0/F_{CO2} ratio if a proper heat recovery is deployed. Moreover, the electricity required to operate a cement plant integrated with a Ca-looping process can be generated in situ by a steam cycle attached to the capture unit without any external source of electricity which would be associated with carbon emissions.

2.7 Concluding Remarks

A way of capturing CO_2 from cement plants by integrating it with a Ca-looping process has been investigated. The cement process simulation implemented in this study was proven to be reliable in that the total energy consumption estimated by the simulation lies within the range of those reported in the literature and the clinker compositions estimated in the simulation are in good agreement with those calculated by the Bogue equation. Among the flue gas streams, the gas stream leaving the 3rd preheater was selected to be the optimal feed suitable for the Ca-looping capture unit since 1) it does not have to be preheated, 2) it has a higher CO_2 partial pressure and a lower total volumetric flowrate, and 3) a simpler design of the steam cycle for heat recovery is possible.

The upper and lower limits of the F_0/F_{CO2} ratio have been set in order to see the effect of F_0/F_{CO2} on the energy consumption. Given 90% carbon capture in the carbonator, the CO_2 avoidance rate ranges from 92% to 99% depending on the F_0/F_{CO2} ratio. The incremental energy consumption by carbon capture decreases with the F_0/F_{CO2} ratio, but with heat recovery from the capture unit, the energy consumption can be almost constant regardless of the ratio. It was observed that the incremental energy consumption estimates remain almost constant even if the CO_2 avoidance rate is fixed at 90%.

It should be noted that there may be a constraint in the minimum fuel supply to the kiln to ensure a stable operation in the kiln as pointed out in the IEA study (2008). Therefore, the actual upper limit of the F_0/F_{CO2} ratio needs to be defined considering plant operability. Moreover, the estimation of the amount of heat that can be recovered from three high temperature sources can be made more accurate by inclusion of a detailed steam cycle in the integrated process flowsheet.

Chapter 3 Alternative CO_2 Capture Technologies for Cement Plants

This chapter is divided into three main sections. Section 3.1 introduces an advanced system combining the Ca-looping process with the chemical looping combustion (CLC) cycle. The process integration of the indirect calcination process is explored in Section 3.2. Furthermore, a comprehensive analysis of the standalone amine process and a hybrid configuration is performed. In Section 3.3, two feed gas locations and several dual-configurations are assessed to investigate the potential of incorporating a membrane separation process.

3.1 Combining Chemical Looping Combustion and Calcium Looping Process

As discussed in Chapter 2, one of the major energy penalties in the Ca-looping process results from the need of an air separation unit (ASU) for the production of high purity CO_2 in the calciner, which also escalates the total capital cost requirement. A novel alternative for the transfer of pure oxygen into a calciner was proposed by Abanades and Murillo (2009). In their work, a CLC system was coupled with a Ca-looping process to provide heat to the calciner by the exothermic reduction of a metal oxide (CuO) as an oxygen carrier with methane.

The schematic diagram of the conventional CLC process is given in Figure 3-1. This system is comprised of an air reactor and a fuel reactor. In the fuel reactor, oxygen from the carrier oxidizes the fuel while the depleted oxygen carrier is regenerated with air in the air reactor. The air reactor always produces heat while the fuel reactor either requires heat or releases heat depending on the types of oxygen carrier and fuel (Adanez et al., 2012). While the reduction of majority of the metal oxides used in the CLC system is endothermic, only a few metal oxides have exothermic reduction reaction, for example, the reactions between CuO and CH_4 or CO or H_2, NiO and CO or H_2, and Mn_2O_3 and CH_4 or CO or H_2 are exothermic.

(N_2, O_2) (CO_2, H_2O)

Air Reactor (Me_xO_{y-1}) **Fuel Reactor**

(Me_xO_y)

Air   Fuel
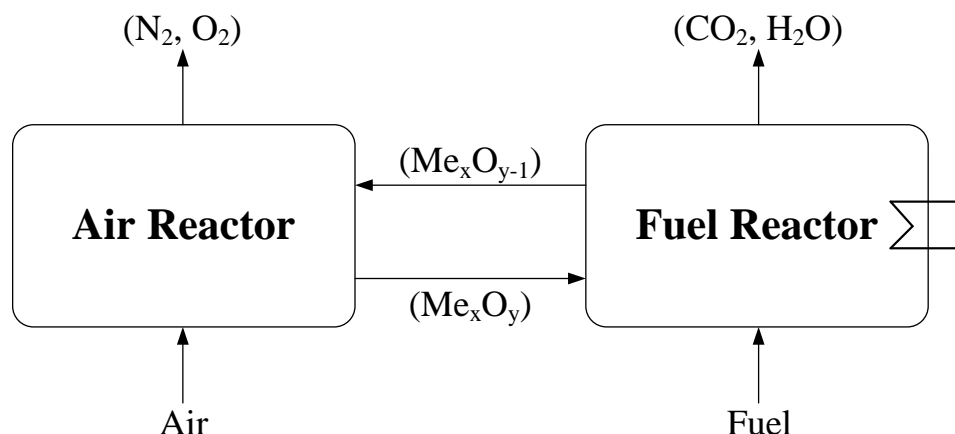
Figure 3-1 Schematic diagram of the conventional CLC process.

In the case of integrating CLC with the Ca-looping process, it is important to satisfy the heat requirement in the fuel reactor (or calciner) because of the limestone calcination. CuO has been defined as the most promising oxygen carrier for this purpose in different studies owing to its highly exothermic reduction with a fuel and high oxygen carrying capacity (Abanades and Murillo, 2009; Abanades et al., 2010; Manovic and Anthony, 2011b; Manovic et al., 2011c). Therefore, there is a heat release in both reactors when CuO is selected as an oxygen carrier in the CLC process. By this way, the exothermic reduction of CuO can provide heat for the endothermic calcination reaction in the calciner. Besides, it is possible to evaporate the water inside the air reactor to control the operating temperature which can increase due to the exothermic oxidation reaction. The heat of fuel combustion in this process is equal to the total heat release in both reactors.

To date, variety of experimental demonstrations using CuO/CaO sorbents have been reported for pre-combustion and post-combustion CO_2 capture applications (Abanades et al, 2010; Manovic and Anthony, 2011d). Al_2O_3 as a support is often included because of the low melting point of CuO (1085°C) and activity loss of CaO due to sintering. Abanades et al. (2010), Fernandez et al. (2012) and Martinez et al. (2014) investigated this combined process for hydrogen production and/or electricity generation from natural gas by sorption enhanced reforming. Abanades and Murillo (2009), and Manovic and Anthony (2011d) proposed different process schemes for its practical implementation for post-combustion applications. Kierzkowska and

Muller (2012) reported that a Ca-Cu composite without any inert support can be manufactured by using a co-precipitation technique. Later, this group indicated that sol-gel derived, calcium-based, copper-functionalised CO_2 sorbents possess excellent oxygen-carrying and stabilised CO_2 uptake capacities (Kierzkowska and Muller, 2013). The performance of MgO supported CaO/CuO (Qin et al., 2012) as well as the effects of thermal pre-treatment of CuO and steam addition on the sorbent performance was also examined (Qin et al., 2013).

The main objective of this section is to investigate the potential combination of the Ca-looping and the CLC processes in order to reduce the energy penalty associated with the use of an ASU in the process scheme presented in Figure 2-4.

3.1.1 Preliminary Analysis

A way of integrating the CLC into the Ca-looping process, hereinafter called Ca-Cu looping process, including three different solid routes is shown in Figure 3-2. This system contains three reactors: a carbonator, a calciner (fuel reactor) and an air reactor. The solids in the system can be circulated in a direction of carbonator → calciner → air reactor → carbonator (Route 1). In addition, Manovic and Anthony (2011d) proposed two other solid circulation routes that are carbonator → calciner → carbonator, labelled as Route 2 and carbonator → air reactor → calciner → carbonator (Route 3) as a reverse of Route 1. In Route 2, an air reactor is not included since it assumes that sufficient oxygen is always present in feed gas to regenerate depleted oxygen carrier. Nevertheless, the oxygen content of cement flue gases (around 1 mol% from 3rd preheater exit) is not enough to oxidize large amounts of oxygen carrier. Therefore, Route 2 has been eliminated. Route 3 is another interesting option and would be a potential candidate. However, the main concern in this scheme is the temperature of the air reactor that needs to be strictly controlled to prevent partial calcination in this reactor. Furthermore, the operating temperature will be lower than that of the calciner which makes the transfer of heat from the air reactor to the calciner unfeasible. Hence, only Route 1 is further analyzed in the rest of this study.
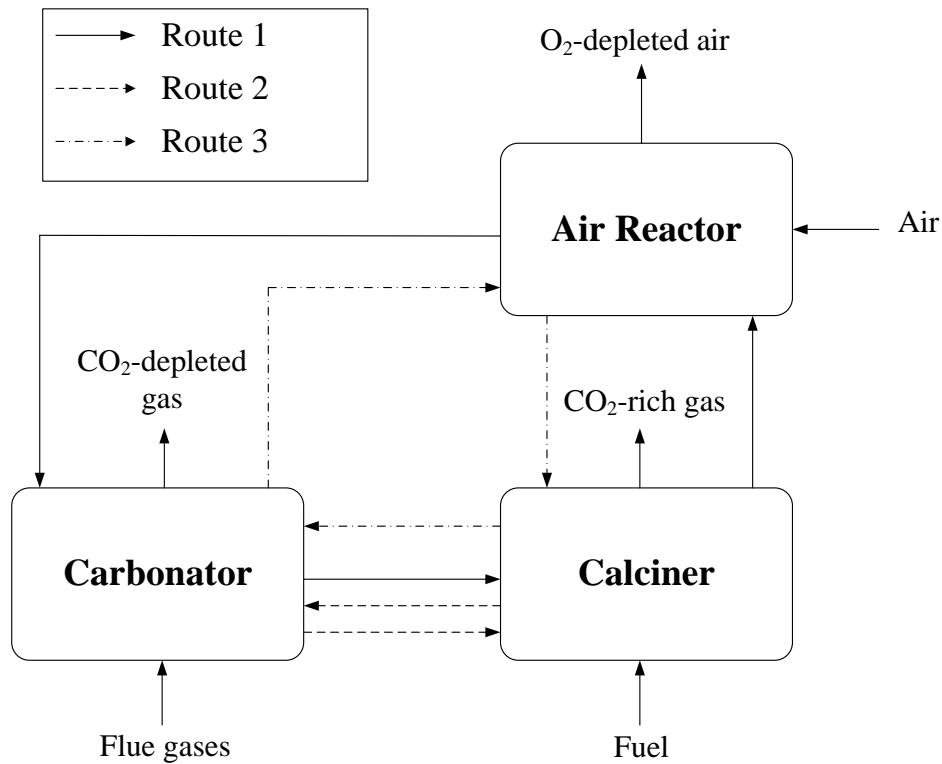
Figure 3-2 Schematic diagram of the Ca-Cu looping process (Manovic and Anthony, 2011d).

It should be noted that the main property of a metal oxide to be employed in this system is its exothermic reduction reaction. In this study a CuO/CaO sorbent supported by Al_2O_3 is used owing to the benefits explained above. Also, methane is used as the fuel, but syngas (CO + H_2) can also be explored as an alternative fuel for the reduction/calcination step. While CaO is the CO_2 capture agent in the carbonator, the heat requirement for the calcination reaction can be satisfied by the reduction of CuO with methane. The Cu leaving the calciner is oxidized back to CuO in the air reactor. All reactions defined in the process simulations are presented in Table 3-1. The sum of oxidation and reduction reactions occurring in two different reactors gives the overall methane combustion reaction as presented below.

$$CH_{4(g)} + 2O_{2\,(g)} \rightarrow CO_{2(g)} + 2H_2O_{(g)} \quad \Delta H = -798\ kJ/mol \quad \text{(Rn. 3.1)}$$
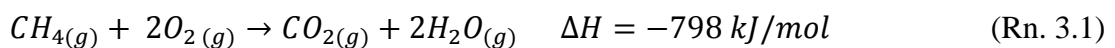
Table 3-1 Chemical reactions defined in the process simulations.

Reaction	Reactor	$\Delta H_{25°C}$ (kJ/mol)
$CaO(s) + CO_2(g) \rightarrow CaCO_3(s)$	Carbonator	−179
$4CuO(s) + CH_4(g) \rightarrow 4Cu(s) + CO_2(g) + 2H_2O(g)$ $CaCO_3(s) \rightarrow CaO(s) + CO_2(g)$	Calciner	−158 +179
$2Cu(s) + O_2(g) \rightarrow 2CuO(s)$	Air reactor	−320

It should be highlighted that only approximately 20% of the heat of methane combustion is usable in the calciner while the remaining should be somehow recovered in the air reactor. Since the main aim is to provide heat into the calciner with less expense in the air reactor, it is clear that a method of heat transfer between the calciner and air reactor is necessary in order to prevent excessive thermal energy requirement in the system. Otherwise, severe heat duties in the capture plant will be required, and there is a strong possibility that those values would be much higher compared to the requirement in the base cement plant.

Rodriguez et al. (2011b) proposed the indirect calcination process that uses high temperature solid circulation from a CFB combustor to a fluidized bed calciner for the purpose of transferring heat required for limestone calcination. In the process, the combustor operates at higher temperatures than the calciner, and heat transferred by hot CaO particles from this reactor satisfies the heat requirement in the calciner. In this manner, the air reactor can be operated at a higher temperature than that of the calciner in Route 1. The surplus heat from this reactor can reduce the heat requirement in the calciner. It would also affect the sorbent composition as well since the required methane and CuO flows reduce parallel with a decrease in the calciner heat requirement. Therefore, the fraction of CuO in the sorbent can potentially be decreased. Another advantage of this approach would be the elimination of cooling requirement in the air reactor. While higher reactor temperatures facilitate heat transfer by reducing solid circulation rates, it is also well-known that they also trigger sorbent degradation due to the sintering.

The air reactor temperature is limited to 950°C, and the effects of high temperature on sorbent performance in the given conditions have been evaluated by experimental analyses. To determine the flow rate of air into the air reactor, the O_2 molar fraction in the O_2-depleted stream is fixed at 3 mol% and complete oxidation is assumed in each cycle (de Diego et al., 2004; Garcia-Labiano et al., 2004). Since the reduction of methane with CuO produces only CO_2 and a significant amount of H_2O lowering the partial pressure of CO_2 in the calciner, the operating temperature of the calciner is set to 880°C by considering a 15°C increase on the equilibrium temperature for complete calcination. The excess CuO ratio is fixed at 30% to guarantee complete reduction of methane in the calciner (Forero et al., 2011). The carbonator operates at 650°C in the previous chapter but the carbonator temperature is set to 700°C in this chapter since it allows the reduction of heat duty in the calciner along with the quantity of solid circulation between the reactors. Although it is well-known that the higher carbonation temperatures reduce the equilibrium carbonation efficiency, this assumption also alleviate the heat requirement in the raw mill at very low F_0/F_{CO2} ratios since the temperature of the CO_2-depleted gas stream sent back to the cement plant will be greater. The rigorous carbonator model has been modified and used for the estimation of the carbonation efficiency.

Due to the expected degradation of the CO_2 uptake capacity as a result of high reactor temperatures, part of the spent sorbent needs to be replaced with fresh sorbent. To capture the CO_2 resulting from calcination of the fresh sorbent, it should be fed to the calciner. If the purge stream is removed from the calciner, the heat released from the Cu oxidation cannot be recovered. To prevent such heat losses, the purge stream should be removed either from the air reactor or the carbonator. At this point, it is not clear in the literature how a purge stream containing $CaO/CaCO_3$, CuO and Al_2O_3 can be utilized. However, CaO and Al_2O_3 are cement raw materials and can potentially be used for clinker production. Kolovos et al. (2005) indicated that the addition of 1 wt% CuO in cement raw meal promotes sintering and improves the burnability of the cement raw meal. Also, its favouring effect on the cement strength development and negligible effect on the physical properties were reported. Ma et al. (2010) mixed a reference cement raw mix with up to 3 wt% CuO. It was demonstrated that CuO promotes CaO consumption and improves the clinkerization

process. CuO content over 1 wt% in the raw meal caused a decrease in the 3-day and 28-day strengths. Thus it is assumed in this study that the purge stream can be removed after the air reactor and used for clinker production with a maximum limit of 1 wt% CuO in the raw meal. However, further studies on this subject is still required since it was reported in another reference (Bhatty et al., 2011) that the copper (I) oxide (Cu_2O) formed under reducing conditions adversely affects the formation of alite and belite phases and significantly decreases the fusion temperature. The use of spent sorbent including CuO would be beneficial for the reduction of the heat requirement in the base cement plant by eliminating the partial need for the limestone calcination, but the operating cost of the system will increase significantly because of the excessive cost of CuO.

It would be preferable to separate the CLC sorbent from the purge and reuse it in the capture system if CuO shows stable oxidation/reduction performances. However, this option requires additional investigation, especially for the separation of the CLC sorbent from the purge and is not considered in the scope of this study. In case of a possibility of the separation of CuO from the purge stream, it would mainly affect the economic performance rather than the process efficiency presented in this section.

3.1.2 Experimental Data for the CLC Sorbent

The experimental CaO and CuO conversion data for the CLC sorbent were provided by Dr. Agnieszka Kierzkowska and Prof. Christoph Müller from the Laboratory of Energy Science and Engineering at ETH Zurich University, Switzerland. The sorbent is a physical mixture of Al_2O_3-stabilized CuO and Al_2O_3-stabilized CaO where the material compositions are 87 wt% CuO and 81 wt% CaO, respectively. The CaO-based sorbent was derived by sol-gel technique while the CuO-based CLC material was co-precipitation based. The details of manufacturing these sorbents were already given in the relevant references (Broda et al., 2012; Imtiaz et al., 2012) and are not repeated here. The CaO and CuO conversion performances of the sorbent were measured by a thermo-gravimetric analysis (TGA). The sorbent was calcined at 850°C under 10% CH_4 for 20 minutes and carbonated at 700°C with 36 mol% CO_2 for 40 minutes. The oxidation took place at 950°C under

10% O_2 for 25 minutes. It should be noted that part of the experimental conditions differ from the simulation inputs, for example air is selected as an oxidation agent in the process simulations and the cycle times are very long for the carbonator model in use. Furthermore, because of the operational limitations of the TGA system, only 10% CH_4 was fed to the system instead of 100% CH_4 assumed in the simulations. The use of diluted CH_4 reduces the effect of sintering related to the CO_2 partial pressure. However, it is acknowledged that the currently available data is sufficient for the preliminary analysis of the proposed configuration with a sensitivity analysis on the sorbent performance.

3.1.3 Modification of the Rigorous Carbonator Model and Process Integration

The following equation proposed by Li et al (2008) was used to fit the experimental CaO conversion data for the sorbent as it provides an accurate regression of the data:

$$X_{max,N} = a_1 f_1^{N+1} + a_2 f_2^{N+1} + b \qquad \text{(Eq. 3.1)}$$

where a_1, a_2, f_1, f_2 and b are the constants, and N is the cycle number.

Another important term that needs to be revised in the rigorous carbonator model, when it is used in the Ca-Cu looping process, is the mass fraction of particles after N cycles, r_N (Eq. B3 in Appendix B). The solids leaving the calciner are fed to the air reactor while the majority of the solid stream leaving this reactor is recycled to the calciner for heat transfer in the Ca-Cu looping process. The effect of high temperatures on sorbent performance in the air reactor has been included in the model by implementing relevant experimental data; however, it needs to be kept in mind that the solid circulation does not exist in the experimental setup. According to the experiments conducted by Grasa and Abanades (2006) where the calcination and carbonation temperatures were set to 950°C and 650°C, respectively using La Blanca limestone, the calcination time is only effective on the sorbent performance for initial cycles, but this effect disappears in the following cycles. Following this argument, we assumed that the circulation of solids between the air reactor and the calciner

corresponds to having longer solid residence times in the calciner since no carbonation occurs in the air reactor. Therefore, Eq. B3 has been kept as it is in the model and the potential effects on the initial performance of the sorbent have been neglected. Nevertheless, it should be noted that the accuracy of this assumption diminishes at high F_0/F_{CO2} ratios because the early performance is more crucial if the sorbent does not stay in the system for a high number of cycles.

The final implementation of the Ca-Cu looping process with the base cement plant is presented in Figure 3-3. Following the proposed process integration of the Ca-looping process with the base cement plant given in Chapter 2, the flue gases from the 3rd preheating stage are diverted to the carbonator for CO_2 capture and the CO_2-depleted stream from this reactor is routed back to the 2nd preheater for raw meal preheating. The heat duty of the CO_2-depleted stream is not enough to satisfy the heat requirement in the raw mill. Thus, the excess air from the clinker cooler should be used for raw material heating as presented. The majority of excess heat from high temperature O_2-depleted gases leaving the air reactor is transferred to the air feed so there is a need for a tubular regenerative air heater (DOE, 2003). The temperature of the O_2-depleted stream can be further reduced by preheating the make-up and methane streams with a final temperature of 150°C. The purge stream containing CaO, CuO and Al_2O_3 from the air reactor is mixed with the pre-calcined raw meal and used for clinker production. Since part of the requirements of CaO and Al_2O_3 are provided from the capture unit, the flow rates of these materials in the cement raw meal have been adjusted in order to keep the clinker production rate similar to that in the base cement plant.

For a direct comparison of the Ca-Cu looping process with the Ca-looping process, in addition to the outcomes of Chapter 2, the process scheme presented in Figure 2-4 has been updated using methane as fuel in the calciner at similar F_0/F_{CO2} ratios determined for the Ca-Cu looping process. There are some benefits of using methane in this scheme compared to a coal-fired calciner even though the cost of coal is usually cheaper than that of the methane. First, since a significant amount of H_2O is formed during combustion in this reactor lowering the CO_2 partial pressure, the required calcination temperature for complete calcination reduces. Furthermore,

the negative effects of sulphur and ash from coal on the sorbent performance can be prevented. To be consistent with the Ca-Cu looping process, the calciner also operates at 880°C in this scheme while the carbonator temperature is set to 700°C. The experimental data for the natural limestone was also provided by the Laboratory of Energy Science and Engineering at ETH Zurich University where the limestone was calcined in 63 mol% CO_2 at 880°C and carbonated at 700°C with 35 mol% CO_2 during the TGA experiments.
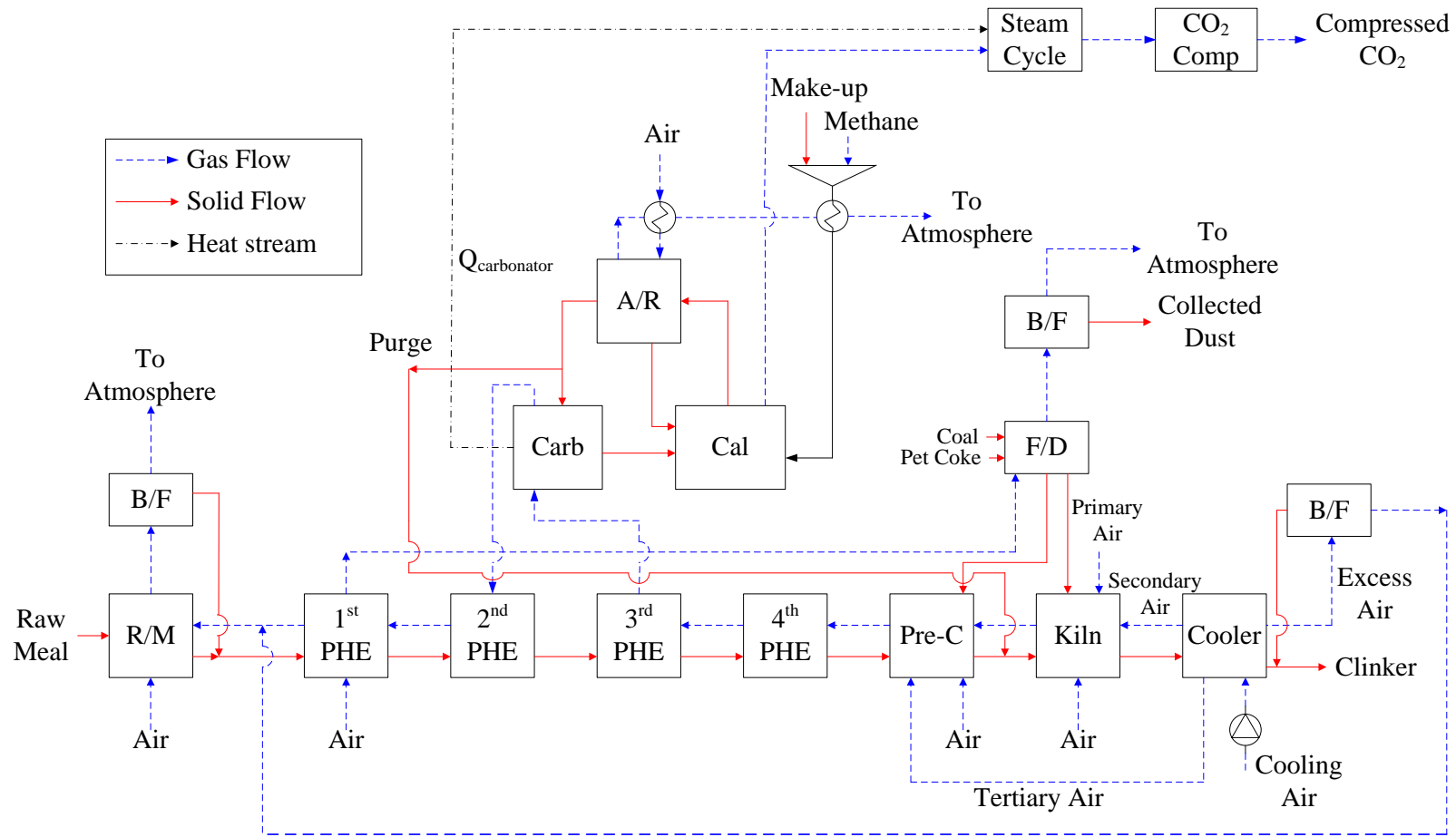
Figure 3-3 Schematic diagram of the process integration of a cement plant with an integrated Ca-looping/CLC unit. Abbreviations: **R/M**, Raw Mill; **B/F**, Bag Filter; **F/D**, Fuel Drying; **PHE**, Preheater; **Pre-C**, Pre-calciner; **Carb**, Carbonator; **Cal**, Calciner (Fuel Reactor); **A/R**, Air Reactor; **CO$_2$ Comp**, CO$_2$ Compression.
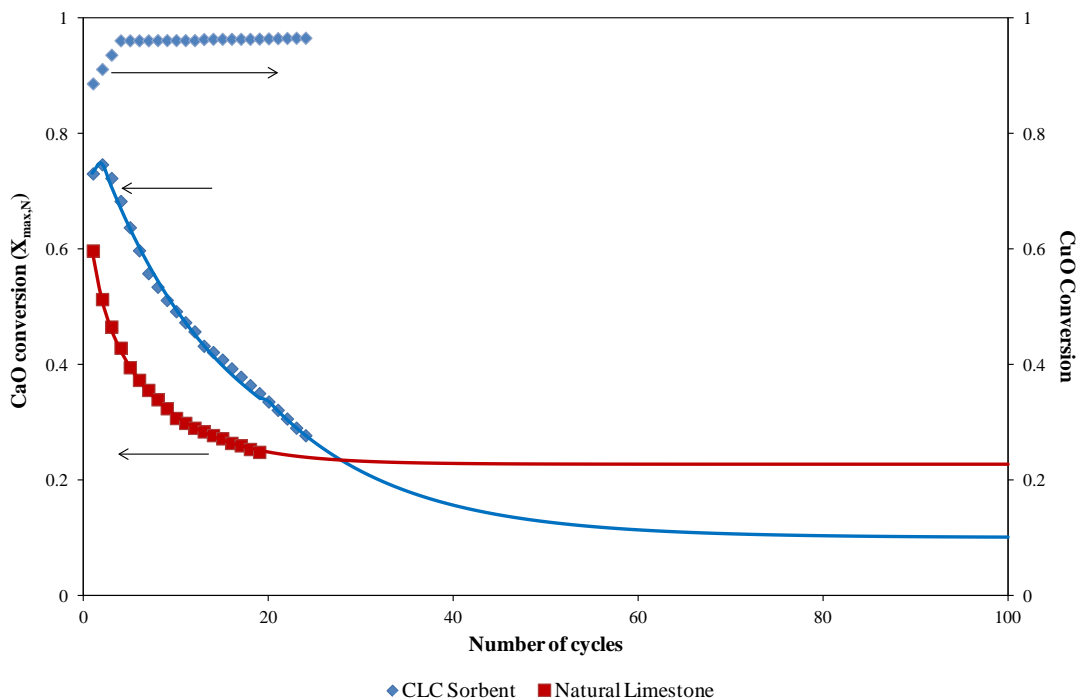
Figure 3-4 Experimental data for the CLC sorbent (74.0 wt% CaO, 7.5 wt% CuO balanced with Al_2O_3) and natural limestone used in the rigorous carbonator model (Ozcan et al., 2013).

3.1.4 Results and Discussion

The experimental performances of the CLC sorbent with a composition of 74.0 wt% CaO and 7.5 wt% CuO balanced with Al_2O_3 and natural limestone are presented in Figure 3-4 (Ozcan et al., 2013). With a support of preliminary mass and energy balance calculations with simultaneous experimental investigations, the composition of the CLC sorbent estimated by the process simulator (75.9 wt% CaO, 5.5 wt% CuO balanced with Al_2O) is close to that of the experimentally tested CLC sorbent. The CaO conversion efficiency is initially higher for the CLC sorbent, but its degradation is more severe compared to the natural limestone, which can be linked to the higher temperature in the air reactor and corresponding sintering effect. The negative effects of sintering can be reduced by operating the air reactor at temperatures lower than 950°C (and above 880°C); however, very low temperature differences would complicate the solid circulation between the air reactor and calciner. The CaO conversion curves were fitted using Eq. 3.1, and the fitting constants are given in Table 3-2. For the CLC sorbent, a two-step fitting procedure has been followed for more accurate regression of the data.

Table 3-2 The fitting parameters for the CLC sorbent and limestone.

	a_1	a_2	f_1	f_2	b
Limestone	0.3836	0.3993	0.8714	0.4437	0.2274
CLC (N≤19)	−25.94	0.7126	0.04966	0.929	0.1801
CLC (N>19)	1.072	2.968	0.9306	0.3252	0.1006

The first set of parameters belongs to cycle numbers ≤19 and the second is for the remaining cycles (up to 24 cycles). It would be preferable to fit the experimental data for the CLC sorbent when its CaO conversion rate becomes constant but the current method is appropriate given the data available. After a rapid increase in CuO conversion rates of the CLC sorbent in the first 4 cycles, it remains stable during the 24 cycle TGA analysis, which proves that there is a strong potential of using purged CuO again in the capture system. This can also be supported by previous experimental studies on the subject (Qin et al., 2012; Kierzkowska and Muller, 2013). As mentioned previously, the reuse of purged CuO will allow significant reductions in the variable cost of the system compared to the case where it is dumped as waste.

The main variables from mass and energy balances including those for the base cement plant are presented in Table 3-3. Two different systems, Ca-looping and Ca-Cu looping processes have been compared, and the impact of the F_0/F_{CO2} ratio has been investigated. The F_0/F_{CO2} ratio is initially assigned and the required F_R/F_{CO2} ratio is calculated to achieve 90% CO_2 avoidance by keeping the CO_2 capture efficiency between 88 – 90% in the carbonator and using an assumption of 100% capture efficiency in the calciner. The F_0/F_{CO2} ratio is limited to 0.15 to produce a CuO weight fraction of 1% in the cement raw meal. A smaller value of 0.02 F_0/F_{CO2} has been included to investigate the effect of purge flow on the process performance. It should be noted that the minimum allowable F_0/F_{CO2} ratio given in Chapter 2 was determined to be 0.20 whereas it can be reduced to 0.15 here since the carbonator operates at 700°C so the CO_2-depleted stream sent to the cement plant is at a higher temperature. Nevertheless, for the 0.02 F_0/F_{CO2} case, the excess air stream fed to the raw mill should be heated up using the hot gas streams available in the capture plant before being sent to the raw mill, which increases the complexity of the system.

Table 3-3 Simulation outputs of the proposed schemes in Section 3.1, including those for the base cement plant.

	Base Cement Plant	Ca-looping (I)	Ca-looping (II)	Ca-Cu looping (I)	Ca-Cu looping (II)
Carbonator model inputs					
F_0/F_{CO2}	-	0.02	0.15	0.02	0.15
F_R/F_{CO2}	-	4.2	3.1	9.4	2.0
CO_2 recovery in the carbonator (%)	-	90.0	88.2	89.7	88.0
CO_2 intensity (ton CO_2/ton clinker)	0.8	0.08	0.08	0.08	0.08
Thermal energy requirements (GJ_{th}/ton clinker)					
Cement plant	3.13	3.09	2.72	3.08	2.67
Capture plant	-	4.30	4.0	7.37	4.38
Power generation (MW_e)					
CO_2-rich gas	-	13.1	13.5	19.0	16.2
Carbonator	-	46.4	36.3	80.4	37.6
Power consumption (MW_e)					
ASU	-	10.0	9.2	-	-
Compression (inc. blowers)	-	14.7	14.0	18.0	14.7
Cement plant auxiliaries	13.7	13.7	13.6	13.7	13.8
Net power (MW_e)	−13.7	21.1	13.0	67.7	25.3
CO_2 avoidance rate (%)	-	90.0	90.0	90.0	90.0
Incremental energy consumption (GJ_{th}/ton CO_2 avoided)	-	2.6	2.5	2.2	1.7
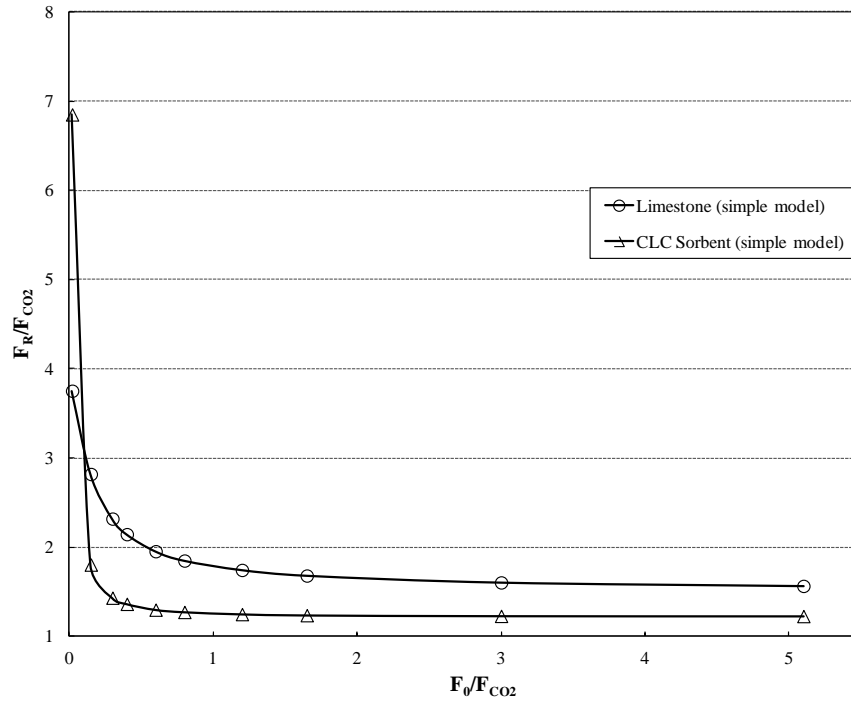
Figure 3-5 Corresponding F_R/F_{CO_2} values estimated by the simple carbonator model for the given range of F_0/F_{CO_2} to reach 90% capture efficiency in the carbonator. The results are shown for two different sorbents, CLC sorbent and natural limestone.

In both configurations, the required F_R/F_{CO_2} ratios decrease with increasing F_0/F_{CO_2} rates as more fresh sorbent enters into the system and improves the activity of the CO_2 sorbent. The level of reduction is greater for the Ca-Cu looping process, mostly because of the change in the average carbonation efficiency (X_{ave}) (see Appendix B). As the simple model is only based on average carbonation efficiency calculations, the F_R/F_{CO_2} estimates for a predefined range of F_0/F_{CO_2} by using this model is shown in Figure 3-5 to support the results obtained by the rigorous model. The required F_R/F_{CO_2} is greater for the CLC sorbent when F_0/F_{CO_2} is smaller than 0.1, but after this point an opposite behaviour is observed. The difference in the behaviour can be related to change in sorbent performance after number of carbonation/calcination cycles as presented in Figure 3-4.

The thermal energy requirement in the cement plant reduces in the capture cases owing to the transfer of pre-calcined limestone from the capture plant, lowering the heat duty in the pre-calciner and kiln. With increasing purge flows, the thermal energy requirement of the cement plant reduces to a minimum of 2.7 GJ_{th}/ton clinker. The modest difference between the 0.15 F_0/F_{CO_2} cases can be associated with Al_2O_3

in the purge of the Ca-Cu looping process as this, when supplied from the capture system, reduces the heat duty associated with its preheating in the cement plant. For all capture cases, the total thermal energy requirement is more than double of that of the base cement plant. It is clear that if the heat transfer between the air reactor and calciner does not exist in the Ca-Cu looping process, the current estimates for this system would further increase significantly.

Part of the energy can be recovered from the carbonator and CO_2-rich gas stream to drive a steam cycle for power generation, which can then be used to meet the demand in the cement and capture plants arising from the cement plant auxiliaries, CO_2 compression unit and ASU, if needed. For this purpose, the methodology explained in Chapter 2 has been retained for the estimation of power generation, and the calculated power generation/consumption values are also summarized in Table 3-3. The difference between the power generation and total power consumption is referred to as net power generation. A negative value was calculated for the base cement plant since the demand in this plant can only be fulfilled by power import. The major advantage of eliminating the need for an ASU is the reduced power consumption in the Ca-Cu looping process. The incremental energy consumption estimates covering also the power requirement for CO_2 compression and ASU (if needed) and considering heat recovery for power generation reduce to 1.7 GJ_{th}/ton CO_2 avoided at 0.15 F_0/F_{CO2} compared with 2.5 GJ_{th}/ton CO_2 for the Ca-looping scheme at the same F_0/F_{CO2}. In comparison with the outcomes of Chapter 2, where the effect of sulphation on the sorbent performance is considered, the incremental energy consumption estimates for the Ca-looping scheme presented in this chapter are smaller at low F_0/F_{CO2} ratios. This can be linked to the reduced total thermal energy requirements as a result of the improved performance of the sorbent.
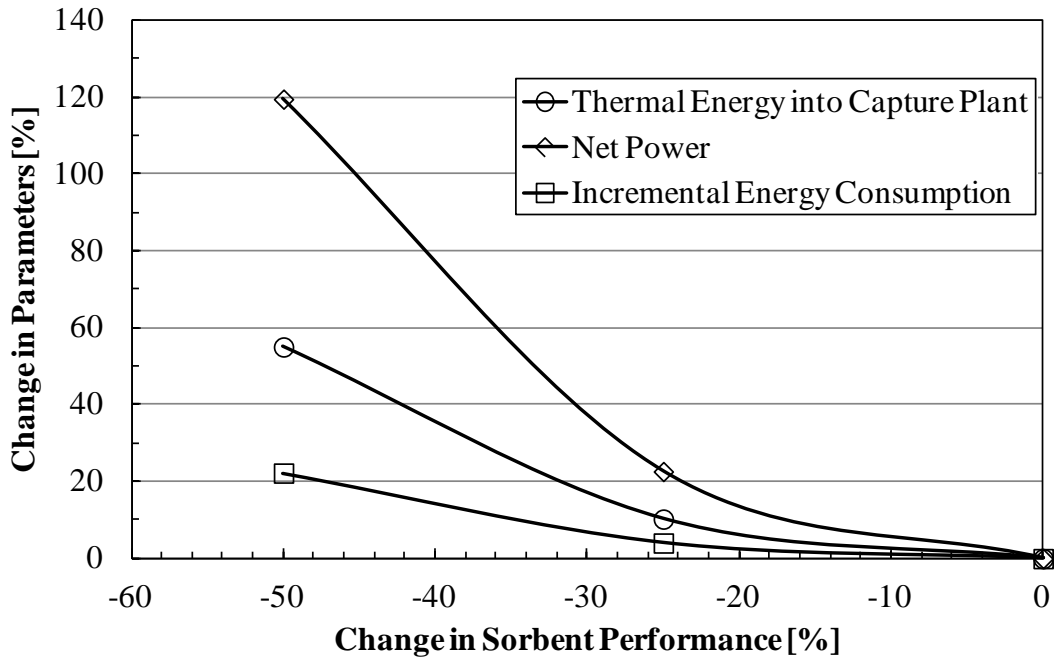
Figure 3-6 The sensitivities of the thermal energy requirement in the capture plant (MW_{th}), net power capacity (MW_e) and incremental energy consumption (GJ_{th}/ton CO_2 avoided) against the change in sorbent performance for the Ca-Cu looping (II) case.

The sensitivity of the main results for the Ca-Cu looping (II) case against the sorbent performance is given in Figure 3-6. Even though it is not possible to predict precisely the CaO conversion behaviour of a sorbent without conducting relevant experiments, the CaO conversion performance of the CLC sorbent has been reduced by 25% and 50% for a brief analysis. The ratio of F_0/F_{CO2} has been retained at 0.15 so the main difference results from the change in required F_R/F_{CO2} to achieve 90% CO_2 avoidance. By lowering the sorbent performance by 25% and 50%, the required F_R/F_{CO2} increases to 3.3 and 9.1, respectively. At very high F_R/F_{CO2} ratios, the amount of solid circulation between the reactors increases, and this triggers the thermal energy requirement in the capture plant. With a reduction of 50% in the sorbent performance, the thermal energy requirement increases by 55% while the net power capacity correspondingly reaches 55.5 MW_e. The incremental energy consumption estimate is calculated to be 2.0 GJ_{th}/ton CO_2 avoided for the worst scenario in proportion to severe thermal energy requirement and compression unit duty in the capture plant, but it is still lower than that of equivalent Ca-looping process for which the results have been given in Table 3-3.

Given the postulate that the limitation of 0.15 F_0/F_{CO2} is only valid for the Ca-Cu looping process to restrict the quantity of CuO in the cement raw meal, this ratio can be set higher for the Ca-looping process as already shown in Chapter 2. The incremental energy consumption for the CO_2 capture in the cement plant by using the Ca-looping process could be reduced to as low as 2.3 GJ_{th}/ton CO_2, which is the value calculated for the 'oxy-calciner only' case at 90% CO_2 avoidance in Chapter 2. However, the energy consumption increases further with a decrease in F_0/F_{CO2} ratio as well as depending on the deficiency in sorbent performance. Therefore, it can be concluded that among the CaO-based carbon capture options presented in Chapter 2 and this chapter, the Ca-Cu looping process requires the lowest incremental energy consumption. If there is an economical way to separate/reuse of CuO/Al_2O_3 sorbent from the purge, the energy consumption in the Ca-Cu looping process is possibly improved further by increasing the F_0/F_{CO2} ratio as demonstrated for the Ca-looping process in Chapter 2. Moreover, the capital cost requirement of the system can potentially be reduced by the elimination of an ASU. However, a detailed economic analysis is necessary to see the impact of the excessive cost of CuO.

3.2 Indirect Calcination Process

In this section, the process integration of the indirect calcination process existing in the literature (Rodriguez et al., 2011b) into the base cement plant is investigated. The indirect calcination process allows separation of CO_2 from limestone calcination in a concentrated form. Even though the reference indirect calcination design was proposed for CO_2 capture from a cement plant, its complete integration has not been analyzed to date. The raw mill, preheater and kiln existing in a conventional cement plant were not included in the process analysis. Furthermore, only the calcination reaction was considered while clay decomposition and clinkerization reactions were not taken into account. The process integration given in this section aims to minimize the total thermal energy requirement by using excess energy from high temperature flue gas streams for raw meal preheating as in the conventional cement manufacturing process. It also considers the use of an additional CO_2 capture unit combined with the indirect calcination process, called hybrid configuration, since the standalone indirect calcination application can only provide a moderate level of CO_2

avoidance. For this purpose, an aqueous amine process removes the remaining CO_2 relating to clinkerization occurring at the cement kiln and fuel combustion for the indirect calcination process.

3.2.1 Fundamentals of the Indirect Calcination Process

Figure 3-7 shows the schematic diagram of a novel indirect calcination process which separates fuel combustion and limestone calcination into two distinct chambers. The calciner operates at 930ºC for the complete calcination of limestone in the raw meal. The high temperature solid stream from the combustor (>1000ºC) is transferred to the calciner to meet the heat requirement for the endothermic calcination reaction. The combustor temperature is initially set to 1050°C but is later altered to illustrate the effect of temperature difference on solid flux and solid circulation rate. The combustor should be designed by adhering to the limits of temperature and solid flux in the commercial CFB combustion systems. High temperature CFB combustion systems are well established technologies for ore roasting, phyrohydrosis of spent potlining and aluminium hydroxide calcination processes with operating temperatures of 1050ºC, 1200ºC and even up to 1450ºC, respectively (Reh, 1995), and allowable solid flux rates of between 10-100 kg/m^{2}s (Bi and Liu, 2012).
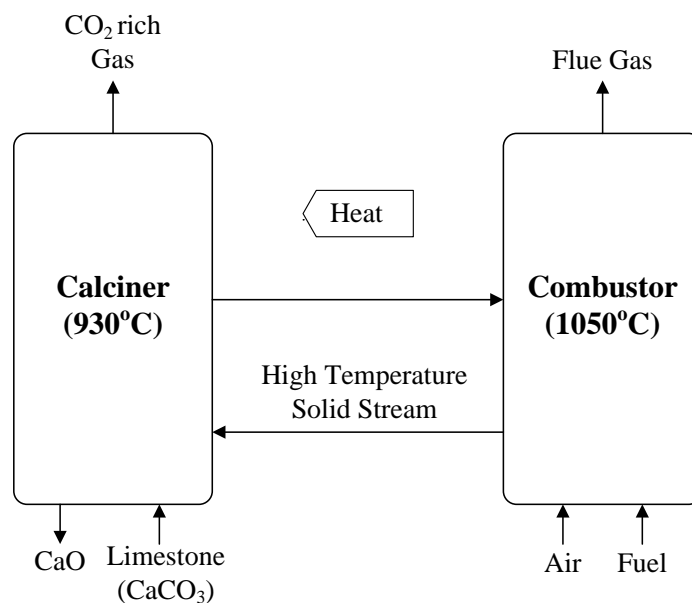
Figure 3-7 Schematic diagram of the indirect calcination process (Rodriguez et al., 2011b).

The high temperatures in the CFB combustor will restrict the fuel characteristics due to ash softening problems. Therefore, the pet coke used in the kiln of the base cement plant, is burnt in the combustor. The composition of the pet coke has already been given in Table 2-5. The use of pet coke with high sulphur content in the combustor exacerbates $CaSO_4$ formation since it is assumed that all of the SO_2 generated in the combustor reacts with CaO and is irreversibly converted to $CaSO_4$.

3.2.2 Process Integration of the Indirect Calcination Process

To prevent the circulation of significant amounts of clay minerals with CaO and their interaction at the given temperature range, limestone and clay minerals are fed into two separate raw mills as presented in Figure 3-8. The moisture-free limestone from the raw mill is fed to a preheater, where its temperature subsequently increases by heat exchange with hot gas streams from the combustor and cooler. The excess air from the cooler is initially at 279°C but is further heated up to 880°C in a regenerative heat exchanger while the CO_2-rich gas stream leaving the calciner at 930°C is cooled to 330°C. While the limestone stream from the preheater is sent to the calciner solely, the product CaO from this reactor is mixed with preheated clay before the kiln stage.

Since high solid temperatures are achieved in the limestone preheater, the assumption of 10% calcination in the preheater given in Chapter 2 has been retained. Accordingly the corresponding CO_2 emissions cannot be captured. Having been cooled to certain temperatures in the limestone preheater, the exit gas stream is able to cover the heat requirement in the limestone raw mill and fuel drying unit. Since there is no combustion occurring in the calciner anymore, the tertiary air at 908°C can be entirely fed to the combustor. The heat requirement in the kiln reduces with the assumption of complete calcination of limestone in the calciner. All surplus secondary air at 1025°C, which is not needed in the kiln anymore, can also be transferred to the combustor. Finally, the excess air from the clinker cooler is able to cover the remaining requirement in the combustor. In the clay preheater, the flue gases from the kiln heats up the clay and leaves the system at 110°C.
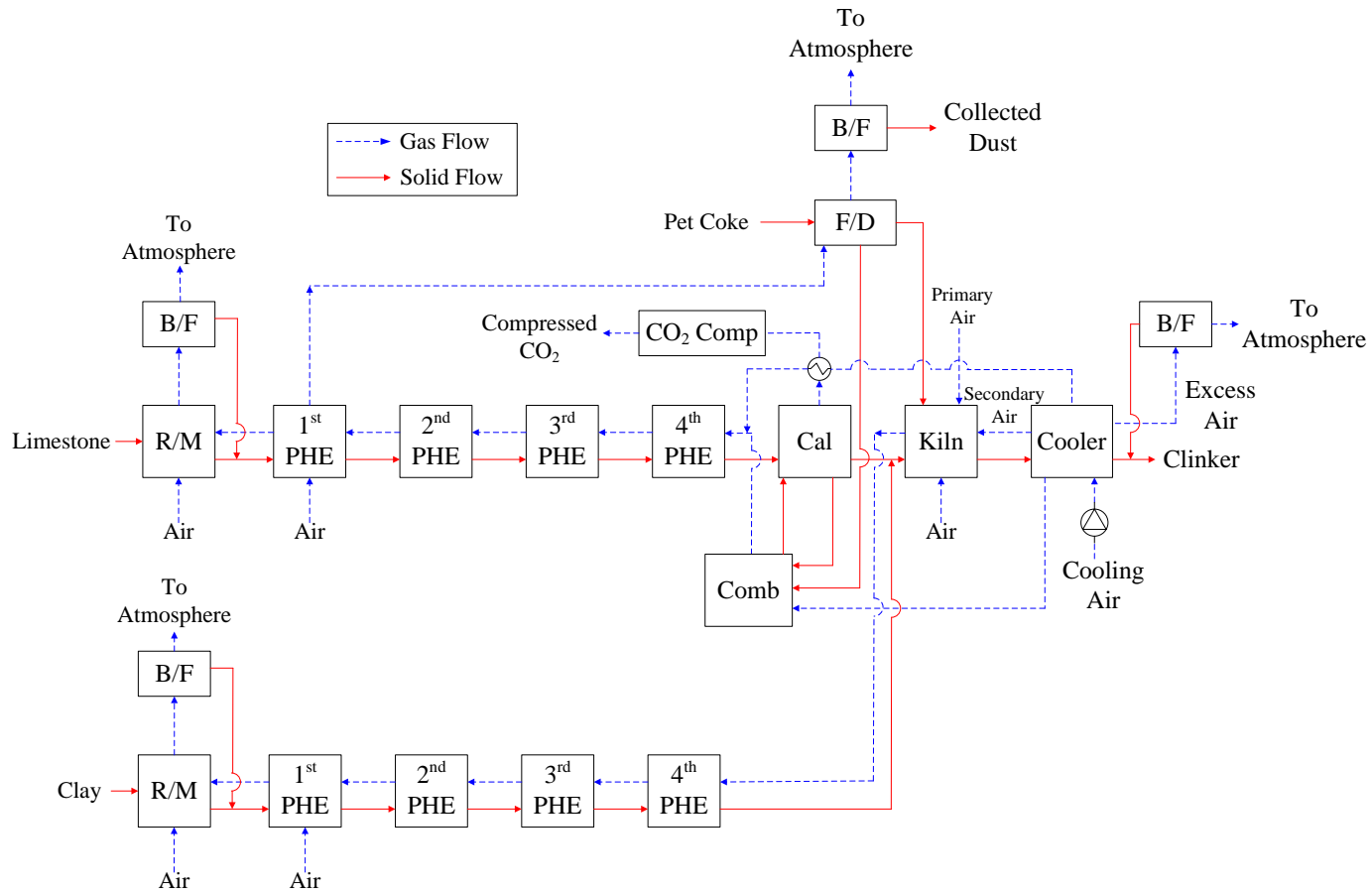
Figure 3-8 Schematic diagram of the process integration of a cement plant with an indirect calcination process. Abbreviations: **R/M**, Raw Mill; **B/F**, Bag Filter; **F/D**, Fuel Drying; **PHE**, Preheater; **Cal**, CFB Calciner; **Comb**, Combustor; **CO₂ Comp**, CO₂ Compression.

The presence of CaO and SiO_2 in a single preheater system leads to formation of belite (C_2S) phase under the conditions of final preheater stage and pre-calciner as detailed in Chapter 2. Since the CaO and clay minerals are mixed just before the kiln stage in this configuration, belite formation is postponed. Thus, it would be needed to adjust the residence time in the kiln by controlling its rotational speed so that the same clinker composition with the base cement plant can be obtained. Accordingly an additional reaction step prior to the kiln stage needs to be included in the simulation of the indirect calcination process where belite formation occurs.

Although air leakages in the raw mills, preheaters and kiln are not so critical for this configuration and included in its simulation, it is very important to minimize air leakage in the calciner to prevent the dilution of the CO_2 rich stream. Also, part of the CO_2 released in the calciner can be transferred to the combustor (or vice versa) on the pores and interparticle voids of the circulated solids even though very low gas transfer rates are expected. In this chapter, air leakages into the new CFB systems have been neglected as in Chapter 2; however, the negative impacts of air leakages on CO_2 purity can clearly be seen in Chapter 5.

3.2.3 Amine Process and Its Process Integration

The schematic diagram of the amine process that is attached to the base cement plant is shown in Figure 3-9. To obtain accurate performance predictions for the absorber and stripper, the add-on amine thermodynamic package in UniSim Design is employed. Since the primary purpose of this section is to evaluate alternative carbon capture options rather than optimization of the absorber and stripper designs, the process conditions given in Ahn et al. (2013) have been adapted. The technical modelling parameters for the amine process are presented in Table 3-4.

The feed gas stream is initially sent to a cooler, where it is cooled to 32°C and part of the water is condensed out. It is then pressurized to 1.31 bar by a blower prior to the absorption stage. The lean amine concentration is set to 30 wt% by adjusting MEA and water make-up flowrates. The CO_2-rich sorbent is pumped to the section at the bottom of the striper that operates at 1.93 bar. A water wash tower is included for the recovery of vaporised MEA which is then sent back to the absorber.
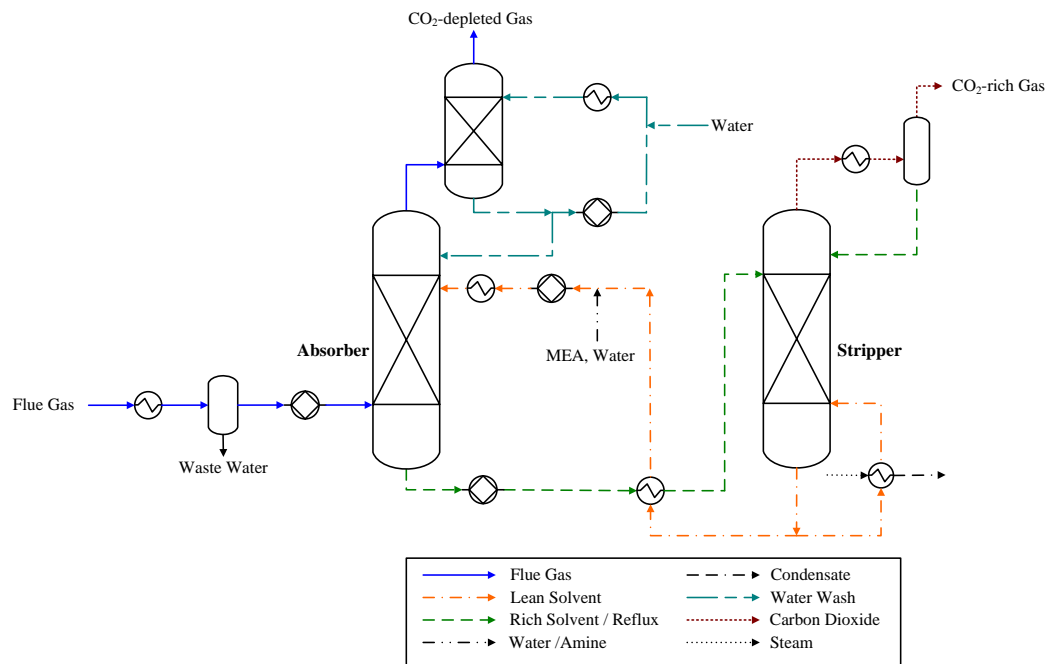
Figure 3-9 Schematic diagram of the amine process (Ahn et al., 2013).

An important design issue for the amine process is to satisfy the heat duty in steam stripper for solvent regeneration. The CHP plant configuration reported by the IEA (2008) is attached to the amine plant configuration, and its schematic diagram is presented in Figure 3-10. In the CHP plant, the main steam at 500°C and 130 bar is blown into a turbine for power generation and is then fed to the reboiler at 144.7°C and 3.5 bar. The power generation in the CHP plant partially/completely fulfils the power requirements in both base cement and carbon capture plants.

Table 3-4 Main modelling parameters for the amine process.

		Unit
Solvent	Monoethanolamine (MEA)	-
MEA concentration	30	wt%
Absorber feed gas temperature	43.5	°C
Absorber feed gas pressure	1.31	bar
Stripper bottom pressure	1.93	bar
Stripper feed temperature	100	°C
Steam source	CHP plant	-
CHP plant steam conditions	500 / 130	°C / bar
Steam provided to the reboiler	144.7 / 3.5	°C / bar
Steam after the reboiler	138.5 / 3.5	°C / bar
NO_x control	Ammonia SCR	-
SO_x control	Wet-limestone FGD	-
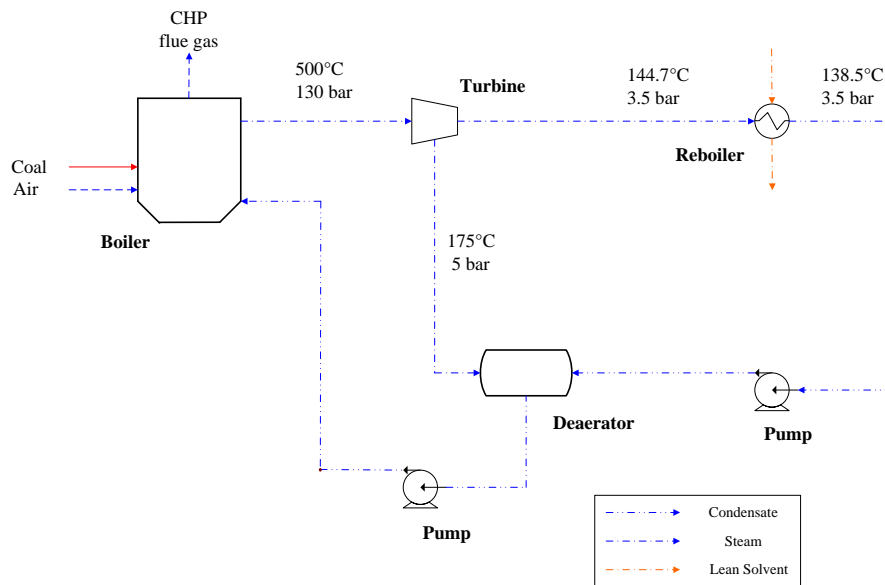
Figure 3-10 Process schematic of the CHP plant (IEA, 2008).

Two different configurations have been assessed for the integration of the amine process into the base cement plant. The corresponding schematic diagrams shown in Figures 3-11(a) and 3-11(b) are for the hybrid configuration and the standalone amine process, respectively. The hybrid configuration is comprised of the indirect calcination process and an amine process. In this system, the excess air from the cooler, after being heated up by hot CO_2-rich gas from the calciner, is fed to the CHP plant instead of the limestone preheater. In that way the temperature of the solid stream in the limestone preheater and relevant partial calcination level can be kept similar to those in the base cement plant. The CHP plant simultaneously generates steam for the solvent regeneration and produces electricity. Therefore, the thermal energy requirement in the CFB combustor located in the hybrid configuration is expected to be higher compared to that in the standalone application of the indirect calcination process. The CHP plant configuration employed in this system would be similar to large scale CFB combustion systems for CHP plants which are commercially in operation and will be scaled up to 600 MW_e in a near future (Nuortimo, 2013). The conventional CHP plant layout presented in Figure 3-10 has been modified in the hybrid configuration to include solid circulation between the reactors while the reference steam conditions have been retained.

(a)

(b)
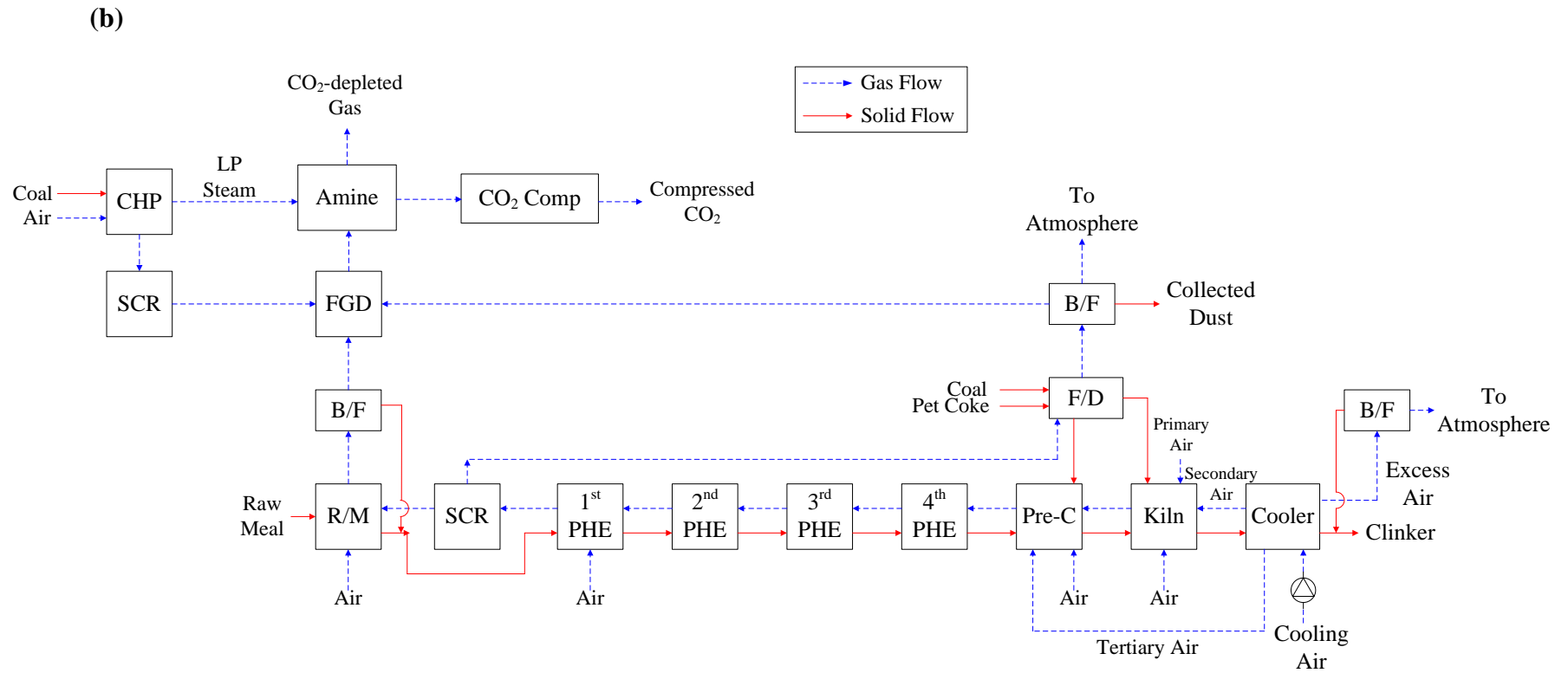
Figure 3-11 Schematic diagram of the process integration of a cement plant with (a) hybrid configuration; (b) standalone amine process. Abbreviations: **R/M**, Raw Mill; **B/F**, Bag Filter; **F/D**, Fuel Drying; **PHE**, Preheater; **Pre-C**, Pre-calciner; **Cal**, CFB Calciner; **CHP**, Combined heat and power plant; **SCR**, Selective Catalytic Reduction Unit; **FGD**, Flue Gas Desulphurization Unit; **Amine**, Amine Scrubbing Process; **CO₂ Comp**, CO_2 Compression.

For the reduction of NO_x in the feed gas stream, two SCR units are located between the raw mills and the preheaters as suggested by IEA (2008). The temperature of the gas streams at these locations is around 320°C, and the reductant in the SCR units is selected to be 25% ammonia solution. The flue gas stream from the bag filters are blown into an FGD unit for SO_x removal before it is fed to the amine process. The solvent flow rate in the amine process is varied in order to achieve 90% CO_2 avoidance in the system.

The second option presented in Figure 3-11(b) shows an end-of-pipe integration of the amine process in the base cement plant. The same type of coal as in the base cement plant is burnt in the CHP plant, the composition of which is already given in Table 2-5. The flue gas stream from the CHP plant, after passing through an SCR unit, is mixed with the flue gas stream from the base cement plant and is fed to an FGD unit. The SO_x- and NO_x-depleted flue gas stream is then transferred to the amine plant. As before, the CO_2 avoidance rate is set to 90% by adjusting the solvent flowrate in the absorber. The CO_2-rich gas stream from the stripper is sent to a CO_2 compression unit in both configurations. The design of this unit is identical to the one detailed in Chapter 2.

3.2.4 Results and Discussion

Figure 3-12 presents the stream properties of the calciner, combustor and kiln system in the standalone indirect calcination process for the production of 113.0 ton clinker/h. As pet coke is fed into the combustor instead of coal as in the pre-calciner of the base cement plant, the ash content of clinker produced in this system is lower. Thus, the slight reduction in the clinker product rate compared to that of the base cement plant (113.8 ton clinker/h) can be associated with the reduced flow rate of ash in the clinker. However, the clinker composition is almost identical in both plants. It is well-known that the perfect match between clinker compositions facilitates the calculation of robust mass and energy balances as a result of the enthalpy changes related to the clinkerization reactions.
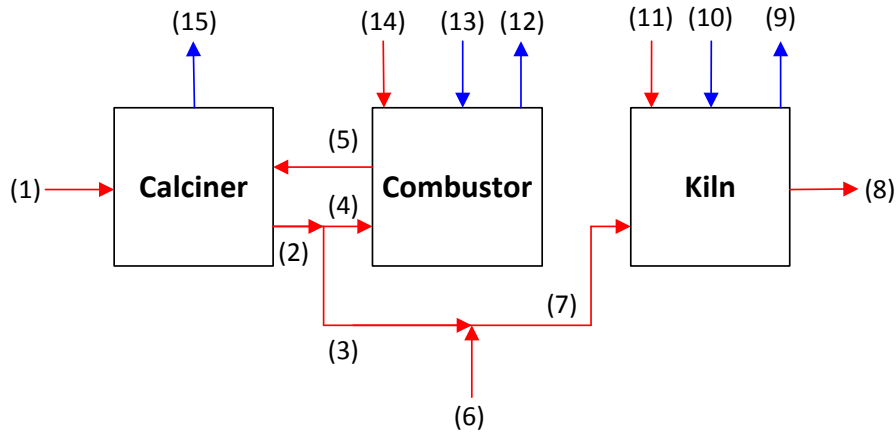
Stream	Description	Temperature (^{o}C)	Mass Flow (ton/h)
(1)	CaO/CaCO$_3$	725	129
(2)	CaO	930	2048
(3)	CaO to kiln	930	78
(4)	CaO to combustor	930	1970
(5)	CaO to calciner	1050	1972
(6)	Clay	750	53
(7)	CaO/Clay	845	131
(8)	Clinker	60	113
(9)	Kiln flue gas	1025	54
(10)	Secondary air/Primary air	1025	33
(11)	Fuel to kiln	101	3
(12)	Combustor flue gases	1050	106
(13)	Air mixture	794	100
(14)	Fuel to combustor	101	8
(15)	CO$_2$-rich gas	930	53

Figure 3-12 Stream properties of the main flows of indirect calcination process integrated into the base cement plant (Figure 3-8).

The temperature of the CaO/CaCO$_3$ stream (stream 1) entering the calciner is 725°C as a result of heat exchange with the hot gases in the limestone preheater. The high solid feed temperatures reduce the thermal energy requirement in the calciner so that it is lower compared to that of the reference indirect calcination configuration (Rodriguez et al., 2011b) where almost the same quantity of limestone is fed to the calciner at the ambient temperature. Accordingly the flow rate of the solid recycle is reduced to 1970 ton/h compared to 3200 ton/h reported in the literature. The recycled solid stream comprises of mainly CaO (97 wt%) with some ash and CaSO$_4$.
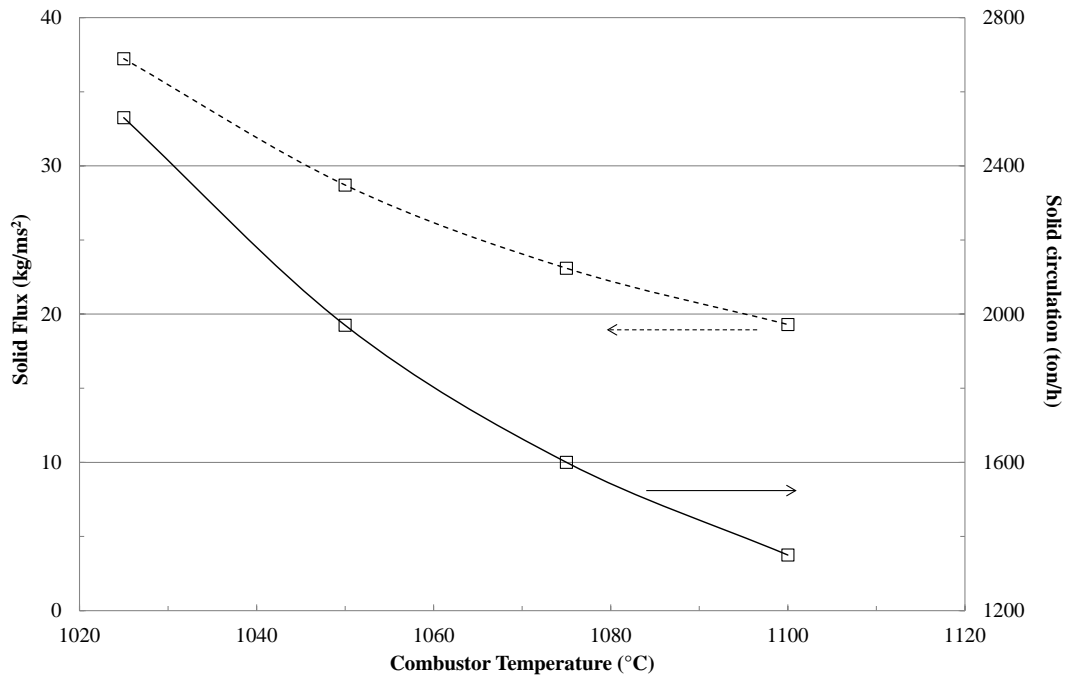
Figure 3-13 Variation of solid flux and solid circulation rate in the combustor at different temperatures.

The temperature of the combustor in the indirect calcination process is altered in a range of 1025 - 1100°C to evaluate its impact on solid flux and solid circulation rate. The results are presented in Figure 3-13. The maximum combustor temperature is limited to 1100°C to prevent the increase in the solid temperature and relevant partial calcination rate in the preheater. To estimate the solid flux, the superficial velocity of gases in the reactor can be assumed to be 5 m/s being a typical value for CFB systems in fast fluidization regime. The solid recycle rate reaches the minimum at 1100°C with a value of 1350 ton/h. The solid flux estimates in the combustor ranges between 19–37 kg/ms^2 at different combustor temperatures and can be handled by the current status of CFB combustors according to Bi and Liu (2012).

To validate the assumption of complete calcination in the calciner, a further analysis has been conducted. Martinez et al. (2010) claimed that the calcination reaction is chemically controlled and the internal mass transfer resistance is negligible up to a particle size of 300 μm.

They proposed the following equation based on the reaction kinetics to calculate the time required for achieving full calcination (t_c^*):

$$t_c^* = \frac{3X_{ave}}{k_c(C_{CO_2,eq} - C_{CO_2})} \qquad \text{(Eq. 3.2)}$$

where X_{ave} (mol $CaCO_3$/mol Ca) is the $CaCO_3$ content of the solid stream entering the calciner, k_c ($m^2 kmol^{-1} s^{-1}$) is the kinetic constant for the calcination reaction. $C_{CO2,eq}$ (kmol/m^3) and C_{CO_2} (kmol/m^3) are the CO_2 concentration at equilibrium and in the gas phase respectively. The value of kinetic constant is estimated by the following equation:

$$k_c = k_{c0}\exp\left(\frac{-E_{ac}}{RT}\right) \qquad \text{(Eq. 3.3)}$$

where k_{c0} ($m^3 kmol^{-1} s^{-1}$) is the pre-exponential factor, and E_{ac} (kJ/mol) is the activation energy of calcination. The kinetic parameters of "limestone A" given in the reference have been selected for use in the calculations, for which k_{c0} is 2.1×10^6 $m^3 kmol^{-1} s^{-1}$, and E_{ac} is 112.4 kJ/mol (Martinez et al., 2010).

The X_{ave} value in Eq. 3.2 is equal to 1 because only fresh limestone is fed to the calciner. The required calcination times for complete calcination at different calciner temperatures are presented in Figure 3-14. Two different calcination atmospheres have been examined: (i) pure CO_2 and (ii) 95% CO_2. The latter is included to consider any unhindered air leakages. It can be proven that the calcination temperature of 930°C selected in this study would allow reaching complete calcination rapidly (less than 25 seconds) even under pure CO_2 atmosphere. Although a detailed design of the calciner has not been investigated, it is expected that estimated solid residence times can easily be achievable in a BFB calciner, which is a potential candidate for the application of this system. At lower temperatures, however, the required calcination time for complete calcination increases further, i.e. over 3 minutes at 900°C.
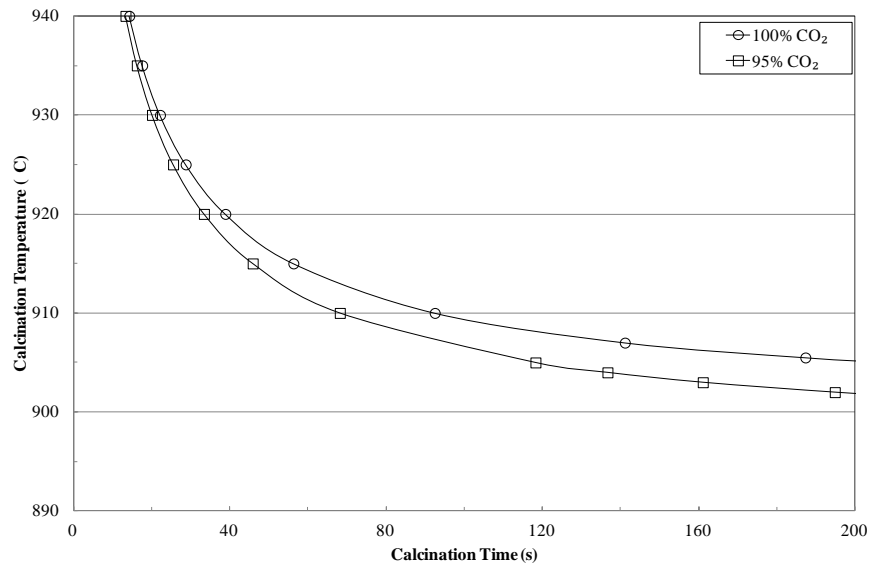
Figure 3-14 Required calcination time at different temperatures and calcination atmospheres to achieve complete calcination.

The process performances of the proposed schemes in this section are compared in Table 3-5. The total thermal energy requirement in the standalone indirect calcination process is slightly lower than that of the base cement plant (see Table 3-3) which can be linked to higher level of heat recovery from the excess air stream. The main energy penalty for this system results from the CO_2 compression unit. The indirect calcination process provides approximately 56% CO_2 avoidance without a need of any additional carbon capture technology. By incorporating the amine process into the indirect calcination process, 90% CO_2 avoidance can be achieved. Although the thermal energy requirement of the cement plant in the hybrid configuration seems to be much lower than the other options, it is because of the pre-calciner duty that is included in the heat requirement of the CHP plant.

In the hybrid configuration, the concentration of the CO_2 in the feed gas entering the absorber is around 14 mol% which is a typical value for a coal-fired combustor whereas this value is around 20 mol% for the standalone application of the amine process. The difference is due to the additional CO_2 emissions resulting from the calcination of limestone. Besides, the molar flow rate of the feed gas is less in the hybrid configuration. In order to reach the avoidance rate of 90%, the CO_2 capture efficiency is set to 85% in the hybrid configuration, while up to 95% capture efficiency is required in the standalone amine process because of the excessive CO_2

generation in the CHP plant. For this reason, the duty of reboiler increases to 3.96 $MJ_{th}/kg\ CO_2$ in the latter.

The power requirement of the capture plant in the hybrid configuration is calculated to be 19.7 MW_e. This requirement arises from the CO_2 compression unit (11.7 MW_e), pumps and compressors in the amine process as well as FGD and SCR units. The total electricity requirement of 42.4 MW_e in the standalone amine process can be met by generation in the CHP plant where an extra 7.8 MW_e can potentially be exported or sold to the grid. Nevertheless, the gross output of the CHP plant located in the hybrid configuration is not enough to meet the entire power requirement so remaining 19.8 MW_e should be imported. Considering all thermal energy and power requirements, the incremental energy consumption goes up to 8.2 $GJ_{th}/ton\ CO_2$ avoided in the standalone amine process while it is calculated to be 3.3 $GJ_{th}/ton\ CO_2$ avoided for the hybrid configuration at the same CO_2 avoidance rate. The incremental energy consumption in the standalone indirect calcination process is found to be only 0.9 $GJ_{th}/ton\ CO_2$ avoided, which reflects the power requirement in the CO_2 compression unit.

Table 3-5 Comparison of the standalone indirect calcination and amine processes, and the hybrid configuration.

	Standalone Indirect Calcination	Standalone Amine Process	Hybrid Configuration
Thermal energy requirement (GJ_{th}/ton clinker)			
in the cement plant	3.08	3.13	0.76
in the CHP plant	-	7.70	4.33
Amine process			
Feed gas composition (mol %)	-	2% H_2O, 4% O_2, 74% N_2, 20% CO_2	2% H_2O, 7% O_2, 77% N_2, 14% CO_2
CO_2 in feed (kmol/h)	-	3891.2	1425.0
CO_2 capture efficiency (%)	-	95	85
CO_2 lean loading (mol/mol)	-	0.23	0.23
CO_2 rich loading (mol/mol)	-	0.46	0.51
Solvent regeneration energy requirement (MJ_{th}/kg CO_2)	-	3.96	3.28
Power consumption (MW_e)			
Cement plant auxiliaries	13.7	13.7	13.7
Capture plant			
CO_2 compression	5.7	15.0	11.7
Amine plant auxiliaries	-	13.7	8.0
Power generation (MW_e)	-	50.2	13.6
Net power (MW_e)	−19.4	7.8	−19.8
CO_2 intensity (ton CO_2/ton clinker)	0.36	0.08	0.08
CO_2 avoidance rate (%)	55.6	90.0	90.0
Incremental energy consumption (GJ_{th}/ton CO_2 avoided)	0.9	8.2	3.3

3.3 Membrane Separation Process

The other advanced technology that has been mostly studied for the purpose of carbon capture from the power generation industry is membrane separation (Zhao et al., 2010; Merkel et al., 2012; Ramasubramanian et al., 2012; Zhai and Rubin, 2013). Even though this technology is still under development and has only been applied to small scale natural gas sweetening and oxygen enrichment applications to date (He and Hagg, 2012), it has been identified as a very promising option for the removal of CO_2 from cement flue gases (ECRA, 2007). However, its sensitivity to sulphur compounds and other trace elements in addition to difficulties in capture of 90% CO_2 in flue gas with a high-purity permeate stream in a single membrane stage has been pointed out as unfavourable characteristics. In the case of the latter, the use of multiple stages and/or recycling has often been suggested as a solution. Subsequent studies have focused on improving the properties of membranes such as CO_2 permeance and CO_2/N_2 selectivity (Zhao et al., 2010). Merkel et al. (2012) successfully developed a multi-stage analysis focusing on a retrofit integration and recycling of part of the CO_2 to the boiler of a power plant. A Polaris^{TM} membrane with a CO_2 permeance of above 1000 GPU (where 1 GPU is equal to 10^{-6} cm^3(STP)/cm^2·s·cmHg or a CO_2 permeability of 1000 Barrers assuming a 1-μm-thick membrane) and a CO_2/N_2 selectivity of 50 at 30°C has been used in their analysis.

The objective of this section is to give an overall insight into the application of the membrane process in the base cement plant for carbon capture. An analysis of a variety of multi-stage membrane configurations has been carried out. The membrane unit operation developed as an extension in UniSim Design by the Carbon Capture Group at University of Edinburgh (Bocciardo et al., 2012; Bocciardo et al. 2013) has been employed in this section.

3.3.1 Modelling of the Membrane Process

The modelling of a membrane for CO_2 separation is not in the scope of this section. In Bocciardo (2014), different membrane models have been developed that allow predicting the behaviour of industrially available membrane permeators. These

models have been incorporated into the base cement plant simulation to avoid 90% CO_2 with the target purity of ≥95 mol%. Under the assumptions of: (i) no pressure drop, (ii) ideal and isothermal behaviour, and (iii) constant permeance along the module, the models chosen for the process simulations are:

- **Non-disperse plug-flow:** the set of differential equations which represent the mass balance for a counter-current flow pattern using a sweep gas in the permeate are for retentate side (Eq. 3.4) and permeate side (Eq. 3.5).

$$\frac{dF_r}{dA} = -\sum_{i=1}^{i=NC} \pi_i \left(P_r x_{ir} - P_p x_{ip} \right)$$ (Eq. 3.4)

$$\frac{dF_p}{dA} = \sum_{i=1}^{i=NC} \pi_i \left(P_r x_{ir} - P_p x_{ip} \right)$$ (Eq. 3.5)

where F is the molar flow rate, P is the pressure, π is the permeance, and x is the molar fraction. Besides, A is the area, and NC refers to number of components. The suffixes r and p refer to retentate and permeate sides, respectively. Following the previous study on post-combustion capture from coal-fired power plants (Bocciardo et al., 2013) where counter-current with sweep has been marked as the best option for high-recovery stages, part of the retentate is chosen as sweep and is recycled to the permeate. The use of a sweep stream reduces the CO_2 partial pressure in the permeate and thereby improves the driving force of separation. In this way, the same overall recovery can be achieved by keeping relatively small membrane areas. This flow pattern can be found in hollow-fibre modules, where fibres with diameters up to mm scale are assembled to achieve area/volume ratio of 10000 m^2/m^3 (Baker, 2004).

- **2-D Cross-flow:** a cross-flow formulation has been adapted to model separation through spiral-wound permeators. The model equations are presented as follows for retentate side (Eq. 3.6) and permeate side (Eq. 3.7), where s and v are the retentate molar flow rates per unit of width (w) and permeate molar flow rate per unit length (l), respectively.

$$\frac{ds}{dl} = -2\sum_{i=1}^{i=NC} \pi_i \left(P_r x_{ir} - P_p x_{ip} \right)$$ (Eq. 3.6)

$$\frac{dv}{dw} = 2\sum_{i=1}^{i=NC} \pi_i \left(P_r x_{ir} - P_p x_{ip} \right)$$ (Eq. 3.7)

3.3.2 Selection of an Optimal Feed Gas Stream

Two feed gas locations have been identified in this section for the integration of a membrane separation into the base cement plant. The flue gas stream leaving the bag filters can be fed to the membrane separation process as an end-of-pipe integration. Alternatively, the flue gas stream from the preheater stage, which has a higher CO_2 concentration, can be preferable for CO_2 capture. The corresponding schematic diagrams for these options are presented in Figure 3-15 and Figure 3-16, respectively.

For the end-of-pipe integration shown in Figure 3-15, there is no significant modification required in the base cement plant except for the additional FGD and SCR units. The NO_x and SO_x emission levels can reach up to 1450 ppm and 1200 ppm, respectively in a cement process (IEA, 2008). The negative effects of minor gas components including NO_x and SO_x on membrane separation performance have been reported in Scholes et al. (2011), but further studies are still required to determine acceptable limits for such impurities. Since majority of the experimental studies have been carried out without having NO_x and SO_x in the feed gas stream, SCR and FGD units have been included in the process simulations as in the reference studies (IECM, 2012; NETL, 2012). The SCR unit is installed between the preheater and raw mill, and the FGD unit is located after the bag filters as in the previous section.

In the alternative option presented in Figure 3-16, the flue gas stream at 320°C from the preheater stage is first passed through an SCR unit and then an electrostatic precipitator (ESP) where solid particulates in the gas stream are removed. Since the flue gas stream leaving the preheater is directly sent to the capture unit rather than the raw mill, the heat requirement in this unit and fuel drying system cannot be satisfied anymore. However, it would be possible to transfer heat from the gas stream leaving the ESP to the CO_2-depleted gas stream from the membrane process in a regenerative heat exchanger. The preheated CO_2-depleted gas stream in addition to the excess air from the cooler will be sufficient to meet the heat demand in the raw mill. Finally, the feed gas stream after being cooled in the regenerative heat exchanger flows through an FGD unit prior to the membrane process.
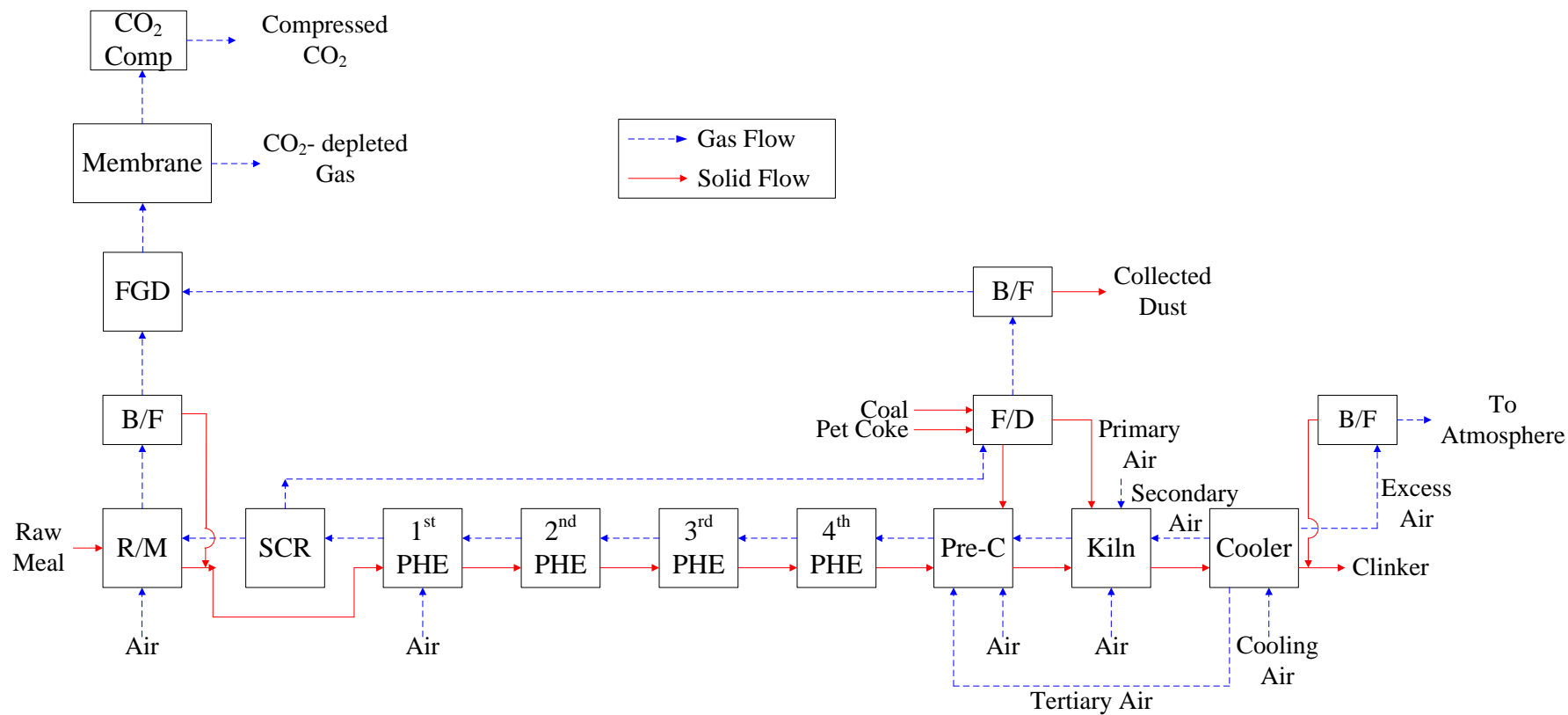
Figure 3-15 Schematic diagram of a cement plant with a membrane-based CO_2 capture unit (The end-of-pipe option). Abbreviations: **R/M**, Raw Mill; **B/F**, Bag Filter; **F/D**, Fuel Drying; **PHE**, Preheater; **Pre-C**, Pre-calciner; **SCR**, Selective Catalytic Reduction Unit; **FGD**; Flue Gas Desulphurization Unit; **CO_2 Comp**, CO_2 Compression.
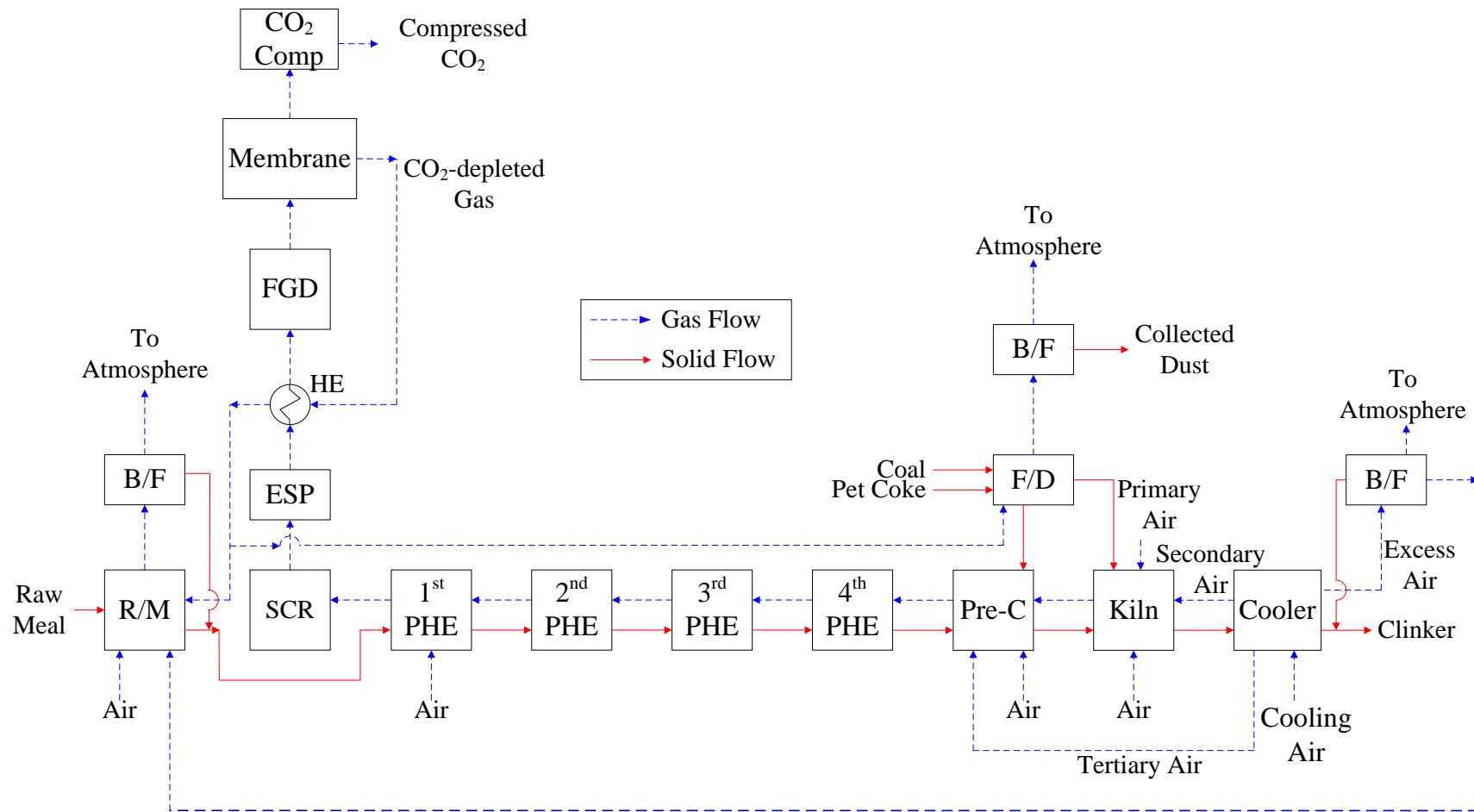
Figure 3-16 Schematic diagram of a cement plant with a membrane-based CO_2 capture unit (An alternative integration option). Abbreviations: **R/M**, Raw Mill; **B/F**, Bag Filter; **F/D**, Fuel Drying; **PHE**, Preheater; **Pre-C**, Pre-calciner; **SCR**, Selective Catalytic Reduction Unit; **FGD**; Flue Gas Desulphurization Unit; **CO₂ Comp**, CO_2 Compression; **HE**, Heat Exchanger.

Table 3-6 Composition of the flue gas stream after the bag filters (end-of-pipe) and the preheater.

	End-of-pipe (mol %)	After Preheater (mol %)
CO_2	22.4	32.3
N_2	58.1	59.7
O_2	6.2	2.4
H_2O	13.2	5.5
SO_2	0.1	0.1
Molar flow (kmol/h)	9398.0	6522.0

As can be seen in Table 3-6, the major benefits of the alternative integration where the preheater gas stream is selected as a feed gas are greater CO_2 concentration (32.3 mol% vs. 22.4 mol%) and lower volumetric gas flow as a result of eliminating the air leakages and moisture in the raw mill.

3.3.3 Membrane Process Configurations

For the membrane separation process, the major concern is dealing with high volume, low pressure feed gas streams when it is implemented in industrial scale applications. The CO_2 permeation of gas separation membranes is directly related to partial pressure difference between the feed and permeate sides. Thus, it is important to select the optimal pressure ratio as this also directly influences the performance of membranes as their properties and CO_2 concentration in the feed gas do.

The cost and energy requirements are the key concerns for generating a pressure difference across a membrane. Pressure ratios between 5 and 10 have been determined as economically affordable for this application (Merkel et al., 2010). Very high pressure ratios can be achievable by the utilization of compressors on the feed gas or by drawing a vacuum on the permeate side, but the main criterion is the selection of an economical way. There are three major advantages of using a gas compressor: (i) the capital cost of a gas compressor is half of that for a vacuum pump (IECM, 2012), (ii) the use of a compressor requires less membrane area compared to a vacuum (Merkel et al., 2010), and (iii) it would be possible to recover part of the energy spent for compression by employing a turbo-expander (Merkel et al., 2010). However, the vacuum operation is favoured owing to reduced energy consumption. A vacuum pressure of 0.22 bar slightly higher than the lowest practical vacuum

pressure (0.2 bar) for CO_2 capture applications is selected in this study following the reference (Merkel et al., 2010). Hence, the feed stream is initially compressed to 1.1 bar to have a pressure ratio of 5.

Promising results have been reported for improvements in membrane properties (Merkel et al., 2010; Favre, 2011). In addition to enhanced membrane permeability and selectivity, researchers have been focusing on the development of highly stable membranes that would be suitable for industrial scale applications. Membranes with higher selectivities are required to make the CO_2 separation process more attractive. In this study, the commercial membrane, Polaris^{TM} (Merkel et al., 2012) with a CO_2 permeance of 1000 GPU and CO_2/N_2 selectivity of 50 has been used adhering to the latest developments in this field. CO_2/O_2 and CO_2/H_2O selectivities have been estimated from the data available in NETL (2012) with the values of 10 and 0.2, respectively. A feed gas temperature is set to 30°C following the reference (Merkel et al., 2010), but the dependence of permeability on the gas temperature is not taken into account. It is not possible to capture 90% of the CO_2 at very high CO_2 purities from a typical feed gas stream by using a single membrane stage regardless of the type of membrane. Therefore, multi-stage configurations are necessary to reach higher degrees of separation as well as the purity.

Two membrane models, 2D cross-flow and counter-current with sweep, called 'cross-flow' and 'counter-current' respectively from now on, have been used in the multi-stage analysis. Four different dual-stage configurations have been evaluated as illustrated in Figure 3-17. The flue gas stream leaving the preheater stage (see Table 3-6) has been selected as a feed gas in all configurations. The feed gas stream is initially compressed to 1.1 bar and then cooled to 30°C while the condensed water is separated. In the first configuration (Conf. 1) shown in Figure 3-17(a), the counter-current stage has been located in the first stage as it provides high recovery, and followed by the cross-flow stage for high purity in the second stage. The feed gas stream is mixed with recycled retentate from the cross-flow stage and then fed to the counter-current stage. Part of the retentate stream, that is 10% for a preliminary analysis, from the counter-current stage is recycled back to the permeate side as a sweep. The remaining retentate stream is marked as CO_2-depleted gas stream.
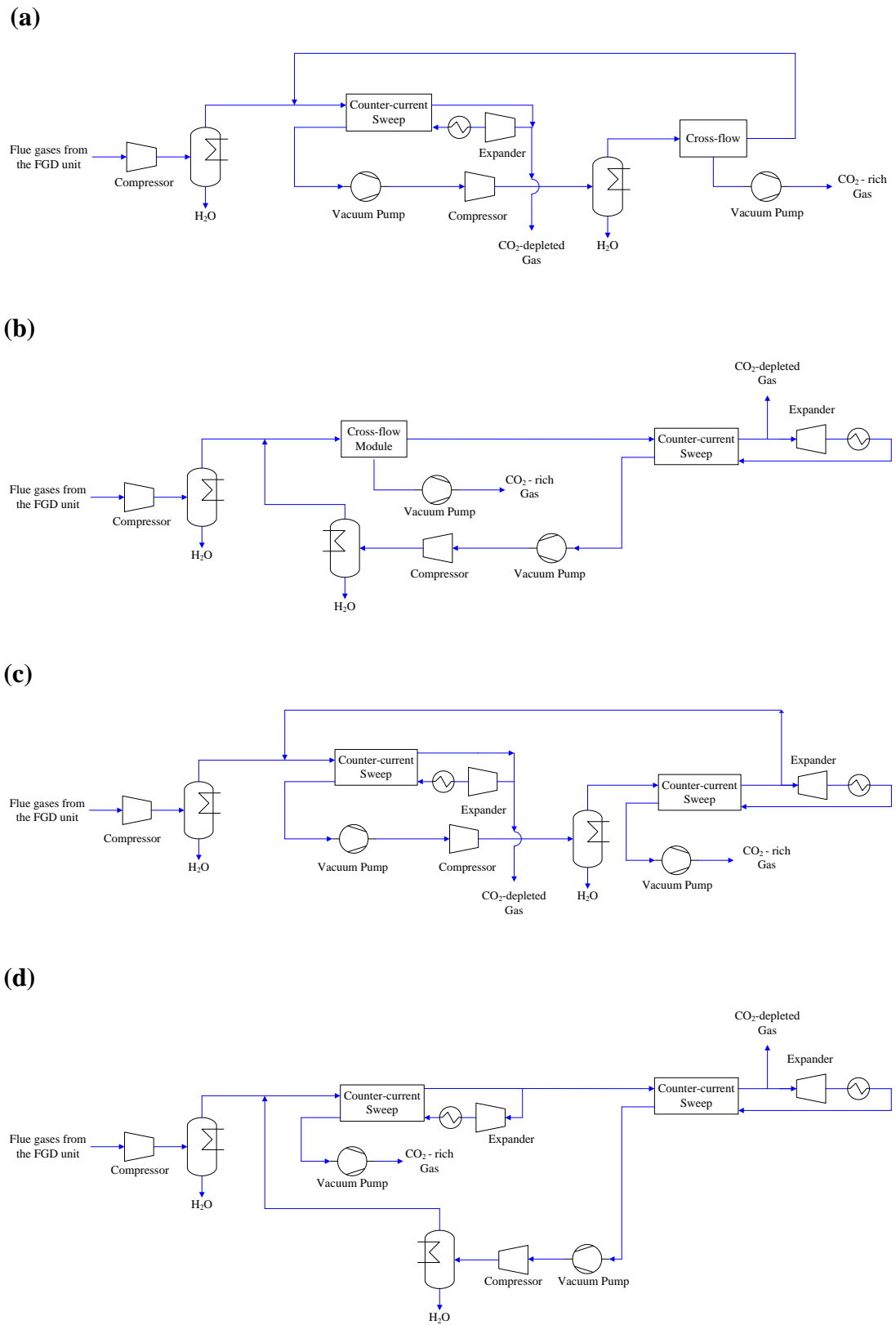
Figure 3-17 Schematic diagrams of the proposed membrane process configurations; (a) Conf. 1, (b) Conf. 2, (c) Conf. 3, (d) Conf. 4.

The permeate stream from the counter-current stage is compressed to 1.1 bar, cooled to 30℃ and sent to the cross flow stage. The CO_2-rich gas stream from the cross-flow stage is ready to be transferred to the CO_2 compression unit, which has a similar configuration to the one detailed in Chapter 2. In addition, three other alternative dual stage configurations have been examined. In Conf. 2, presented in Figure 3-17(b), a cross flow stage is followed by a counter current stage. A dual counter current configuration, Conf. 3, is presented in Figure 3-17(c). Finally, another dual counter current design with different gas recycle option is given in Conf. 4 shown in Figure 3-17(d). For all cases, the feed gas stream is taken from the preheater and the sweep/retentate (S/R) ratio is fixed at 0.1.

3.3.4 Results and Discussion

The outcomes of the dual-stage membrane configurations providing 90% CO_2 avoidance are compared in Table 3-7. It should be noted that the tabulated results are the best estimates obtained by multiple trials to achieve the target avoidance rate and purity with minimum energy consumption and membrane area. However, an optimization work would allow further reduction in the current estimates. The power consumptions of the pumps and compressors, including those in the CO_2 compression unit, are converted to thermal energy by using a power plant efficiency of 0.4 as before. It is clear from the results that the target purity can be achieved successfully by only Conf. 1 and Conf. 2, and among these two configurations, Conf.1 requires slightly less membrane area and energy consumption. On the other hand, the proposed dual counter-current configurations (Conf. 3 and Conf. 4) could reach up to 92.5 mol% CO_2 purity. Nevertheless, they are not favourable as Confs. 1 and 2 since an additional step is needed to increase the CO_2 purity further up to 95 mol%, which definitely increases the energy consumption and/or membrane area as well as the capital cost requirement. By comparing the energy consumptions and membrane area requirements for different configurations, it can be proven that further investigations should be based on Conf. 1 as it would potentially provide the lowest cost requirement for the carbon capture in the current analysis.

Table 3-7 Comparison of various membrane configurations at 90% overall CO_2 avoidance rate.

Configuration	Total membrane area ($\times 10^3$ m^2)	Incremental energy consumption (GJ$_{th}$/ton CO_2 avoided)	CO_2 purity (mol %)
After preheater			
Conf. 1	271	2.0	>95.0
Conf. 2	272	2.2	>95.0
Conf. 3	280	2.0	92.5
Conf. 4	172	1.9	70.0
End-of-pipe			
Conf. 1	402	2.1	>95.0

To determine the impact of different feed gas conditions, Conf. 1 is also employed in the end-of-pipe integration presented in Figure 3-15. The higher volumetric gas flow rate and lower CO_2 concentration of the feed gas stream in this option results approximately 48% increase in the membrane area. In addition, the energy consumption increases to 2.1 GJ$_{th}$/ton CO_2 avoided. The results indicate that the major difference in terms of process economics, when two different ways of integration are compared, will potentially be the cost of membrane modules since the power requirements are very similar in both options.

3.3.4.1 Sensitivity Analysis of Membrane Parameters

It is necessary to investigate the impact of S/R ratio fixed initially at 0.1 on membrane area and energy consumption estimations. Furthermore, a sensitivity analysis on the CO_2 permeance and CO_2/N_2 selectivity will reveal how the recent developments on membranes properties will influence the current estimates. To conduct a sensitivity analysis, the feed gas conditions given in Table 3-6 for the preheater gas stream and Conf. 1 have been used. The variation in the membrane area and energy consumption between 0-0.3 S/R is presented in Figure 3-18. It is observed that the membrane area increases significantly when S/R reduces. This proves that sweep stream improves the driving force of separation. On the other hand, very high sweep flow implies higher duty for the vacuum pump at the permeate side. Thus, following the minimum energy consumption at 0.075 S/R, a sharp increase is encountered after 0.1 S/R. Since none of examined S/R values provides minimum membrane area and energy consumption simultaneously, an economic analysis is needed to reveal the best value for S/R.
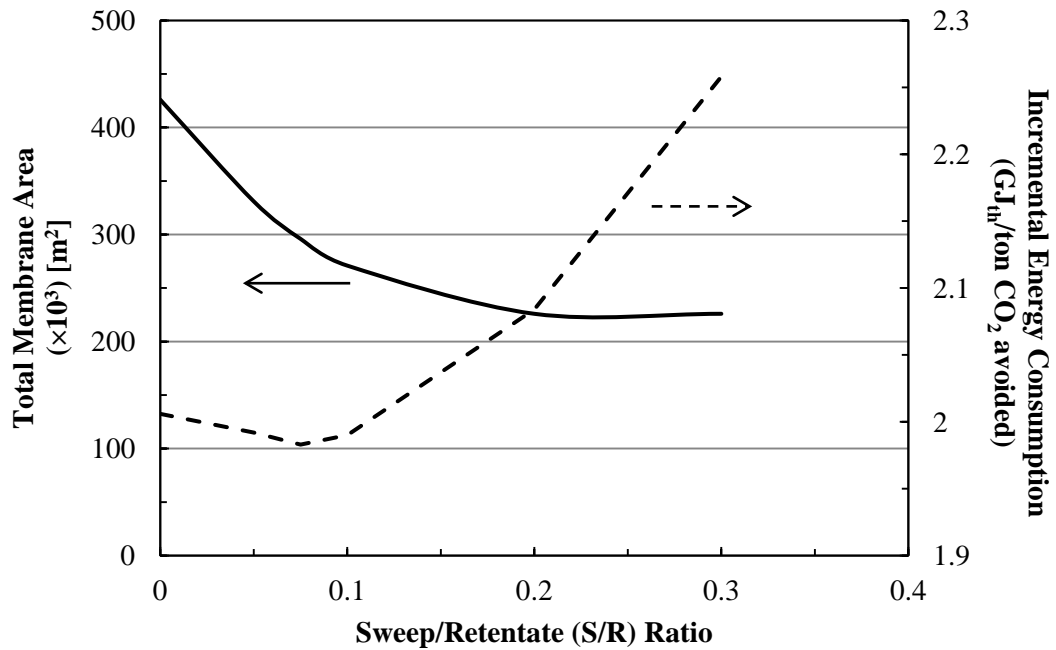
Figure 3-18 The impact of sweep/retentate ratio (S/R) on membrane area and incremental energy consumption.

In the second part of the sensitivity analysis, the CO_2 permeance assumed to be 1000 GPU initially has been varied between 1000-12000 GPU by keeping the CO_2/N_2, CO_2/O_2 and CO_2/H_2O selectivities constant, and the results are presented in Figure 3-19(a). No change in the energy consumption estimates is observed while the major impact of the CO_2 permeance appears to be an increase in the membrane area. Membranes having very low CO_2 permeance require very high membrane areas, and it is shown here that the membrane area can be potentially reduced to 23×10^3 m^2 when the CO_2 permeance is increased to 12000 GPU. The impact of CO_2/N_2 selectivity on both membrane area and consumption is significant as shown in Figure 3-19(b). The energy consumption estimates reduce gradually with an increase in the CO_2/N_2 selectivity and reach the maximum at the lowest selectivity. By changing the CO_2/N_2 selectivity from 25 to 75, a variation of 12% in the energy consumption estimates is observed. Clearly the duty of the vacuum pump makes the largest contribution at low CO_2/N_2 selectivities. An opposite impact has been observed on membrane area estimates which show increase at high selectivities because of the reduction in the driving force for CO_2 permeation. The membrane area increases to 307×10^3 m^2 at the selectivity of 75.

(a)
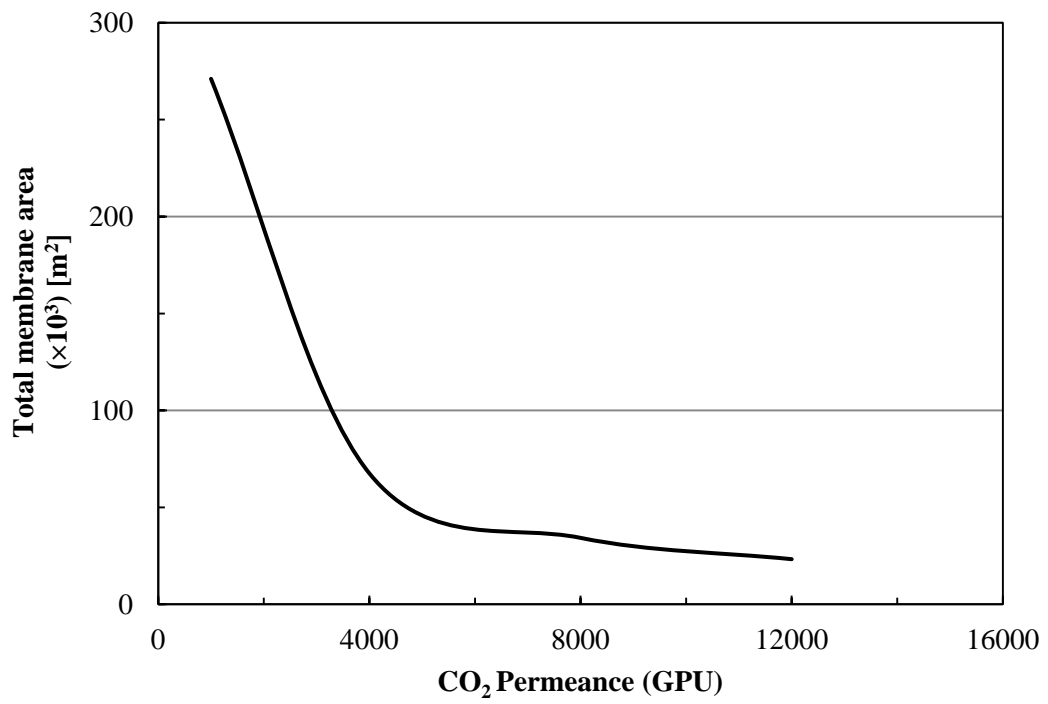
(b)
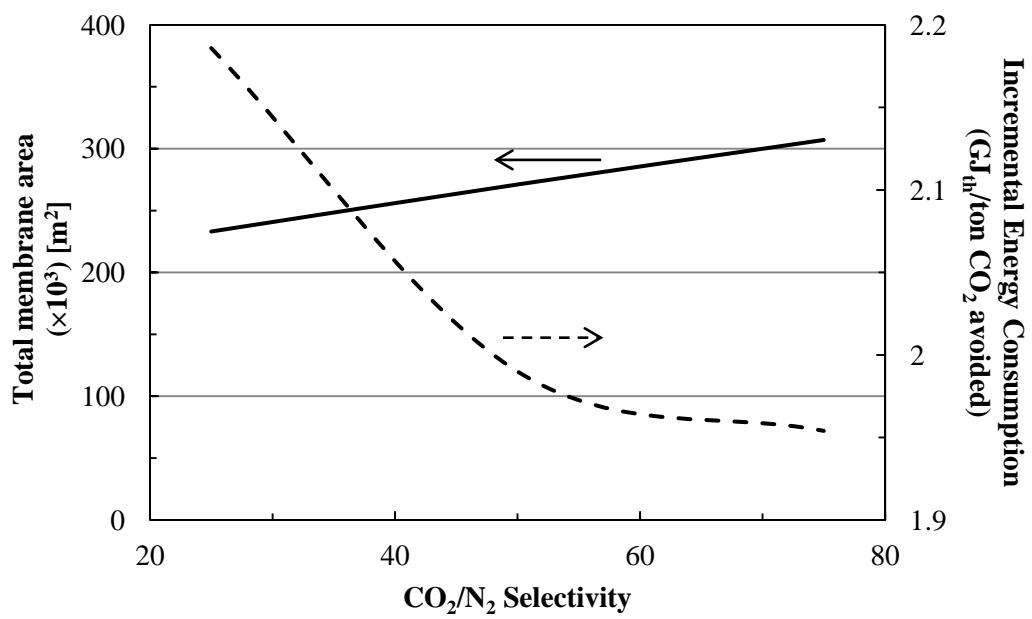
Figure 3-19 The effects of (a) the CO_2 permeance on membrane area; (b) CO_2/N_2 selectivity on membrane area and incremental energy consumption.

The volume of each membrane module can roughly be estimated by using the membrane area and packing density data given in Bocciardo (2014), where an average packing density was reported to be 1300 m^2/m^3 for the cross-flow spiral-wound modules and 7300 m^2/m^3 for the counter-current modules. Therefore, the total membrane area of 307×10^3 m^2 corresponds to an approximate volume of 60 m^3.

3.4 Concluding Remarks

This chapter describes the application of alternative carbon capture technologies to reduce the CO_2 emissions from the base cement plant. In the first section, the Ca-looping process has been coupled with a CLC cycle to eliminate the requirement of an energy intensive ASU. Within the different ways of solid transfer between the reactors, a process configuration with a solid route of carbonator $\rightarrow$ calciner $\rightarrow$ air reactor $\rightarrow$ carbonator has been selected to enable heat transfer between the air reactor and the calciner as this is a requirement to avoid unfeasible heat duties in the capture system. As a method of heat transfer, a hot solid stream from the air reactor has been recycled to the calciner operating at a lower temperature. The air reactor operates at 950°C to provide a sufficient temperature difference. The upper limit of 0.15 F_0/F_{CO2} has been determined to restrain the amount of CuO to a value of 1 wt% in the cement raw meal. To achieve 90% CO_2 avoidance, the capture efficiency of the carbonator is varied between 88 - 90%. The minimum incremental energy consumption for this process and for the others estimated in Chapters 2 and 3 are reported in Table 3-8 for ease of discussion. It was indicated that the energy consumption of the Ca-Cu looping process can be fairly lower than that of the Ca-looping process depending on F_0/F_{CO2} ratio and sorbent performance.

The indirect calcination process can provide partial CO_2 reduction and energetic efficiency improvements when it is properly located in the cement plant. Approximately 56% of CO_2 emissions from the cement plant can be prevented without requirement of an additional post-combustion carbon capture process. An aqueous amine process was coupled with the indirect calcination process to increase CO_2 avoidance rate further up to 90%. The incremental energy consumption of the hybrid configuration was found to be lower than that of the standalone integration of

the amine process (3.3 GJ_{th}/ton CO_2 avoided vs. 8.2 GJ_{th}/ton CO_2 avoided), but it was almost double of that of the Ca-Cu looping process.

Finally, a potential strategy for effective process integration of a membrane separation process into the base cement plant has been proposed. Two feed gas locations have been identified, among which the preheater gas stream requires less energy consumption and membrane area due to higher CO_2 concentration and lower volumetric flow rate. Since it is not possible to reach very high capture rates along with stringent CO_2 purity requirements by a single stage membrane, a membrane configuration comprised of a counter-current module with a sweep following by a cross-flow module has been selected as an optimal configuration as it provides the target CO_2 avoidance rate and purity at minimum expense. It was concluded by comparing the energy consumption estimates that membrane separation can be a promising alternative for the Ca-looping process, but an economic study is required to support this argument.

Table 3-8 Minimum incremental energy consumption estimates for the carbon capture processes evaluated in Chapters 2 and 3.

	Incremental Energy Consumption (GJ_{th}/ton CO_2 avoided)
Ca-looping process	2.5
Ca-Cu looping process	1.7
Indirect calcination process	0.9
Hybrid configuration	3.3
Standalone amine process	8.2
Membrane process	2.0
'Oxy-calciner only' case	2.3

Chapter 4 Economic Analysis

The final comparison of different CO_2 capture technologies should take economic criteria into account. Thus, the aim of this chapter is to provide a simple and transparent economic analysis for the estimation of costs of cement production and CO_2 avoided associated with the capture technologies evaluated in Chapters 2 and 3. Although the literature regarding carbon capture economics in the cement industry is limited, the available methodologies are also summarized in this chapter.

4.1 A Review of Existing Studies

For the indirect calcination process, Rodriguez et al. (2008b) used the following equation for the calculation of cost of CO_2 avoided (AC).

$$AC = \frac{\frac{\Delta TCR\ FCF}{CF} + FC\ \Delta H + COE_{comp}}{CO_2 t\ cement_{ref}^{-1} - CO_2 t\ cement_{capture}^{-1}} \qquad \text{(Eq. 4.1)}$$

where TCR is the specific total capital requirement; FCF is the fixed charge factor (to amortize the TCR for the plant lifetime and discount rate assumptions); CF is the capacity factor; FC and COE_{comp} refer to the fuel and compressor electricity costs, respectively; and ΔH is the thermal energy requirement. The terms in the denominator are the CO_2 intensities of a reference cement plant with and without carbon capture. FCF and CF values are fixed at 0.1 and 0.9, respectively. The assumption implicit in Eq. 4.1 is that the capture plant is of a type and design equivalent to the reference cement plant. Thus, when a capture unit is incorporated, Eq. 4.1 calculates the increment in the total cost and allows for comparison of the average cost of reducing CO_2 emissions for the same product capacity base plant. The TCR of the capture plant is critical to calculations using Eq. 4.1, and in the absence of a detailed cost analysis for the indirect calcination process, its similarity of existing CFB combustion systems is often taken into account. In Rodriguez et al. (2008b), the cost of the CFB combustor was assumed to be 30% of the TCR of an equivalent CFB power plant, while the compression unit cost was estimated by using 86 $/kW, which was given by Rubin et al. (2007).

The latest article on the indirect calcination process (Rodriguez et al., 2011) proposes a more detailed economic analysis. It also incorporates the cost of a steam cycle because the excess heat recovered from the high temperature gas streams was used to drive a steam cycle. The reference cost of 500 $/kW$_e$ given in the DOE report (2007) was employed for the estimation of the steam cycle cost. Since all excess heat was used for power generation instead of reducing the thermal energy requirement in the calciner by preheating the solid feed, as proposed in Chapter 3, there was surplus power generation. A revenue of 0.05 $/kWh was included, under the assumption that the surplus electricity can be sold to the grid, which gave a negative electricity cost estimation. The avoided cost was calculated to be 12 $/ton CO_2 at 38% efficiency. The primary reason behind such a low avoided cost is the profit gained from surplus power generation.

The economic analysis proposed by Romeo et al. (2010) was applied to a system comprised of a power plant, a cement plant and a Ca-looping carbon capture process. Romeo et al. (2012) also employed Eq. 4.1 in their study to estimate the cost of CO_2 avoided. The specific TCR of a reference air-fired power plant was assessed to be 1100 €/kW$_e$, while that of the calciner was estimated by assuming that the cost of the boiler represents 40% of the TCR of the power plant. Even though the need to use scale factor in the cost estimations was mentioned because the size of the reference plant differs from the actual capacity, this option was skipped in the calculations. Unfortunately, there is not any reference that particularly presents a way to estimate the cost of a carbonator in the literature. Hence, to estimate the cost of the carbonator in their study, Romeo et al. (2010) calculated the TCR of an air-fired power plant based on the net power generation capacity of the capture plant, assuming that the carbonator and heat exchanger costs can replace the cost of the boiler in the power plant, including the steam cycle cost. ASU and compression costs were added according to the methodology of Rubin et al. (2007). The cost of CO_2 avoided was reported to be 12.4 €/ton CO_2 for this system, which was stated to be lower than the individual application of the Ca-looping process for power and cement plants.

The process scheme presented in Rodriguez et al. (2012) has some similarities with the system explained in Chapter 2, except for the way of integrating the capture plant. In the reference, the economic performances of the oxy-fired CFB calciner and Ca-looping cases were compared. For the oxy-fired calciner case, the cost of a pre-calciner in the base cement plant was discounted since this unit was replaced by an oxy-fired calciner. A cost of 20 $/annual ton clinker was assumed for the existing pre-calciner. Since the economic data for an oxy-fired calciner are scarce, those available for an equivalent oxy-fired CFB power plant were taken from the European Commission's SETIS Energy Information System (SETIS, 2013). The calculated TCR was 3125 $/kW$_e$ which covers the costs of an oxy-fired boiler, an ASU, a gas processing system including CO_2 compression, a steam cycle and utilities. For the Ca-looping case, the carbonator cost was calculated as a modest fraction (10%) of the TCR of the additional oxy-fired CFB power plant. The cost of cement (COC$_{ref}$) was given according to the following equation:

$$COC_{ref} = \frac{\Delta TCR_{ref}\, FCF}{CF} + FC\, H_{ref} + COE \qquad \text{(Eq. 4.2)}$$

This is very similar to Eq. 4.1 but was adapted for cement production. Here, TCR$_{ref}$ refers to the total capital cost requirement of a reference cement plant, and H$_{ref}$ is the thermal energy requirement. The cost of electricity (COE) covers the entire electricity requirements for the plant. For the proposed carbon capture processes, TCR and H values increase because of the additional reactors, steam cycle, ASU, and gas processing system, but the COE can be reduced, since majority of the power requirement can potentially be satisfied by a heat recovery steam cycle. The cost of CO_2 avoided was then calculated according to the following equation:

$$AC = \frac{COC_{CO2-capture} - COC_{ref}}{(CO_2/ton\,of\,cement)_{ref} - (CO_2/ton\,of\,cement)_{CO2-capture}} \qquad \text{(Eq. 4.3)}$$

where 'CO_2-capture' and 'ref' refer to the capture and reference cases, respectively, and the CO_2 intensity estimations in the denominator reflect the process simulations. With these assumptions, the cost of CO_2 avoided was calculated to be 16 $/ ton of CO_2 and 23 $/ton of CO_2 for the oxy-fired calciner and Ca-looping systems, respectively.

In a more recent paper (Romano et al, 2013), the combined cost of a calciner and a carbonator was estimated using the following equation as a function of reactor volume (V) and thermal energy requirement in the calciner (Q).

$$C_{CaL}[\text{€}] = C_0 \left[\alpha \left(\frac{Q_{LHV,calc}}{Q_0} \right)^{SF,Q} + (1 - \alpha) \left(\frac{V_{calc}}{V_0} \right)^{SF,V} + (1 - \alpha) \left(\frac{V_{carb}}{V_0} \right)^{SF,V} \right] \text{(Eq. 4.4)}$$

where scale factor values, SF,Q and SF,V, are assumed to be 0.9 and 0.67, respectively, and α is assumed to be 0.85, representing the ratio of heat transfer surfaces on the total cost of a cooled CFB reactor. Additionally, parameters C_0, Q_0 and V_0 refer to the TCR of the boiler, the thermal energy input, and the volume of the boiler, respectively.

Liang and Li (2012) conducted a more detailed economic analysis based on a case study of a cement plant in China. An amine-scrubbing post combustion process was implemented to capture 85% of the CO_2 from a cement plant. Through a static cash flow analysis, the cost of CO_2 avoided by the proposed design, including a new 200 MW_e CHP plant, was estimated to be 70 $/ton CO_2 at a 14% discount rate, with the assumption of a lifetime of 25 years. Although the TCR of the system was calculated by estimating the cost of each unit, the details of the calculation method were not exhibited. Li et al. (2013) added an oxy-fired system for comparison with the amine-scrubbing process. The calculated avoided cost was above 60 $/ton of CO_2. It was emphasized that public financial support is essential for applications of such technologies in a cement plant since the current market conditions can only provide limited financial support.

4.2 Method of Economic Analysis

The economic study reported in this chapter describes the assessment of total capital requirement, operating & maintenance (O&M) and variable costs of the carbon capture technologies presented in Chapters 2 and 3, in addition to, the various sensitivities of cost parameters. The economic analysis was based on the approach given by IEA (2008). Similar to the levelised cost of energy (LCOE) which is applicable for power plants (DECC, 2012), levelised cost of cement (LCOC) that refers the ratio of the net present value of total capital requirement, O&M and

variable costs of a cement plant to the net present value of cement production over its operating life has been calculated. The formulation of the LCOC is given by the following equation:

$$LCOC = \frac{\sum_{t=1}^{n} \frac{TCR_t + M_t + V_t + (TCR_{t,cc} + M_{t,cc} + V_{t,cc})}{(1+r)^t}}{\sum_{t=1}^{n} \frac{C_t}{(1+r)^t}}$$ (Eq. 4.5)

where TCR_t is the total capital requirement, M_t is the O&M cost, V_t is the variable cost, and C_t denotes the cement production rate. The suffix cc refers to carbon capture process, and t and r are the operating year and discount rate, respectively. By knowing the difference between the LCOC estimations for the base cement plant and a capture case, and the CO_2 emissions for each case, the cost of CO_2 avoided can be calculated according to the following equation:

$$Cost\ of\ CO_2\ avoided = \frac{LCOC_{cc} - LCOC_{base}}{[ton\ CO_2/ton\ cement]_{base} - [ton\ CO_2/ton\ cement]_{CC}}$$ (Eq. 4.6)

The main financial assumptions were taken from IEA (2008) and IEA GHG R&D programme Technical & Financial Assessment Criteria (IEA GHG, 2003) for a cement plant located in Scotland, UK and are summarized in Table 4-1. In the economic analysis of the capture cases, the main issue is the estimation of TCR of each system. The routine and breakdown maintenance is allowed for at 3.5% per year of the TCR for the plants handling solids and at 1.7% per year for the plants handling gases and liquids according to the IEA report (2008). The operating labour is assumed to work in a 5 shift pattern with an annual salary of €40000/yr. An allowance of 20% of the operating cost is added to cover supervision and an additional 30% for administration and general overheads. To cover specific services, e.g. local rates and insurance, 1.7% of the TCR is included. An escalation factor of 1.5% is included for the estimation of O&M cost during the operating life. Although a more complex model can be used for financing assumptions (ZEP, 2011), the cost model used in this dissertation is assumed to be sufficient for the comparison of different carbon capture technologies.

IEA (2008) reported the reference cement plant capital cost allocation, and the calculations and assumptions have been replicated here for the base cement plant. The reference capital cost data for the capture processes reported in Table 4-2 were obtained from the relevant references (DOE, 2003; Fisher et al., 2004; IEA, 2008). The similarity of the Ca-looping process with an existing CFB oxy-fired power plant was taken into consideration. The TCR of the reference oxy-fired power plant is comprised of the costs of a CFB oxy-fired boiler, an ASU, a steam cycle and a gas processing system including CO_2 compression. The total cost was divided under four titles, as presented in Table 4-2 with their capacities. A further 10% of the TCR of a complete oxy-fired power plant was added to cover carbonator cost as suggested by Abanades et al. (2007) and Rodriguez et al. (2012). Since the flow rate of raw meal into the base cement plant decreases with increasing purge flow rate in the Ca-looping and Ca-Cu looping processes, the costs of the preheater and pre-calciner existing in the base cement plant have been discounted with respect to the flow rate of the raw meal. The preheater and pre-calciner costs were given as 13.6 M€ and 1.1 M€ at 189 ton raw meal/h, respectively (IEA, 2008).

The main components of the TCR in the indirect calcination process are a CFB combustor and a gas processing system. Because, the first is similar to the boiler of an air-fired CFB power plant, the TCR estimations given in DOE (2003) for this plant were divided into two categories: boiler island and steam cycle. The cost of the CFB combustor in the indirect calcination process was then calculated based on the total thermal energy requirement in this reactor.

Table 4-1 The main financial assumptions (IEA, 2008).

	Value	Unit
'S' curve of expenditure		
1st Year	20	%
2nd Year	45	%
3rd Year	35	%
Design life	25	Years
Load (or capacity) factor		
1st Year	60	%
2nd Year	90	%
Escalation factor	1.5	%
Discount factor	10	%
Conversion factor ($ to €)	0.77	-

Table 4-2 Reference capital cost data.

	Capacity	Cost	Reference
Reference cement plant	114.9 ton clinker/h	263 M€	(IEA, 2008)
CFB oxy-fired combustor (calciner)	1877 GJ_{th}/h*	94.5 M$	(DOE, 2003)
ASU	37.5 MW_e	76.8 M$	(DOE, 2003)
Steam cycle	209.9 MW_e	85 M$	(DOE, 2003)
Gas processing system	26.9 MW_e	72.2 M$	(DOE, 2003)
CFB air reactor/fuel reactor	1845 GJ_{th}/h*	122 M$	(DOE, 2003)
CFB air-fired combustor	1884 GJ_{th}/h*	164 M$	(DOE, 2003)
Absorber (MEA)	1110 m^3	8.3 M$	(Fisher et al., 2004)
Stripper (MEA)	238 m^3	1.9 M$	(Fisher et al., 2004)
Reboiler (MEA)	125 MW_{th}	2.4 M$	(Fisher et al., 2004)
CHP	746 GJ_{th}/h*	146.4 M€	(IEA, 2008)
FGD	143 m^3/s at 50°C	49.8 M€	(IEA, 2008)
SCR	89 m^3/s at 320°C	10.2 M€	(IEA, 2008)
ESP	76.8 m^3/s at 110°C	4.6 M€	(IEA, 2008)

* LHV Basis

The reference TCR of the CLC system was taken from the similar process configurations detailed in the report by the DOE (2003). Despite this system's similarities to the Ca-looping process, it does not include an ASU. For the amine process, the cost structure was designed to include the absorber, desorber, compressors, pumps, heat exchangers and gas processing system. The reference heat transfer coefficients required sizing the heat exchangers and heat exchanger types in the amine process were taken from the similar type of work, in addition to the costs of the absorber, desorber and reboiler at known capacity (Fisher et al., 2004). The costs associated with the heat exchangers, pumps and compressors were calculated using the CAPCOST software (Turton et al., 2009). The absorber and stripper were sized by the Tray Sizing Tool in UniSim based on packed bed column using Flexipac 250Y and IMTP #40, respectively. Since it is not possible to size some auxiliaries in the amine process such as reflux accumulator, filtration and reclaimer by the process simulator, the costs of these units were assumed to be 8% of the TCR of the amine process according to Fisher et al. (2004). The cost of a CHP plant including an SCR unit was estimated based on the thermal energy demand of this plant. Even though the costs of the FGD and SCR units were estimated based on volumetric gas flow rate, it is worth to mention that more accurate predictions can only be achieved if detailed cost data for such systems are provided.

For the membrane process, the contributions in cost of the membrane module, membrane frame and material replacement can be estimated based on the following equations:

$$TCR_{membrane-module} = A_m c_m \qquad \text{(Eq. 4.7)}$$

$$TCR_{membrane-frame} = (A_m/2000)^{0.7} c_{mf} \qquad \text{(Eq. 4.8)}$$

$$TCR_{membrane-replacement} = (A_m \vartheta) c_{rm} \qquad \text{(Eq. 4.9)}$$

In all three of these equations, the following apply: A_m refers to the required membrane area; c_m, c_{mf} and c_{rm} are set to 50 \$/m^2, 0.238 M\$ and 10 \$/m^2, respectively (IECM, 2012); and the annual material replacement rate (ϑ) is fixed at 20%. In addition, a loading of 40% for contingencies and remaining fees needs to be included (IECM, 2012). The material replacement cost has been included as an O&M cost. The costs of compressors, vacuum pumps and expanders in this system were also calculated by using the CAPCOST software.

According to the six-tenths rule, the approximate capital requirement of a plant or a unit can be estimated if the cost and size of similar items are known. Moreover, historical cost predictions can be adjusted to current prices due to inflation and deflation by using the Marshall&Swift (M&S) index. The following equation demonstrates the use of the six-tenths rule and the M&S index:

$$TCR_B = TCR_A \times \left(\frac{C_B}{C_A}\right)^{0.6} \times \left(\frac{M\&S_B}{M\&S_A}\right) \qquad \text{(Eq. 4.10)}$$

where TCR_A is the known cost of an item with size C_A; TCR_B is the estimated cost of the equipment with size C_B; and the term M&S refers to the index value on a base year. Therefore, Eq. 4.10 has been applied on the available capital cost data in order to estimate current prices. An exception is given for the membranes for which scale factor is assumed to be 1 since they are modular. The fuel and raw material costs were taken from IEA (2008) and are summarized in Table 4-3. These values have been updated using 1.5% escalation factor per year to estimate current prices (ZEP, 2011).

Table 4-3 Reference variable cost data. * The cost of SCR catalyst has been adjusted based on the actual SCR capacity in each case.

	Cost	Unit	Reference
Raw material + Process water	6.1	€/ton cement	(IEA, 2008)
Limestone for FGD	3.0	€/ton	(IEA, 2008)
Ammonia	2000	€/ton	(IEA, 2008)
MEA	1100	€/ton	(IEA, 2008)
SCR catalyst	1.19*	M€/year	(IEA, 2008)
Pet coke	80.0	€/ton	(IEA, 2008)
Coal	65.0	€/ton	(IEA, 2008)
Electricity	0.05	€/kWh	(IEA, 2008)
Copper	6.8	$/kg	(LME, 2013)
Alumina	0.8	$/kg	(INDMIN, 2013)
Natural Gas	4.9	$/1000 ft^3	(EIA, 2013)

The electricity cost was set to 0.05 €/kWh. As a base approach, the same electricity cost was utilized as revenue for surplus power generation (IEA, 2008; Rodriguez et al., 2011b). An average annual escalation factor of 1.5% has also been considered in all variable cost calculations for the subsequent years. To estimate the cost of CuO/Al_2O_3 sorbent in the Ca-Cu looping process, the following equation proposed by Abad et al (2007) has been employed.

$$C_{OC} = x_{CuO} C_{CuO} + x_{Al2O3} C_{Al2O3} + C_m \qquad \text{(Eq. 4.11)}$$

where x and C refer to component mass fractions and cost, respectively for oxygen carrier (OC) and its constituents; CuO and Al_2O_3. The approximate manufacture cost of oxygen carrier, C_m, was given as 1 $/kg OC in Abad et al (2007).

4.3 Results and Discussion

4.3.1 Base Cement Plant and Ca-looping Process

The calculated LCOC estimates presented in Figure 4-1 are for the base cement plant, Ca-looping options at three different F_0/F_{CO2} ratios providing >90% CO_2 avoidance (see Figure 2-8), and the oxy-calciner only case from Chapter 2. A sample economic analysis spreadsheet for the Ca-looping process at 1.65 F_0/F_{CO2} is attached in Appendix C.
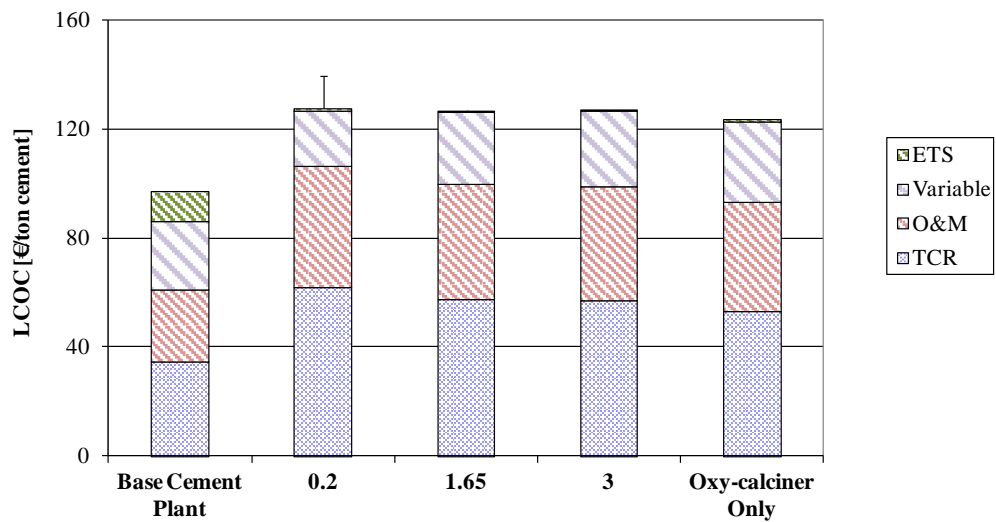
Figure 4-1 LCOC estimates for the base cement plant, three Ca-looping options at different F_0/F_{CO2} (see Figure 2-8) and oxy-calciner only case. The error bar reflects the increase in variable cost if there is no surplus power revenue.

Table 4-4 The composition of the TCRs for the Ca-looping and 'oxy-calciner only' processes presented in Figure 4-1.

Unit	0.2 ($\times 10^6$ €)	1.65 ($\times 10^6$ €)	3.0 ($\times 10^6$ €)	Oxy-calciner ($\times 10^6$ €)
Calciner	51.2	45.9	46.1	44.0
Steam Cycle	45.9	33.0	31.2	26.7
ASU	42.0	37.7	37.8	36.1
Gas processing system	57.6	52.8	52.5	48.9
Carbonator	19.7	16.9	16.8	-
Cyclone	1.9	1.2	1.0	-
Total	**218.3**	**187.5**	**185.4**	**155.7**

Upon further consideration, a significant difference between the TCR of the base cement plant and that of the capture options can be observed. The increment reaches a maximum at 0.2 F_0/F_{CO2} due to the excessive thermal energy requirement in this system. The composition of TCR estimations for the capture plants is given in Table 4-4. In parallel with a reduction in the thermal energy requirement, the TCR estimates decrease by around 15% for 1.65 F_0/F_{CO2} and 3.0 F_0/F_{CO2} cases.

Although the cost of the calciner is the lowest at 1.65 F_0/F_{CO2} among the Ca-looping options owing to the minimum thermal energy requirement in this system as presented in Figure 2-6(a), the lowest TCR estimate belongs to the oxy-calciner only case mainly because of the absence of the costs of the carbonator and additional cyclone. The O&M estimates are directly related to the TCR estimates so a more pronounced effect is observed at 0.2 F_0/F_{CO2}. The main components of the variable

cost in the base cement plant and Ca-looping processes are the costs of raw material, fuel and electricity. The base plant should pay for the electricity as it is imported, while in the other cases, either all (0.2 F_0/F_{CO2}) or partial (1.65 and 3.5 F_0/F_{CO2}, and the oxy-calciner only case) requirement can be met by on-site power generation. As indicated previously, the surplus power generation at 0.2 F_0/F_{CO2} has been included as revenue in the cost model. However, the surplus power revenue will also vary on a location basis: if for example the infrastructure for the electricity grid is not able to take large amounts of electricity from the cement plant, the cement plant will not be able to sell the surplus electricity. Therefore, an error bar is also included in Figure 4-1 to reflect the case where surplus power generation cannot be considered as revenue, increasing the variable cost further.

The variable cost of the Ca-looping process at 0.2 F_0/F_{CO2} which is the case with the greatest power generation is slightly lower, despite having the highest cost associated with fuel consumption. The trade-off between the fuel and electricity costs keeps the variable costs of the 1.65 F_0/F_{CO2} and 3.0 F_0/F_{CO2} cases at the same level while further increase is observed in the oxy-calciner only case. To reveal the potential advantages of cement plants with CO_2 capture, the additional benefits from the Emission Trading System (ETS) is included in the economic analysis. According to the ETS, industries emitting CO_2 pay a variable amount for the emission credits, depending on market conditions. As a reference value of this emission credit, 14 €/ton CO_2 has been adopted as this was the value used in the IEAGHG report (2009). The contribution of the ETS price is the highest for the base cement plant since all CO_2 generated in this system is directly emitted whereas it is significantly less for the Ca-looping processes where more than 90% CO_2 avoidance can be achieved. At 3.0 F_0/F_{CO2}, the minimum ETS price is utilized since the highest CO_2 avoidance rate has been achieved in this case (see Figure 2-8). Even at the different F_0/F_{CO2} ratios, the LCOC estimates for the Ca-looping process remains constant at approximately 127 €/ton cement (140 €/ton excluding surplus power revenue at 0.2 F_0/F_{CO2}), while that of the base cement and the oxy-calciner only plants was calculated to be 97 €/ton cement and 124 €/ton cement, respectively.
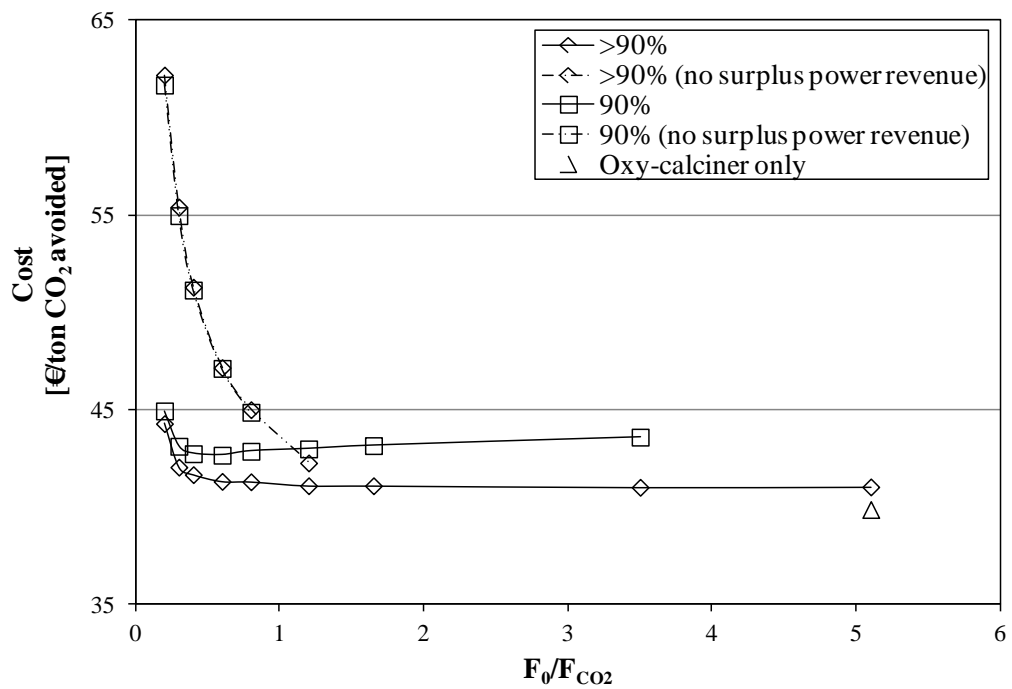
Figure 4-2 The cost estimates for the Ca-looping and 'oxy-calciner only' processes. For the Ca-looping process, the CO_2 avoidance rate is either fixed at '90%' or '>90%', reflecting the results given in Chapter 2.

The use of LCOC results in Eq. 4.6 enables the calculation of the cost of CO_2 avoided. The results shown in Figure 4-2 are for the Ca-looping process at two different CO_2 avoidance rates; (i) 90% (see Figure 2-9) and (ii) >90% (see Figure 2-8), and for the oxy-calciner only case. Given the fact that the revenue of surplus power generation depends on demand in the grid, additional results have been included for the cases at <1.5 F_0/F_{CO2}, assuming no surplus power revenue. The cost of CO_2 avoided is the highest at the lowest F_0/F_{CO2} owing to the greater thermal energy and oxygen requirements and reduces if the avoidance rate is more than 90%. The main difference between the '90%' and '>90%' cases is the amount of sorbent circulated between the reactors which affects the heat requirement in the calciner, whereas the volumetric flow rate of the feed flue gas from the cement plant as well as the purge flow rate is almost similar. In addition, the crucial term in the cost of CO_2 avoided calculations (Eq. 4.6) is the CO_2 intensity which decreases as the CO_2 avoidance rate increases.

The cost of CO_2 avoided estimates at 90% CO_2 avoidance show a similar trend to the heat requirement in the calciner as presented in Figure 2-6(a), while the others at >90% CO_2 avoidance stay almost constant after 0.4 F_0/F_{CO2} with a value of 41 €/ton CO_2 avoided. The cost associated with the oxy-calciner only case is around 1 €/ton CO_2 avoided lower than that of the Ca-looping plant (minimum 2 €/ton CO_2 avoided at 90% case). Without any revenue for surplus power generation, a severe increment in the cost estimates is observed especially at 0.2 F_0/F_{CO2} where the cost reaches 62 €/ton CO_2 avoided.

4.3.2 Ca-Cu Looping Process

Even though the Ca-Cu looping process provides an improvement in the energetic efficiency, the major drawback on the process economics results from the cost of the oxygen carrier that is purged from the system. The LCOC estimates for the Ca-Cu looping process and the Ca-looping process using methane as fuel in the calciner are presented in Figure 4-3 with error bars reflecting the conditions with no surplus power revenue. The breakdown of TCR calculations for the capture plants is illustrated in Table 4-5. Here, cases A and B refer to the Ca-looping process using natural gas as a fuel at 0.02 F_0/F_{CO2} and 0.15 F_0/F_{CO2}, respectively while the same purge ratios refer to cases C and D for the Ca-Cu looping process. The CO_2 avoidance rate in both processes has been fixed at 90%. Predictably, the TCR estimates for the cases A and B are lower compared to equivalent configurations at low F_0/F_{CO2} burning pet-coke (see Figure 4.1). This occurs because of the reduction in thermal energy requirements of the calciner in the cases A and B as a result of the absence of negative SO_2 and ash effects on the sorbent performance. The elevated thermal energy requirement increases the reactor and steam cycle costs and leads to the highest TCR found in case C, even though an ASU does not exist in this system. It is convenient to assume that the cost of the carbonator in case D should be similar to that in case B as both systems have similar thermal energy requirements in the capture plants, CO_2 and sorbent flow rates as well as heat exchange area requirements in the carbonators according to Table 3-4. Thus, to estimate the cost of the carbonator in cases C and D, a further 11.2% of the TCR of the CLC plant has been added to be consistent with that of the Ca-looping processes.
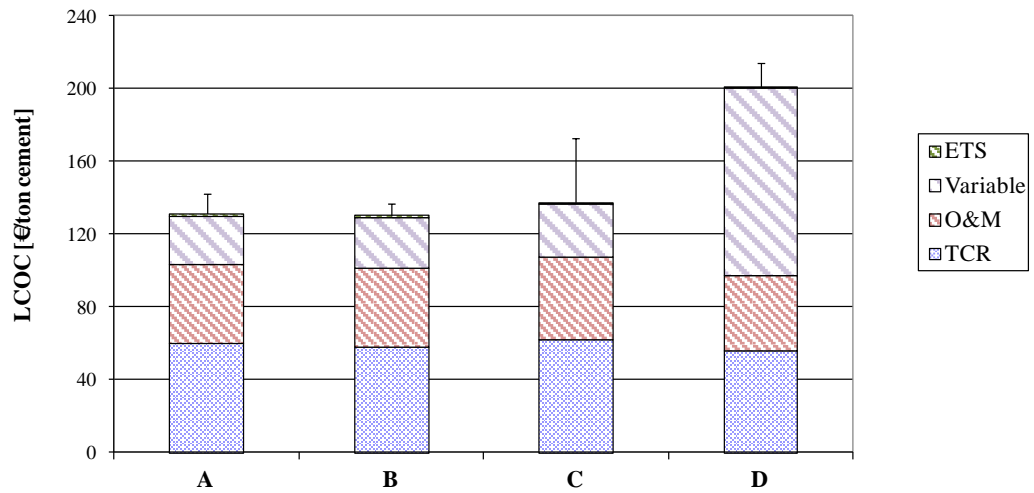
Figure 4-3 The LCOC estimates for the Ca-looping process using methane as a fuel (cases A and B) and the Ca-Cu looping process (cases C and D). Cases A and C refer to the results at 0.02 F_0/F_{CO2} while cases B and D refer to those at 0.15 F_0/F_{CO2}. The error bars reflect the increase in the variable cost if there is no surplus power revenue.

Table 4-5 The composition of the TCRs for the Ca-looping process using methane (cases A and B) and the Ca-Cu looping process (cases C and D) presented in Figure 4-3.

Unit	A ($\times 10^6$ €)	B ($\times 10^6$ €)	C ($\times 10^6$ €)	D ($\times 10^6$ €)
Calciner	44.6	42.8	-	-
Steam Cycle	42.3	38.0	58.3	40.4
ASU	36.7	35.2	-	-
Gas processing system	49.9	48.3	53.0	47.2
Air Reactor/Fuel Reactor	-	-	80.4	59.0
Carbonator	17.4	16.4	21.5	16.4
Cyclone	2.1	2.0	2.1	2.0
Total	**193.0**	**182.7**	**213.0**	**163.3**

Notably, when the 0.02 F_0/F_{CO2} cases are compared, it can be realized that regardless of the excessive cost of oxygen carrier in the Ca-Cu looping process, the estimated variable cost is close to that of the Ca-looping case. It can be associated to very small flow of CuO in the purge. However, without any revenue of surplus power generation, the LCOC estimates increase in all cases, particularly in Case C. The cost of sorbent is very prominent at in case D, and this option is not competitive with the other cases.

The LCOC estimates are in the range of 130 €/ton cement to 138 €/ton cement for most of the cases but reaches a maximum of 201 €/ton cement in case D including the ETS price. Without any surplus power revenue, a severe jump in the cost estimate of case C can be marked, indicating the importance of the export of surplus power for this case. The cost of CO_2 avoided estimates for the Ca-looping process using methane and the Ca-Cu looping process are presented in Figure 4-4. The results are divided into four different options: the first option (Option 1) directly represents the conditions applied in Figure 4-3; the second option (Option 2) shows the electricity selling price has increased to 0.1 €/kWh which is an advantage for the processes generating great amount of electricity; the third option (Option 3) is opposite to Option 2 where there is no revenue of surplus power generation; and the fourth option represents the best scenario applicable for the Ca-Cu looping process where entire purged CuO/Al_2O_3 sorbent is separated and reused in the system.

The cost estimates for cases A and B according to Option 1, are around 50 €/ton CO_2 avoided; these values are slightly higher than the previous '90%' case using pet-coke as presented in Figure 4-2 because of the higher cost of natural gas than pet-coke. At 0.02 F_0/F_{CO2}, the Ca-Cu looping process is more competitive compared to the Ca-looping options, but the sorbent cost becomes challenging at 0.15 F_0/F_{CO2} where the cost increases to 157 €/ton CO_2 avoided. Additionally, the electricity selling price impacts the total variable cost estimates, and this value is kept at 0.05 €/kWh initially but changed to 0.1 €/kWh in Option 2. For the processes importing the electricity, as in the base cement plant, an increase in the electricity cost triggers the variable costs. However, for the capture processes where power generation is possible, the increase causes a reduction in the variable cost. The profit is more obvious for the cases at 0.02 F_0/F_{CO2} since the power generation capacities are higher. Because the power generation capacity is the greatest in case C, one should expect severe variation in the cost of this system compared to the others. For this case, the cost of CO_2 avoided takes a negative value. Conversely, for an opposite scenario presented in Option 3, the cost increases to 114 €/ton CO_2 avoided in case C.
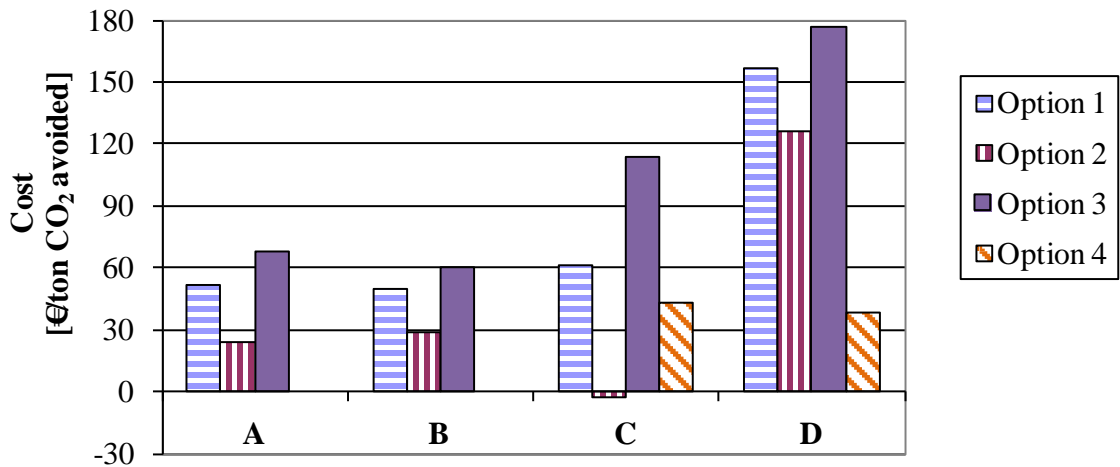
Figure 4-4 The cost of CO_2 avoided estimates for the Ca-looping process using methane (A and B) and the Ca-Cu looping process (C and D).

Although it was not considered in the process simulations presented in Chapter 3 and the CuO content in the clinker is limited to 1 wt%, the possible recovery of the CuO/Al_2O_3 sorbent leaving in the purge stream will reduce the variable cost significantly. In Option 4, the reduction in the cost of CO_2 avoided is more prominent in case D. It decreases to 38 €/ton CO_2 avoided exclusive of cost of solid separation. The results suggest that if there is an economical way to separate CuO/Al_2O_3 from the solid mixture, the Ca-Cu looping process will be more competitive with the Ca-looping process in terms of process economics. Furthermore, this will also allow the operation of the system with high F_0/F_{CO2}, reducing the cost of CO_2 avoided further.

4.3.3 Indirect Calcination, Hybrid and Standalone Amine Processes

The TCR estimates for the standalone indirect calcination, hybrid and standalone amine processes are presented in Table 4-6. The TCR of the standalone indirect calcination process is comprised of the costs of a CFB combustor, a gas processing system and a regenerative heat exchanger to heat up the excess air stream by heat exchange with the CO_2-rich gas stream. The total TCR of the standalone amine process is significantly higher than that of the base cement plant, whereas the hybrid configuration provides around a 30% improvement in the TCR even though both processes provide 90% CO_2 avoidance. It should be noted that the TCRs of the hybrid and standalone amine processes include also the costs of the FGD and SCR

units, causing reduction of SO_x and NO_x in the final gas stream, while these units do not exist in the standalone indirect calcination process.

The LCOC estimates for these systems are shown in Figure 4-5. Similarly, an error bar indicates the increase in the variable cost if there is no revenue for surplus power generation. The cement cost calculated for the standalone indirect calcination process is only 12 €/ton cement higher compared to the base cement plant. Although the TCR and O&M costs are greater for the indirect calcination process, the total difference reduces with the inclusion of the ETS price.

Table 4-6 The composition of the TCRs for the standalone indirect calcination, hybrid configuration and standalone amine process.

	Standalone indirect calcination (×10^6 €)	Hybrid configuration (×10^6 €)	Standalone amine process (×10^6 €)
Amine Process			
Flue gas blower	-	2.3	4.5
Absorber	-	7.4	14.1
Rich amine pump	-	0.04	0.09
Stripper	-	1.3	3.2
Reflux condenser	-	0.8	2.0
Reboiler	-	1.3	2.9
Rich/lean amine heat exchanger	-	5.9	10.0
Lean amine pump	-	0.005	0.04
Lean amine cooler	-	0.3	3.7
Inlet gas cooler	-	1.6	2.9
Other auxiliaries	-	2.3	3.8
CFB combustor	53.2	-	-
CHP plant	-	120.8	170.8
SCR unit	-	4.3	10.8
FGD unit	-	38.5	55.4
Gas processing system	30.2	46.2	53.8
Regenerative heat exchanger	0.5	0.5	-
Total	**83.9**	**233.0**	**338.0**
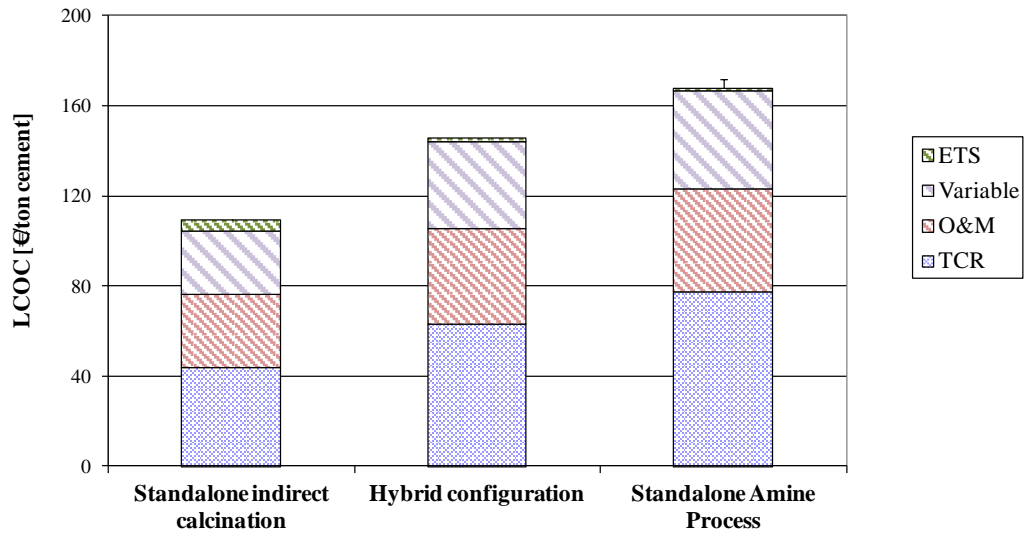
Figure 4-5 The LCOC estimates for the standalone indirect calcination, hybrid configuration and standalone amine process. The error bar reflects the increase in variable cost if there is no surplus power revenue.

The LCOC increases to 146 €/ton cement for the hybrid process and 168 €/ton cement (172 €/ton cement without the surplus power revenue) for the standalone amine process. Even though there is no power generation facility in the standalone indirect calcination process, its variable cost estimation is very low due to the absence of excessive costs of fuel and solvent.

The cost of CO_2 avoided estimates are shown in Figure 4-6. For the standalone indirect calcination process, the estimated cost is around 29 €/ton CO_2 avoided, which is the lowest among the different options compared in this dissertation despite the fact that the CO_2 avoidance rate provided by this process is only 56%. By adding an amine process, 90% CO_2 avoidance can be attained causing the cost to increase to 73 €/ton CO_2 avoided, which is up to 80% higher than that of the Ca-looping process. However, compared to the standalone amine process, it provides more than a 30% improvement in the cost.
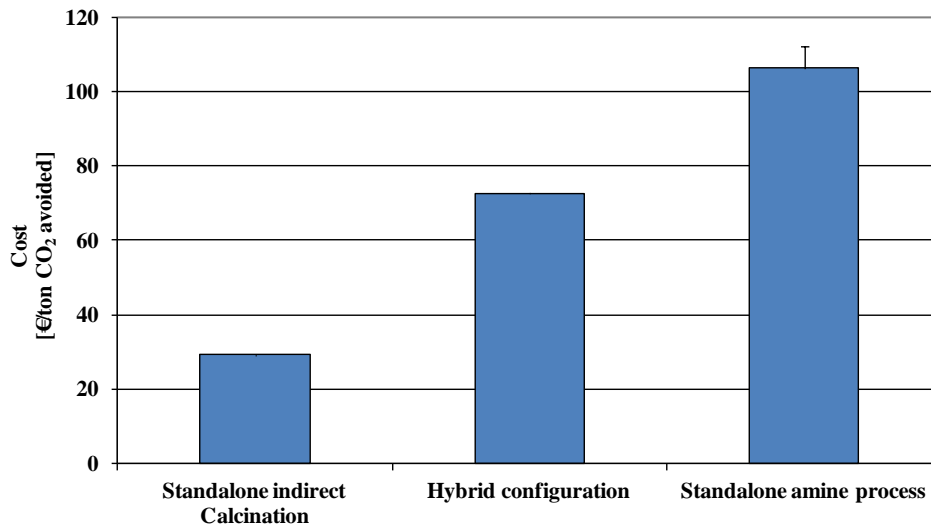
Figure 4-6 The cost of CO_2 avoided estimates for the indirect calcination, hybrid configuration and standalone amine process. The error bar reflects the case where there is no revenue for surplus power generation.

4.3.4 Membrane Process

For the membrane process, the impact of the predefined range of S/R ratios on the LCOC estimates has initially been examined, and the results are presented in Figure 4-7. The cost results are given for two cases: in Option 1, the feed stream is the gas stream leaving the preheater while it is the gas stream after the bag filters (end-of-pipe) in Option 2. It can be concluded that even though distinctive values of the membrane areas and energy consumptions have been calculated at different S/R ratios, as already shown in Figure 3-18, the effect is almost negligible on LCOC estimates. This occurs because of the trade-off between the costs of membrane module, vacuum pumps and compressors. The LCOC estimates are close at 0.1 S/R and 0.2 S/R but around 1 €/ton cement higher at 0.05 S/R. Despite the membrane area is 48% higher in Option 2; the LCOC predictions based on two feed locations are not significantly different from each other.

The breakdown of TCR estimates for the membrane process based on Options 1 and 2 at 0.1 S/R is given in Table 4-7. The total cost of the heat exchangers includes the one needed in Option 1 to heat the CO_2-depleted gas stream. Therefore, only the total heat exchanger cost is greater in Option 1 while all remaining are higher in Option 2 owing to larger membrane area requirement and greater volumetric flow rate of the feed gas.

136
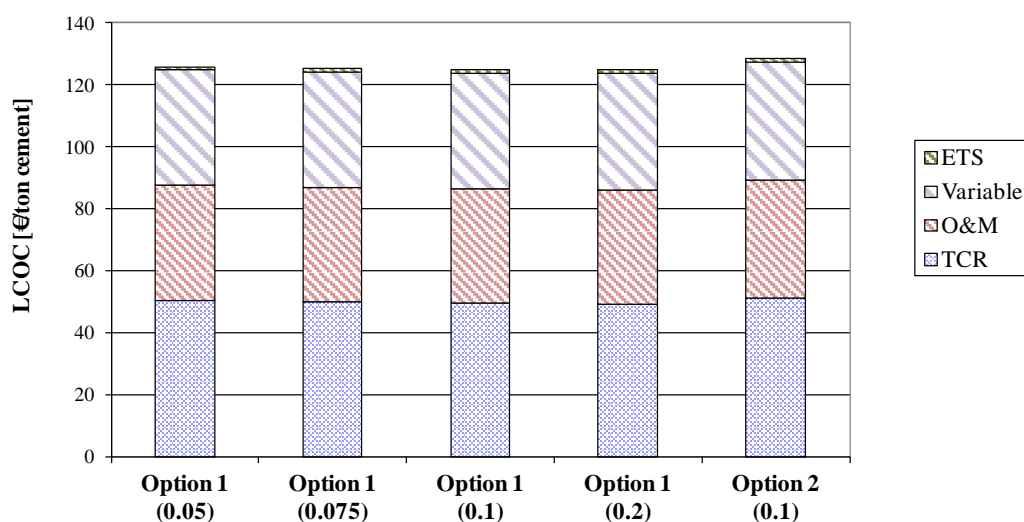
Figure 4-7 The LCOC estimates for Options 1 and 2 at different S/R ratios. The S/R ratios are shown in the parentheses.

Table 4-7 The composition of the TCRs for the membrane process at two different feed gas locations.

	Option 1 ($\times 10^6$ €)	Option 2 ($\times 10^6$ €)
Total membrane (module + frame)	22.7	32.3
Heat exchangers	1.2	0.8
Compressors, vacuum pumps and expanders	6.9	8.2
SCR	10.8	10.8
FGD	27.7	34.5
Gas processing system	39.1	39.1
ESP	3.9	-
Total	**112.3**	**125.7**

The cost estimates for the membrane process are compared in Figure 4-8 for Options 1 and 2. With this technology, the cost can be reduced to approximately 42 €/ton CO_2 avoided if the feed gas location is selected as the exit of the preheater. If a complete retrofit option is preferred, the cost will increase to 47 €/ton CO_2 avoided. The cost estimate for the membrane process taking the feed stream from the exit of the preheater is up to 1 €/ton CO_2 avoided higher than that of the Ca-looping process as presented in Figure 4-2. Even though the TCR and O&M cost are higher for the latter, the variable cost requirement in this system is lower because of the on-site power generation. However, the footprint of the membrane process would be smaller so it may be more attractive in the case of retrofits to existing plants with limited availability of land.
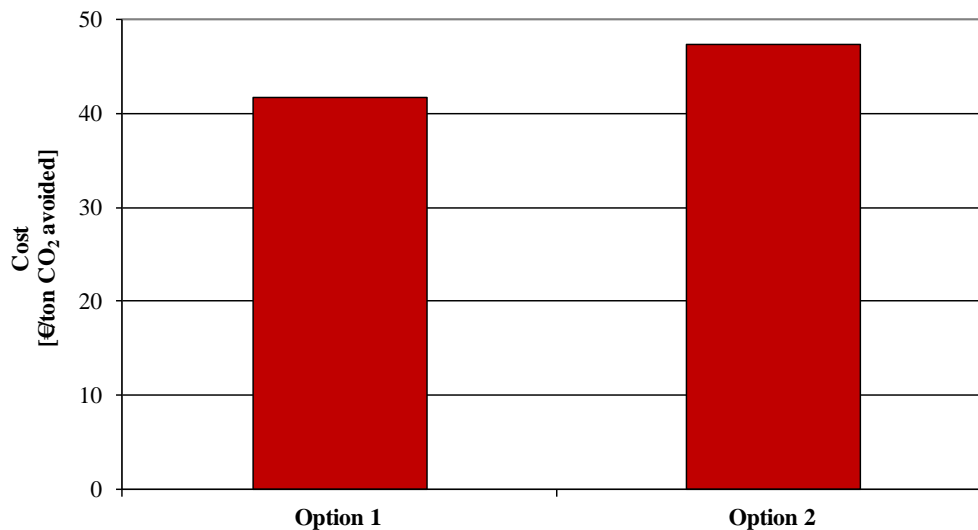
Figure 4-8 The cost of CO_2 avoided estimates for the membrane process at two different feed gas locations.

4.3.5 Sensitivity Analysis

In the final stage of this chapter, sensitivities of TCR, O&M cost, fuel and power costs, discount rate, scale factor and ETS cost based on a variation of ±25% have been examined. In addition, three additional scenarios, where (i) CO_2 saving by on-site power generation, (ii) inclusion of FGD and SCR units in all process schemes, and (iii) replacement of the ASU in the Ca-looping process with oxygen purchasing have been taken into the consideration. The sensitivity analysis has been developed for seven different carbon capture options: (i) Ca-looping process at 1.2 F_0/F_{CO2} (the case where the CO_2 avoidance rate is ≥90% and the entire electricity requirement can be met by on-site power generation with an excess of less than 2 MW_e), (ii) Ca-Cu looping process at 0.02 F_0/F_{CO2}, (iii) standalone indirect calcination process, (iv) hybrid configuration, (v) standalone amine process, (vi) membrane process (at 0.1 S/R, Option 1), and (vii) oxy- calciner only case. First, the results for the sensitivities of TCR and O&M cost are shown in Figure 4-9.

(a)

(b)
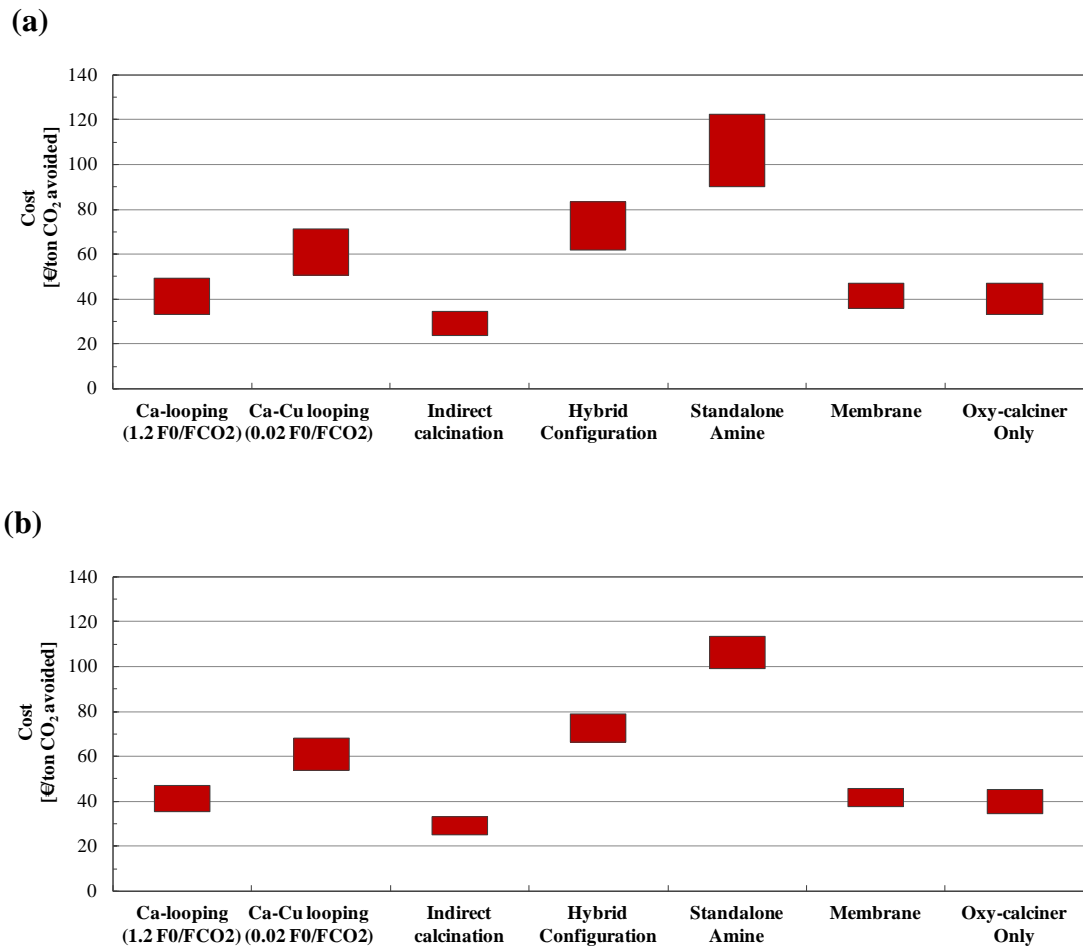
Figure 4-9 Sensitivities of (a) TCR and (b) O&M.

While the variation in TCR is greater for the standalone amine process as the cost estimate for this system is the highest, it changes in a small range for the standalone indirect calcination and membrane processes. In Figure 4-9(b), the sensitivities of O&M cost indicate that similar to the variation in the TCR, the fluctuation is severe for the Ca-Cu looping process, hybrid configuration and standalone amine process.

(a)

(b)
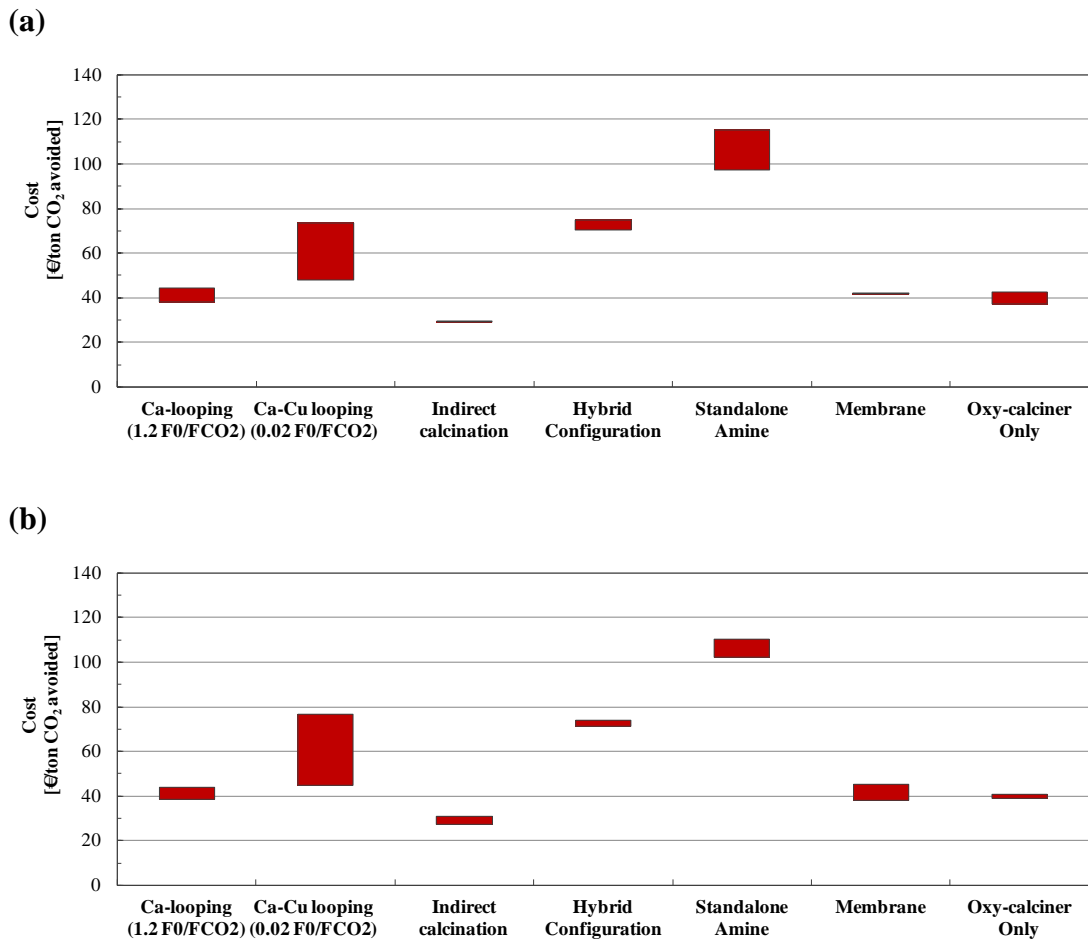
Figure 4-10 Sensitivities of (a) fuel cost and (b) power cost.

The sensitivities of fuel and power costs are presented in Figure 4-10. In Figure 4-10(a), there is not a significant change in the costs of the indirect calcination process and the membrane process, since the total thermal energy requirement in these systems are similar to that of the base cement plant. A change in the fuel cost affects the variable cost in both the base cement plant and these capture processes, therefore, this effect disappears for the cost of CO_2 avoided estimates because the increase in the cost is similar. A more pronounced effect is observed for the Ca-Cu looping process and the standalone amine process due to the excessive thermal energy requirements in these systems.

The impact of a change in power cost, shown in Figure 4-10(b), is different for the capture cases. There is power generation in the majority of the configurations except the indirect calcination and membrane processes. For these exceptions, an increment in the electricity cost causes the cost of CO_2 avoided to increase, while the converse occurs for the remaining processes. Although the CHP plant located in the hybrid configuration provides electricity to be used in the system, the final electricity cost is still higher than that of the base cement plant. Therefore, it is preferable for this option to pay less for the electricity. Conversely, in the oxy-calciner only case, the need for electricity is lower than that in the base cement plant, so the cost of CO_2 avoided is lower at high electricity cost.

The sensitivities of discount rate and the scale factor that is assumed to be 0.6 initially are presented in Figure 4-11. In parallel to an excessive TCR estimate for the standalone amine process, the cost of CO_2 avoided calculated for this system ranges between 95 €/ton CO_2 avoided to 119 €/ton CO_2 avoided based on ±25% variation of the discount rate. For the remaining cases up to 30% variation is observed depending on the severity of TCR estimates. The sensitivity on scale factor, presented in Figure 4-11(b), is only applicable to the processes for which the cost estimations are based on Eq. 4.10. Even though the costs of the absorber, desorber, reboiler and gas processing unit existing in the hybrid and standalone amine processes have been calculated by using the same equation, the costs of the compressors, expanders and heat exchangers in these systems have been taken from the CAPCOST software. For this reason, the results shown in Figure 4-11(b) are only for the Ca-looping, Ca-Cu looping process, indirect calcination and the oxy-calciner only processes. For the selected systems, an increment in the scale factor reduces the cost of CO_2 avoided since the reference cost data for these systems is at higher capacity, leading the cost to be reduced to 22 €/ton CO_2 avoided for the indirect calcination process and to 33 €/ton CO_2 avoided for the Ca-looping process.

(a)

(b)
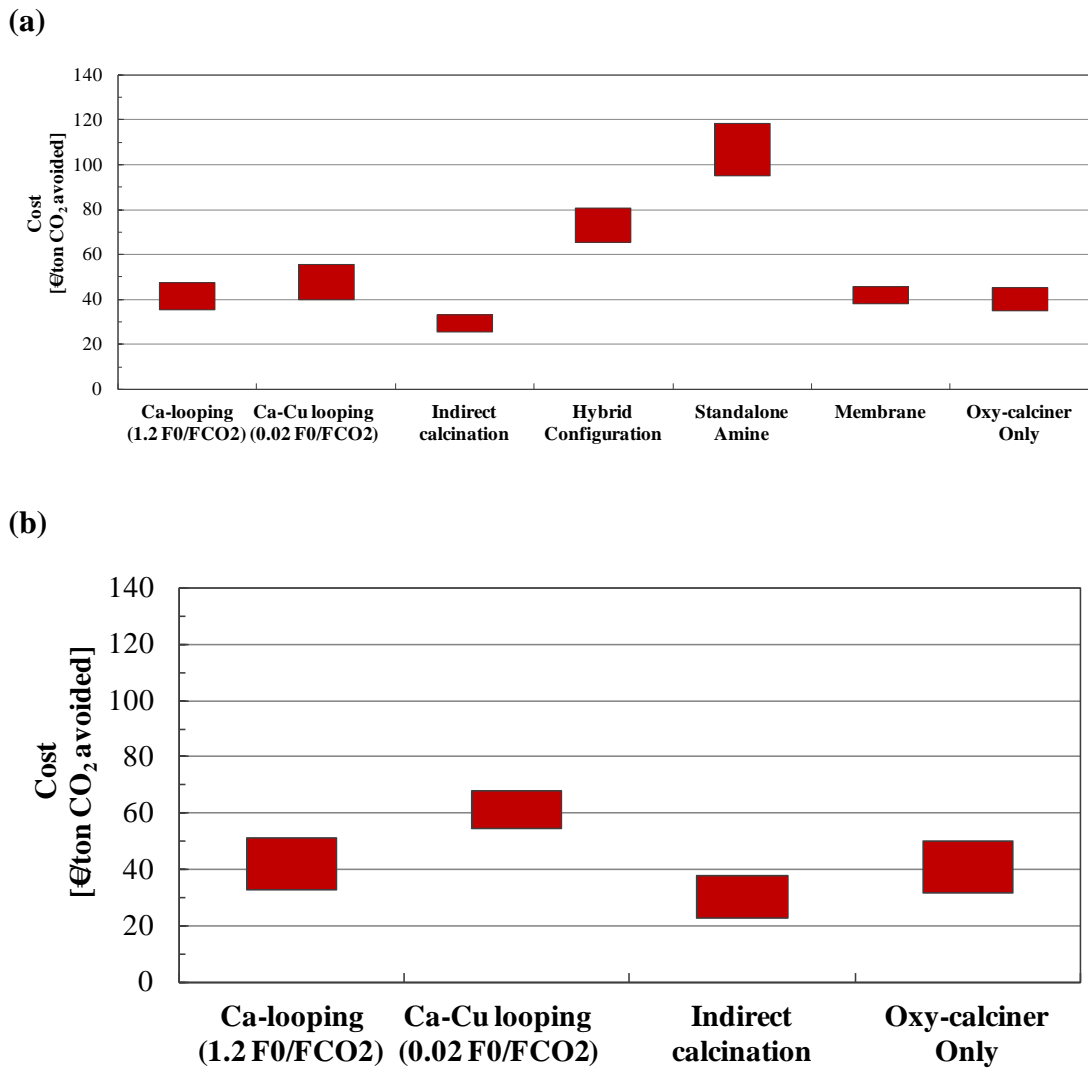
Figure 4-11 Sensitivities of (a) discount rate and (b) scale factor.

Finally, the sensitivity of the cost of CO_2 avoided estimates against the ETS cost is given in Figure 4-12. An increase in the ETS cost is necessary to make the capture processes competitive with the base cement plant as it allows a reduction in the cost of CO_2 avoided. An additional 25% increase in the ETS cost reduces the cost of the Ca-looping process to 37 €/ton CO_2 avoided while that of the indirect calcination process reduces to 25 €/ton CO_2 avoided. If the ETS cost is set to 50 €/ton CO_2, the cost model gives almost zero cost of CO_2 avoided estimate for the Ca-looping case, which will facilitate the use of Ca-looping process in the cement industry.
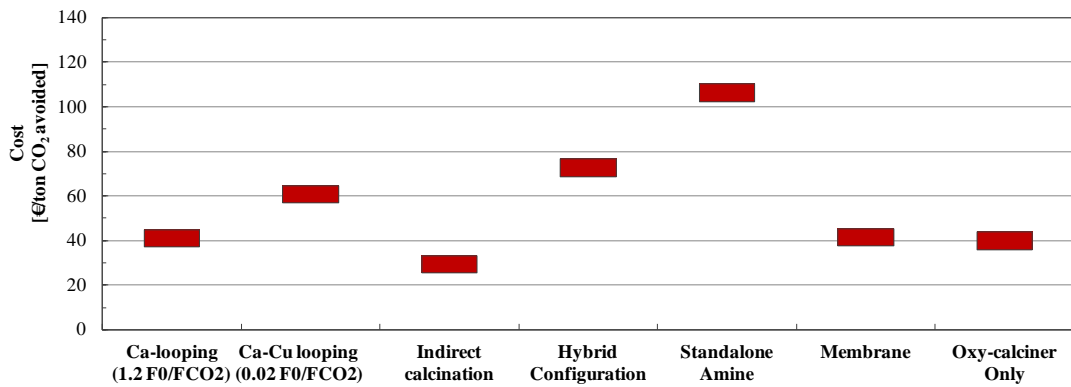
Figure 4-12 Sensitivity of ETS cost.

4.3.5.1 The Effect of Grid Emission Factor

The emission factor for average grid electrical consumption refers to the CO_2 emitted during electricity generation. An average value of 520 kg/MWh is invoked as a reference value in the course of this analysis; this value has been derived from the IEA (2008), which appropriated the emission factors supplied by DEFRA, as well as the energy statistics that were reported in the Digest of UK Energy Statistics (DUKES).

In particular, the emissions from coal, oil, gas, nuclear, renewable and other types of energy and energy generating mechanisms, such as wind turbines, were divided by the total electricity supplied to the grid. The use of the grid emission factor in the calculations will highlight the CO_2 emissions in the base cement plant; it will also emphasise options where electricity is imported. To simplify the use of the grid emission factor, negative emissions that are generated as a result of surplus power generation are not taken into account. For example, in cases such as the Ca-looping process, the Ca-Cu looping process and the standalone amine process, wherein there is surplus power generation, the CO_2 emissions that relate to the use of electricity is set to zero instead of considering a negative value.

Table 4-8 The cost of CO_2 avoided estimates using the grid emission factor.

	Cost ($€$/ton CO_2 avoided)
Ca-looping (1.2 F_0/F_{CO2})	38.0
Ca-Cu looping (0.02 F_0/F_{CO2})	56.1
Indirect calcination	31.5
Hybrid configuration	75.6
Standalone amine process	98.1
Membrane process (0.1 S/R)	47.1
Oxy-calciner only	38.7

Table 4-8 presents the cost of CO_2 avoided estimates, which have been modified to include the grid emission factor. The table clearly illustrates that the cost decreases to 38 $€$/ton CO_2 avoided for the Ca-looping option. Similarly, the cost estimates are reduced for the Ca-Cu looping, standalone amine and oxy-calciner only processes. Nevertheless, the cost estimate increases to around 47 $€$/ton CO_2 avoided for the membrane processes as the electricity is imported in this case.

4.3.5.2 Inclusion of FGD and SCR Units in All Configurations

In the cement industry, SO_2 is formed due to the combustion of fuel in the pre-calciner and kiln, and oxidation of sulfur in raw meal in the preheater stage. Although the SO_2 formed by fuel combustion is mostly absorbed by feed materials in the process, part of the SO_2 generated by the raw meal oxidation is emitted. Based on the given raw meal composition in Table 2-3 where there is only 0.3 wt% sulfur in the raw meal and following the design basis in IEA (2008), FGD and SCR units have not been included in the base cement plant described in Chapter 2. However, these units should be included when amine and membrane separation processes are retrofitted to prevent the negative effects of SO_x and NO_x in the feed gas stream. Various solutions exist to keep these impurities in cement flue gases below the environmental limits even for S-rich raw meal as explained in details in IEA (2008). However, to give more flexibility in terms of fuel selection, and considering that the environmental regulations will become more stringent in the future, the cost results have been updated to include FGD and SCR units in all capture processes including the base cement plant.

Table 4-9 Variation in the cost of CO_2 avoided estimates when the capital costs of FGD and SCR units are included in all configurations.

	Cost ($€$/ton CO_2 avoided)
Ca-looping (1.2 F_0/F_{CO2})	38.0 (-8%)
Ca-Cu looping (0.02 F_0/F_{CO2})	60.0 (-2%)
Indirect calcination	35.8 (+22%)
Hybrid configuration	55.5 (-24%)
Standalone amine process	89.2 (-16%)
Membrane process (0.1 S/R)	24.4 (-41%)
Oxy-calciner only	33.0 (-17%)

The updated cost estimates including their variation against the previously reported values in Figures 4-2, 4-4, 4-6 and 4-8 are presented in Table 4-9. Since the TCR of the base cement plant also increases due to the additional costs of FGD and SCR units, the cost of CO_2 avoided estimates reduces in majority of the cases except the indirect calcination process. In this process, the volumetric flow rate of the flue gas stream fed to the FGD and SCR units is greater as a result of using part of excess air for the combustion of fuel and raw meal preheating. Part of the gas stream is diverted to the carbonator in the Ca-looping and Ca-Cu looping processes where SO_2 can be removed by reaction with CaO, and also NO_x emissions can be minimized in the CFB combustion systems (DOE, 2003). Thus, the cost estimates of these capture processes including that of the oxy-calciner only case reduce. In the base cost scenario, TCRs of the hybrid configuration, standalone amine and membrane processes already include the cost of FGD and SCR units. For this reason, the cost of CO_2 avoided reduces in these cases, providing the minimum cost of 24.4 $€$/ton CO_2 avoided for the membrane process.

Following the same argument, a different scenario can be applicable to membrane and amine processes, where the latest developments in this field provide opportunity to manufacture membranes or solvents having resistance against impurities (SO_x, NO_x, etc.) in the feed gas stream. Unless the environmental regulations are so strict, there will not be any requirement for the FGD and SCR units in this scenario. Therefore, this will also reduce the cost associated with these systems and possibly favour the membrane process over the other options for the reduction of CO_2 emissions from a cement plant.
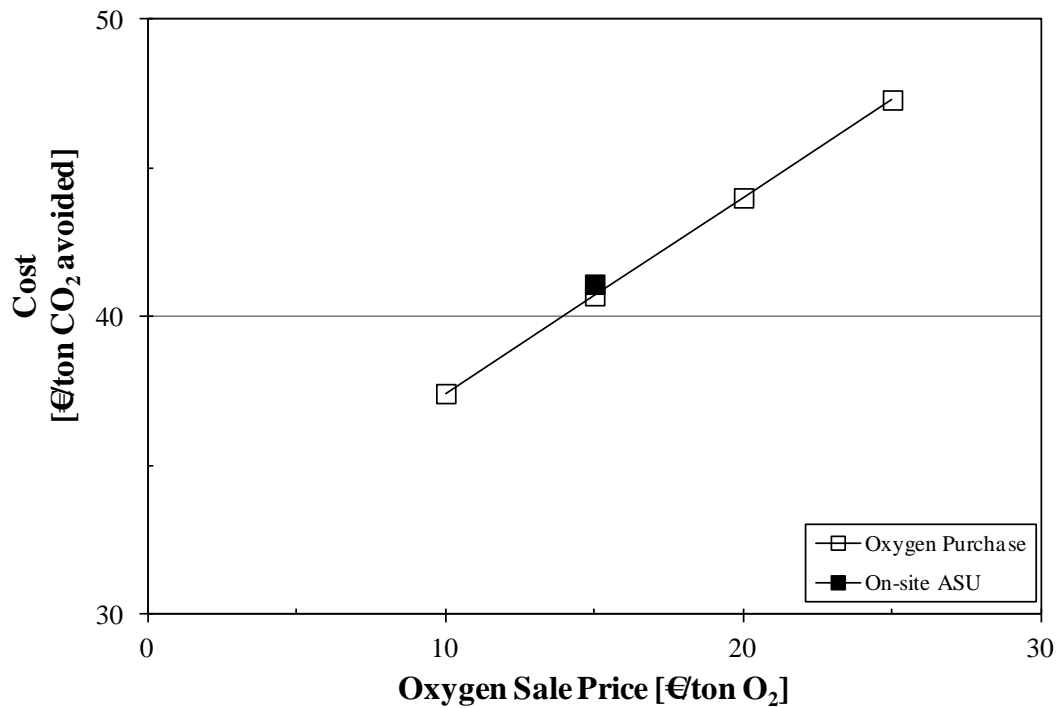
Figure 4-13 Variation in the cost of CO_2 avoided estimate of the Ca-looping option when the ASU existing in the system is replaced by oxygen purchase.

4.3.5.3 Replacement of the ASU in the Ca-looping Process with Oxygen Purchase

The oxygen requirement in the Ca-looping process can also be supplied by purchasing oxygen product instead of having an on-site ASU. To reflect such an option, the cost associated with the ASU has been subtracted from the TCR estimate of the Ca-looping process, and cost of oxygen has been added in place as a variable cost. It was reported that the oxygen production cost can be reduced to 15.5 $/ton O_2 compared to DOE/NETL target of 20 $/ton O_2 (Alptekin et al., 2008). A range of (10 – 25 €/ton O_2) oxygen selling prices have been implemented in the cost model, and the results are illustrated in Figure 4-13. The cost of CO_2 avoided estimate for a system with the ASU is also included for a comparison. The avoided cost is slightly lower when the oxygen selling price is set to 10 €/ton O_2 compared to having an ASU in the system. The cost estimates are almost similar when the selling price increases to 15 €/ton O_2 (around 20 $/ton O_2), while further increase in the oxygen price makes the ASU option more economical.

4.4 Concluding Remarks

The costs of the CO_2 capture technologies evaluated in Chapters 2 and 3 have been reported. A detailed cost model based on LCOC estimations has been proposed for the comparison of these processes in terms of cost of CO_2 avoided. Even though the cost data for the capture units are scarce since most of these technologies are still in a development stage, consideration of their similarity with the existing power systems is the key assumption in the cost model, which allows a reliable estimate. The reference cost data have been updated using the six-tenths rule and M&S index to take the capacity of the unit and historical inflation/deflation rates into account. The ETS price has also been included in the final cost comparisons to expose the advantage of carbon capture from cement plants. The cost and process efficiency estimates for the capture technologies reported in Chapters 2 and 3 are summarized in Table 4-10 for ease of discussion.

Among various options where the F_0/F_{CO2} ratio has been changed in the Ca-looping process, there was no significant effect on costs estimates after 0.4 F_0/F_{CO2}. The TCR estimates reduce when the CO_2 avoidance rate is fixed at 90% compared to the case where it is above 90%, but the specific cost per ton of CO_2 avoided was found to be lower for the latter. The cost was estimated to be around 41 €/ton CO_2 avoided for the Ca-looping process, and it was around 1 €/ton CO_2 avoided lower for the oxy-calciner only case, but the first can provide a higher CO_2 avoidance rate as indicated in Table 4-10. In some circumstances where the assumption of revenue for surplus power generation is not applicable, the avoided cost estimates severely increase below 1.5 F_0/F_{CO2} while the others remain constant. Oxygen purchase with a cost of ≤15 €/ton O_2 was found to be an alternative option to meet the oxygen demand in the Ca-looping process in place of an on-site ASU.

The Ca-Cu looping process offers a reduction in TCR compared to equivalent Ca-looping process, which is mostly related to the absence of an ASU. However, the sorbent cost is the main contributor to the cost estimations. The calculated LCOC for the Ca-Cu looping process is significant at high purge rates, but gets close to that of the Ca-looping process if the purge rate is kept low. Despite this, the cost of CO_2

avoided estimate for the 0.02 F_0/F_{CO2} case is still slightly higher than that of the equivalent Ca-looping process. Further reduction in the cost of the Ca-Cu looping process can be achieved by either an increase in the revenue of power generation or separating CuO/Al_2O_3 sorbent in the purge for reuse.

The standalone indirect calcination process requires the minimum TCR among different carbon capture options compared in this dissertation because this system does not include an additional capture unit but only a gas processing system. The hybrid configuration, combining the indirect calcination and amine processes, results in minor gains to the LCOC estimate, compared to the standalone application of the amine process. Despite this, the final cost of this system is still greater than that of the Ca-looping process.

It was shown that the impact of S/R ratio on cost estimates is negligible for the membrane process as a result of a trade-off between membrane area and energy consumption. The LCOC estimates based on the two feed locations considered were close; with the cost of CO_2 avoided for the membrane process is slightly higher than the value calculated for the Ca-looping process. It seems to be more advantageous to apply the Ca-looping if the revenue of power generation is high, whereas in contrary cases, the membrane process will be the option. The possible future developments of membrane systems with high resistance against SO_x and NO_x in flue gases would eliminate the requirement of FGD and SCR units and further improve the cost of this process.

The sensitivity analysis on the economic indices reveals that a change in the fuel cost results in vast fluctuations in the cost estimations especially for the Ca-Cu looping process and the standalone amine process, for which the energy requirement is severe. When the power cost deviates by ±25%, the cost of the Ca-Cu looping process at 0.02 F_0/F_{CO2} varies significantly because of larger surplus power generation in this system. If the surrounding area has electrical needs and there is a possibility to sell the surplus electricity for profitable prices, this option would be favourable.

Table 4-10 The summary of cost and process efficiency estimates for the capture processes evaluated in Chapters 2 and 3. The values in the parentheses reflect the case where there is no surplus power revenue.

	CO$_2$ avoidance rate (%)	Energy consumption (GJ$_{th}$/ton CO$_2$ avoided)	TCR (€/ton cement)	O&M Cost (€/ton cement)	Variable Cost inc. ETS (€/ton cement)	Cement Cost (€/ton cement)	Cost of CO$_2$ avoided (€/ton CO$_2$ avoided)
Base plant	-	-	34.8	26.1	36.5	97.4	-
Ca-looping	90-99	2.5 – 3.0	55.6 – 61.8	41.4 - 44.6	21.2 – 29.3 (33.3)	125.7 – 127.5 (139.7)	41.0 – 45.0 (61.7)
Oxy-calciner only	90	2.3	53.2	40.1	30.5	123.8	40.0
Ca-Cu looping	90	1.7 – 2.2	55.8 – 62.3	41.4 – 45.0	29.3 – 102.9(116)	137.6 – 201.3 (214.4)	60.8 – 157.0 (176.6)
Indirect Cal.	56	0.9	43.8	32.6	33.0	109.4	29.2
Hybrid Conf.	90	3.3	63.0	42.7	39.8	145.5	72.6
Amine Process	90	8.2	77.5	45.5	44.9 (48.6)	167.9 (171.6)	106.3 (112.0)
Membrane	90	2.0 – 2.1	50.2 – 51.4	37.3 – 38.0	38.4 – 39.2	125.9 – 128.6	42.0 – 47.0

Chapter 5 Process and Cost Analysis of a Biomass Power Plant

In this chapter, a novel concept is presented to capture CO_2 from a large-scale (>100 MW_e) dedicated biomass-fired power plant by using CaO as the CO_2 sorbent. Biomass is burnt in a circulating fluidized bed at sufficiently low temperature to allow in-situ CO_2 capture at atmospheric pressure. A detailed process analysis is carried out to reveal process performance and economics of the proposed power plant which is compared against biomass-air-fired and biomass-oxy-fired power plants. A heat exchanger network is designed using a pinch analysis aimed at the recovery of the maximum amount of excess heat from high temperature gas and solid streams in the plant while the recovered heat is transferred into a subcritical steam cycle for power generation. The entire process simulation also includes a CO_2 purification and compression unit that allows reaching more than 95 mol% CO_2 purity. Work presented in this chapter is the outcome of my visit to Instituto Nacional del Carbón (INCAR, Spain) where the part of work was carried out and has resulted in one published article as detailed in Appendix E. Prof. Carlos Abanades and Dr. Monica Alonso are co-authors of the publication and contributed with their guidance and expertise.

5.1 Background

The use of sustainably-grown biomass as a renewable energy source in combustion systems can be defined as a potential way to reduce CO_2 emissions, as this is associated with zero net CO_2 emissions (Faaij et al., 1998). In Europe, it is expected that the targets of 20% reduction in CO_2 emissions by 2020 and increase in the share of renewable energy to 20% can be partially achieved by replacing coal with biomass in coal fired power generation systems (Maciejewska et al., 2006; Böhringer et al., 2009).

Large scale ($\geq$100 MW_e) dedicated biomass-power plants have not been deployed in the past for critical economic reasons linked to the limited local availability of biomass sources, low energy density, higher moisture content and variability of fuel

characteristics. Most of the proposed solutions to introduce biomass in the power generation sector have been aimed at co-firing biomass with coal in existing power plants (Dai et al., 2008; Demirbas et al., 2009). It is generally agreed that co-firing up to 20% biomass with coal is technically feasible with relatively modest modifications of the existing system (Demirbas, 2003). However, further increases in biomass content generate problems. For example high mixing ratios can create more difficulties to fuel preparation and milling stages, boiler capacity and performance as well as the utilization of ash, which reveals the requirement of a dedicated biomass infrastructure (Maciejewska et al., 2006). In addition to a reduction of CO_2 emissions, co-firing of biomass with high-sulphur coal can provide a reduction in NO_x and SO_x emissions (Baxter, 2005). In the EU many countries have established green certificate incentives for biomass use and this has led to an international market of biomass feedstock for power generation (Schaeffer et al., 2013).

The latest developments in CFB technology are enabling a niche market in the power sector for biomass combustion and gasification plants with net power generation capacities between 100 and 250 MW_e in standalone configurations or linked to larger fossil plants (Stevens, 2001; IEAGHG, 2009). In particular, CFB combustion systems for biomass have been defined as an ideal technology to be deployed at large scale power generation from biomass co-firing owing to inherently low emissions, high availability and superior fuel flexibility with high system efficiencies (Hotta, 2010). The current CFB technology of dedicated biomass firing is available up to 300 MW_e and that for co-firing 50% biomass with coal can reach 600 MW_e, while the maximum steam conditions for clean biomass firing can approach 570°C and 180 bar, and for 50% biomass 585°C and 290 bar (Jäntti and Nuortimo, 2012). The Foster Wheeler large scale utility at 300 MW_e using an advanced bio CFB boiler generates steam at 568/566°C and 179/43.6 bar and this concept is market-ready (Jäntti and Nuortimo, 2012).

It should be noted that with current technology only subcritical steam cycles are available for dedicated biomass-fired power plants while the supercritical steam cycle conditions are only feasible for coal co-firing because of the high furnace tube material temperatures and the requirement of tube materials to protect against

corrosion (Jäntti and Nuortimo, 2012). This limitation is linked, among other factors, to the need to moderate combustion temperatures in the biomass combustor to minimize risks of bed agglomeration, fouling and corrosion of the convective surfaces (Leckner, 1998; Werther et al., 2000; Khan et al., 2009). Vaporized biomass alkalis react with flue gas constituents and fly ash, producing low-melting species. The potential of agglomeration, fouling and corrosion tendencies is linked to the chlorine and sulphur contents and alkali composition so that the risks are more severe for straw than for wood chips, sawdust and husk (rice) (Hiltunen et al., 2008; Jäntti and Nuortimo, 2012).

5.2 Application of CO$_2$ Capture to Biomass-fired Systems

The application of CO$_2$ capture and permanent geological storage to biomass fired systems leads to processes with negative emissions of CO$_2$ (Ishitani and Johansson, 1996; Obersteiner et al., 2001; Rhodes and Keith, 2008). In theory all the CO$_2$ capture technologies (pre-combustion, post-combustion and oxy-combustion) are applicable for this purpose. The conceptual integration of a Ca-looping process for in-situ CO$_2$ capture from a dedicated biomass-fired power plant was proposed in a previous study and is represented in Figure 5-1 (Abanades et al., 2011a). In the combustor-carbonator reactor, biomass is fired with air and the CO$_2$ generated in this reactor is captured by CaO flowing from a calciner according to the following reaction.

C (from biomass) + O$_2$ (from air) + CaO $\rightarrow$ CaCO$_3$ + Heat $\hspace{2cm}$ (Rn. 5.1)
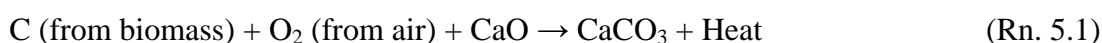
The main additional product of the combustion is water, while for air the presence of 79 mol% inert nitrogen is assumed. The experimental performance of the proposed design has been investigated in a 30 kW$_{th}$ test facility (Alonso et al., 2011a) and scaled up to a 300 kW$_{th}$ pilot plant (Alonso et al., 2013). Although the work is still in progress to characterize and optimize the operation of the larger pilot plant, the operation of the simultaneous combustion-carbonation step in this system was found to be technically feasible from a reactor perspective as combustion of biomass at around 700ºC is known to yield high combustion efficiencies.
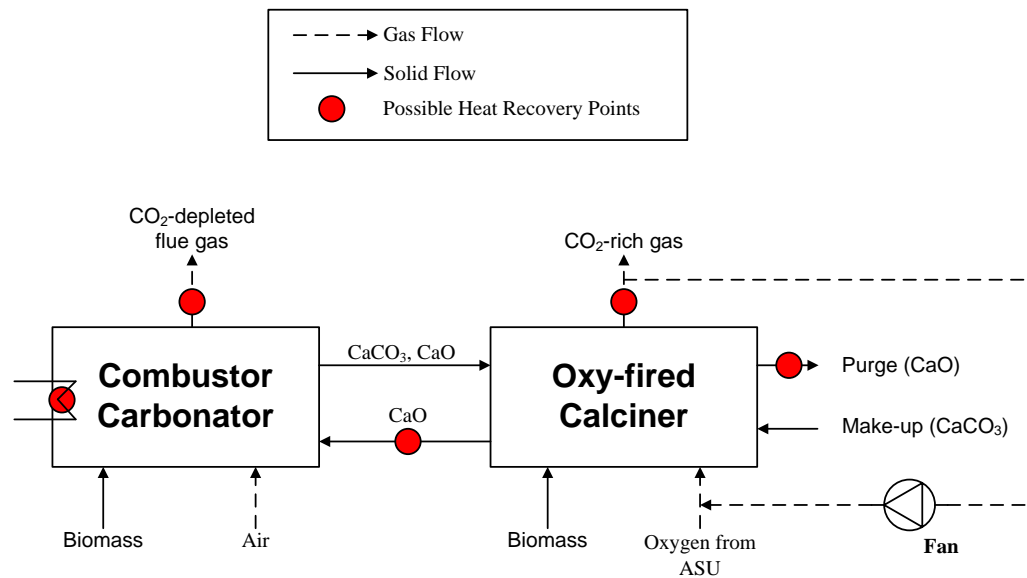
Figure 5-1 Basic schematic diagram of the in-situ Ca-looping plant (Abanades et al., 2011a).

The combustor temperature of 700ºC also allows for theoretical CO_2 capture efficiencies over 80% when sufficiently active CaO is present in the combustor-carbonator reactor which has been validated experimentally (Abanades et al., 2011b; Alonso et al., 2011a; Alonso et al., 2011b). Despite the potential importance of the concept shown in Figure 5-1 as a future application of bio-energy with CO_2 capture and storage (BECCS) technologies, there has not been a comprehensive process analysis of the system and only a rough analysis of the cost structure has been published so far (Abanades et al. 2011a). Therefore, the objective in this chapter is to evaluate the system of Figure 5-1 in sufficient detail to allow for a comprehensive cost analysis of the proposed system against similar alternatives for biomass combustion with and without CO_2 capture. A number of promising configurations have been developed and the results have been compared against dedicated biomass-air-fired and biomass-oxy-fired power plants in terms of net power generation efficiency, CO_2 capture rate and cost of CO_2 avoided.

5.3 Reference Power Plants

5.3.1 Biomass-air-fired Power Plant

The CFB biomass-air-fired power plant used as a reference in this work has been simulated according to relevant published reports (DOE, 2003; IEAGHG,2009) and

its schematic diagram including the detailed steam cycle configuration (DOE, 2007) is shown in Figures 5-2(a) and 5-2(b), respectively. The plant uses a subcritical steam cycle with a single reheat (166.5 bar/565.6°C/565.6°C). The steam cycle stream properties for the plant from the simulations are given in Appendix D along with a simulation of the effect of higher moisture contents. The steam cycle simulation used in this study is calibrated against the reported data detailed in Ahn et al. (2013). As the current biomass combustion technology does not allow severe steam generation conditions, only the subcritical steam cycle is investigated for the proposed dedicated biomass-fired power plant configurations (DOE, 2003; McIlveen-Wright et al., 2011; Jäntti and Nuortimo, 2012).

The design parameters for the biomass-air-fired plant are given in Table 5-1. The biomass-air-fired plant is an exemplary 135 MW$_e$ net output power plant with 40.9% net efficiency based on lower heating value (LHV) of the design biomass (Abanades et al., 2011a). The design biomass, with an LHV value of 20.08 MJ$_{th}$/kg estimated by the simulator, is burnt in 15% excess air to guarantee complete combustion. The total thermal energy input from biomass combustion is 329.8 MW$_{th}$. The contents of ash and alkalis in the biomass are not considered as limiting factors; although, depending on the quality of the biomass, there would be the requirement for some modifications in the steam cycle design. In the schematic diagram shown in Figure 5-2(a), the combustion air is passed through a fan to provide 0.2 bar to overcome the pressure drop in the combustor. The flue gases from the convection pass heat exchangers are further cooled down to 135°C by pre-heating the inlet combustion air, and then flow into a dust collector where particulates such as fly ashes are removed (DOE, 2003). The CFB biomass-air-fired power plant includes an infiltration air flow rate estimated to be 2 wt% of total gas flow rate from the combustor (DOE, 2003; DOE, 2007). The full process has been simulated in UniSim Design and the outputs of the simulation are summarized in Table 5-1. The results are in close agreement with those reported in the by the IEAGHG (2009) and provide a base for comparison with simulations of the biomass-oxy-fired and in-situ Ca-looping concepts described in the next paragraphs.

(a)
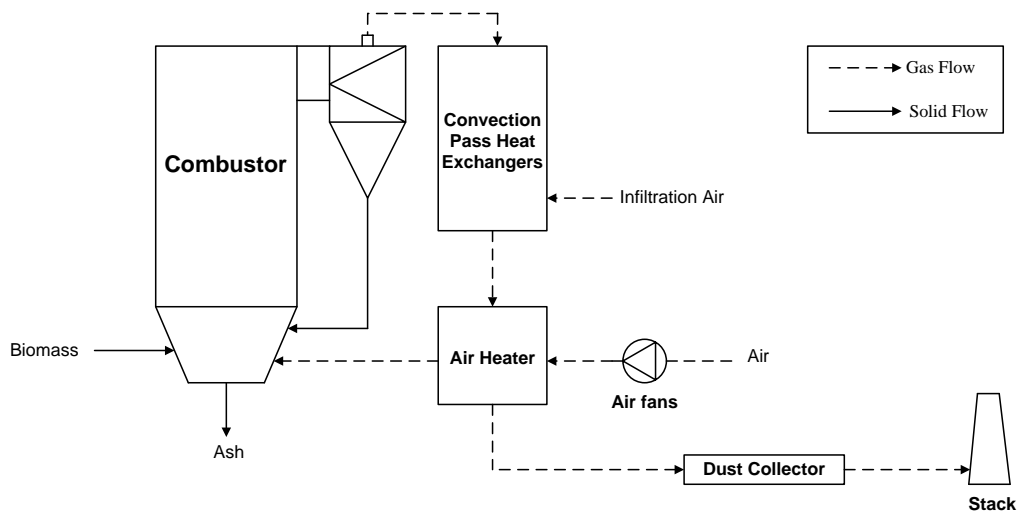
(b)
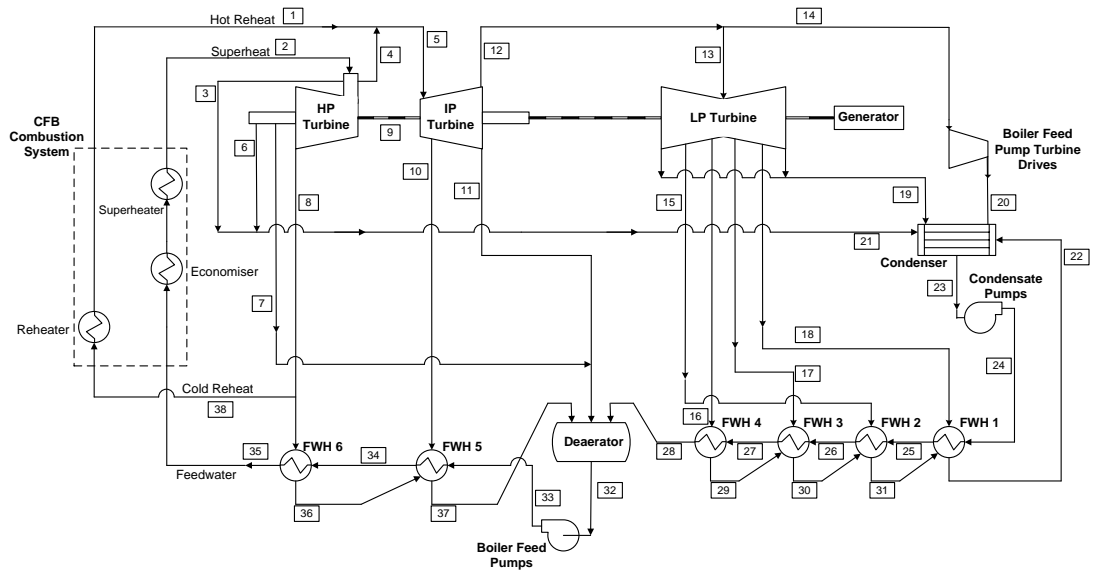
Figure 5-2 Simplified schematic diagrams of the (a) biomass-air-fired power plant (DOE, 2003) and (b) integrated subcritical steam cycle (IEAGHG, 2009). (**HP**: High Pressure; **IP**: Intermediate Pressure; **LP**: Low Pressure; **FWH**: Feedwater Heater)

Table 5-1 Design specifications and performance summaries of the dedicated biomass-air-fired and biomass-oxy-fired power plants.

	Biomass-air-fired Power Plant	Biomass-oxy-fired Power Plant
Fuel	Biomass	Biomass
Fuel Composition (wt %)	5.4% H, 39.9% O, 0.7% N, 5.4% Ash, 41.4% C, 7.2% Moisture	5.4% H, 39.9% O, 0.7% N, 5.4% Ash, 41.4% C, 7.2% Moisture
Fuel Flow Rate (ton/h)	59.14	59.14
Fuel Lower Heating Value, LHV (MJ$_{th}$/kg)	20.08 (simulated)	20.08 (simulated)
Heat of Combustion (MW$_{th}$)	329.8	329.8
Air/Oxygen Flow Rate (ton/h)	343.3	71.0
Infiltration Air Flow Rate (ton/h)	8.0	4.8
Steam Cycle Conditions (bar/°C/°C)	166.5/565.6/565.6	166.5/565.6/565.6
Gross Power Generation (MW$_e$)/Efficiency (%)	143.8 / 43.6	147.6 / 44.8
Auxiliary Power (MW$_e$)	8.8	8.0
Air Separation Unit Power (MW$_e$)	-	16.4
CO$_2$ Purification and Compression Power (MW$_e$)	-	11.5
Net Power Generation (MW$_e$)/Efficiency (%)	135.0 / 40.9	111.7 / 33.9
Overall CO$_2$ Capture Efficiency (%)	-	93
CO$_2$ purity (mol %)	-	97

5.3.2 Biomass-oxy-fired Power Plant

In the dedicated CFB biomass-oxy-fired plant, the thermal energy input from biomass combustion is set to be the same as that in the biomass-air-fired plant, i.e. 329.8 MW_{th}. The plant parameters for the biomass-oxy-fired plant are also reported in Table 5-1. The oxygen feed at 99.1 mol% purity from an ASU is mixed with the part of CO_2-rich gases leaving the convection pass heat exchangers and is fed to the combustor. The oxygen concentration in this mixture is fixed at 40 mol% to limit flame temperatures in the combustor but it has a potential to be even higher (70 mol%) according to the DOE report (2003). The ASU power requirement is set as 231 kWh per ton of oxygen at 1.2 bar (DOE, 2003), which is identical to that used in Chapter 2. The circulated CO_2-rich gases are initially passed through a fan with a final pressure of 1.2 bar to overcome pressure drop along the combustor. The gas flowrate into the combustor is determined by setting the oxygen molar fraction in the CO_2-rich gas stream to 3 mol% and complete combustion is assumed. The CO_2-rich gases from the convection pass heat exchangers that are not recirculated to the combustor feed, are initially cooled down to 172°C by exchanging heat with the inlet oxygen feed and then further cooled down to 80°C in the second feedwater heater (FWH2) shown in Figure 5-2(b) (DOE, 2003; DOE, 2010). Air infiltration is also included as for the biomass-air-fired plant.

5.3.3 Power Plant Auxiliaries

In the two dedicated biomass power plants described above, a biomass drying unit is not included. The limits of NO_x emissions for biomass combustion systems can be met by firing the boiler with low furnace exit temperatures, which can be completely eliminated in the oxy-combustion systems (DOE, 2003; IEAGHG, 2009). Therefore, there is no need for an SCR unit. Moreover, because of negligible content of sulphur in the design biomass used in this study, an external FGD unit or limestone injection is not included. The flow of infiltration air in the biomass-oxy-fired plant reduces the CO_2 concentration in the gas streams and leads to the requirement for a CO_2 purification unit in order to achieve the target purity of ≥95 mol%.
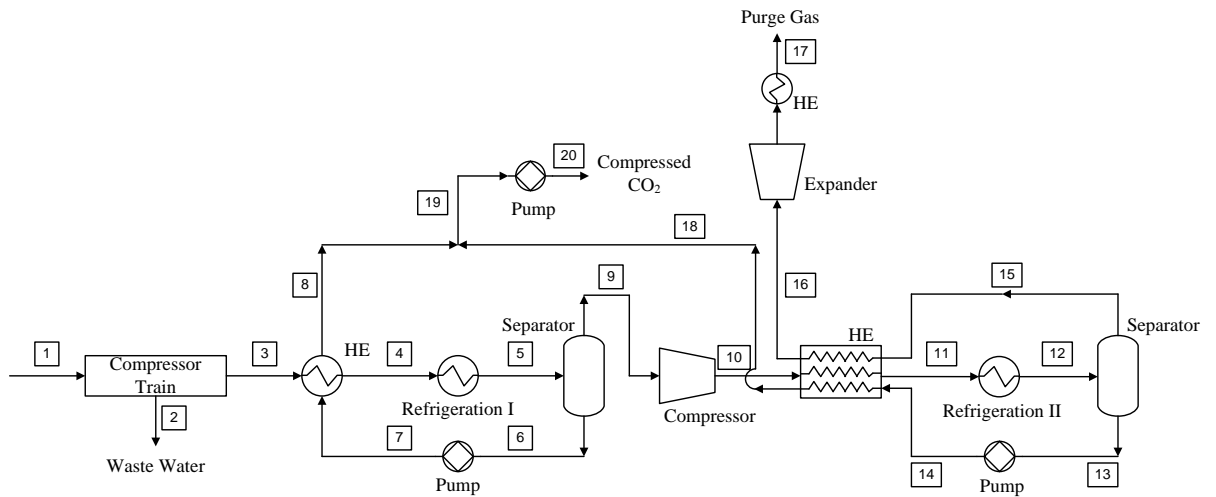
Figure 5-3 Schematic diagram of the cryogenic CO_2 purification and compression unit (Xu et al., 2012). (**HE**: Heat exchanger)

A CO_2 purification and compression stage (final pressure of 150 bar) is added to the biomass-oxy-fired plant and the Peng-Robinson equation of state (Honeywell, 2010) is used as the thermodynamic model to calculate the phase equilibrium and fluid properties. While only a simple CO_2 compression design is needed owing to the absence of air infiltration assumption in the Ca-looping and Ca-Cu looping process schemes evaluated in Chapters 2 and 3, it is clear that a more advanced gas processing system will be required in reality if there are any air-leakages into the oxy-fired combustor (or calciner).

The configuration of the CO_2 cryogenic liquefaction and separation system proposed by Xu et al. (2012) has been adapted to the present case. The reference cryogenic system comprises a two-stage compression, a two-stage refrigeration, a two-stage separation and an energy recovery component. The pressure drops in the heat exchangers will result in a maximum additional power requirement of 0.5 MW$_e$ and as a result are not considered further. The cryogenic process has been modified slightly because of the different feed gas compositions compared to 80 mol% in Xu et al. (2012). In this study, the CO_2 molar fraction in the feed is only 49 mol%, which becomes 87 mol% on a dry basis and differs from the 80 mol% of Xu et al. (2012). By adjusting slightly the gas pressure to reach it is possible to reach the targeted CO_2 purity. The corresponding schematic diagram is presented in Figure 5-3 and the stream compositions are given in Appendix D.

The CO_2-rich gas stream is initially compressed to 24 bar by a series of compressors with intermediate cooling to 35°C. The compressed gas is further cooled to −20°C initially by heat exchange with liquid CO_2 and then to −35°C by a refrigeration cycle. The fluid refrigerant R502 with a boiling point of −45.4°C is chosen for the first stage of refrigeration because of its acceptable thermodynamic performance (Xu et al., 2012). Liquid CO_2 from the first separator is pumped to 80 bar. In the second stage, the remaining gases are first further compressed to 54 bar and then cooled to −18°C by heat exchange with liquid CO_2 and purge gas from the second separation stage. The refrigerant, R502, is also used in the second stage to reduce the gas temperature to −35°C. The minimum temperature difference in the low temperature heat exchanger is more than 2.1°C. The heat released during the expansion of exhaust stream (No 16) is used to cool down the feed gas in the compressor train. Finally, the liquid CO_2 from the both stages of the cryogenic separation process is pumped to 150 bar. The adiabatic efficiency of compressors and pumps has been assumed to be 80%. The overall CO_2 capture efficiency in the cryogenic separation system is 93% with CO_2 purity of ~97 mol%. The average performance of vapour compression cycle coefficient (COP) was taken as 1.36 for the first and second stages of refrigeration in order to estimate power use (Xu et al., 2012).

5.3.4 Results and Discussion

The gross power generation capacity, presented in Table 5-1, is estimated to be 143.8 and 147.6 MW_e for the biomass-air-fired and biomass-oxy-fired plants, respectively. The difference in these values can be linked to the preheating requirement of nitrogen in the air as well as lower level of heat recovery from the flue gas stream which is fed to the stack at 135°C, compared to 80°C of the CO_2 rich stream in the biomass-oxy-fired plant. The power requirements associated with auxiliaries (8.0 MW_e), ASU (16.4 MW_e) and CO_2 purification and compression (11.5 MW_e) in the biomass-oxy-fired plant results in a reduction of the net power output down to 111.7 MW_e with 33.9% LHV-based efficiency. The overall capture efficiency and CO_2 purity of the biomass-oxy-fired plant are directly related to the

efficiency in the CO_2 purification and compression stage, which are 93% and 97 mol%, respectively.

5.4 In-situ Ca-looping Power Plant

5.4.1 Combustor-Carbonator Model

The key issue in the combustor-carbonator design is the selection of the operating temperature since this is based on the equilibrium of CO_2 over CaO and the simultaneous combustion of biomass (Abanades et al., 2011a). It was concluded that a reactor temperature of 700°C allows sufficiently high CO_2 capture and combustion efficiencies. At this temperature tar formation and the associated emissions of hydrocarbons may be an issue for further research if the technology evolves towards larger scale demonstration. However, considering the catalytic effect of CaO particles on tar cracking reported by several authors in similar biomass gasification processes in fluidized beds (Koppatz et al., 2009; Soukup et al., 2009) together with the oxidizing nature of the combustor-carbonator, only minor traces of these contaminants should be expected in the proposed systems and no cost penalty has been allocated to treat them.

There are two heat sources in the combustor-carbonator which are the biomass combustion and the exothermic carbonation reaction. Thus, a heat recovery system is necessary to keep the reactor at the desired temperature. As for the previous designs full conversion of the fuel is assumed. However, the detailed description of the in situ Ca-looping plant requires additional assumptions on the level of conversion of CaO to $CaCO_3$ and the required level of solid circulation between the reactors. Even though the rigorous carbonator model is employed in Chapters 2 and 3 for the prediction of carbonation efficiency, the model is not applicable for this system where simultaneous combustion and carbonation take place. Therefore, in this chapter, the efficiency of carbonation is estimated by setting the conversion level of CaO to $CaCO_3$ (X_{ave}) at 0.1 and the maximum average conversion rate of CaO ($X_{max,ave}$) at 0.15 considering that the sorbent is derived from a natural limestone (Grasa and Abanades, 2006). The value of 0.05 ($X_{active} = X_{max,ave} - X_{ave}$) as active fraction of CaO particles is assumed to be enough to capture 80% of CO_2 generated

in the carbonator which is in an agreement with the previous experimental work where this was demonstrated (Alonso et al., 2011). Since the sorbent loses its absorption capacity through cyclic carbonation and calcination cycles, part of the sorbent is replaced with make-up sorbent that is assumed to be 100% $CaCO_3$.

The quantity of purge flow rate has been calculated by using (Rodriguez et al., 2010):

$$X_{max,ave} = \frac{a_1 f_1^2 F_0}{F_0 F_R f_{carb}(1-f_1)} + \frac{a_2 f_2^2 F_0}{F_0 F_R f_{carb}(1-f_2)} + b \qquad \text{(Eq. 5.1)}$$

where a_1, a_2, b, f_1 and f_2 are decay constants obtained from experimental data available for the CaO-based sorbent produced from natural limestone and taken as 0.1045, 0.7786, 0.07709, 0.9822 and 0.7905 respectively (Rodriguez et al., 2010). f_{carb} refers to $X_{ave}/X_{max,ave}$ ratio. With the known CO_2 molar flow rate (F_{CO2}), F_R can be calculated from the following equation where E_{CO2} refers to the carbonation efficiency.

$$E_{CO_2} = \frac{F_R X_{ave}}{F_{CO2}} \qquad \text{(Eq. 5.2)}$$

5.4.2 Assumptions to Build Mass and Energy Balances

The temperature of the calciner is set to 890°C which is 15°C higher than the equilibrium temperature (Garcia-Labiano et al., 2002) and complete calcination is assumed. The heat requirement mainly for the endothermic calcination reaction is provided by combustion of biomass with oxygen from an ASU. A biomass-drying unit is not included for consistency with the previous cases and also because in this case it leads to a reduced CO_2 partial pressure in the calciner, which allows to operate the calciner at lower temperatures. Furthermore, it is shown that steam addition into the calciner may potentially improve the cyclic stability and performance of CaO-based sorbents (Rong et al., 2013). As in the previous oxy-fired reference case, the purity of oxygen fed to the calciner is assumed to be 99.1 mol% at 1.2 bar and part of the exiting CO_2-rich gases are circulated to lower oxygen concentration in the feed gas to prevent high flame temperatures inside the calciner. A circulation fan is required on the circulated CO_2-rich gases to overcome pressure

drop in the calciner. As before, the inlet oxygen concentration was set equal to 40 mol%. The combustion air flowing into the combustor-carbonator is initially passed through a fan to boost of the gas stream pressure by 0.2 bar to overcome the pressure drop.

The overall mass and energy balances, presented in Table 5-2 for the schematic diagram in Figure 5-4, have been conducted to achieve 80% CO_2 capture efficiency in the combustor-carbonator and 100% calcination efficiency. The resulting sorbent to feed ratio (F_R/F_{CO2}) and purge rate ratio (F_0/F_{CO2}) are estimated to be 8 and 0.07, respectively. The infiltration air flow rate into both reactors has been estimated to be 2% of total gas flow rate as for the previous cases. It has been assumed that 80% of ashes from biomass combustion leave the system as fly ash. Moreover, 10% of make-up ($CaCO_3$) escapes the system as CaO in the fly ash because of sorbent attrition. This portion of CaO is linked to a small additional energy penalty due to the energy required for its calcination. It should be noted here that the assumptions of fly ash and CaO attrition that improve the accuracy of process simulations are only occupied in this chapter whereas they are not taken into consideration in Chapters 2 and 3. The total thermal energy input for the in-situ Ca-looping plant, which is the sum of that for the combustor-carbonator and that for the calciner, is set to 329.8 MW_{th} as before. Almost 64% of this energy needs to be supplied to the combustor-carbonator while the rest is provided to the calciner.

5.4.3 Heat Recovery Steam Cycle

An important design issue for the in-situ Ca-looping plant is heat recovery from high temperature gas and solid streams. There are five different heat recovery locations on the diagram shown in Figure 5-1: combustor-carbonator; CO_2-depleted flue gas stream leaving the carbonator; CO_2-rich gas from the calciner; solid purge stream; and solid stream from the calciner to the combustor-carbonator. The last is important since it reduces the quantity of heat that needs to be recovered in the combustor-carbonator as well as the required heat transfer area in this reactor.
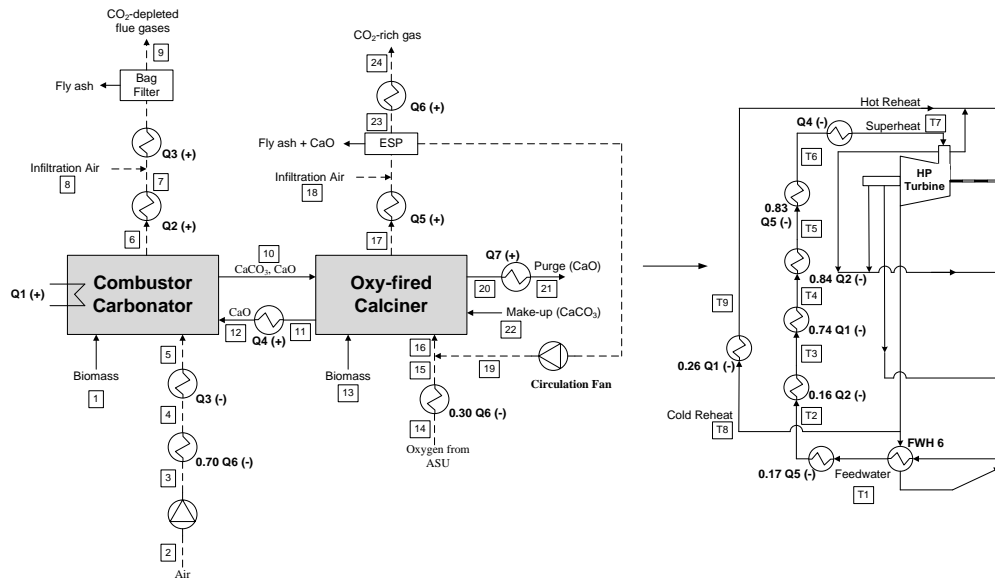
Figure 5-4 Detailed presentation of the heat recovery from the in-situ Ca-looping plant and its integration with the reference steam cycle shown in Figure 5-2(b). The flow rate of steam in the steam cycle is 400 t/h.

A heat exchanger network design is necessary to recover the maximum amount of heat from this process, which can be then transferred to the steam cycle for power generation. Even though a predefined gross efficiency has been employed to estimate power generation capacity from high temperature sources in Chapters 2 and 3, the steam cycle configuration described for the reference systems (Figure 5-2(b)) has been modified in this chapter in order to recover heat from the recovery points summarized above for the in-situ Ca-looping plant. The detailed integration of steam cycle with the in-situ Ca-looping plant is shown in the right inset in Figure 5-4 and corresponding stream conditions are presented in Table 5-2. The pinch methodology is applied to estimate minimum energy requirement (MER) as well as to develop a heat exchanger network design. The objective of pinch method is the reduction of external energy requirements (heating or cooling) by maximizing heat transfer between hot and cold streams (Linnhoff et al., 1978). A minimum temperature difference of 20°C in the heat exchangers is assumed (Lara et al., 2013), while the heat exchangers in the base steam cycle design have a minimum temperature difference of 5°C (DOE, 2007).

Table 5-2 The stream properties and compositions for the in-situ Ca-looping plant presented in Figure 5-4.

Stream No	1	2	3	4	5	6	7	8	9	10	11	12
T (°C)	15	15	34.2	99	294	700	320	15	135	700	890	500
m (ton/h)	37.7	219.1	219.1	219.1	219.1	210.6	210.6	4.2	213.2	700.8	654.6	654.6
Composition (wt %)												
CO_2	-	-	-	-	-	5.4	5.4	-	5.4	-	-	-
O_2	-	23.5	23.5	23.5	23.5	4.1	4.1	23.5	4.5	-	-	-
N_2	-	76.5	76.5	76.5	76.5	79.7	79.7	76.5	80.3	-	-	-
CaO	-	-	-	-	-	-	-	-	-	74.9	89.1	89.1
$CaCO_3$	-	-	-	-	-	-	-	-	-	14.9	-	-
C	41.4	-	-	-	-	-	-	-	-	-	-	-
H	5.4	-	-	-	-	-	-	-	-	-	-	-
S	-	-	-	-	-	-	-	-	-	-	-	-
O	39.9	-	-	-	-	-	-	-	-	-	-	-
N	0.7	-	-	-	-	-	-	-	-	-	-	-
H_2O	7.2	-	-	-	-	10.0	10.0	-	9.8	-	-	-
Ash	5.4	-	-	-	-	0.8	0.8	-	-	10.2	10.9	10.9
LHV (MJ_{th}/kg)	20.08	-	-	-	-	-	-	-	-	-	-	-
Total Stream Enthalpy (GJ_{th}/h)	−71.23	−2.3	−2.0	16.6	61.1	−236.9	−335.0	−0.04	−357.0	−7757.0	−7076.0	−7322.0

Stream No	13	14	15	16	17	18	19	20	21	22	23	24
T (°C)	15	15	248	279.3	890	15	294.0	890	150	15	267.4	80
m (ton/h)	21.4	26.8	26.8	76.7	148.8	3.0	49.9	5.9	5.9	10.4	100.4	100.4
Composition (wt %)												
CO_2	-	-	-	53.7	83.3	-	82.6	-	-	-	82.6	82.6
O_2	-	99.2	99.2	36.6	2.6	23.5	3.0	-	-	-	3.0	3.0
N_2	-	0.8	0.8	2.0	1.1	76.5	2.6	-	-	-	2.6	2.6
CaO	-	-	-	-	0.4	-	-	89.1	89.1	-	-	-
$CaCO_3$	-	-	-	-	-	-	-	-	-	100	-	-
C	41.4	-	-	-	-	-	-	-	-	-	-	-
H	5.4	-	-	-	-	-	-	-	-	-	-	-
S	-	-	-	-	-	-	-	-	-	-	-	-
O	39.9	-	-	-	-	-	-	-	-	-	-	-
N	0.7	-	-	-	-	-	-	-	-	-	-	-
H_2O	7.2	-	-	7.7	12.0	-	11.8	-	-	-	11.8	11.8
Ash	5.4	-	-	-	0.6	-	-	10.9	10.9	-	-	-
LHV (MJ_{th}/kg)	20.08	-	-	-	-	-	-	-	-	-	-	-
Total Stream Enthalpy (GJ_{th}/h)	−40.4	−0.25	5.6	−427.6	−1211.0	−0.03	−433.3	−63.7	−67.7	−125.7	−874.7	−895.2

Stream No	T1	T2	T3	T4	T5	T6	T7	T8	T9
T (°C)	251.5	262.0	270.0	361.7	365.1	391.4	565.6	365.9	565.6

The pinch analysis specifications are summarized in Table 5-3 including all heat duties. The target temperatures for the hot streams as well as the cold ones in the steam cycle can be predefined whereas those for the combustion air and oxygen streams should be calculated according to the energy balance after the steam cycle integration. To reach maximum heat recovery with high power generation efficiency the two primary target cold streams are feedwater at ~252°C and cold reheat at ~366°C in the reference steam cycle presented in Figure 5-2(b). The hot streams can be cooled down to only 272°C, because of the minimum temperature difference of 20°C, when only those two streams are targeted. Further heat recovery from these streams can be made either to the combustion air and oxygen streams or to the feedwater heaters (FWH 1-6) in the steam cycle. In this study, the excess heat from the CO_2-rich gas and CO_2-depleted gas streams are initially transferred to the feedwater stream as shown in Figure 5-4 with final gas temperatures of 272°C and 320°C, respectively. Since the aim is to generate more steam at high temperature, the remaining excess heat from those gas streams is transferred to the combustion air and oxygen streams.

The feedwater is then further heated to the desired steam conditions by additional heat from the combustor-carbonator and circulated solids at high temperature, while the remaining heat from the combustor-carbonator is then sufficient to heat up the cold reheat as suggested in Figure 5-4. Once this heat exchanger network arrangement is defined, the flow rate of steam in the steam cycle is adjusted to minimize the heat requirement of hot and cold utilities. With a steam flow rate of 400 ton/h, the MER is estimated to be almost zero, leading to the maximum theoretical heat recovery from the in-situ Ca-looping plant to the steam cycle. For this threshold problem, the pinch point is located at 870 - 890°C and the corresponding Grand Composite Curve (GCC) is shown in Figure 5-5. It should be mentioned that potential heat transfer from the purge stream to the steam cycle is not considered because of its low heat duty. There would be a marginal increase in the required total heat exchange area in the in-situ Ca-looping configuration as the combustor is operated at a lower temperature than commercial boilers (~850°C) but this issue is not considered in the current level of development.

Table 5-3 Pinch analysis specifications for the in-situ Ca-looping plant.

Heat Recovery Point	Supply Temperature (°C)	Target Temperature (°C)	Heat Duty (MW$_{th}$)	Stream	Stream Type
Combustor-Carbonator (C-C)	700.0	700.0	183.8	+Q1	Hot
CO$_2$-depleted Gas	700.0	135.0	39.6	+(Q2+Q3)	Hot
Solids from Calciner to C-C	890.0	500.0	68.3	+Q4	Hot
CO$_2$-rich Gas (from calciner)	890.0	272.0	32.8	+Q5	Hot
CO$_2$-rich Gas (to compression)	267.4	80.0	5.7	+Q6	Hot
Purge from Calciner	890.0	150.0	1.1	+Q7	Hot
Combustion Air into C-C	34.2	294.0	16.4	−(Q3+0.71 Q6)	Cold
Oxygen into Calciner	15.0	248.0	1.7	−(0.30 Q6)	Cold
Cold Reheat	365.9	565.6	48.0	−(0.26 Q1)	Cold
Feed-water	251.5	565.6	264.1	−(0.74 Q1+Q2+Q4+Q5)	Cold
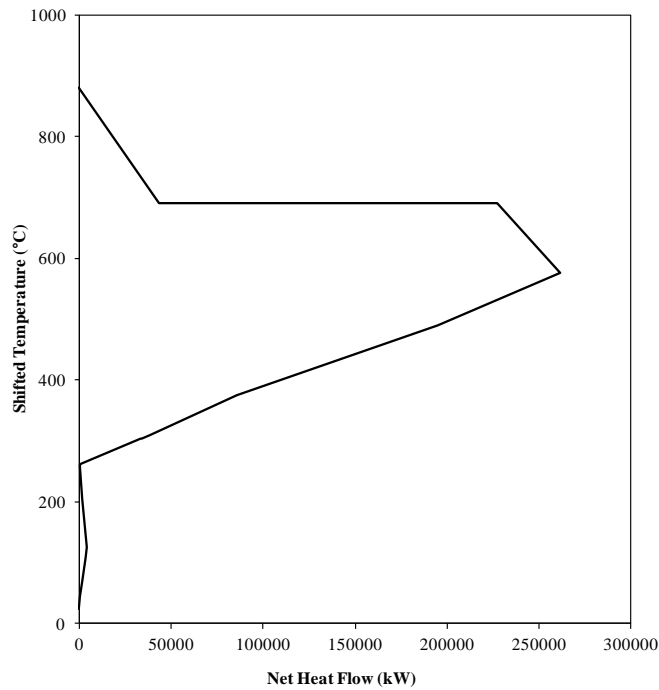
Figure 5-5 The grand composite curve prepared according to the specifications given in Table 5-3.

5.4.4 Results and Discussion

Table 5-4 shows the energy balances around the proposed power plant schemes. The difference between the total enthalpies of the inlet and outlet streams is resulting from the amount of heat transferred into the steam cycle and the energy consumed by the fans. The enthalpy of the biomass feed is same in the all cases due to the constant flow rate of the biomass whereas the air/oxygen flow rate including the infiltration air differs between cases. The major term having priority on the gross power generation efficiency estimations is the total heat transfer into the steam cycle. This value is the greatest for the biomass-oxy-fired plant. The expectation would be that the in-situ Ca-looping plant would be second as it includes both air-fired and oxy-fired combustors. However, due to the calcination energy requirement (5.2 MW$_{th}$) and heat losses from the purge stream (1.1 MW$_{th}$); it turns out that the heat flow from the in-situ Ca-looping process into the steam cycle is slightly lower than that for the biomass-air-fired plant. The heat spent for calcination can be discounted if the purge stream is used in a cement plant but this option has not been considered here. There are two components in the heat flow to the steam cycle from the biomass-oxy-fired plant: the majority of heat flow (321 MW$_{th}$) is used to generate steam and on the cold

reheat stream while the remaining 4.0 MW$_{th}$ reduce the heat duty on the second feed water heater. The other two configurations only use energy for steam generation and for the cold reheat.

The key design parameters and outcomes of the in-situ Ca-looping plant simulation are summarized in Table 5-5. The CO$_2$ purification unit is essential to increase the CO$_2$ purity to the target purity of more than 95 mol%. The cryogenic CO$_2$ purification-compression process is very similar to the one described previously and presented in Figure 5-3. The corresponding power requirement is reported in Table 5-5. The final CO$_2$ product is compressed to 150 bar as for the biomass-oxy-fired plant. The thermal energy transferred into the steam cycle is consistent with the case compiled in Table 5-4, and the gross power generation capacity of this plant is 143.0 MW$_e$. This value reduces to 117.9 MW$_e$ (35.7% net efficiency) when additional power losses linked to auxiliaries, ASU and CO$_2$ purification-compression are included. The CO$_2$ capture efficiency obtained is 88% before the CO$_2$ purification-compression stage and reduces to 84% when the efficiency of the cryogenic separation is included. Overall, the net power generation efficiency of the in-situ Ca-looping plant is higher than that for the biomass-oxy-fired plant but it should be noted that the capture efficiency is higher for the latter.

Table 5-4 Energy balances of the proposed dedicated biomass power plants.

	Biomass-air-fired Power Plant (MW$_{th}$)	Biomass-oxy-fired Power Plant (MW$_{th}$)	In-situ Ca-looping Power Plant (MW$_{th}$)
Enthalpy In (A)			
Biomass	−31.0	−31.0	−31.0
Air/Oxygen	−1.0	−0.2	−0.7
Make-up	-	-	−34.9
Enthalpy Out (B)			
Fly/Bottom Ashes	−12.1	−12.1	−11.5
Exit Gas Streams	−331.9	−343.1	−347.9
Purge	-	-	−17.7
Heat of Compression by Fans (C)	1.8	1.0	1.6
Heat into the Steam Cycle (D)	313.8	321.0 + 4.0	312.1
Net ((B−A)+(D−C))	**0**	**0**	**0**

Table 5-5 The in-situ Ca-looping plant process specifications and performance summary.

	In-situ Ca-looping Power Plant
Fuel	Biomass (see Table 5-1 for composition)
Heat of Combustion (MW$_{th}$)	
Combustor/Carbonator	210.4
Calciner	119.4
Air/Oxygen Flow Rate (ton/h)	219.1 / 26.8
Flue Gas Composition before CO$_2$ Purification (mol %)	3.5% O$_2$, 3.4% N$_2$, 24.1% H$_2$O, 69.0% CO$_2$
Flue Gas Composition after CO$_2$ Purification (mol %)	1.6% O$_2$, 1.3% N$_2$, 0.3% H$_2$O, 96.8% CO$_2$
Steam Cycle Conditions (bar/°C/°C)	166.5/565.6/565.6
Gross Power Generation (MW$_e$)/Efficiency (%)	143.0 / 43.3
Auxiliary Power (MW$_e$)	8.5
Air Separation Unit Power (MW$_e$)	6.2
CO$_2$ Purification and Compression Power (MW$_e$)	10.4
Net Power Generation (MW$_e$)/Efficiency (%)	117.9 / 35.7
CO$_2$ Capture Efficiency before the Purification Stage (%)	88.0
Overall CO$_2$ Capture Efficiency (%)	84.1

5.5 Economic Analysis

The aim of this section is to provide a simple and transparent economic analysis for the estimations of costs of electricity (COE) and CO$_2$ avoided associated with the biomass-fired power plants discussed in this chapter. The following equation has been used to estimate COE (€/kWh$_e$) (Abanades et al., 2007; Abanades et al., 2011a). The specifications of the economic analysis have been summarized in Table 5-6.

$$COE = \frac{TCR \times FCF + FOM}{CF \times 8760} + VOM + \frac{FC}{\eta} \qquad \text{(Eq. 5.3)}$$

where TCR (€/kW$_e$) is the total capital requirement and FCF is the fixed charge factor which is assumed to be 0.1 (Abanades et al., 2011a). FOM refers to the fixed operating and maintenance costs and is taken as 3.70% of the TCR (SETIS, 2013). CF is described as the capacity factor and set to 90% for all cases. For the sake of simplicity, the variable operating and maintenance costs, VOM, is fixed at 0.01 €/kWh$_e$ (SETIS, 2013). FC (€/kWh$_{th}$) is the fuel cost and selected depending the type of fuel (either coal or biomass) and η (kWh$_e$/kWh$_{th}$) is the net electrical efficiency.

Table 5-6 The main specifications used for the economic analysis.

	Value
Reference Biomass-air-fired CFB Power Plant*	
Capacity (MW$_{th}$)**	654.0
Capital Cost, TCR (×1000€)	
Solid Storage and Handling	49,000
Boiler Island	204,000
Power Island	60,800
Utilities & Offsites	56,400
Base Year	2009
Fixed Fraction Cost, FOM (% TCR)	3.70
Capacity Factor, CF (%)	90
Fixed Charge Factor, FCF	0.1
Variable Cost, VOM (€/kWh$_e$)	0.01
Coal Cost (€/kWh$_{th}$)	0.01
Biomass Cost (€/kWh$_{th}$)	0.03
ETS (€/ton CO$_2$)	14
Green Certificate (€/MWh$_e$)	50
Scale Factor	0.6

* Data from IEAGHG (2009).
** Based on LHV of the fuel.

The TCR of the reference biomass-air fired plant has been taken from the study on biomass plants with CCS (IEAGHG, 2009) and is reported in Table 5-6 together with its thermal energy capacity and base year. The TCR of this plant comprises of the costs of solid storage and handling unit; boiler island; power island and utilities. The cost data available for the biomass-oxy-fired case is scarce in the literature. However, the similarities of biomass-fired systems with existing coal-fired CFB power systems can be taken into consideration. According to DOE (2003), the total TCR of the boiler island in a coal-air-fired plant is 60% higher than that for a coal-oxy-fired plant at same thermal energy input, which can be linked to the volume of the boilers. Thus, it is possible to estimate the cost of the boiler island from the values given for the reference biomass-air-fired plant. In addition, the TCRs of the ASU and CO$_2$ purification-compression unit in the biomass-oxy-fired plant have been calculated based on their power requirements compared to the reference units given in Table 4-2 (DOE, 2003).

For all proposed cases, TCR calculations have been based on the same thermal energy input, 329.8 MW$_{th}$. The six-tenths rule and the M&S index detailed in Chapter 4 are used to approximate TCR of a plant or a unit. Calculations for the biomass-air-fired and biomass-oxy-fired plants are straight forward. However, more

attention has to be given for the case of the in-situ Ca-looping plant. This system contains an air-fired CFB combustor and an oxy-fired CFB combustor at smaller scale. Also, the ASU and CO_2 purification-compression unit existing in this system are smaller compared to these in the biomass-oxy-fired plant. As indicated, approximately 64% of the total thermal energy input is supplied into the combustor-carbonator as an air-fired CFB combustor. The rest of energy is used in the calciner, as an oxy-fired CFB combustor. Thus, the air- and oxy-fired combustors in the in-situ Ca-looping plant have been scaled based on the individual thermal energy input into these reactors whereas the TCRs of the solid storage and handling unit, power island and utilities have been estimated based on the total thermal energy input as these units are shared by both combustors. As mentioned previously, the heat exchange area requirement in the combustor-carbonator should be higher than the reference CFB boiler operated at higher temperature. However, the cost increase linked to variation in the heat transfer area is not considered in this study and a more detailed study is required to calculate the heat transfer area in both cases.

The calculated TCR results are shown in Table 5-7, together with COE and cost of CO_2 avoided estimations. To compare the economic performance of the biomass power plants against a CFB coal-air-fired power plant, the specific CO_2 emission and the TCR of a reference CFB coal-air-fired plant are taken from the DOE report (2003). To have a more accurate estimation, the TCR of the reference coal-fired plant is adjusted by the six-tenths rule and the M&S index based on the same thermal energy input given for the biomass power plants. The estimated TCRs of the coal- and biomass-fired CFB power plants, presented in Table 5-7, are lower than those of the capture options since there are no ASU and CO_2 purification-compression unit. One could expect a lower TCR for the in-situ Ca-looping plant since the capacity of the ASU for this system is lower compared to the biomass-oxy-fired plant. The calculated TCRs are very close and this can be explained by the difference in the capital costs of air- and oxy-fired CFB boilers as well as the use of the scale factor in the calculations. While the estimated COE is the lowest for the coal-air-fired plant, the addition of capture units increases the cost further with a maximum of 139 €/MWh$_e$ estimated for the biomass-oxy-fired plant.

Table 5-7 Comparison of the dedicated biomass-fired power plants in terms of costs of electricity (COE) and CO_2 avoided.

	Coal-fired CFB	Biomass-air-fired	Biomass-oxy-fired	In-situ Ca-looping
Specific CO_2 Emission (kg CO_2/MWh$_e$)	998	665	56	127
CO_2 emission factor (kg CO_2/MWh$_e$)	998	0	−744	−672
TCR (€/kW$_e$)	1660	1903	3012	2816
COE (€/MWh$_e$)	60	109	139	132
COE inc ETS (€/MWh$_e$)	74	109	128	122
COE inc ETS and GC (€/MWh$_e$)	74	59	78	72
Cost of CO_2 Avoided (€/ton CO_2 avoided)	-	49	45	43
Cost of CO_2 Avoided inc ETS (€/ton CO_2 avoided)	-	35	31	29
Cost of CO_2 Avoided inc ETS and GC (€/ton CO_2 avoided)	-	−15.3	2.4	−1.1
Case A				
TCR (€/kW$_e$)	-	-	2887	2697
Cost of CO_2 Avoided* (€/ton CO_2 avoided)	-	-	1.5	−2.1
Case B				
TCR (€/kW$_e$)	-	1759	2628	2084
Cost of CO_2 Avoided* (€/ton CO_2 avoided)	-	−17.2	−0.5	−6.9

* Including ETS and green certificate (GC) incentives.

The additional benefits from the ETS as in Chapter 4 and green certificates (IEAGHG, 2009) have been included in the economic analysis. The reference ETS price is fixed at 14 €/ton CO_2. The green certificates are used to include the environmental value of renewable energy and set to 50 €/MWh$_e$. With the introduction of the ETS and green certificate incentives, the COE estimations for the capture cases, biomass-oxy-fired and in-situ Ca-looping plants, drastically decrease in comparison with the coal-fired plant. The COE of the in-situ Ca-looping plant reduces to 72 €/MWh$_e$ and it becomes even lower for the biomass-air-fired plant (59 €/MWh$_e$).

To calculate cost of CO_2 avoided (€/ton CO_2 avoided) for the biomass combustion systems (bio), the following general equation can be used.

$$Cost\ of\ CO_2\ avoided = \frac{COE_{bio} - COE_{coal-fired}}{CO_2\ emission\ factor_{coal-fired} - CO_2\ emission\ factor_{bio}} \quad \text{(Eq. 5.4)}$$

where the CO_2 emission factor$_{coal-fired}$ is equal to the specific CO_2 emission in the coal reference plant. However, the definition of the CO_2 emission factor for the biomass combustion systems must consider the neutral character assumed for the carbon from biomass and the overall efficiency of CO_2 captured (E_{capt}). In the case of the biomass air-fired plant, the emission factor is zero (IEAGHG, 2009), while this takes negative values when CO_2 capture is applied to the plant. The CO_2 emission factors as well as the specific CO_2 emissions for all the systems considered in this work are also summarized in Table 5-7. For the biomass-oxy-fired and in-situ Ca-looping plants referred as 'bio,cc', the CO_2 emission factor is calculated by:

$$CO_2\ emission\ factor_{bio,cc} = -specific\ CO_2\ emissions_{bio,cc} \frac{E_{capt}}{(1 - E_{capt})} \quad \text{(Eq. 5.5)}$$

The cost is the minimum for the in-situ Ca-looping process at 43 €/ton CO_2 avoided, when excluding ETS and green certificate incentives whereas this decreases to −1.1 €/ton CO_2 avoided when the incentives are included. An even more attractive negative avoided cost result is calculated for the biomass-air–fired plant mainly because of the inclusion of green certificates. The cost of CO_2 avoided results calculated for the biomass-oxy-fired and in-situ Ca-looping plants are similar. While

net power generation efficiency of the in-situ Ca-looping plant is slightly higher than that for the biomass-oxy-fired plant, the overall CO_2 capture efficiency is greater for the latter. Thus, the similarity can be explained by a trade-off between those values.

Two different additional approaches have been considered for TCR estimations of the dedicated biomass-fired power plants when they are built next to other combustion systems. The results of these cases can also be seen in Table 5-7. In Case A, it is considered that biomass-oxy-fired and in-situ Ca-looping plants are able to share their oxygen supply with another oxy-fired system located nearby. In this case, it is assumed that the total oxygen requirement in the plants, a dedicated biomass-fired power plant with CO_2 capture and the other oxy-fired plant, equals that of the reference ASU shown in Table 4-2. The capital cost of the ASU in the biomass-fired plants can be then calculated from the flow of oxygen to these systems. In other words, this is equivalent to eliminating the scale factor in TCR calculations for the ASU. The total TCR estimations reduce to 2887 and 2697 €/kW$_e$ for the biomass-oxy-fired and in-situ Ca-looping plants, respectively while the corresponding cost including ETS and green certificate incentives decreases to −2.1 €/ton CO_2 avoided for the latter.

In more advanced process integrations (Case B in Table 5-7), the biomass-fired plants can be coupled directly with another fossil-based power generation systems to reduce CO_2 emissions since biomass-firing is linked to zero CO_2 emission, for example parallel co-firing, where coal and biomass are burnt in separate boilers. In this type of integration, the biomass-air-fired plant can share power island and utilities costs with the other power plant while biomass-oxy-fired plant can also benefit from a larger ASU and CO_2 purification-compression unit if it is integrated into an oxy-fired power plant. For the in-situ Ca-looping plant, in addition to above benefits, the most advantageous integration can be achieved if this process is coupled with another post-combustion Ca-looping unit that is used to capture CO_2 from a power plant. The availability of CaO from the calciner at larger scale will eliminate the requirement of an additional calciner as well as its capital requirement. The capital cost of a calciner in the in-situ Ca-looping plant can be estimated based on its energy requirement over the total thermal energy input into the larger scale calciner.

For Case B calculations, similar to Case A, it is assumed that the total thermal energy requirement in a biomass-fired plant and a fossil-based power system equals to that for the reference biomass-air-fired plant given in Table 5-6. Further reduction in total TCR can be achieved in Case B while the level of reduction is more severe for the in-situ Ca-looping process because the units existing in this system are normally at smaller scale compared to the other biomass-fired plants. The cost reduces down to -17.2 €/ton CO_2 avoided for the biomass-air-fired plant and -6.9 €/ton CO_2 avoided for the in-situ Ca-looping plant but the specific CO_2 emission is much lower for the latter. In summary, owing to the six-tenths rule, this exercise indicates that substantial reductions in the avoided cost can be obtained if the small scale biomass systems can use specific capital cost characteristic of much larger power generation systems through integration. It is important to note here that direct co-firing in the existing systems could also be an option, but there is a general trend in reducing the legislative financial support to biomass co-firing and in practice it may be economically more favourable to build a separate unit which uses only biomass. For example in the UK biomass co-firing will attract only 0.5 Renewable Obligation Certificates (ROCs) per MWh of electricity produced, while a dedicated biomass plant will receive 1.4 ROCs for the same output (DECC, 2012b).

Finally, the sensitivities of the cost calculations with respect to some of the cost parameters adopted above have been examined based on a ±25% variation (see Figure 5-6). The CO_2 avoided estimations including ETS and green certificate incentives already shown in Table 5-7, excluding Cases A and B, are selected as bases for the sensitivity analyses. The influence of the biomass cost is the largest, especially on the biomass air-fired plant. The green certificate subsidy has a similar influence, as it directly affects the effective fuel cost for the power plants. In cost scenarios where the ETS price is sufficiently high the biomass oxy-fired system becomes the preferred option. The in-situ Ca-looping technology is only slightly more economical when both ETS and green certificate incentives are in place. The impact of scale factor is milder in the sensitivity analyses compared to the advanced cases (A and B) investigated above since it also changes the TCR of the reference coal-air-fired plant.

(a)
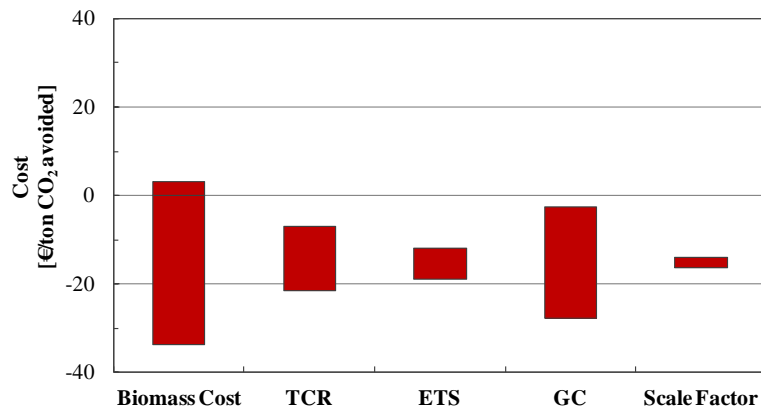
(b)
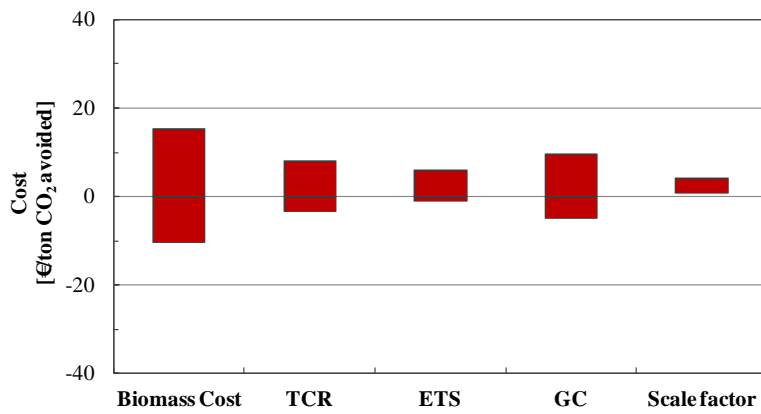
(c)
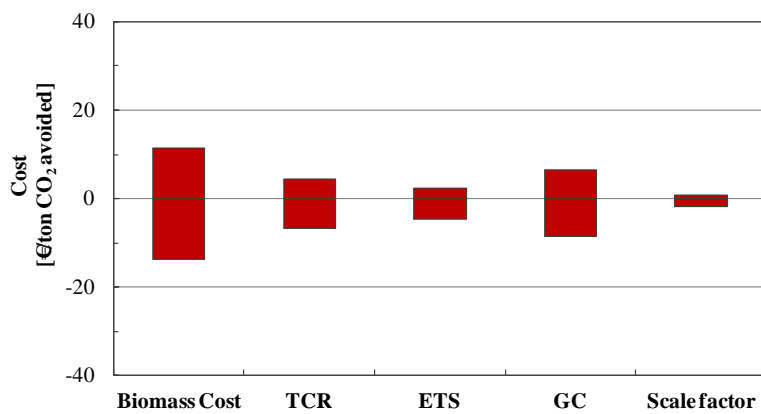
Figure 5-6 Sensitivity analysis on cost parameters for the a) biomass-air-fired plant; b) biomass-oxy-fired plant; c) in-situ Ca-looping plant. (**TCR**: Total Capital Requirement; **ETS**: European Trading Scheme CO_2 cost; **GC**: Green Certificates)

The option of a biomass air-fired plant clearly becomes the most competitive option to avoid CO_2 emissions at present because many countries have adopted a policy of green certificates, while the ETS is very low. If this policy is sustained, this could lead to a deployment of air-fired CFBC systems with no CO_2 capture. If there was later a policy to favour CCS systems (much higher cost of ETS credits), the retrofitting of existing air-fired CFB biomass combustion plants to CCS could be facilitated with the in situ Ca-looping system as this would allow not only the capture of the CO_2 generated in the oxy-fired calciner but also the capture of the CO_2 generated in the existing air-fired plant. This added flexibility in the in-situ system has not been incorporated in the cost analysis as it is too sensitive to uncertain assumptions on the residual value of the air-fired plant. It is sufficient to conclude at present that all three systems discussed in this work have a chance to be highly competitive to avoid CO_2 emissions depending on political incentives determining the values of ETS or green certificates.

On the other hand, the current capacity of the dedicated biomass power plants in the UK was reported to be 400 MW_e, and that for co-firing is 255 MW_e (DECC, 2014). It is estimated that around 1700 km^2 of land to grow the fuel on will be required if these plants are running with 90% capacity and using only energy crops (DECC, 2014). Therefore, it is worth to consider that there would be limitations on the availability of biomass if several large scale dedicated biomass power plants become operational.

5.6 Concluding Remarks

The conceptual process integration of an in-situ Ca-looping process with a dedicated biomass power plant allows effective removal of CO_2 from biomass combustion when the combustor-carbonator operates at around 700°C. Thanks to the biomass-fired oxy-calciner, most of the CO_2 from combustor-carbonator as well as the entire fraction of CO_2 from biomass combustion in this reactor can be removed at high purity. This system, with a heat exchanger network design, is capable of achieving a greater net power generation efficiency compared to a biomass-oxy-fired plant. An overall CO_2 capture efficiency of 84% is achieved by capturing 80% CO_2

resulting from biomass combustion in the combustor-carbonator while 93 % capture efficiency is estimated for the biomass-oxy-fired plant. The net power generation efficiency decreases from 40.9% for the biomass-air-fired plant to 35.7% in the proposed system mainly because of the requirements of the ASU and CO_2 purification-compression sections.

A detailed cost analysis has been presented which allows the estimation of electricity and cost of CO_2 avoided with and without incentives, i.e. ETS carbon price and green certificates. The lowest cost of electricity is obtained for a coal-fired power plant without CO_2 capture due to lower cost of coal compared to biomass. With the inclusion of ETS and green certificate incentives (14 €/ton CO_2 and 50 €/MWh$_e$, respectively), the cost of electricity is found to be minimum for the biomass-air-fired plant. The cost of CO_2 avoided estimates for the biomass-oxy-fired and in-situ Ca-looping plants are close but the gap widens with different process integration possibilities. The sensitivity analyses on economical estimations reveal that costs of biomass and revenue from green certificates have significant impacts on cost of CO_2 avoided calculations. Although several different large-scale dedicated biomass power systems with CO_2 capture have been studied in this chapter, this approach may not be the optimal one for smaller scale biomass plants, which are more common, and that further studies are needed to evaluate this.

Chapter 6 Conclusions and Recommendations for Future Work

The objective of this dissertation is to conduct the techno-economic assessment of carbon capture technologies to reduce CO_2 emissions from cement and biomass-fired power plants. The Ca-looping process has emerged as a leading option for this purpose because of the use of low cost sorbent, the relatively small energy penalty, and the possibility of using purged sorbent for clinker production. Various alternative carbon capture technologies including membrane, amine, oxy-combustion and indirect calcination processes have also been investigated, and the comparison of these processes with the Ca-looping process has been conducted. Detailed process flowsheets have been generated using Honeywell's UniSim R400 to reveal process performance and economics of the proposed carbon capture technologies. The most significant conclusions and recommendations for future work are outlined in this chapter.

6.1 Conclusions

6.1.1 Ca-looping Process for Cement Plants

A way of capturing CO_2 from cement plants by using the Ca-looping process has initially been investigated. The base cement process simulation implemented in this study was proven to be reliable by comparing the estimated composition of clinker and thermal energy requirement with those reported in the literature. The flue gas stream leaving the 3rd preheater has been selected to be the optimal feed for the carbonator because: (i) it has higher CO_2 concentration and a lower total volumetric flowrate; (ii) it does not have to be preheated; and (iii) it facilitates the design of a heat exchanger network for heat recovery. The CO_2-rich gas stream from the calciner was directly sent to the CO_2 compression unit rather than the preheater (Rodriguez et al., 2012) as this may result significant reduction in CO_2 purity if any air-leakage into this unit cannot be prevented. A model for a carbonator, where hydrodynamics in fast fluidisation, reaction kinetics as well as active fraction of the sorbent are taken into account, has been incorporated into the cement process flowsheet. The Ca-looping

process can achieve over 90% CO_2 avoidance with energy consumption ranges from 2.5 to 3.0 GJ_{th}/ton CO_2 avoided depending on the F_0/F_{CO2} ratio.

6.1.2 Ca-Cu Looping Process for Cement Plants

The potential of incorporating a CLC cycle into the Ca-looping process as an alternative way to transfer oxygen into the calciner was carefully investigated. The configuration with a solid route of carbonator → calciner (fuel reactor) → air reactor → carbonator has been selected to provide an opportunity for heat transfer between the calciner and air reactor by hot solid circulation. To the best of our knowledge, this was the first approach that addressed the need of heat transfer between these reactors to prevent severe heat requirements in the proposed system. Up to 1 wt% CuO from the purge was allowed in the cement raw meal for clinker production, which corresponds to a F_0/F_{CO2} ratio of 0.15. The incremental energy consumption required by this system was estimated to be as low as 1.7 GJ_{th}/ton CO_2 avoided, which is at least 30% lower than that of the conventional Ca-looping process.

6.1.3 Alternative Carbon Capture Technologies for Cement Plants

A detailed process integration of the indirect calcination process into the base cement plant has been analysed. The major advantage of the proposed configuration is the use of surplus heat from high temperature gas streams for raw meal preheating rather than power generation suggested in Rodriguez et al. (2011b). The incremental energy consumption of this system was estimated to be 0.9 GJ_{th}/ton CO_2 avoided at 56% CO_2 avoidance. The energy consumption increases to 3.3 GJ_{th}/ton CO_2 avoided in the new hybrid configuration which includes an additional amine capture unit, while that of the standalone amine process was calculated to be 8.2 GJ_{th}/ton of CO_2 avoided. Furthermore, a dual stage membrane configuration comprised of a counter-current module with a sweep, followed by a cross flow model has been implemented for two feed gas locations, i.e. preheater gas or end-of-pipe gas. It was observed that the membrane area was 48% higher for the latter case. The incremental energy consumption for the membrane process was calculated to be as low as 2.0 GJ_{th}/ton CO_2 avoided at 90% CO_2 avoidance, which is less than that of the equivalent Ca-looping process.

6.1.4 Economic Analysis of the Carbon Capture Technologies Applied to Cement Plants

A method of economic analysis has been applied to evaluate the cost performance of the proposed carbon capture technologies. The close similarity of the CFB reactors existing in certain carbon capture systems with commercial CFB power plants were taken into account for capital cost estimations. The LCOC for the base cement plant increases from 97 €/ton cement to around 127 €/ton cement when the Ca-looping process is incorporated and stays almost constant at different F_0/F_{CO2} ratios. Including the ETS price, the avoided cost was calculated to be around 41 €/ton CO_2 for the Ca-looping process. The economic performance of the Ca-Cu looping process is not competitive with the Ca-looping process at very high F_0/F_{CO2} ratios because of the severe variable cost associated with the purged CuO/Al_2O_3. The avoided cost increases up to 157 €/ton CO_2 for the Ca-Cu looping process at 0.15 F_0/F_{CO2}. It is clear that separation and reuse of the purged CuO/Al_2O_3, depending on the stability of the sorbent, are necessary to make this process more economical.

Amongst the various carbon capture technologies compared in this dissertation, the minimum cost belongs to the standalone indirect calcination process with a value of 29 €/ton CO_2 avoided. This cost further increases to 73 €/ton CO_2 avoided in the hybrid configuration aiming at 90% CO_2 avoidance, but it is around 30% lower compared to that of the standalone amine process. In the case of the membrane process, the LCOC increases to 125 €/ton cement for the preheater integration and 129 €/ton cement for the end-of-pipe integration. The cost of CO_2 avoided for these cases were calculated to be 42 €/ton CO_2 and 47 €/ton CO_2, respectively. It should be highlighted that although the Ca-looping process requires greater energy requirement, the final cost estimate for this process and membrane process are very similar owing to the benefit of on-site power generation.

6.1.5 Dedicated Biomass Power Plant with in-situ Ca-looping Process

The first comprehensive process analysis of a large-scale dedicated biomass power plant with in-situ CO_2 capture using the Ca-looping process has been reported. This system was compared against similar alternatives, biomass-air-fired and

biomass-oxy-fired power plants in terms of process and cost performances. A subcritical steam cycle with a single reheat that is currently the only available technology for biomass combustion has been included in the process configurations. The net LHV-based power efficiency of 40.9% for the biomass-air-fired power plant reduces to 33.9% for the biomass-oxy-fired power plant. The net efficiency of the in-situ Ca-looping plant achieving 84% overall CO_2 capture efficiency was calculated to be 35.7%, representing an energy penalty of 5.2%. Furthermore, the COE estimate increases from 109 €/MW_e for the biomass-air-fired plant to 139 €/MW_e and 132 €/MW_e for the biomass-oxy-fired and in-situ Ca-looping plants, respectively. With the inclusion of the ETS price and green certificate incentives, the COE reduces to 59 €/MW_e and 72 €/MW_e for the biomass-air-fired and the in-situ Ca-looping plants, respectively. It reflects a negative cost of CO_2 avoided estimate for the in-situ Ca-looping plant with a value of -1.1 €/ton CO_2 avoided. It was concluded that the biomass-air-fired plant taking the advantage of green certificates is the preferable option if the ETS price is very low, whereas the capture processes will be favourable if the ETS price is much higher.

6.2 Recommendations for Future Work

Further work may be carried out based on the following recommendations.

- A detailed steam cycle configuration and a heat exchanger network design were explored for heat recovery from the biomass power plant with in-situ Ca-looping system detailed in Chapter 5. The same methodology can be adapted in Chapters 2 and 3 for the post-combustion Ca-looping and Ca-Cu looping processes to improve the prediction of power generation efficiency in these systems.
- The use of more realistic assumptions regarding sorbent attrition and air-leakage in the Ca-looping, Ca-Cu looping and indirect calcination processes presented in Chapters 2 and 3 would improve the accuracy of current predictions. It is expected that the sorbent attrition results an increase in calciner heat duty and variable cost, while any air-leakage into the calciner will arise the requirement of CO_2 purification stage as presented in Chapter 5.

- Oxy-kiln would be a possible alternative to increase CO_2 avoidance rate more than 90% when it is coupled with an oxy-fired calciner if the future studies approve the utilization of oxy-combustion in the kiln.

- If detailed calciner (fuel reactor) and air reactor modelling studies are conducted, more accurate predictions can be obtained for the calcination, oxidation and reduction efficiencies in these reactors.

- The limit of using purged CuO, CaO and Al_2O_3 for clinker production needs to be revised, preferably with the support of experimental analyses.

- Possibility of separating CuO/Al_2O_3 sorbent from the purge stream would allow significant reductions in the variable cost as presented in Chapter 4. Thus, it is worth to investigate potential technologies for this purpose.

- Further experimental studies would verify the stability and performance of the CLC sorbent to support the idea of reusing purge sorbent in the Ca-Cu looping process.

- The use of syngas ($CO+H_2$) from gasification of solid fuels, such as coal, petroleum coke and biomass as an alternative fuel to methane in the calciner would reduce the variable cost of this system as mentioned in Chapter 4. A follow-up study may be conducted to investigate this option.

- An alternative method of providing steam into the stripper rather than having an on-site CHP plant, i.e. availability of steam source in nearby locations, would be an option to reduce the energy consumption associated with the amine process.

- The application of the advanced solvent systems, requiring less energy consumption for carbon capture than an amine process and having improved tolerance to SO_x and NO_x, deserves to be investigated further.

- Although a remarkable amount of dual-stage membrane process schemes have been investigated in this study, the number of possible configuration can still be expanded to improve the energy consumption and cost requirements.

- Further studies needs to be conducted to improve the accuracy of the membrane models in use.

- A detailed combustor-carbonator model would allow more accurate prediction of combustion and carbonation efficiencies in this reactor.

References

Abad, A., Adanez, J., Garcia-Libiano F., de Diego, L.F., Gayan, P. and Celaya, J., 2007. Mapping of the Range of Operational Conditions for Cu-, Fe-, and Ni-based Oxygen Carriers in Chemical-looping Combustion. Chem. Eng. Sci. 62, 533–549.

Abanades, J.C., 2002. The maximum capture efficiency of CO_2 using a carbonation/calcination cycle of $CaO/CaCO_3$. Chemical Engineering Journal 90, 303-306.

Abanades, J.C., Alvarez, D., 2003. Conversion limits in the reaction of CO_2 with lime. Energy&Fuels 17,308–316.

Abanades, J. C., Anthony, E. J., Lu, D. Y., Salvador, C., Alvarez, D., 2004. Capture of CO_2 from combustion gases in a fluidized bed of CaO. AIChE Journal 50(7), 1614-1622.

Abanades, J.C., Anthony, E.J., Wang, J., Oakey, J.E., 2005. Fluidized bed combustion systems integrating CO_2 capture with CaO. Environ Sci Technol. 39, 2861–2866.

Abanades, J. C., Grasa, G., Alonso, M., Rodriguez, N., Anthony, E. J., Romeo, L. M., 2007. Cost structure of a postcombustion CO_2 capture system using CaO. Environmental science & technology 41(15), 5523-5527.

Abanades, J. C., Murillo, R., 2009. Method of Capturing CO_2 by Means of CaO and the Exothermal Reduction of a Solid. European Patent Application EP2305366 A1.

Abanades, J.C., Murillo, R., Fernandez, J.R., Grasa, G., Martinez, I., 2010. New CO_2 Capture Process for Hydrogen Production Combining Ca and Cu Chemical Loops. Environ. Sci. Technol. 44, 6901–6904.

Abanades, J. C., Alonso, M., Rodríguez, N., 2011a. Biomass Combustion with in Situ CO_2 Capture with CaO. I. Process Description and Economics. Industrial & Engineering Chemistry Research 50(11), 6972-6981.

Abanades, J. C., Alonso, M., Rodriguez, N., 2011b. Experimental validation of in-situ CO_2 capture with CaO during the low temperature combustion of biomass in a fluidized bed reactor. International Journal of Greenhouse Gas Control 5(3), 512-520.

Adanez, J., Abad, A., Garcia-Labiano, F., Gayan, P., de Diego, L. F., 2012. Progress in chemical-looping combustion and reforming technologies. Progress in Energy and Combustion Science 38(2), 215-282.

Ahn, H., Luberti, M., Liu, Z., Brandani, S., 2013. Process configuration studies of the amine capture process for coal-fired power plants. International Journal of Greenhouse Gas Control 16, 29-40.

Albrecht, K. O., 2008a. Development and testing of a combined catalyst/sorbent core-in-shell material for the production of high concentration hydrogen. PhD Thesis, Iowa State University.

Albrecht, K. O., Wagenbach, K. S., Satrio, J. A., Shanks, B. H., Wheelock, T. D., 2008b. Development of a CaO-based CO_2 sorbent with improved cyclic stability. Industrial & Engineering Chemistry Research 47(20), 7841-7848.

Alonso, M., Rodríguez, N., Grasa, G., Abanades, J. C., 2009. Modelling of a fluidized bed carbonator reactor to capture CO_2 from a combustion flue gas. Chemical Engineering Science 64(5), 883-891.

Alonso, M., Rodríguez, N., González, B., Grasa, G., Murillo, R., Abanades, J.C., 2010. Carbon dioxide capture from combustion flue gases with a calcium oxide chemical loop. Experimental results and process development. International Journal of Greenhouse Gas Control 4, 167-173.

Alonso, M., Rodríguez, N., González, B., Arias, B., Abanades, J. C., 2011a. Biomass combustion with in Situ CO_2 capture by CaO. II. Experimental results. Industrial & Engineering Chemistry Research 50(11), 6982-6989.

Alonso, M., Rodriguez, N., Gonzalez, B., Arias, B., Abanades, J. C., 2011b. Capture of CO_2 during low temperature biomass combustion in a fluidized bed using CaO. Process description, experimental results and economics. Energy Procedia 4, 795-802.

Alonso, M., Diego, M.E., Abanades, J.C., Perez, C., Chamberlain, J., 2013. In Situ CO_2 Capture with CaO in a 300 Kw Fluidized Bed Biomass Combustor, in TCCS-7, Trondheim.

Alptekin, G.O., Jayaraman, A., Dubovik, M., Brickner, L., 2008. Oxygen Sorbents for Oxy-Fuel Combustion. Presented at 2008 AIChE Annual Meeting, Philadelphia, USA.

Alsop, P.A., Chen, H., Tseng, H., 2007. The Cement Plant Operations Handbook, Tradeship Publications Ltd, Surrey, UK.

Arias, B., Abanades, J. C., Anthony, E. J., 2011. Model for self-reactivation of highly sintered CaO particles during CO_2 capture looping cycles. Energy & Fuels 25(4), 1926-1930.

Arias, B., Diego, M.E., Abanades, J.C., Lorenzo, M., Diaz, L., Martinez, D., Alvarez, J., Sanchez-Biezma, A., 2013. Demonstration of steady state CO_2 capture in a 1.7 MWth calcium looping pilot. International Journal of Greenhouse Gas Control 18, 237-245.

Bhatty, J.I., Miller, F.M., Boahn, R.P., 2011. Innovations in Portland Cement Manufacturing, Portland Cement Assn; 2nd edition.

Baker, R.W., 2002. Future directions of membrane gas separation technology. Industrial & Engineering Chemistry Research 41(6), 1393-1411.

Baker, R.W., 2004. Membrane technology and applications. John Wiley & Sons, Ltd.

Bandyopadhyay, A., 2011. Amine versus ammonia absorption of CO_2 as a measure of reducing GHG emission: a critical analysis. Clean Technologies and Environmental Policy 13(2), 269-294.

Baxter, L., 2005. Biomass-coal co-combustion: opportunity for affordable renewable energy. Fuel 84(10), 1295-1302.

Berstad, D., Anantharaman, R., Jordal, K., 2012. Post-combustion CO_2 capture from a natural gas combined cycle by $CaO/CaCO_3$ looping. International Journal of Greenhouse Gas Control 11, 25-33.

Bhatia, S. K., Perlmutter, D. D., 1983. Effect of the product layer on the kinetics of the CO_2-lime reaction. AIChE Journal 29(1), 79-86.

Bi, X.T., Liu, X., 2012. High density and high solid flux CFB risers for steam gasification of solids fuels. Fuel Processing Technology 91 (8), 915-920.

Blamey, J., Anthony, E.J., Wang, J., Fennell, P.S., 2010. The calcium looping cycle for large-scale CO_2 capture, Prog. Energy Combust. Sci. 36, 260–279.

Blamey, J., Paterson, N. P., Dugwell, D. R., Stevenson, P., Fennell, P. S., 2011. Reactivation of a CaO-based sorbent for CO_2 capture from stationary sources. Proceedings of the Combustion Institute 33(2), 2673-2681.

Bocciardo, D., Ferrari, M.C., Brandani, S., 2012. Customising UniSim Design: membrane separation and its application to carbon capture, in EMEA HUG 2012, Istanbul.

Bocciardo, D., Ferrari, M.C., Brandani, S., 2013. Modelling and multi-stage design of membrane processes applied to carbon capture in coal-fired power plants. Energy Procedia 37, 932-940.

Bocciardo, D., 2014. Optimisation and integration of membrane processes in coal-fired power plants with carbon capture and storage. PhD Thesis, University of Edinburgh.

Bogue, R.H., 1929. Calculation of the Compounds in Portland Cement. Industrial & Engineering Chemistry Analytical Edition 1 (4), 192-197.

Boot-Handford, M. E., Abanades, J. C., Anthony, E. J., Blunt, M. J., Brandani, S., Mac Dowell, N., ... Fennell, P. S, 2014. Carbon capture and storage update. Energy & Environmental Science 7(1), 130-189.

Bosoaga, A., Masek, O., Oakey, J.E., 2009. CO_2 capture technologies for cement industry. Energy Procedia 1(1), 133-140.

Böhringer, C., Rutherford, T., Tol, R., 2009. The EU 20/20/20 targets; an overview of the EMF assessment. Energy Economics 31, 268-273.

Broda, M., Kierzkowska, A. M., Müller, C. R., 2012. Application of the Sol–Gel Technique to Develop Synthetic Calcium-Based Sorbents with Excellent Carbon Dioxide Capture Characteristics. ChemSusChem 5(2), 411-418.

CCSGI "CCS Global Institute", 2010. The Status of CCS Projects Interim Report, Canberra, Australia.

Chang, M. H., Huang, C. M., Liu, W. H., Chen, W. C., Cheng, J. Y., Chen, W., ..., Hsu, H. W., 2013. Design and Experimental Investigation of Calcium Looping Process for 3-kWth and 1.9-MWth Facilities. Chemical Engineering & Technology 36(9), 1525-1532.

Charitos, A., Rodriguez, N., Hawthorne, C., Alonso, M., Zieba, M., Arias, B., Kopanakis, G.,Scheffknecht, G., Abanades, J.C., 2011.Experimental validation of the calcium looping CO_2 capture process with two circulating fluidized bed carbonator reactors. Ind. Eng. Chem. Res. 50, 9685–9695.

Chrissafis, K., Dagounaki, C., Paraskevopoulos, K. M., 2005. The effects of procedural variables on the maximum capture efficiency of CO_2 using a carbonation/calcination cycle of carbonate rocks. Thermochimica acta 428(1), 193-198.

CO2CRC, 2014. CO_2 capture/separation technologies. Co2crc.com.au. Retrieved February 26, 2014, from

(http://www.co2crc.com.au/aboutccs/cap_absorption.html).

Coppola, A., Montagnaro, F., Salatino, P., Scala, F., 2012. Fluidized bed calcium looping: The effect of SO_2 on sorbent attrition and CO_2 capture capacity. Chemical Engineering Journal 207, 445-449.

Curran, G. P., Fink, C. E., Gorin, E., 1967. Carbon dioxide-acceptor gasification process: studies of acceptor properties. Advanced Chemistry Services 69, 141-165.

CW Group, 2012. Global Cement Volume Forecast Report.

Dai, J., Sokhansanj, S., Grace, J. R., Bi, X., Lim, C. J., Melin, S., 2008. Overview and some issues related to co-firing biomass and coal. The Canadian Journal of Chemical Engineering 86(3), 367-386.

de Diego, L. F., García-Labiano, F., Adánez, J., Gayán, P., Abad, A., Corbella, B. M., María Palacios, J., 2004. Development of Cu-based oxygen carriers for chemical-looping combustion. Fuel 83(13), 1749-1757.

Dean, C. C., Blamey, J., Florin, N. H., Al-Jeboori, M. J., Fennell, P. S., 2011a. The calcium looping cycle for CO_2 capture from power generation, cement manufacture and hydrogen production. Chemical Engineering Research and Design 89(6), 836-855.

Dean, C. C., Dugwell, D., Fennell, P. S., 2011b. Investigation into potential synergy between power generation, cement manufacture and CO_2 abatement using the calcium looping cycle. Energy & Environmental Science 4(6), 2050-2053.

DECC, 2012a. UK Electricity Generation Costs Update.

DECC, 2012b. Government response to the consultation on proposals for the levels of banded support under the Renewables Obligation for the period 2013-17 and the Renewable Obligation Order 2012. Presented to Parliament by the Secretary of State for Energy and Climate Change: London, U.K.

DECC, 2014. DECC 2050 Pathways Calculator.

(http://2050-calculator-tool.decc.gov.uk/)

Demirbas, A., 2003. Sustainable cofiring of biomass with coal. Energy Conversion and Management 44(9), 1465-1479.

Demirbas, M. F., Balat, M., Balat, H., 2009. Potential contribution of biomass to the sustainable energy development. Energy Conversion and Management 50(7), 1746-1760.

Dieter, H., Bidwe, A.R., Varela-Duelli, G., Charitos, A., Hawthorne, C., Scheffknecht, G., 2014. Development of the calcium looping CO_2 capture technology from lab to pilot scale at IFK, University of Stuttgart. Fuel (127), 23-37.

Dlugokencky, E., Tans, P., 2014, NOAA/ESRL.

(http://www.esrl.noaa.gov/gmd/ccgg/trends/)

DOE, 1999. Carbon sequestration: research and development. U.S. Department of Energy Report, Office of Science, Office of Fossil Energy, U.S. Department of Energy.

DOE, 2003. Greenhouse Gas Emissions Control By Oxygen Firing In Circulating Fluidized Bed Boilers: Phase 1 - a Preliminary Systems Evaluation. Alstom Power Inc. and National Energy Technology Laboratory, US Department of Energy.

DOE, 2007. Cost and performance baseline for fossil energy plants. Volume 1: Bituminous coal and natural gas to electricity final report. National Energy Technology Laboratory.

DOE, 2010. Cost and performance for Low-Rank Pulverized Coal Oxycombustion Energy Plants. Final Report, NETL-401/093010.

Dong, R.F., Lu, H.F., Yu, Y.S., Zhang, Z.X., 2012. A feasible process for simultaneous removal of CO_2, SO_2 and NO_x in the cement industry by NH_3 scrubbing. Applied Energy 97, 185–191.

ECRA, 2007. Technical Report: Carbon Capture Technology – Options and Potentials for the Cement Industry.

ECRA, 2009. Technical Report: ECRA CCS Project – Report about Phase II.

ECRA, 2012. Technical Report: ECRA CCS Project – Report on Phase III.

EG Science "EU Climate Change Expert Group", 2008. The 2°C target Information Reference Document.

(http://www.climateemergencyinstitute.com/uploads/2C_EU.pdf)

EIA, U.S. Energy Information Administration, 2013. (http://www.eia.gov/dnav/ng/hist/n3035us3m.htm)

EPRI, 2009. Updated Cost and Performance Estimates for Clean Coal Technologies Including CO_2 Capture – 2009, Electric Power Research Institute, Palo Alto, California.

Faaij, A., Meuleman, B., Turkenburg, W., van Wijk, A. D., Bauen, A., Rosillo-Calle, F., Hall, D., 1998. Externalities of biomass based electricity production compared with power generation from coal in the Netherlands. Biomass and Bioenergy 14(2), 125-147.

Favre, E., 2011. Membrane processes and postcombustion carbon dioxide capture: challenges and prospects. Chemical Engineering Journal 171(3), 782-793.

Fennell, P. S., Davidson, J. F., Dennis, J. S., Hayhurst, A. N., 2007. Regeneration of sintered limestone sorbents for the sequestration of CO_2, from combustion and other systems. J. Energy Inst. 80, 116–119.

Fernández, J. R., Abanades, J. C., Murillo, R., Grasa, G., 2012. Conceptual design of a hydrogen production process from natural gas with CO_2 capture using a Ca–Cu chemical loop. International Journal of Greenhouse Gas Control 6, 126-141.

Figueroa, J. D., Fout, T., Plasynski, S., McIlvried, H., Srivastava, R. D., 2008. Advances in CO_2 capture technology—The US Department of Energy's Carbon Sequestration Program. International Journal of Greenhouse Gas Control 2(1), 9-20.

Finkenrath, M., 2011. Cost and performance of carbon dioxide capture from power generation (No. 2011/5). OECD Publishing.

Fisher, K. S., Beitler, C., Rueter, C., Searcy, K., Rochelle, G., Jassim, M., 2005. Integrating MEA Regeneration with CO_2 Compression and Peaking to Reduce CO_2 Capture Costs (No. DOE/ER/84111). Trimeric Corporation.

Florin, N., Fennell, P., 2010. Carbon capture technology: future fossil fuel use and mitigating climate change. Grantham Institute for Climate Change, briefing paper, (3).

Forero, C. R., Gayán, P., García-Labiano, F., De Diego, L. F., Abad, A., Adánez, J., 2011. High temperature behaviour of a $CuO/\gamma Al_2O_3$ oxygen carrier for chemical-looping combustion. International Journal of Greenhouse Gas Control 5(4), 659-667.

Garcia-Labiano, F., Abad, A., de Diego, L.F., Gayan, P., Adanez, J., 2002. Calcination of calcium-based sorbents at pressure in a broad range of CO_2 concentrations. Chemical Engineering Science 57, 2381-2393.

García-Labiano, F., De Diego, L. F., Adánez, J., Abad, A., Gayán, P., 2004. Reduction and oxidation kinetics of a copper-based oxygen carrier prepared by impregnation for chemical-looping combustion. Industrial & engineering chemistry research 43(26), 8168-8177.

Grasa, G.S., Abanades, J.C., 2006. CO_2 capture capacity of CaO in long series of carbonation/calcinations cycles. Industrial & Engineering Chemistry Research 45, 8846–8851.

Grasa, G., González, B., Alonso, M., Abanades, J. C., 2007. Comparison of CaO-based synthetic CO_2 sorbents under realistic calcination conditions. Energy & Fuels 21(6), 3560-3562.

Grasa, G.S., Abanades, J.C., Alonso, M., Gonzalez, B., 2008a. Reactivity of highly cycled particles of CaO in a carbonation/calcination loop. Chemical Engineering Journal 137 (3), 561 – 567.

Grasa, G. S., Alonso, M., Abanades, J. C., 2008b. Sulfation of CaO particles in a carbonation/calcination loop to capture CO_2. Industrial & Engineering Chemistry Research 47(5), 1630-1635.

Harlick, P.J.E., Tezel, F.H., 2004. An experimental adsorbent screening study for CO_2 removal from N_2. Microporous and Mesoporous Materials 76, 71–76.

Harrison, D. P., 2008. Sorption-Enhanced Hydrogen Production: A Review. Ind. Eng. Chem. Res. 47, 6486–6501.

Hasanbeigi, A., Price, L., Lin, E., 2012. Emerging energy-efficiency and CO_2 emission-reduction technologies for cement and concrete production: a technical review. Renewable and Sustainable Energy Reviews 16, 6220–6238.

Hassan, S.M.N., 2005. Techno-economic study of CO_2 capture process for cement plants. Masters Thesis, Chemical Engineering. University of Waterloo, Canada.

He, X., Hagg, M. B., 2012. Membranes for environmentally friendly energy processes. Membranes 2(4), 706-726.

Hiltunen, M., Barišić, V., Coda Zabetta, E., 2008. Combustion of different types of biomass in CFB boilers. In 16th European Biomass Conference.

Honeywell, 2010. Unisim Design Simulation Basis Reference Guide, R400 Release; Honeywell: London.

Hossain, M. M., de Lasa, H. I., 2008. Chemical-Looping Combustion (CLC) for Inherent CO_2 Separations - A Review. Chem. Eng. Sci. 63, 4433–4451.

Hotta, A., 2010. Foster wheeler's solutions for large scale CFB boiler technology: features and operational performance of Łagisza 460 MWe CFB boiler. In Proceedings of the 20th international conference on fluidized bed combustion (pp. 59-70). Springer Berlin Heidelberg.

Hu, X., Mangano, E., Friedrich, D., Ahn, H., Brandani, S., 2014. Diffusion mechanism of CO_2 in 13X zeolite beads. Adsorption 20(1), 121-135.

Huang, C. H., Chang, K. P., Yu, C. T., Chiang, P. C., Wang, C. F., 2010. Development of high-temperature CO_2 sorbents made of CaO-based mesoporous silica. Chemical Engineering Journal 161(1), 129-135.

Hurst, T. F., Cockerill, T. T., Florin, N. H., 2012. Life cycle greenhouse gas assessment of a coal-fired power station with calcium looping CO_2 capture and offshore geological storage. Energy & Environmental Science 5(5), 7132-7150.

IEA, 2007. Greenhouse Gas R&D Programme. Improved Oxygen production technologies. IEA report 2007/14.

IEA, 2008. CO_2 Capture in the Cement Industry, July 2008/3.

IEA, 2009a. World Energy Outlook 2009.

(http://www.worldenergyoutlook.org/publications/weo-2009/)

IEA, 2009b. Carbon Emission Reductions up to 2050. In Cement Technology Roadmap 2009.

IEA, 2009c. Energy Technology Transitions for Industry: Strategies for the Next Industrial Revolution. International Energy Agency: Paris.

IEA, 2010. Energy Technology Perspectives 2010: Scenarios & Strategies to 2050, Paris, France.

IEA, 2012. World Energy Outlook 2012.

(http://www.worldenergyoutlook.org/publications/weo-2012/).

IEA Clean Coal Center, 2011. CO_2 abatement in the cement industry.

IEA GHG, 2003. Technical & Financial Assessment Criteria. Revision B2.

IEA GHG, 2009. Biomass CCS Study: Techno-Economic Evaluation of Biomass Fired or Co-Fired Power Plant with Post-Combustion CO_2 Capture, IEAGHG: Cheltenham, U.K.

IECM "Integrate Environmental Control Model", 2012. Technical Documentation: Membrane-based CO_2 Capture Systems for Coal-fired Power Plants. Carnegie Mellon University, Pittsburgh, USA.

Imtiaz, Q., Kierzkowska, A. M., Müller, C. R., 2012. Coprecipitated, Copper-Based, Alumina-Stabilized Materials for Carbon Dioxide Capture by Chemical Looping Combustion. ChemSusChem 5(8), 1610-1618.

INDMIN, Industrial Minerals, 2013. (www.indmin.com/)

IPCC, 2005. Carbon Dioxide Capture and Storage, Cambridge University Press, UK.

IPCC, 2007. Climate Change 2007: Mitigation. Contribution of Working Group III to the Fourth Assessment Report of the Intergovernmental Panel on Climate Change. Cambridge University Press, Cambridge, United Kingdom and New York, NY, USA.

IPCC, 2014. Climate Change 2013: The Physical Science Basis. Contribution of Working Group I to the Fifth Assessment Report of the Intergovernmental Panel on Climate Change. Cambridge: Cambridge University Press, at press.

Ishida, M., Jin, H., 1994. A New Advanced Power-Generation System Using Chemical-Looping Combustion. Energy 19 (4), 415–422.

Ishitani, H., Johansson, T.B., 1996. Energy supply mitigation options, in Climate Change 1995: Impacts, Adaptations, and Mitigation of Climate Change: Scientific-Technical Analyses; Cambridge University Press: Cambridge, UK.

Jäntti, T., Nuortimo, K., 2012. Foster Wheeler Advanced Bio CFB Technology for Large Scale Biomass & Peat Firing Power Plants. Presented at Russia Power, Moscow, Russia.

Jaramillo, P., Griffin, W. M., McCoy, S. T., 2009. Life cycle inventory of CO_2 in an enhanced oil recovery system. Environmental science & technology 43(21), 8027-8032.

Jared, C.P., Sean, P.I., Lynn, B., Andrew, J., Gregson, V., Shiaoguo, C., 2010. DOE/NETL advanced carbon dioxide capture R&D program: technology update, September 2010.

Kapetaki, Z., Ahn, H., Brandani, S., 2013. Detailed process simulation of pre-combustion IGCC plants using coal-slurry and dry coal gasifiers. Energy Procedia 37, 2196-2203.

Khan, A. A., De Jong, W., Jansens, P. J., Spliethoff, H., 2009. Biomass combustion in fluidized bed boilers: Potential problems and remedies. Fuel processing technology 90(1), 21-50.

Khinast, J., Krammer, G. F., Brunner, C., Staudinger, G., 1996. Decomposition of limestone: The influence of CO_2 and particle size on the reaction rate. Chemical engineering science 51(4), 623-634.

Kierzkowska, A.M., Müller, C.R., 2012. Development of calcium-based, copper-functionalised CO_2 sorbents to integrate chemical looping combustion into calcium looping, Energy Environ. Sci. 5, 6061-6065.

Kierzkowska, A.M., Müller, C.R., 2013. Sol–gel derived, calcium-based, copper-functionalised CO_2 sorbents for an integrated chemical looping combustion-calcium looping CO_2 capture process ChemPlusChem 78, 92–100.

Kolovos, K., Barafaka, S., Kakali, G., Tsivilis, S., 2005. CuO and ZnO addition in the cement raw mix: effect on clinkering process and cement hydration and properties. Ceramics 49, 205–212.

Koppatz, S., Pfeifer, C., Rauch, R., Hofbauer, H., Marquard-Moellenstedt, T., Specht, M., 2009. H_2 rich product gas by steam gasification of biomass with in situ CO_2 absorption in a dual fluidized bed system of 8 MW fuel input. Fuel Process. Technol. 90, 914-921.

Kunii, D., Levenspiel, O., 1991. Fluidization Engineering, second ed. Butterworth-Heinemann, Boston.

Kuramochi, T., Ramírez, A., Turkenburg, W., Faaij, A., 2012. Comparative assessment of CO_2 capture technologies for carbon-intensive industrial processes. Progress in energy and combustion science 38(1), 87-112.

Kyoto, 1997. Kyoto Protocol to the United Nations Framework Convention on Climate Change, Kyoto, 11 December 1997.

Lara, Y., Lisbona, P., Martínez, A., Romeo, L. M., 2013. Design and analysis of heat exchanger networks for integrated Ca-looping systems. Applied Energy 111, 690-700.

Lasheras, A., Ströhle, J., Galloy, A., Epple, B., 2011. Carbonate looping process simulation using a 1D fluidized bed model for the carbonator. International Journal of Greenhouse Gas Control 5(4), 686-693.

Leckner, B., 1998. Fluidized bed combustion: mixing and pollutant limitation. Progress in Energy and Combustion Science 24(1), 31-61.

Leion, H., Mattisson, T., Lyngfelt, A., 2009. Use of ores and industrial products as oxygen carriers in chemical-looping combustion. Energy & Fuels 23(4), 2307-2315.

Li, Z-s., Cai, N-s, Croiset, E., 2008. Process analysis of CO_2 capture from flue gas using carbonation/calcination cycles. AlChE J 54, 1912-1925.

Li, J., Tharakan, P., Macdonald, D., Liang, X., 2013. Technological, economic and financial prospects of carbon dioxide capture in the cement industry. Energy Policy 61, 1377-1387.

Liang, X., Li, J., 2012. Assessing the value of retrofitting cement plants for carbon capture: A case study of a cement plant in Guangdong, China. Energy Conversion and Management 64, 454-465.

Linnhoff, B., Flower, J. R., 1978. Synthesis of heat exchanger networks: I. Systematic generation of energy optimal networks. AIChE Journal 24(4), 633-642.

LME, London Metal Exchange, 2013. (http://www.lme.com/)

Lu, H., Reddy, E.P., Smirniotis, P.G., 2006. Calcium oxide based sorbents for capture of carbon dioxide at high temperatures. Ind. Eng. Chem. Res. 45, 3944–3949.

Lu, D. Y., Hughes, R. W., Anthony, E. J., 2008. Ca-based sorbent looping combustion for CO_2 capture in pilot-scale dual fluidized beds. Fuel Processing Technology 89(12), 1386-1395.

Lyon, R. K., Cole, J. A., 2000. Unmixed Combustion: An Alternative to Fire. Combust. Flame 121, 249–261.

Lysikov, A. I., Salanov, A. N., Okunev, A. G., 2007. Change of CO_2 carrying capacity of CaO in isothermal recarbonation-decomposition cycles. Industrial & Engineering Chemistry Research 46(13), 4633-4638.

Ma, X., Chen, H., Wang, P., 2010. Effect of CuO on the formation of clinker minerals and the hydration properties. Cement and Concrete Research 40, 1681–1687.

Maciejewska, A., Veringa, H., Sanders, J., Peteves, S. D., 2006. Co-firing of biomass with coal: constraints and role of biomass pre-treatment. Petten, The Netherlands: Institute for Energy 113, 100.

MacKenzie, A., Granatstein, D. L., Anthony, E. J., Abanades, J. C., 2007. Economics of CO_2 capture using the calcium cycle with a pressurized fluidized bed combustor. Energy & fuels 21(2), 920-926.

Manovic, V., Anthony, E. J., 2007. Steam reactivation of spent CaO-based sorbent for multiple CO_2 capture cycles. Environmental science & technology 41(4), 1420-1425.

Manovic, V., Anthony, E. J., 2008. Thermal activation of CaO-based sorbent and self-reactivation during CO_2 capture looping cycles. Environmental science & technology 42(11), 4170-4174.

Manovic, V., Lu, D., Anthony, E. J., 2008. Steam hydration of sorbents from a dual fluidized bed CO_2 looping cycle reactor. Fuel 87(15), 3344-3352.

Manovic, V., Anthony, E. J., 2009a. Screening of Binders for Pelletization of CaO-Based Sorbents for CO_2 Capture. Energy & Fuels 23(10), 4797-4804.

Manovic, V., Anthony, E.J., 2009b. CaO-based pellets supported by calcium aluminate cements for high-temperature CO_2 capture. Environ. Sci. Technol. 43, 7117-7122.

Manovic, V., Anthony, E. J., 2009c. Long-term behavior of CaO-based pellets supported by calcium aluminate cements in a long series of CO_2 capture cycles. Industrial & Engineering Chemistry Research 48(19), 8906-8912.

Manovic, V., Anthony, E. J., 2010. CO_2 carrying behavior of calcium aluminate pellets under high-temperature/high-CO_2 concentration calcination conditions. Industrial & Engineering Chemistry Research 49(15), 6916-6922.

Manovic, V., Anthony, E. J., 2011a. Reactivation and remaking of calcium aluminate pellets for CO_2 capture. Fuel 90(1), 233-239.

Manovic, V., Anthony, E. J., 2011b. CaO-Based Pellets with Oxygen Carriers and Catalysts. Energy Fuels 25 (10), 4846 – 4853.

Manovic, V., Wu, Y., He, I., Anthony, E. J., 2011c. Core-in-shell CaO/CuO-based composite for CO_2 capture. Ind. Eng. Chem. Res. 50, 12384−12391.

Manovic, V., Anthony, E. J., 2011d. Integration of Calcium and Chemical Looping Combustion using Composite CaO/CuO-Based Materials. Environ. Sci. Technol. 45, 10750−10756.

Martinez, I., Grasa, G., Murillo, R., Arias, B., Abanades, J.C., 2010. Kinetics of Calcination of Partially Carbonated Particles in a Ca-looping System for CO_2 Capture. Energy&Fuels 26 (2), 1432-1440.

Martinez, I., Romano, M. C., Fernández, J. R., Chiesa, P., Murillo, R., Abanades, J. C., 2014. Process design of a hydrogen production plant from natural gas with CO_2 capture based on a novel Ca/Cu chemical loop. Applied Energy 114, 192-208.

McIlveen-Wright, D. R., Huang, Y., Rezvani, S., Mondol, J. D., Redpath, D., Anderson, M., Williams, B. C., 2011. A techno-economic assessment of the reduction of carbon dioxide emissions through the use of biomass co-combustion. Fuel 90(1), 11-18.

Mellows-Facer, A., 2010. Key issues for the new parliament. House of Commons Library Research. (http://goo.gl/Gdv1n0)

Merkel, T. C., Lin, H., Wei, X., Baker, R., 2010. Power plant post-combustion carbon dioxide capture: an opportunity for membranes. Journal of Membrane Science 359(1), 126-139.

Merkel, T. C., Zhou, M., Baker, R. W., 2012. Carbon dioxide capture with membranes at an IGCC power plant. Journal of Membrane Science 389, 441-450.

McCauley, K. J., Farzan, H., Alexander, K. C., McDonald, D. K., 2009. Commercialization of Oxy-Coal Combustion: Applying Results of a Large 30 MW_{th} Pilot Project. Energy Procedia 1, 439–446.

Naranjo, M., Brownlow, D. T., Garza, A., 2011. CO_2 capture and sequestration in the cement industry. Energy Procedia 4, 2716-2723.

NETL, 2012. Current and Future Technologies for Power Generation with Post-Combustion Carbon Capture - Final Report, in DOE/NETL-2012/1557.

Nuortimo, K., 2013. Large scale CHP with CFB technology. Presented at 4th European Conference of Renewable Heating and Cooling, Dublin, Ireland.

Obersteiner, M., Azar, C., Kauppi, P., Möllersten, K., Moreira, J., Nilsson, S., Van Ypersele, J. P., 2001. Managing climate risk. Science 294(5543), 786-787.

Olivier, J. G., Janssens-Maenhout, G., Muntean, M., Peters, J. A., 2013. Trends in global CO_2 emissions 2013 report. PBL Netherlands Environmental Assessment Agency.

Ozcan, D. C., 2010. Development of a sorbent for carbon dioxide. MSc Thesis, Iowa State University.

Ozcan, D. C., Shanks, B. H., Wheelock, T. D., 2011. Improving the stability of a CaO-based sorbent for CO_2 by thermal pretreatment. Industrial & Engineering Chemistry Research 50(11), 6933-6942.

Ozcan, D.C., Ahn, H., Kierzkowska, A.M., Müller, C.R., Brandani, S., 2013. Process integration of chemical looping combustion into calcium looping for CO_2 capture from a cement plant, 5th HTSLCN Meeting, Cambridge, UK.

Pacciani, R., Müller, C. R., Davidson, J. F., Dennis, J. S., Hayhurst, A. N., 2008. Synthetic Ca-based solid sorbents suitable for capturing CO_2 in a fluidized bed. The Canadian journal of chemical engineering 86(3), 356-366.

Pan, X., Clodic, D., Toubassy, J., 2013. CO_2 capture by antisublimation process and its technical economic analysis. Greenhouse Gases: Science and Technology 3 (1), 8–20.

Pennline, H. W., Luebke, D. R., Jones, K. L., Myers, C. R., Morsi, B. I., Heintz, Y. J., Ilconich, J. B., 2008. Progress in Carbon Dioxide Capture and Separation Research for Gasification-Based Power Generation Point Sources. Fuel Process. Technol. 89, 897–907.

Plötz, S., Bayrak, A., Galloy, A., Kremer, J., Orth, M., Wieczorek, M., Ströhle, J., Epple, B., 2012. First carbonate looping experiments with a 1 MWth test facility consisting of two interconnected CFBs. In: 21st International conference on fluidized bed combustion, Naples (Italy), 421–428.

Qin, C., Yin, J., Liu, W., An, H., Feng, B., 2012. Behavior of CaO/CuO based composite in a combined calcium and copper chemical looping process. Ind. Eng. Chem. Res. 51, 12274−12281.

Qin, C., Yin, J., Luo, C., An, H., Liu, W., Feng, B., 2013. Enhancing the performance of CaO/CuO based composite for CO_2 capture in a combined Ca-Cu chemical looping process. Chemical Engineering Journal 228, 75-86.

Ramasubramanian, K., Verweij, H., Winston Ho, W. S., 2012. Membrane processes for carbon capture from coal-fired power plant flue gas: A modeling and cost study. Journal of Membrane Science 421, 299-310.

Rampinelli, G., 2010. Modello matematico di un reattore per la cattura della CO2 post-combustione tramite ossido di calcio. Masters Thesis. Politecnico di Milano, Italy.

Rao, A. B., Rubin, E. S. A., 2002. Technical, Economic, and Environmental Assessment of Amine-Based CO_2 Capture Technology for Power Plant Greenhouse Gas Control. Environ. Sci. Technol. 36, 4467– 4475.

Reh, L., 1995. New and efficient high-temperature processes with circulating fluid bed reactor. Chemical Engineering & Technology 18 (2), 75-89.

Rhodes, J. S., Keith, D. W., 2008. Biomass with capture: negative emissions within social and environmental constraints: an editorial comment. Climatic Change 87(3), 321-328.

Robeson, L. M., 2008. The upper bound revisited. Journal of Membrane Science 320(1), 390-400.

Rodriguez, N., Alonso, M., Grasa, G., Abanades, J. C., 2008a. Heat requirements in a calciner of $CaCO_3$ integrated in a CO_2 capture system using CaO. Chemical Engineering Journal 138(1), 148-154.

Rodriguez, N., Alonso, M., Grasa, G., Abanades, J. C., 2008b. Process for capturing CO_2 arising from the calcination of the $CaCO_3$ used in cement manufacture. Environmental science & technology 42(18), 6980-6984.

Rodriguez, N., Alonso, M., Abanades, J.C., Grasa, G., Murillo, R., 2009. Analysis of a process to capture the CO_2 resulting for pre-calcination of the limestone feed to a cement plant. Energy Procedia 1, 141–148.

Rodríguez, N., Alonso, M., Abanades, J. C., 2010. Average activity of CaO particles in a calcium looping system. Chemical Engineering Journal 156(2), 388-394.

Rodríguez, N., Alonso, M., Abanades, J.C., 2011a. Experimental investigation of a circulating fluidized-bed reactor to capture CO_2 with CaO. AIChE J. 57, 1356-1366.

Rodríguez, N., Murillo, R., Alonso, M., Martinez, I., Grasa, G., Abanades, J.C., 2011b. Analysis of a process for capturing the CO_2 resulting for pre-calcination of limestone in a cement plant. Industrial & Engineering Chemistry Research 50 (4), 2126–2132.

Rodriguez, N., Murillo, R., Abanades, J.C., 2012. CO_2 Capture from Cement Plants Using Oxyfired Precalcination and/or Calcium Looping. Environmental Science & Technology 46 (4), 2460-2466.

Romano, M. C., 2012. Modeling the carbonator of a Ca-looping process for CO_2 capture from power plant flue gas. Chemical Engineering Science 69(1), 257-269.

Romano, M. C., Spinelli, M., Campanari, S., Consonni, S., Cinti, G., Marchi, M., Borgarello, E., 2013. The Calcium Looping Process for Low CO_2 Emission Cement and Power. Energy Procedia 37, 7091-7099.

Romeo, L.M., Abanades, J.C., Escosa, J.M., Pano, J., Gimenez A., 2008. Oxyfuel carbonation/calcination cycle for low cost CO_2 capture in existing power plants. Energy Convers Manage 49:2809–2814.

Romeo, L.M., Lara, Y., Lisbona, P., Escosa, J.M., 2009. Optimizing make-up flow in a CO_2 capture system using CaO. Chem Eng J 147, 252–258.

Romeo, L.M., Catalina, D., Lisbona, P., Lara, Y., Martínez, A., 2011. Reduction of greenhouse gas emissions by integration of cement plants, power plants, and CO_2 capture systems. Greenhouse Gases: Science and Technology 1, 72–82.

Rong, N., Wang, Q., Fang, M., Cheng, L., Luo, Z., Cen, K., 2013. Steam Hydration Reactivation of CaO-Based Sorbent in Cyclic Carbonation/Calcination for CO_2 Capture. Energy & Fuels 27(9), 5332-5340.

Rubin, E. S., Yeh, S., Antes, M., Berkenpas, M., Davison, J., 2007. Use of experience curves to estimate the future cost of power plants with CO_2 capture. International journal of greenhouse gas control 1(2), 188-197.

Ryu, H. J., Grace, J. R., Lim, C. J., 2006. Simultaneous CO_2/SO_2 capture characteristics of three limestones in a fluidized-bed reactor. Energy & fuels 20(4), 1621-1628.

Sakadjian, B. B., Iyer, M. V., Gupta, H., Fan, L. S., 2007. Kinetics and structural characterization of calcium-based sorbents calcined under subatmospheric conditions for the high-temperature CO_2 capture process. Industrial & Engineering Chemistry Research 46(1), 35-42.

Salvador, C., Lu, D., Anthony, E. J., Abanades, J. C., 2003. Enhancement of CaO for CO_2 capture in an FBC environment. Chemical Engineering Journal 96(1), 187-195.

Schaeffer, G. J., Boots, M. G., Mitchell, C., Timpe, C., Cames, M., Anderson, T., 2013. The implications of tradable green certificates for the deployment of renewable electricity: mid-term report. Policy Studies 2012, 2011.

Scholes, C. A., Chen, G. Q., Tao, W. X., Bacus, J., Anderson, C., Stevens, G. W., Kentish, S. E., 2011. The effects of minor components on the gas separation performance of membranes for carbon capture. Energy Procedia 4, 681-687.

SETIS, 2013. Calculation of Energy Production Costs. Institute for Energy, Directorate-General Joint Research Centre: Petten, The Netherlands. (http://setis.ec.europa.eu/EnergyCalculator/)

Shimizu, T., Hirama, T., Hosoda, H., Kitano, K., Inagaki, M., Tejima, K., 1999. A twin fluid-bed reactor for removal of CO_2 from combustion processes. Chem Eng Res Des 77, 62–68.

Squires, A. M., 1967. Cyclic use of calcined dolomite to desulfurize fuels undergoing gasification. Adv. Chem. Ser. 69, 205–229.

Silaban, A., Harrison, D.P., 1995. High-temperature capture of carbon dioxide: characteristics of the reversible reaction between CaO (s) and CO_2 (g). Chemical Engineering Communications 137,177–190.

Silaban, A., Narcida, M., Harrison, D. P., 1996. Characteristics of the reversible reaction between CO_2(g) and calcined dolomite. Chemical Engineering Communications 146: 149-162.

Soukup, G., Pfeifer, C., Kreuzeder, A., Hofbauer, H., 2009. In situ CO_2 capture in a dual fluidized bed biomass steam gasifier - Bed material and fuel variation. Chemical Engineering and Technology 32, 348-354.

Srivastava, R. K., Jozewicz, W., Singer, C., 2001. SO_2 scrubbing technologies: a review. Environmental Progress 20(4), 219-228.

Stadler, H., Beggel, F., Habermehl, M., Persigehl, B., Kneer, R., Modigell, M., Jeschke, P., 2011. Oxyfuel coal combustion by efficient integration of oxygen transport membranes. International Journal of Greenhouse Gas Control 5(1), 7-15.

Stallmann, O., 2013. Integrated carbon dioxide capture for cement plants. Publication No. WO/2013/024340.

Stevens, D. J., 2001. Hot gas conditioning: recent progress with larger-scale biomass gasification systems. NREL Subcontractor Report (NREL/SR-510-29952).

Sun, P., Grace, J. R., Lim, C. J., Anthony, E. J., 2007. Removal of CO_2 by calcium-based sorbents in the presence of SO_2. Energy & fuels 21(1), 163-170.

Sun, P., Grace, J. R., Lim, C. J., Anthony, E. J., 2008. Investigation of Attempts to Improve Cyclic CO_2 Capture by Sorbent Hydration and Modification. Ind. Eng. Chem. Res. 47, 2024–2032.

Sun, R., Li, Y., Liu, H., Wu, S., Lu, C., 2012. CO_2 capture performance of calcium-based sorbent doped with manganese salts during calcium looping cycle. Applied Energy 89(1), 368-373.

Taylor, H.F.W., 1990. Cement Chemistry, Academic Press Ltd, New York.

Telesca, A., Calabrese, D., Marroccoli, M., Tomasulo, M., Valenti, G.L., Montagnaro, F., 2014. Spent limestone sorbent from calcium looping cycle as a raw material for the cement industry. Fuel 118, 202-205.

Torp, T., Gale, J., 2004. Demonstrating storage of CO_2 in geological reservoirs: The Sleipner and SACS projects. Energy 29, 1361– 1369.

Tuinier, M. J., Hamers, H. P., van Sint Annaland, M., 2011. Techno-economic evaluation of cryogenic CO2 capture - A comparison with absorption and membrane technology. International Journal of Greenhouse Gas Control 5(6), 1559-1565.

Turton, R., Bailie, R.C., Whiting, W.B., Shaeiwitz, J.A., Bhattacharyya, D., 2009. Analysis, Synthesis, and Design of Chemical Processes (third ed.), Prentice Hall.

U. K. Parliament (UKP), 2008. Climate change act 2008. London, UK.

United Nations Framework Convention on Climate Change (UNFCC), 2007. Article 2, Bali 3–15 December 2007.

Vera, E.R.M., 2009. Method for capturing CO_2 produced by cement plants by using the calcium cycle. Publication No. US20090255444 A1.

Wang, Y., Lin, S., Suzuki, Y., 2008. Limestone calcination with CO_2 capture (II): Decomposition in CO_2/steam and CO_2/N_2 atmospheres. Energy & Fuels 22(4), 2326-2331.

Wang, W., Ramkumar, S., Wong, D., Fan, L. S., 2012. Simulations and process analysis of the carbonation–calcination reaction process with intermediate hydration. Fuel 92(1), 94-106.

WBCSD, 2009. Cement Industry and CO_2 Performance. 'Getting the Numbers Right', Cement Sustainability Initiative, Geneva.

Weimer, T., Berger, R., Hawthorne, C., Abanades, J. C., 2008. Lime enhanced gasification of solid fuels: Examination of a process for simultaneous hydrogen production and CO_2 capture. Fuel 87(8), 1678-1686.

Werther, J., Saenger, M., Hartge, E. U., Ogada, T., Siagi, Z., 2000. Combustion of agricultural residues. Progress in energy and combustion science 26(1), 1-27.

WWF, 2008. Blueprint for the Cement Industry: How to Turn Around the Trend of Cement Related Emissions in the Developing World.

Xu, G., Li, L., Yang, Y., Tian, L., Liu, T., Zhang, K., 2012. A novel CO_2 cryogenic liquefaction and separation system. Energy 42(1), 522-529.

ZEP, 2011. The Cost of CO_2 Capture, Transport and Storage. Post-demonstration CCS in the EU, Technology Platform for Zero Emission Fossil Fuel Power Plants, Brussels.

Zhai, H., Rubin, E. S., 2013. Techno-Economic Assessment of Polymer Membrane Systems for Postcombustion Carbon Capture at Coal-Fired Power Plants. Environmental science & technology 47(6), 3006-3014.

Zhao, L., Riensche, E., Blum, L., Stolten, D., 2010. Multi-stage gas separation membrane processes used in post-combustion capture: Energetic and economic analyses. Journal of Membrane Science 359(1), 160-172.

Appendix A

Mass and energy balance calculations for the base cement plant, Ca-looping process and preliminary steam cycle design detailed in Chapter 2
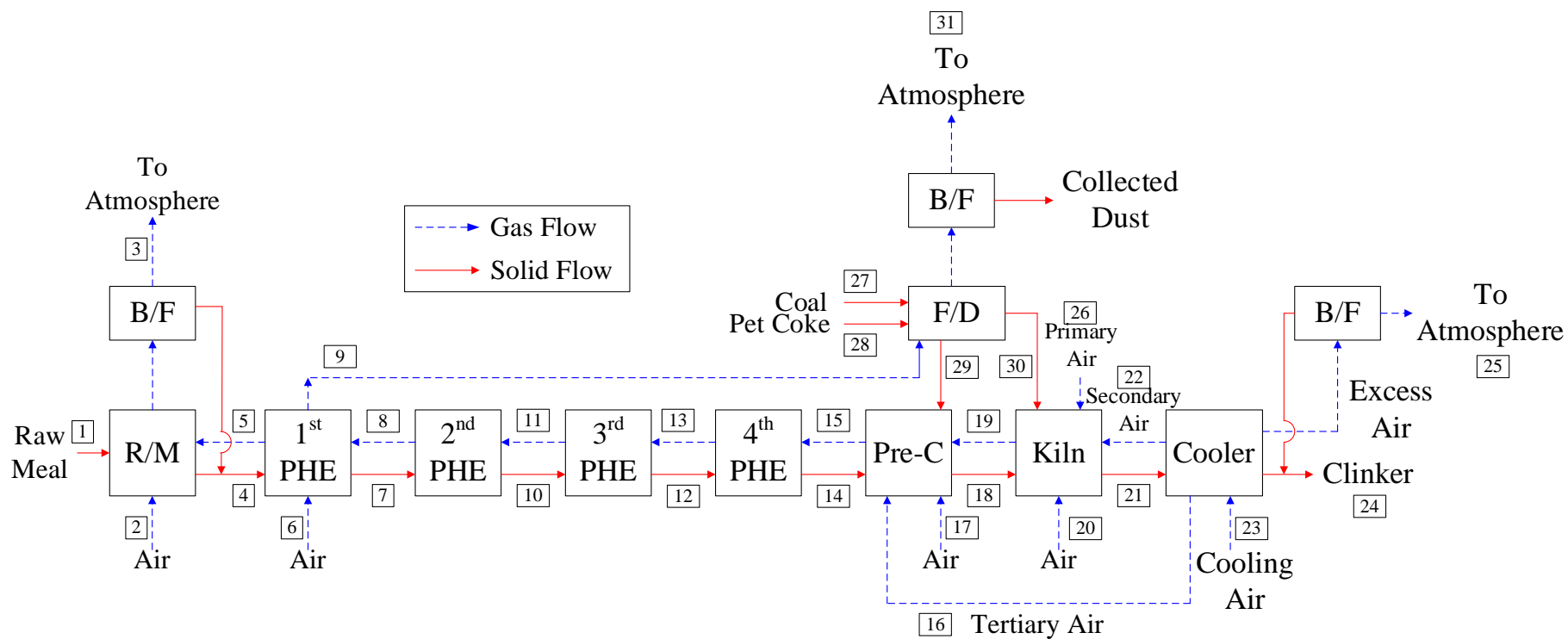
Figure A1 Schematic diagram of a cement plant without a CO_2 capture unit (Base Case) (IEA, 2008). Abbreviations: **R/M**, Raw Mill; **B/F**, Bag Filter; **F/D**, Fuel Drying; **PHE**, Preheater; **Pre-C**, Pre-calciner.

Table A1 Stream compositions for base cement plant (only two digits after decimal have been shown).

Stream Number		1	2	3	4	5	6	7	8	9	10	11	12	13	14	15	16	17
Stream Name		Raw meal	Air In-leak	B/F Exit Gas	R/M Exit	Preheater Exit Gas	Air In-leak	1st PHE Exit	2nd PHE Exit Gas	1st PHE Exit Gas to Fuel Drying	2nd PHE Exit	3rd PHE Exit Gas	3rd PHE Exit	4th PHE Exit Gas	4th PHE Exit	Pre-C Exit Gas	Tertiary Air	Air In-leak
Component																		
CO_2	kg/s			23.97		23.97			25.73	1.76		25.73		25.73		23.66		
$CaCO_3$	kg/s	37.94			40.49	2.55		42.86	5.10	0.19	45.91	8.49	46.24	8.49	33.94	0.90		
$CaSO_4$	kg/s										0.01	0.01	0.08	0.08	0.33	0.33		
H_2	kg/s																	
O_2	kg/s		3.75	5.06		1.31	0.97		0.49	0.1		0.49		0.49		0.49	3.81	1.13
SO_2	kg/s			0.1		0.11												
N_2	kg/s		12.2	40.45		28.23	3.18		27.13	2.07		27.13		27.13		27.16	12.42	3.68
Ash	kg/s										0.02	0.03	0.03	0.11	0.11			
C	kg/s																	
S	kg/s	0.16			0.17			0.12	0.01		0.13	0.02	0.03	0.03	0.11			
H_2O	kg/s	4.19		5.87		1.67			1.80	0.12		1.79		1.79		1.62		
C_2S	kg/s							0.07	0.07		0.67	0.67	3.79	3.79	15.16	6.48		
C_3A	kg/s												0.05	0.05	0.19	0.19		
C_3S	kg/s										0.05	0.05	0.26	0.26	1.04	1.04		
C_4AF													0.04	0.04	0.14	0.14		
Fe_2O_3	kg/s										0.03	0.03	0.15	0.15	0.60	0.31		
Al_2O_3	kg/s										0.06	0.06	0.33	0.33	1.30	0.66		
SiO_2	kg/s	3.16			3.37	0.21		3.57	0.42	0.02	3.78	0.63	3.59	0.44	1.76	0.34		
AS_4H	kg/s	4.74			5.06	0.32		5.35	0.63	0.02	5.69	0.97	5.49	0.77	3.07			
AS_2H_2	kg/s	1.27			1.35	0.08		1.43	0.17		1.52	0.26	1.46	0.21	0.82			
$2FeO \cdot OH$	kg/s	0.95			1.01	0.06		1.07	0.13		1.14	0.19	1.10	0.15	0.62			
CaO	kg/s															3.01		
Total Flow	kg/s	52.41	15.96	75.44	51.46	58.52	4.15	54.48	61.7	4.3	58.99	66.21	62.72	69.94	59.20	66.46	16.23	4.81
Temperature	°C	9	9	110	110	309	9	309	490	309	490	634	634	760	760	915	908	9
Pressure	atm	-	1	1	-	1	1	-	1	1	-	1	-	1	-	1	1	1
Total Stream Enthalpy	GJ/h	-2415	-0.95	-1044	-2310	-938.5	-0.25	-2405	-1101	-68.96	-2561	-1256	-2689	-1382	-2524	-1217	+56.64	-0.29

Stream Number		18-1	18-2	19-1	19-2	20	21-1	21-2	22-1	22-2	23	24	25	26	27	28	29	30	31
Stream Name		Pre-C Exit	Pre-C Exit	Kiln Exit Gas	Kiln Exit Gas	Air In-leak	Kiln Exit	Kiln Exit	Secondary Air	Secondary Air	Cooling Air	Clinker	B/F Exit Gas	Primary Air	Coal	Pet-coke	Dry Coal	Dry Pet-Coke	B/F Exit Gas
Component																			
CO_2	kg/s			4.82	4.82														1.76
$CaCO_3$	kg/s	2.51	2.51														0.19		
$CaSO_4$	kg/s	0.92	0.92	0.12	0.12		0.80	0.80				0.80							
H_2	kg/s														0.10	0.04	0.10	0.04	2.07
O_2	kg/s			0.31	0.31	0.38			2.65	2.65	16.78		10.33	0.36	0.16	0.02	0.16	0.02	0.01
SO_2	kg/s			0.12	0.12														
N_2	kg/s			11.03	11.03	1.22			8.64	8.64	54.73		33.67	1.14	0.03	0.02	0.03	0.02	
Ash	kg/s	0.32	0.32	0.04	0.04		0.28	0.28				0.28			0.28		0.28		
C	kg/s														1.46	1.01	1.46	1.01	
S	kg/s														0.02	0.06	0.02	0.06	
H_2O	kg/s			0.37	0.37										0.21	0.02			0.36
C_2S	kg/s	17.94	17.94	0.82	0.82		5.42	5.43				5.43							
C_3A	kg/s	0.52	0.52	0.52	0.52		3.44	3.44				3.44							
C_3S	kg/s	2.89	2.89	2.89	2.89		19.08	19.08				19.08							
C_4AF		0.39	0.39	0.39	0.39		2.59	2.59				2.59							
Fe_2O_3	kg/s	0.85	0.85																
Al_2O_3	kg/s	1.84	1.84																
SiO_2	kg/s	0.93	0.93														0.02		
AS_4H	kg/s																0.02		
AS_2H_2	kg/s																		
$2FeO \cdot OH$	kg/s																		
CaO	kg/s	8.36	8.36																
Total Flow	kg/s	37.5	37.5	21.44	21.44	1.60	31.61	31.61	11.29	11.29	71.52	31.61	44.00	1.50	2.26	1.18	2.29	1.16	4.30
Temperature	°C	915	1250	1450	1025	9	1450	1370	1025	1245	9	60	279	9	9	9	110	110	110
Pressure	atm	-	-	1	1	1	-	-	1	1	1	-	1	1	-	-	-	-	1
Total Stream Enthalpy	MJ/h	-1582	-1541	-264.3	-305.5	-0.09	-1260	-1270	+45.0	+55.71	-4.2	-1424	41.73	-0.09	-25.6	+0.52	-22.73	+2.21	-73.50

Figure A2 Schematic diagram of the proposed process integration of a cement plant with a Ca-looping unit. Abbreviations: **R/M**, Raw Mill; **B/F**, Bag Filter; **F/D**, Fuel Drying; **PHE**, Preheater; **Pre-C**, Pre-calciner; **Carb**, Carbonator; **Calc**, Calciner; **ASU**, Air Separation Unit; **CO₂ Comp**, CO₂ Compression.

Table A2 Stream compositions for cement plant with a Ca-looping unit at 1.65 F_0/F_{CO2} (only two digits after decimal have been shown).

Stream Number		1	2	3	4	5	6	7	8	9	10	11	12	13	14	15
Stream Name		Raw meal	Air In-leak	B/F Exit Gas	R/M Exit	Preheater Exit Gas	Air In-leak	1st PHE Exit	2nd PHE Exit Gas	1st PHE Exit Gas to Fuel Drying	2nd PHE Exit	3rd PHE Exit Gas	3rd PHE Exit	4th PHE Exit Gas	4th PHE Exit	Pre-C Exit Gas
Component																
CO_2	kg/s			0.69		0.69			0.77	0.09		7.77		7.77		7.30
$CaCO_3$	kg/s	8.62			9.17	0.55		9.70	1.15	0.07	10.38	1.85	10.46	1.92	7.68	0.21
$CaSO_4$	kg/s										0.01	0.01	0.08	0.08	0.30	0.30
H_2	kg/s															
O_2	kg/s		1.47	8.29		0.43	0.38		0.16	0.06		0.16		0.16		0.16
SO_2	kg/s			0.1		0.10				0.01						
N_2	kg/s		4.79	37.38		11.76	1.25		12.02	1.50		12.02		12.02		12.02
Ash	kg/s														0.04	0.04
C	kg/s															
S	kg/s	0.16			0.17			0.12	0.01		0.13	0.02	0.13	0.03	0.10	
H_2O	kg/s	1.64		2.55		0.91			1.02	0.12		1.02		1.02		0.85
C_2S	kg/s							0.02	0.02		0.16	0.16	0.89	0.89	3.56	2.64
C_3A	kg/s												0.05	0.05	0.19	0.19
C_3S	kg/s										0.05	0.05	0.26	0.26	1.03	1.03
C_4AF	kg/s												0.04	0.04	0.14	0.14
Fe_2O_3	kg/s										0.03	0.03	0.15	0.15	0.60	0.31
Al_2O_3	kg/s										0.06	0.06	0.33	0.33	1.30	0.66
SiO_2	kg/s	3.16			3.36	0.20		3.57	0.44	0.03	3.94	0.81	4.58	1.45	5.79	1.68
AS_4H	kg/s	4.74			5.04	0.30		5.33	0.63	0.04	5.66	0.96	5.46	0.77	3.06	
AS_2H_2	kg/s	1.27			1.35	0.08		1.42	0.17	0.01	1.51	0.26	1.46	0.20	0.82	
$2FeO·OH$	kg/s	0.95			1.00	0.06		1.07	0.13		1.13	0.19	1.09	0.15	0.61	
CaO	kg/s															
Total Flow	kg/s	20.54	6.25	49.00	20.10	15.09	1.63	21.25	16.54	1.93	23.07	25.38	24.97	27.28	25.21	27.51
Temperature	°C	9	9	110	110	291.4	9	291.4	456.2	291.4	456.2	588	588	701	701	915
Pressure	atm	-	1	>1	-	>1	1	-	>1	>1	-	>1	-	>1	-	>1
Total Stream Enthalpy	GJ/h	-993	-0.37	-130.9	-949.6	-109.1	-0.1	-995	-167.9	-13.92	-1065	-453	--1137	-524.3	-1129	-516

Stream Number		16	17	18-1	18-2	19-1	19-2	20	21-1	21-2	22-1	22-2	23	24	25	26	27
Stream Name		Tertiary Air	Air In-leak	Pre-C Exit + Purge	Pre-C Exit + Purge	Kiln Exit Gas	Kiln Exit Gas	Air In-leak	Kiln Exit	Kiln Exit	Secondary Air	Secondary Air	Cooling Air	Clinker	Excess Air to R/M	Primary Air	Coal
Component																	
CO_2	kg/s					2.63	2.63										
$CaCO_3$	kg/s			0.57	0.57												
$CaSO_4$	kg/s			1.50	1.50	0.20	0.20		1.30	1.30				1.30			
H_2	kg/s																0.03
O_2	kg/s	0.39	1.13			0.20	0.20	0.38			1.43	1.43	16.78		6.39	0.36	0.05
SO_2	kg/s					0.08	0.08										
N_2	kg/s	1.27	3.68			7.06	7.06	1.22			4.67	4.67	54.73		20.83	1.14	
Ash	kg/s			0.11	0.11	0.01	0.01		0.10	0.10				0.10			0.08
C	kg/s																0.44
S	kg/s																
H_2O	kg/s					0.24	0.24										0.07
C_2S	kg/s			7.32	7.32	0.81	0.81		5.33	5.33				5.33			
C_3A	kg/s			0.52	0.52	0.52	0.52		3.44	3.44				3.44			
C_3S	kg/s			2.85	2.85	2.85	2.85		18.88	18.88				18.88			
C_4AF	kg/s			0.39	0.39	0.39	0.39		2.59	2.59				2.59			
Fe_2O_3	kg/s			0.85	0.85												
Al_2O_3	kg/s			1.84	1.84												
SiO_2	kg/s			4.65	4.65												
AS_4H	kg/s																
AS_2H_2	kg/s																
$2FeO \cdot OH$	kg/s																
CaO	kg/s			16.16	16.16												
Total Flow	kg/s	1.66	4.81	36.76	36.76	14.98	14.98	1.60	31.72	31.72	6.10	6.10	71.52	31.72	27.22	1.50	0.68
Temperature	°C	908	9	921	1109	1450	1025	9	1450	1370	1025	1400	9	60	279	9	9
Pressure	atm	>1	1	-	-	>1	>1	1	-	-	>1	>1	>1	-	>1	>1	-
Total Stream Enthalpy	MJ/h	+5.80	-0.29	-1508	-1479	-225.2	-253.7	-0.09	-1259	-1270	+24.33	+35.17	-4.25	-1425	+25.82	-0.09	-7.7

Stream Number		28	29	30	31	32	33	34	35	36	37	38	39	40
Stream Name		Pet-coke	Dry Coal	Dry Pet-Coke	B/F Exit Gas	Hot Air to Steam Cycle	Purge	CO_2 depleted gas	CaO to Carbonator	$CaCO_3$ to Calciner	CO_2 rich gas	Oxygen	Make-up	Pet-coke
Component														
CO_2	kg/s				0.09			0.77			33.60		29.33	
$CaCO_3$	kg/s		0.07							15.92				
$CaSO_4$	kg/s						0.66		0.89	0.89				
H_2	kg/s	0.03	0.03	0.03										0.15
O_2	kg/s	0.01	0.05	0.01	0.06	8.61		0.16			1.14	12.48		0.08
SO_2	kg/s				0.01									
N_2	kg/s	0.01		0.01	1.50	28.10		12.02			0.13	0.05		
Ash	kg/s		0.08				0.01		0.01	0.01				0.01
C	kg/s	0.65	0.44	0.65										3.74
S	kg/s	0.04		0.04										0.16
H_2O	kg/s	0.01			0.19			1.02			3.99		2.55	0.08
C_2S	kg/s													
C_3A	kg/s													
C_3S	kg/s													
C_4AF	kg/s													
Fe_2O_3	kg/s													
Al_2O_3	kg/s													
SiO_2	kg/s		0.03											
AS_4H	kg/s		0.04											
AS_2H_2	kg/s		0.01											
$2FeO \cdot OH$	kg/s													
CaO	kg/s						16.16		21.60	12.68				
Total Flow	kg/s	0.76	0.77	0.74	1.85	36.71	16.83	13.98	22.50	29.50	38.87	12.53	31.88	4.29
Temperature	°C	9	110	110	110	646	930	650	930	650	930	9	9	9
Pressure	atm	-	-	-	>1	>1	-	>1	-	-	>1	>1	-	-
Total Stream Enthalpy	MJ/h	+0.33	-10.98	+1.41	-11.75	+88.10	-634	-37.78	-847.3	-1176	-1122	-0.67	-1422	-0.23
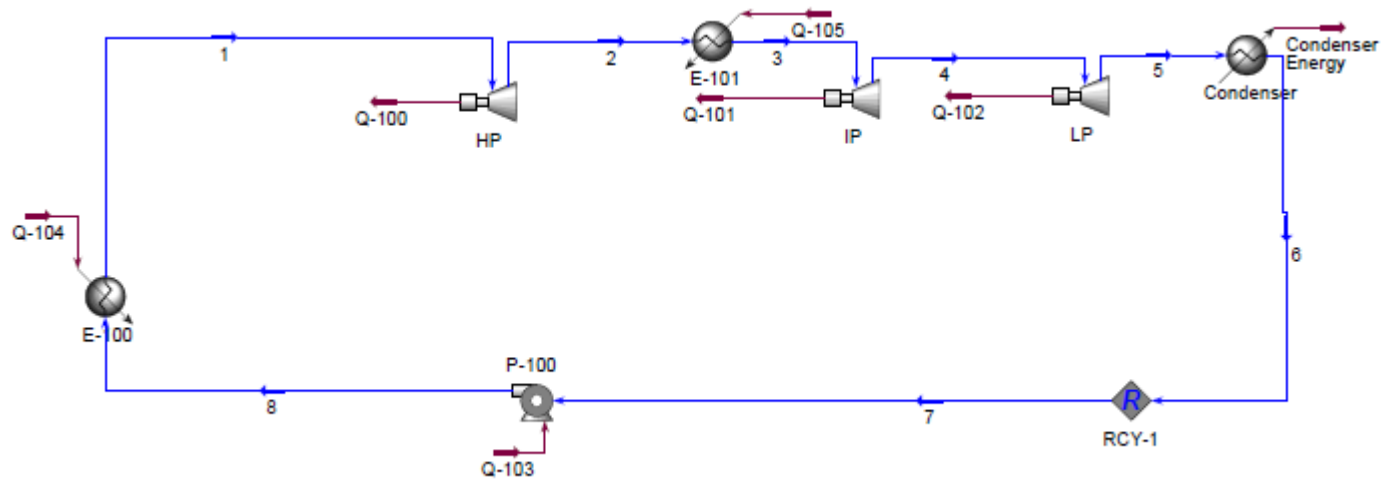
Figure A3 Schematic diagram of the steam cycle design (The below equation has been used to estimate the lumped conversion factor.

The adiabatic efficiencies in HP, IP and LP turbines were assumed to be 86%, 86% and 95%, respectively (Ahn et al., 2013) and that for the pump was taken as 75%).

$$\eta = \frac{W_{ideal,HP}.\eta_{ad,HP} + W_{ideal,IP}.\eta_{ad,IP} + W_{ideal,LP}.\eta_{ad,LP} - W_{ideal,pump}.\eta_{ad,pump}}{Q_{total}}$$ (Eq. A1)

Table A3 Stream compositions for the preliminary steam cycle design.

Stream Number	Molar Flow [kmol/h]	Temperature [°C]	Pressure [bar]	Total Stream Enthalpy [GJ/h]
1	1	565	167	-0.2244
2	1	347.3	38	-0.2312
3	1	565	38	-0.2221
4	1	469.1	20	-0.2256
5	1	28.98	0.04	-0.2460
6	1	25	0.04	-0.2850
7	1	25	0.04	-0.2850
8	1	26.69	167	-0.2846

Stream	Power (MW$_e$)
Q-100	1.894e-3
Q-101	9.76e-4
Q-102	5.646e-3
Q-103	1.118e-4
	Power (MW$_{th}$)
Q-104	1.674e-2
Q-105	2.511e-3
Condenser Energy	1.085e-2

Appendix B Carbonator Design and Customization of UniSim Design

B.1 Carbonator Design

In the simple model, the maximum average carbonation degree of sorbent in the solid population is defined as Eq. B1 (Abanades, 2002) where $X_{max,N}$ is the maximum carbonation degree after N cycles of carbonation/calcination in Eq. B2 (Grasa and Abanades, 2006) and r_N is the mass fraction of particles calculated from mass balance in Eq. B3 (Abanades, 2002). The CO_2 capture efficiency in the carbonator (E_{CO_2}) is defined as Eq. B4.

$$X_{max,ave} = \sum_{N=1}^{N=\infty} r_N X_{max,N} \tag{B1}$$

$$X_{max,N} = \frac{1}{1/(1-X_r)+kN} + X_r \tag{B2}$$

$$r_N = \frac{F_0 F_R^{N-1}}{(F_0+F_R)^N} \tag{B3}$$

$$E_{CO_2} = \frac{F_R X_{max,ave}}{F_{CO_2}} \tag{B4}$$

X_r and k are constants specific to the type of limestone. For non-sulfated Piaseck limestone the values of the constants are $X_r=0.0969$ and $k=0.66$ (Grasa et al., 2008b; Romano, 2012). The capture efficiency calculated from this model is shown in Figure B1. The maximum carbonation efficiency is also limited by the equilibrium of CO_2 over CaO as shown in Eq. B5 (Garcia-Labiano et al., 2002). The equilibrium at 650°C is shown as a horizontal dotted line in Figure B1.

$$P_{CO2,eq} = 4.137 \times 10^{12} \exp\left(-\frac{20474}{T}\right) \tag{B5}$$

As it can be noticed from Figure B1, various sets of F_0/F_{CO_2} and F_R/F_{CO_2} can provide capture efficiency of 90% in the carbonator according to Eqs. B1 to B4. However, an advanced carbonator model is necessary in order to deal with the hydrodynamics of a fluidized bed system.
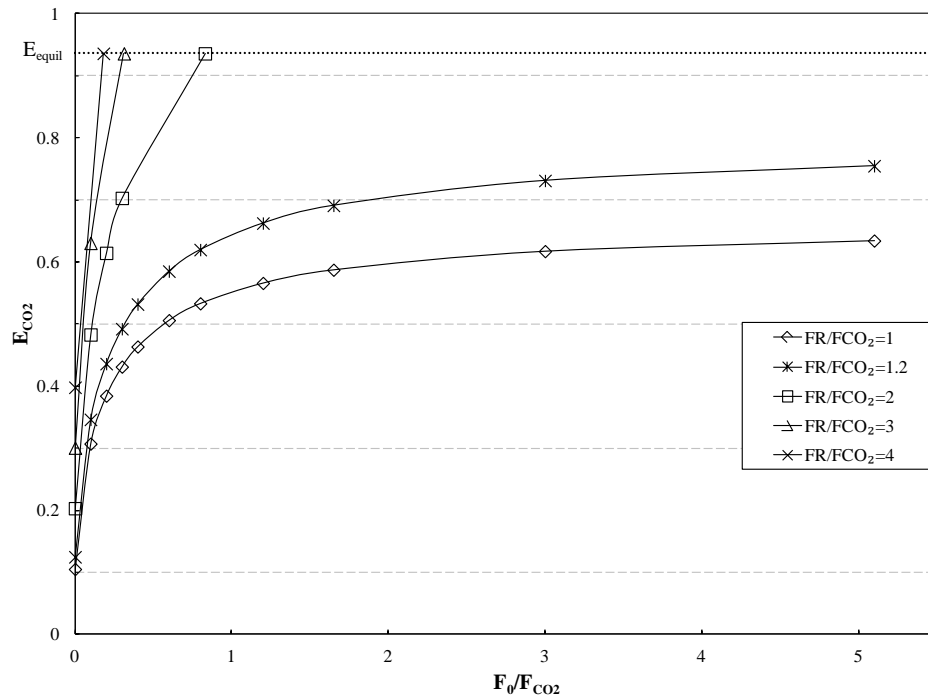
Figure B1 Graphical explanation of Eq. B5 at 650°C (k=0.66 and Xr=0.0969).

Detailed carbonator designs have been investigated including the design of a BFB (Abanades et al., 2004) and a fast fluidized bed (Lasheras et al., 2011; Romano, 2012). Therefore, in this study, the detailed CFB model for fast fluidization has been employed based on the approach proposed in the literature (Rampinelli, 2010; Romano, 2012) and named rigorous model. This model is briefly described here but further details can be found in the literature (Romano, 2012).

In the rigorous model, the flow regime needs to be determined before the prediction of the behaviour of gas-solid reaction. Kunii and Levenspiel (1991) constructed Figure B2 for the whole range of gas-solid contact regimes while the letters A, B, C and D refer to Geldart classification of the solids.
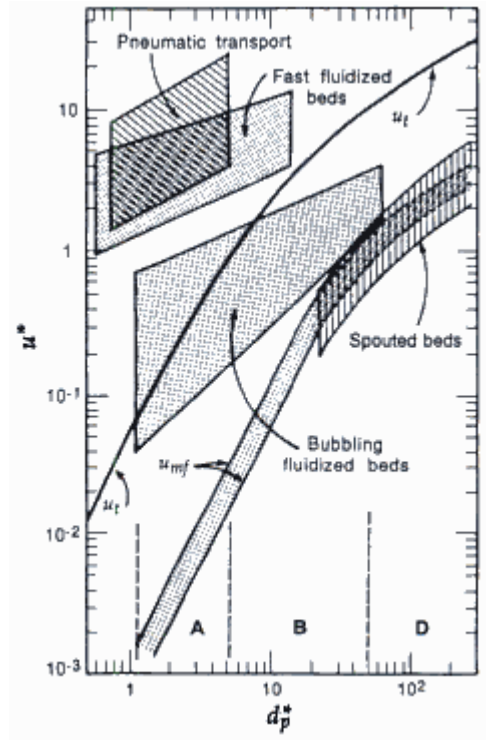
Figure B2 General flow regime diagram for a gas-solid system (Kunii and Levenspiel, 1991).

The dimensionless particle size d_p^* and the dimensionless gas velocity u^* can be calculated to map the constructed chart according to the following equations:

$$u^* = \left[\frac{18}{(d_p^*)^2} + \frac{0.591}{(d_p^*)^{0.5}}\right]^{-1} \text{ for spherical particles} \tag{B6}$$

$$d_p^* = d_p \left[\frac{\rho_g(\rho_s - \rho_g)g}{\mu^2}\right]^{1/3} \tag{B7}$$

where d_p is the particle size of a sorbent and μ is the viscosity. ρ_g and ρ_s refer to gas and solid densities, respectively.

The solid distribution part of the rigorous model has been based on the Kunii-Levenspiel model for CFBs (Kunii and Levenspiel, 1991), and the reactor is divided into two sections, a lower dense region and an upper lean region. To calculate the values of H_l (height of the upper lean region) and $\varepsilon_{s,e}$ (exiting solid fraction), the particle distribution equations (Eqs. B8 and B9) need to be solved simultaneously.

$$\varepsilon_{s,e} = \varepsilon_s^* + (\varepsilon_{s,d} - \varepsilon_s^*)e^{-aH_l} \tag{B8}$$

$$\frac{W_s}{A_t\rho_s} = \frac{(\varepsilon_{s,d}-\varepsilon_{s,e})}{a} + H_t\varepsilon_{s,d} - H_l(\varepsilon_{s,d} - \varepsilon_s^*) \tag{B9}$$

where ε_s^* is the asymptotic solid volumetric fraction and is assumed to be 0.01 for a fast fluidized bed. $\varepsilon_{s,d}$ is the volume fraction of solids in the lower dense region and is set equal to 0.15. 'a' is the decay constant of solid concentration in the lean region, and to estimate this constant, a value of 3 s^{-1} for a.u$_0$ is taken from the values ranging from 2 to 7 s^{-1} in Kunii and Levenspiel (1991). W_s is the solid inventory in the carbonator and determined by setting the pressure drop in the carbonator to 0.1 bar.

The solution of the gas phase material balance in the CFB which can be rearranged with the first order kinetic law for the carbonation reaction (Eq. 2.5 in Chapter 2) leads to two final equations, B10 and B11 which give CO$_2$ concentrations at the top of the dense region (C$_{CO_2,d}$) and at the reactor exit (C$_{CO_2,out}$), respectively.

$$C_{CO_2,d} =$$
$$C_{CO_2,eq} + (C_{CO_2,in} - C_{CO_2,eq})e^{-[\xi\varepsilon_{s,c}\delta k_{ri,ave}+1/((1/\delta K_{cw})+1/(\xi\varepsilon_{s,w}(1-\delta)k_{ri,ave}))]H_d/u_0} \tag{B10}$$

$$C_{CO_2,out} = C_{CO_2,eq} + (C_{CO_2,d} - C_{CO_2,eq})e^{-(k_{ri,ave}/u_0)(x+y)} \tag{B11}$$

$$x = \xi\varepsilon_s^*\left[H_l - \frac{1-\eta_{sd}}{b}(1 - e^{-bH_l})\right] \tag{B12}$$

$$y = \xi(\varepsilon_{s,d} - \varepsilon_s^*)\left[\frac{1-e^{-aH_l}}{a} - \frac{1-\eta_{sd}}{a+b}(1 - e^{-(a+b)H_l})\right] \tag{B13}$$

The average kinetic constant (k$_{ri,ave}$) and volume fraction of potentially active solids (ξ) should be known initially to solve Eqs. B10 and B11. Therefore, as another approach, the considerations of solid composition in the carbonator, probability density function (f$_t$), i.e. the fraction of particles with certain residence times, in Eqs. B14-16 and the distribution of the particle based on the number of carbonation-calcination cycles as given in Eq. B3 allow the calculation of the average carbonation level, X$_{ave}$, (Eq. B17) as well as k$_{ri,ave}$ (Eq. B18) and ξ.

$$f_t = \frac{1}{\tau}e^{-(t/\tau)} \tag{B14}$$

$$\tau = \frac{n_{s,a}}{F_R} \tag{B15}$$

$$n_{s,a} = \frac{W_s}{M_s}(1 - x_{ash} - x_{CaSO_4}) \tag{B16}$$

$$X_{ave} = \sum_{N=1}^{+\infty} r_N \left(\int_0^{t_{lim}} f_t X(t, N, C_{CO_2}^*) dt + \int_{t_{lim}}^{\infty} f_t X_{max,N} \, dt \right) \tag{B17}$$

$$kri, ave = \frac{\rho_{s,a}}{M_{s,a}} \sum_{N=1}^{+\infty} r_N \int_0^{t_{lim}} f_t k_s S_N (1 - X(t, N, C_{CO_2}^*))^{2/3} \, dt \tag{B18}$$

It should be noted that, the effect of sulphation on the maximum carbonation degree in the rigorous model was considered by adjusting the k and X_r constants (Eq. B2) corresponding to the sulphation level of Piaseck limestone (Grasa et al., 2008b; Romano, 2012). The given equations are only valid up to a sulphation level of 1%.

$$\Delta X_{CaSO_4} = F_S/(F_R + F_0) \tag{B19}$$

$$k = 0.026 \times (\Delta X_{CaSO_4} \times 100)^2 + 0.219 \times (\Delta X_{CaSO_4}) + 0.660 \quad 0 \leq \Delta X_{CaSO_4} \leq 0.01 \tag{B20}$$

$$X_r = (-0.1118 \times \Delta X_{CaSO_4} \times 100) + 0.0969 \quad 0 \leq \Delta X_{CaSO_4} \leq 0.005 \tag{B21}$$

$$X_r = (-0.0298 \times \Delta X_{CaSO_4} \times 100) + 0.0559 \quad 0.005 < \Delta X_{CaSO_4} \leq 0.01 \tag{B22}$$

The capture efficiency can be calculated by two different ways, Eq. B23 and Eq. B24.

$$E'_{CO_2} = \frac{F_R X_{ave}}{F_{CO_2}} \tag{B23}$$

$$E''_{CO2} = \frac{F_{CO_2} - V_{g,out} C_{CO_2,out}}{F_{CO_2}} = \frac{V_{g,in} C_{CO_2,in} - V_{g,out} C_{CO_2,out}}{V_{g,in} C_{CO_2,in}} \tag{B24}$$

The values for the variables required for the carbonator calculation are imported from the cement plant simulation via a COM interface (F_{CO_2}, F_0, F_R, F_{ash}, F_S, u_0, d_p, T, M_s, p, μ, $C_{CO_2,in}$, $V_{g,in}$, W_s, H_t, x_{CaSO_4}, x_{ash}). The area of the reactor (A_t), average solid density (ρ_s) and average molar mass values (M_s) are initially calculated. By assuming a CO_2 concentration inside the carbonator ($C_{CO_2}^*$), X_{ave} is obtained using Eqs. B14 to B17 and the first capture efficiency, E'_{CO_2} is calculated using Eq. B23.

The length of dense and lean regions is determined by Eqs. B8 to B9, given the total height of carbonator, H_t. The average kinetic constant of the carbonation reaction, $k_{ri,ave}$, can be calculated using Eq. B18 with the same $C_{CO_2}^*$ used in the E'_{CO_2} calculation. Using the $k_{ri,ave}$, the CO_2 concentration at the outlet is calculated by Eqs. B10 to B13. Finally the second capture efficiency, E''_{CO2} can be obtained using Eq. B24. An iterative calculation is applied to obtain same capture efficiency from the two different methods. Once the same capture efficiency is reached, it is possible to calculate a new A_t using the average value of inlet and outlet flowrates and a new M_s based on the X_{ave}. Based on the new A_t and M_s, the new $C_{CO_2}^*$ needs to be calculated to give same capture efficiency, ie. another iterative loop is set to obtain A_t and M_s outside the iterative loop for $C_{CO_2}^*$.

B.2 Customization of UniSim Design

The behaviour of a user defined operation in the UniSim Design can be defined by compiling a Visual Basic code. Two different ways of implementing an external program into UniSim environment are proposed. These methods include direct integration of a Matlab code or an executable file as a solver. The basic user defined operation appears as shown in Figure B3. The design tab of this unit contains three main sections: connections, code and variables among which the last two are crucial for the customization. A Visual Basic code is written inside the code section while the external user defined parameters, i.e. height of a reactor and solid particle diameter for the carbonator design, can be identified in the variables section. The code environment comprises of three sub-titles as follows.

B.2.1 Sub Initialize

It is the section to activate the inlet and outlet streams and to set up the unit operation. The below command allows the activation of the first feed stream that is named 'Gas Feed'. Similar commands can be repeated for the activation of all inlet and outlet streams.

- ActiveObject.Feeds1Name = "Gas Feed"
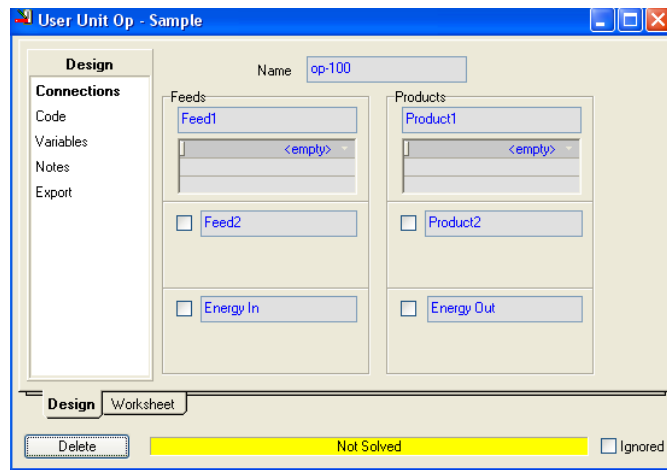
Figure B3 The view of a user defined operation in UniSim Design.

B.2.2 Sub Execute

It is the main section to transfer of the stream properties into the unit operation. In addition, a user defined variable can be created as an external input. The model equations are compiled in this section while any changes on the stream properties or the external inputs trigger the solver. The following command is employed to create a user defined variable called "Pressure", and the term 'uctPressure' assigns a unit selection for this variable.

- ActiveObject.CreateUserVariable("Prs", "Pressure", uvtReal, uctPressure, Scalar)

A crutial step, after compiling model equations, is the transfer of variables from UniSim environment to an external program. Two different procedures are followed for this purpose. First, if the external program is Matlab, the following commands: (i) activate Matlab solver that runs in the background, (ii) add a path to the folder referred as "folder" under C:\, and (iii) assign "MF1" value in the user defined operation as "Massgas" in the Matlab environment. In the final line, the Matlab file named "sample" is executed.

- Dim MatLab As Object
- Dim Result As String
- Set MatLab = CreateObject("Matlab.Application")

- Result = MatLab.Execute("cd c:\folder")
- Call MatLab.PutWorkspaceData("Massgas", "base", MF1)
- Result = MatLab.Execute("sample")

The assigned "Massgas" variable in the Matlab Workspace can be referred as "Massgas_M" by using the below command if it is needed.

- Massgas_M = evalin('base','Massgas')

After Matlab solver terminates, the outputs can be sent to UniSim environment by using "assignin" command. In the following example, the variable "M_result" from Matlab is assigned as "U_result" in UniSim Design.

- assignin('base','U_result',M_result)

If an external model is written in any other programming languages in the form of an executable file, the following procedure is applicable. This option is more challenging since transferred data needs to be stored in input and output files. It is also possible to adapt an executable file from a Matlab code if it is converted to an executable by using Matlab Compiler.

(1) Any variables from a unit operation can be transferred into an input file by using the following command. Here, the input file, "file.txt", is initially cached. Then, the term "ref" in the input file is replaced by a variable, "U_value".
- sname = "C:\folder\file.txt"
- lOpenFile = FreeFile
- Open sname For Input As lOpenFile
- cached = Input(LOF(lOpenFile), lOpenFile)
- cached = Replace(cached, "ref", U_value)
(2) The executable solver ("solver.exe") that requires an input file ("file.txt" in this case) can be run by using the following:
- Dim wsh As Object
- Set wsh = CreateObject("WScript.Shell")
- Dim waitOnReturn As Boolean
- waitOnReturn = True

- Dim windowStyle As Integer
- windowStyle = 1
- wsh.Run("C:\folder\solver.exe C:\folder\file",windowStyle, waitOnReturn)

  UniSim solver waits until the external solver stops running.

(3) In the final stage, any outputs of the external solver in the form of a text file can be read by UniSim solver. In the final command line, the variable 'Value' is set equal to the second variable of the output (srtCDRackk).

- sFileName = "c:\folder\output.txt"
- lOpenFile = FreeFile
- Open sFileName For Input As lOpenFile
- sFileText = Input(LOF(lOpenFile), lOpenFile)
- strCDRackk = Split(sFileText)
- Close lOpenFile
- Value=strCDRackk(2)

The returned variables from an external model using the above implementation methods can be then employed in the unit operation or transferred to the outlet streams. For each outlet stream; temperature, pressure, mass or molar flow rate and composition values have to be provided for activation. The following command is to set the temperature of 'SolidOut' stream to the value of 'Mtemp'.

- SolidOut.Temperature.Calculate(Mtemp)

B.2.3 Sub StatusQuery

This section is to update of status information. Any error and warning messages for missing streams, connections or external variables can be assessed. The error messages not only appear in UniSim status bar but also are illustrated at the bottom of the user defined operation. The final form of the implementation of the Ca-looping process using an external carbonator model and the developed interface are presented in Figure B4. The proposed integration allows rapid data transfer whenever any model inputs are changed, and the customised error messages let the user to understand the source of an error.

(a)
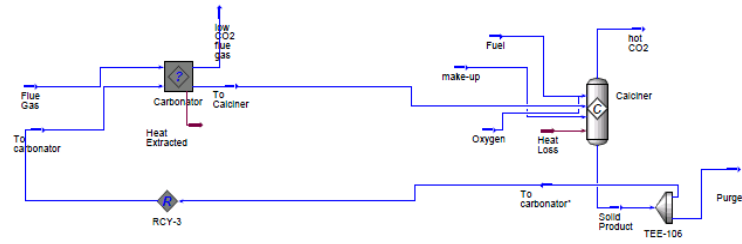
(b)

Figure B4 a) The view of Ca-looping process in the simulation environment, and b) the interface of the carbonator in UniSim.

Appendix C

A sample economic analysis spreadsheet for the Ca-looping process

Table C1 Economic analysis spreadsheet for the Ca-looping process at 1.65 F_0/F_{CO2}.

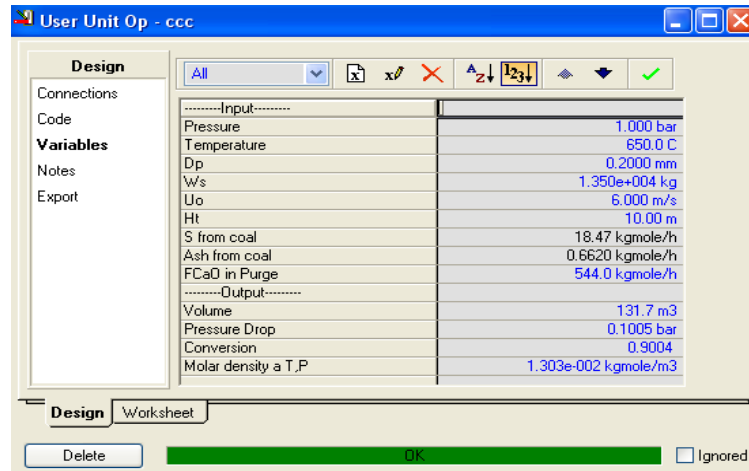|	2013	2014	2015	2016	2017	2018	2019	2020	2021	2022	2023	2024	2025	2026	2027	2028	2029	2030	2031	2032	2033	2034	2035	2036	2037	2038	2039	2040	2041
Year				1	2	3	4	5	6	7	8	9	10	11	12	13	14	15	16	17	18	19	20	21	22	23	24	25	26
Load Factor				60	90	90	90	90	90	90	90	90	90	90	90	90	90	90	90	90	90	90	90	90	90	90	90	90	90
Equivalent yearly hours				5256	7884	7884	7884	7884	7884	7884	7884	7884	7884	7884	7884	7884	7884	7884	7884	7884	7884	7884	7884	7884	7884	7884	7884	7884	7884
Expenditure Factor		20	45	35																									
Operating Costs																													
Fuel				9.47	14.41	14.63	14.85	15.07	15.29	15.52	15.76	15.99	16.23	16.48	16.72	16.97	17.23	17.49	17.75	18.02	18.29	18.56	18.84	19.12	19.41	19.70	20.00	20.30	0
Power				0.24	0.37	0.38	0.38	0.39	0.40	0.40	0.41	0.41	0.42	0.43	0.43	0.44	0.45	0.45	0.46	0.47	0.47	0.48	0.49	0.49	0.50	0.51	0.52	0.53	0
Raw materials + Cooling water				4.48	6.82	6.92	7.02	7.13	7.23	7.34	7.45	7.56	7.68	7.79	7.91	8.03	8.15	8.27	8.39	8.52	8.65	8.78	8.91	9.04	9.18	9.32	9.46	9.60	0
ETS				0.20	0.30	0.30	0.30	0.30	0.30	0.30	0.30	0.30	0.30	0.30	0.30	0.30	0.30	0.30	0.30	0.30	0.30	0.30	0.30	0.30	0.30	0.30	0.30	0.30	
Maintenance				11.23	17.09	17.35	17.61	17.87	18.14	18.41	18.69	18.97	19.25	19.54	19.84	20.13	20.44	20.74	21.05	21.37	21.69	22.02	22.35	22.68	23.02	23.37	23.72	24.07	0
Labour & Supervision				4.38	6.66	6.76	6.86	6.97	7.07	7.18	7.29	7.40	7.51	7.62	7.73	7.85	7.97	8.09	8.21	8.33	8.46	8.58	8.71	8.84	8.97	9.11	9.25	9.38	0
Administration, Local Rates&Insurance				6.93	10.55	10.70	10.86	11.03	11.19	11.36	11.53	11.70	11.88	12.06	12.24	12.42	12.61	12.80	12.99	13.18	13.38	13.58	13.79	13.99	14.20	14.42	14.63	14.85	0
Fixed Capital Expenditures		91.79	206.52	160.62																									
Total cash flow (yearly)		91.79	206.52	197.54	56.20	57.04	57.89	58.76	59.64	60.53	61.43	62.35	63.28	64.22	65.18	66.15	67.14	68.14	69.16	70.19	71.24	72.31	73.39	74.48	75.59	76.72	77.87	79.03	0
Total cash flow (cumulated)		91.79	298.30	495.85	552.05	609.09	666.99	725.75	785.38	845.91	907.34	969.68	1032.96	1097.18	1162.36	1228.51	1295.65	1363.79	1432.95	1503.14	1574.38	1646.69	1720.08	1794.56	1870.15	1946.87	2024.74	2103.78	2103.78
Cement production	0	0	0	0.60	0.90	0.90	0.90	0.90	0.90	0.90	0.90	0.90	0.90	0.90	0.90	0.90	0.90	0.90	0.90	0.90	0.90	0.90	0.90	0.90	0.90	0.90	0.90	0.90	22.20
																													Sum
Discount rate	0.1																												
Discount factor	1	0.91	0.83	0.75	0.68	0.62	0.56	0.51	0.47	0.42	0.39	0.35	0.32	0.29	0.26	0.24	0.22	0.20	0.18	0.16	0.15	0.14	0.12	0.11	0.10	0.09	0.08	0.08	
Total cash flow		83.44	170.68	148.42	38.39	35.42	32.68	30.15	27.82	25.67	23.68	21.85	20.16	18.60	17.16	15.84	14.61	13.48	12.44	11.48	10.59	9.77	9.02	8.32	7.67	7.08	6.53	6.03	826.98
Output				0.45	0.61	0.56	0.51	0.46	0.42	0.38	0.35	0.32	0.29	0.26	0.24	0.22	0.20	0.18	0.16	0.15	0.13	0.12	0.11	0.10	0.09	0.08	0.08	0.07	6.53
Operating sum				10.66	14.75	13.61	12.56	11.59	10.69	9.87	9.11	8.40	7.75	7.15	6.60	6.09	5.62	5.19	4.79	4.42	4.07	3.76	3.47	3.20	2.95	2.73	2.51	2.32	
Fixed sum				16.93	23.43	21.62	19.95	18.41	16.98	15.67	14.46	13.34	12.31	11.36	10.48	9.67	8.93	8.24	7.60	7.01	6.47	5.97	5.51	5.08	4.69	4.33	3.99	3.68	
Capital		83.44	170.68	120.68																									
ETS				0.15	0.21	0.19	0.17	0.16	0.14	0.13	0.12	0.11	0.10	0.09	0.08	0.07	0.07	0.06	0.05	0.05	0.05	0.04	0.04	0.03	0.03	0.03	0.03	0.02	

Summary		
Operating (€/ton cement)	26.64	
Fixed (€/ton cement)	42.31	Cost of base 97.33 (€/t cement)
Capital (€/ton cement)	57.43	CO2 avoided 41.11 €/ton CO2 avoided
ETS (€/ton cement)	0.34	
Sum	126.72	

Appendix D

Stream properties for the steam cycle of biomass-air-fired power plant, and CO$_2$ purification and compression unit, and the effect of fuel moisture on gross capacity of the biomass-air-fired plant described in Chapter 5

Table D1 The steam cycle stream properties for the biomass-air-fired plant presented in Figure 5-2(b).

| Stream No	1	2	3	4	5	6	7	8	9	10
T (°C)	565.6	565.6	565.6	565.6	565.6	365.9	365.9	365.9	565.6	496.9
P (bar)	38.31	166.5	166.5	166.5	38.31	42.78	42.78	42.78	166.5	24.16
m (ton/h)	368.5	401.6	0.11	0.41	368.9	0.40	0.80	396.8	3.1	18.60
Stream No	**11**	**12**	**13**	**14**	**15**	**16**	**17**	**18**	**19**	**20**
T (°C)	395.2	395.2	395.2	395.2	110.7	276.9	229.6	72.0	38.73	46.40
P (bar)	11.56	11.56	11.56	11.56	0.81	4.42	2.87	0.34	0.069	0.103
m (ton/h)	28.31	325.1	308.9	16.26	11.12	8.65	20.08	10.5	258.5	16.26
Stream No	**21**	**22**	**23**	**24**	**25**	**26**	**27**	**28**	**29**	**30**
T (°C)	395.7	69.67	38.39	38.68	56.74	78.19	116.3	131.7	130.9	93.61
P (bar)	42.78	0.34	0.069	27.23	27.23	27.23	27.23	27.23	4.42	2.87
m (ton/h)	0.51	50.35	325.6	325.6	325.6	325.6	325.6	325.6	8.65	28.73
Stream No	**31**	**32**	**33**	**34**	**35**	**36**	**37**	**38**		
T (°C)	72.44	184	188.3	218.1	251.5	223.4	193.8	365.9		
P (bar)	0.81	10.98	214.5	214.5	214.5	42.78	24.16	42.78		
m (ton/h)	39.84	401.6	401.6	401.6	401.6	28.26	46.86	368.5		
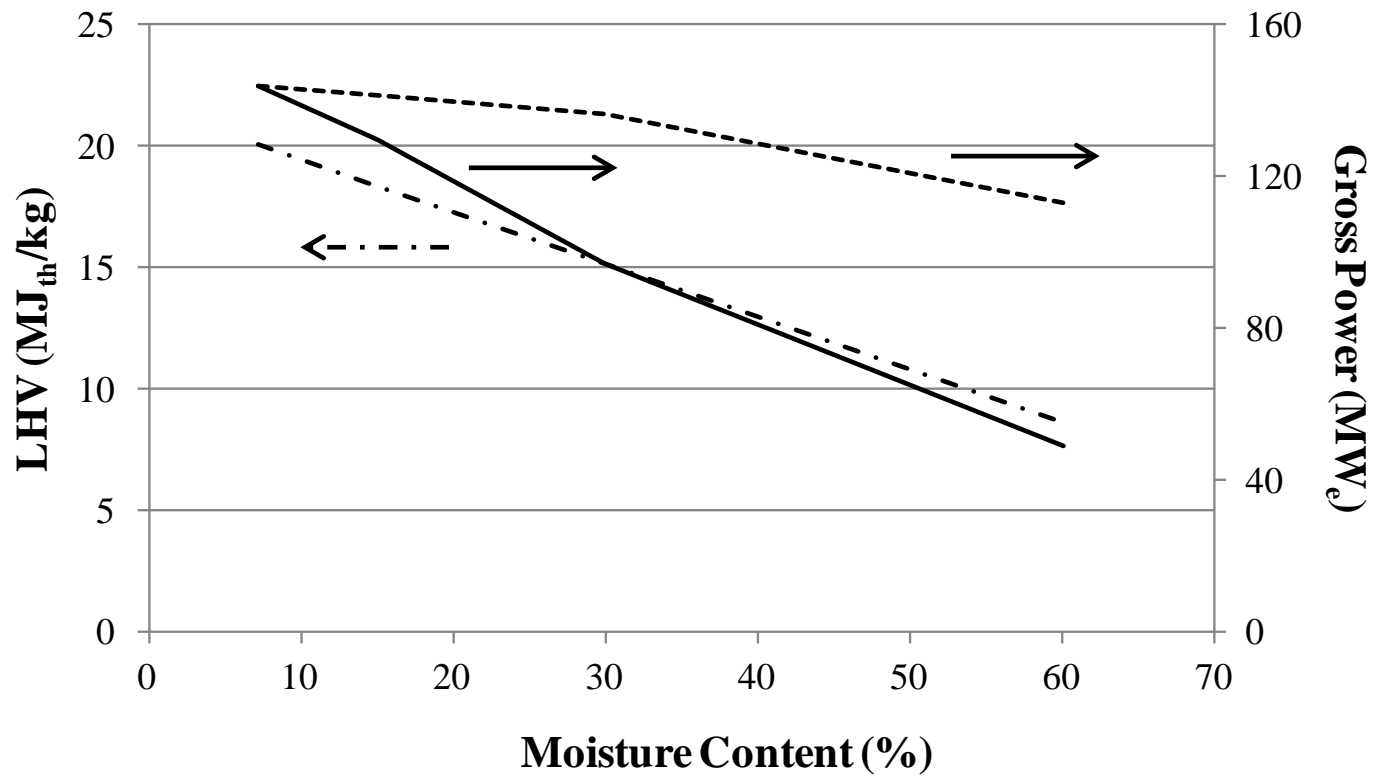
Figure D1 The effect of moisture content on the LHV (MJ_{th}/kg biomass) of the biomass and gross power generation capacity of the biomass-air-fired plant. Dashed line corresponds to the gross power with the same mass of biomass on a dry basis. Continuous line corresponds to the gross power with the same mass of wet biomass.

Table D2 The stream properties and compositions for the cryogenic CO_2 purification and compression unit (Figure 5-3) added to the biomass-oxy-fired plant.

Stream No	1	2	3	4	5	6	7	8	9	10
T (°C)	80	34.7	35	−20	−35	−35	−32	28.2	−35	33.2
P (bar)	1.013	1.013	24	24	24	24	80	80	24	54
Molar Flow Rate (kgmole/h)	4168.3	1832.1	2336.2	2336.2	2336.2	1748.4	1748.4	1748.4	587.8	587.8
Composition (mole %)										
CO_2	48.9	1.0	86.5	86.5	86.5	97.2	97.2	97.2	54.8	54.8
O_2	3.4	-	6.1	6.1	6.1	1.3	1.3	1.3	20.5	20.5
N_2	4.0	-	7.1	7.1	7.1	1.2	1.2	1.2	24.7	24.7
H_2O	43.7	99.0	0.3	0.3	0.3	0.3	0.3	0.3	-	-
Total Stream Enthalpy (GJ_{th}/h)	−1235.0	−527.4	−798.6	−811.3	−828.5	−700.1	−699.6	−686.8	−128.5	−127.3
Stream No	**11**	**12**	**13**	**14**	**15**	**16**	**17**	**18**	**19**	**20**
T (°C)	−18	−35	−35	−33.2	−35	8	25	15	26.3	43.4
P (bar)	54	54	54	80	54	54	1.12	80	80	150
Molar Flow Rate (kgmole/h)	587.8	587.8	225.0	225.0	362.8	362.8	362.8	225.0	1973.4	1973.4
Composition (mole %)										
CO_2	54.8	54.8	91.3	91.3	32.1	32.1	32.1	91.3	96.5	96.5
O_2	20.5	20.5	4.5	4.5	30.4	30.4	30.4	4.5	1.7	1.7
N_2	24.7	24.7	4.2	4.2	37.5	37.5	37.5	4.2	1.5	1.5
H_2O	-	-	-	-	-	-	-	-	0.3	0.3
Total Stream Enthalpy (GJ_{th}/h)	−129.3	−131.5	−84.4	−84.3	−47.1	−46.5	−45.9	−83.0	−769.9	−768.7

Appendix E

E.1 Publications

- Ozcan, D.C., Alonso, M., Ahn, H., Abanades, J.C., Brandani, S., 2014. Process and Cost Analysis of a Biomass Power Plant with In-situ Calcium Looping CO_2 Capture Process. Industrial & Engineering Chemistry Research 53 (26), 10721-10733.
- Ozcan, D.C., Ahn. H., Brandani, S., 2013. Process Integration of a Ca-looping Process with a Cement Plant for Carbon Capture. International Journal of Greenhouse Gas Control 19, 530-540.
- Romano, M. C., Anantharaman, R., Arasto, A., Ozcan, D.C., Ahn, H., Dijkstra, J.W., Carbo, M., Boavida, D., 2013. Application of Advanced Technologies for CO_2 Capture from Industrial Sources. Energy Procedia 37, 7176-7185.
- Romano, M.C., Martínez, I., Murillo, R., Arstad, B., Blom, R., Ozcan, D.C., Ahn, H., Brandani, S., 2013. Process Simulation of Ca-Looping Process: Review and Guidelines. Energy Procedia 37, 142-150.
- Romano, M.C., Martínez, I., Murillo, R., Arstad, B., Blom, R., Ozcan, D.C., Ahn, H., Brandani, S., 2012. Guidelines for modelling and simulation of Ca-looping processes. EERA CCS report.

E.2 Presentations

- Ozcan, D.C., 2014. Carbon Capture from Industrial Sources. Association of British and Turkish Academics (ABTA) Doctoral Researcher Awards Ceremony, May 25, London, UK.
- Ozcan, D.C., Bocciardo, D., Ferrari, M.C., Ahn, H., Kierzkowska, A.M., Muller, C.R., Brandani, S., 2013. Comparison of Various Carbon Capture Technologies to Reduce CO_2 emissions From a Cement Plant. AIChE 2013 Annual Meeting, November 3-8, San Francisco, USA.
- Ozcan, D.C., 2013. Selection of an appropriate carbon capture technology for the reduction of CO_2 emissions from a cement plant. 25th Annual Honeywell Users Group EMEA Conference, November 4-7, Nice, France.

- Ozcan, D.C., Ahn, H., Kierzkowska, A.M., Muller, C.R., Brandani, S., 2013. Process Integration of Chemical Looping Combustion into Calcium Looping for CO_2 Capture from a Cement Plant. 5th IEAGHG HTSLCN Meeting, September 2-3, Cambridge, UK.

- Ozcan, D.C., Ahn, H., Brandani, S., 2012. Techno-Economic Study of Ca-Looping Processes for Carbon Capture from Cement Plants. AIChE 2012 Annual Meeting, October 28 – November 2, Pittsburgh, USA.

- Ozcan, D.C., Ahn, H., Brandani, S., 2012. Fully integrated simulation of a cement plant with a carbon capture Ca-looping process. 4th IEAGHG HTSLCN Meeting, August 19-21, Beijing, China.

- Ozcan, D.C., Ahn, H., Brandani, S., 2011. Design of a Ca-looping Process for Carbon Capture in a Cement Plant. CCS – Development of Improved Technologies for Chemical Looping Combustion & Carbonate Looping Meeting, November, Zabrze, Poland.

- Ozcan, D.C., Ahn, H., Brandani, S., 2011. Process Integration of a Ca-looping process with a cement manufacturing plant. Joint UKCCSRC and CO2CHEM Meeting, July, Nottingham, UK.

E.3 Honours & Awards

- Honorable Mention Award from Association of British and Turkish Academics (ABTA) in 2014.
- Winner of the Honeywell UniSim® Design Challenge for the Europe, Middle East, Africa (EMEA) region in 2013.